**UNIVERSITAT JAUME I**

**Departament de Química Inorgànica i Orgànica**

**Àrea de Química Inorgànica**

# Homogeneous Catalysts for Green Processes and Non-Conventional NHC-Based Complexes

**Doctoral Thesis**

**Candela Segarra Almela**

**PhD. supervisors: Eduardo Peris and Elena Mas**

**Castelló de la Plana, May 2014**

**Prof. Dr. Eduardo Peris Fajarnés, Catedràtic de l'àrea de Química Inorgànica i Dra. Elena Mas Marzá, contractada Ramón y Cajal de l'àrea de Física Aplicada, pertanyents al Departament de Química Inorgànica i Orgànica i el Departament de Física, respectivament, de la Universitat Jaume I,**

**Certifiquen:** Que la Tesis Doctoral amb el títol 'Homogeneous Catalysts for Green Processes and Non-Conventional NHC-Based Complexes' ha sigut desenvolupada baix la seva direcció, en l'àrea de Química Inorgànica del Departament de Química Inorgànica i Orgànica de la Universitat Jaume I, per Candela Segarra Almela.

Castelló de la Plana, a 9 de Maig de 2014

Ft.: Prof. Dr. Eduardo Peris Fajarnés Ft.: Dra. Elena Mas Marzá

**AKNOWLEDGEMENTS/AGRAÏMENTS**

En primer lloc m'agradaria expressar la meua gratitud d'una manera molt sincera al meu director de tesi, Eduardo Peris, per l'oportunitat que m'ha donat de formar part del seu grup d'investigació, pels seus consells i pel seu suport constant. A la meua codirectora de tesi y amiga, Elena Mas per ajudar-me tant i tant i tant... i estar ahí sempre que la necessite, tant en lo professional com en lo personal. MOLTES GRÀCIES ALS DOS!!!

A tots els meus companys de lab. que amb l'aportació individual de cadascú formem un grup molt heterogeni, però compacte. Tantes hores de debat al lab, festes per Castelló, Villareal, La Vilavella i altres llocs de la geografia espanyola... mai vos oblidaré amics!!!. Del més gran al més petit: Jose, Maca, Goyo, (estos son els papis, Jose i Maca m'han acompanyat durant tot el procés, i m'han ajudat molt i Goyo ara al final s'ha bolcat molt en mi). Sergio II (el més bon xic del món amb ell sempre pots contar). Sara (ai la meua Sareta, si ens ho hem passat bé! que eixa alegria que te caracteritza segueixca in Dublin!!. Hugo (mi informático favorito! jejeje que hubiera hecho sin ti?). Sheila (a la que més coses li pasen, però sempre en un somriure en la cara... companya d'un del viatges més increïbles que he fet). Carmen (que caràcter! però amb un cor que no li cap en el pit) Els que ja no estan: Míriam, Sergio I, Aless, Fernando, André, Ampa, Arturo, Jo, Marco (ací vull fer menció especial a Ampa i Arturo dels que he aprés tant i han sigut com un guia per a mi) i, per últim, les noves incorporacions: Víctor, David i Diego! (segur que vos va super bé).

Als meus companys de QIO, amb els que ho passem tan bén en Magdalena! a tots els companys i amics que he anat coneixent durant els dos màsters, cursos, congressos, estades, especialment a Nuria i Lorena i als tècnics de servei central que tanta falta mos fan! A Jens Linke, per la síntesi del TBTQ.

A la Universitat Jaume I per la primera beca d'investigació FPI i al Ministeri per la Segona, una beca PFU que estic disfrutant actualment i que ja s'acaba.

A tots el professors dels quals he rebut algun tipus d'ajuda, ja siga per haver fet alguna estada breu o col·laboració: Mike Whittlesey, Dmitri Gusev, Ekkehart Hahn, Dietmar Kuck, Beatriz Royo. Especialment a Martin Albrecht que ara me dona l'oportunitat de fer una estada post-doctoral amb ell.

Als meus amics de sempre Marta, Rocio i Sergi (els que sempre estan quan els necessites) i la resta de RVK i Tubarro, als de la Uni Eva i Richo (sempre vos tinc present encara que ens veiem molt) i la resta de Carbonatos, totes les amistats sorgides gràcies al pàdel i també a l'Apalanka i novies.

I finalment a la meua família per ser els millors. Als meus pares, Amparo i Emilio, per que gràcies a ells he arribat a ser la persona que soc hui en dia, a la meua germana Amparo, la meua nebodeta Alejandra i el meu cunyat Javi per estar al meu costat sempre, la família política (Maijo, Pepe, Rocio i Javi), les meues ueles, ties i tios, cosins i cosines, en especial al meu cosí Fern per l'ajuda en la maquetació de la tesi. I molt especialment a la millor persona i company de vida, Aitor, per entendre com d'important és per a mi la meua formació, fer tots el sacrificis que siguen necessaris i per fer-me feliç. Vos vull molt a tots!

Als meus pares

---

## NOMENCLATURE

The nomenclature employed to name the compounds described in this work is:

Ligands: letters of the alphabet (**A-M**).

Precursor salts of ligands: the ligand letter with the acidic protons and its counterion. For example, **[EH$_2$]I$_2$** is the precursor salt of ligand **E** which contains two acidic C-H bonds and two iodides as counterions. In order to avoid misunderstandings letter **H** has been omitted in the nomenclature chosen for the ligands.

Metallic complexes obtained in this work: the number followed by the letter of the coordinated ligand. The complexes have been sorted in order to appearance.

## LIST OF ABBREVIATIONS

| | |
|---|---|
| Δ | refluxing temperature |
| η | ligand hapticity |
| μ | bridge ligand |
| *a*NHC | *abnormal* N-heterocyclic carbene |
| BimMe$_2$ | 1,3-dimethylbenzimidazolylidene |
| BimN*t*Bu$_2$ | 1,3-di(*tert*-butyl)benzimidazolylidene |

| | |
|---|---|
| cat. | catalyst |
| *C,C'*-imz-pyr | imidazolylidene-pyridylidene |
| COA | cyclooctane |
| COD | 1,5-cyclooctadiene |
| COE | cyclooctene |
| Conv. | conversion |
| $Cp^*$ | 1,2,3,4,5-pentamethylcyclopentadiene |
| CV | Cyclic Voltammetry |
| DFT | Density Functional Theory |
| DMF | dimethylformamide |
| DMSO | dimethylsulfoxide |
| DPV | Differential Pulse Voltammetry |
| EA | elemental analysis |
| ESI-MS | Electrospray Ionization Mass Spectrometry |
| ESI-TOF-MS | Electrospray Ionization Time-of-flight Mass Spectrometry |
| Et | ethyl |
| EtOAc | ethyl acetate |
| EtOH | ethanol |
| $Et_2O$ | diethyl ether |
| GC | Gas Chromatography |
| gCOSY | gradient Correlation Spectroscopy |
| gHMBC | gradient Heteronuclear Multiple bond Correlation |
| gHSQC | gradient Heteronuclear Single Quantum Coherence |
| gNOESY | gradient Nuclear Overhauser Effect Spectroscopy |
| h | hour |
| HRMS | High Resolution Mass Spectrometry |
| imz | imidazole |
| IPr·HCl | 1,3-bis(2,6-diisopropylphenyl)imidazolium chloride |

| | |
|---|---|
| *i*PrOH | *iso*-propanol |
| IR | infrared |
| KHMDS | potassium bis(trimethylsilyl)amide |
| M | metal |
| Me | methyl |
| mesityl | 2,4,6-trimethylphenyl |
| MIC | mesoionic carbene |
| MW | microwave |
| NaHMDS | sodium bis(trimethylsilyl)amide |
| NaOAc | sodium acetate |
| NaO*t*Bu | sodium *tert*-butoxide |
| NBD | 2,5-norbornadiene |
| *n*Bu | *n*-butyl |
| *n*BuLi | *n*-butyl lithium |
| *N*,*C*-pyr-pyr | pyridine-pyridylidene |
| NHC | N-heterocyclic carbene |
| *n*Hex | *n*-hexyl |
| NMR | Nuclear Magnetic Resonance |
| δ | chemical shift |
| br | broad |
| d | doublet |
| dd | doublet of doublets |
| *J* | coupling constant |
| m | multiplet |
| ppm | parts per million |
| s | singlet |
| t | triplet |
| *n*NHC | *normal* N-heterocyclic carbene |

| | |
|---|---|
| *n*Pr | *n*-propyl |
| OAc | acetate |
| OTf | triflate |
| PEPPSI | Pyridine Enhanced Precatalyst Preparation, Stabilization and Initiation |
| Ph | phenyl |
| PIBs | Pyrene-based-bisazoliums |
| Pyr | pyridine |
| *r*NHC | *remote* N-heterocyclic carbene |
| RT | room temperature |
| t | time |
| T | temperature |
| TBABr | tetrabutylammonium bromide |
| TBTQ | tribenzotriquinacene |
| *t*Bu | *tert*-butyl |
| *t*BuNH$_2$ | *tert*-butylamine |
| TEP | Tolman Electronic Parameter |
| THF | tetrahydrofurane |
| TON | Turnover Number |
| US | ultrasound |
| % $V_{Bur}$ | buried volume |

# CHAPTER 1

# GENERAL INTRODUCTION AND OBJECTIVES

# 1.1 GENERAL INTRODUCTION: N-HETEROCYCLIC CARBENES (NHCs)

## 1.1.1 Metal-carbene complexes

Carbenes are described as neutral species containing a divalent carbon atom with only six valence electrons and two substituents ($:CR^1R^2$). Carbenes can coordinate to a metal fragment, forming, at least formally, a M=C double bond. However, when a carbene binds to a metal, its six electron count turns into an octet character in the complex, a fact that has to be taken into account in order to avoid misinterpretations of the carbene character of a number of carbene-type ligands, especially when referring to the so-called mesoionic carbenes (MICs), as will be mentioned later. Depending on the coordination, metal-carbene complexes can be classified in two extreme types: *Fischer*[1] and *Schrock*[2]. Each type constitutes an extrem different formulation of the bond of the carbene ($:CR^1R^2$) and the metal, and real cases often lie between the two of them.

Fischer carbene complexes, $L_nM=CR^1R^2$, contain late transition metals in low oxidation states, π-acceptor ligands and π-donor $R^1/R^2$ substituents (-OR, $-NR_2$) on the carbene carbon. Fischer carbenes are electrophilic, as a consequence of the $\partial^+$ charge on the carbene carbon. Schrock carbene complexes often contain early transition metals in high oxidation states, σ-donor ligands and alkyl/aryl substituents on the carbene carbon. Schrock carbenes are nucleophilic, because they bear a $\partial^-$ charge on the carbene carbon.

The polarity of the metal-carbene bond determines if a carbene complex has a Fischer or Schrock character. The charge on the carbon atom of the carbene is determined by the relative $M(d_\pi)$ orbital energy. The stability of $M(d_\pi)$ orbitals increases along the transition metal row; thus, late transition metals have more stable $M(d_\pi)$ orbitals and are more electronegative than early transitions metals, which present a more electropositive character.

In a Fischer (singlet state) carbene, a lone pair of electrons is donated from the singlet carbene to the empty $d_\sigma$ orbital on the metal (σ-bonding), and a lone pair is back-donated from a filled $M(d_\pi)$ to the empty $C(p_z)$ orbital of the carbene carbon (π-backbonding) (Figure 1.1). Consequently, the $:CR^1R^2$ ligand is considered in this case

to act as an L-type ligand. The electrons remain on the metal because is more stable, leading to an electrophilic carbene carbon, whose electron deficiency is compensated by π-donating substituents.

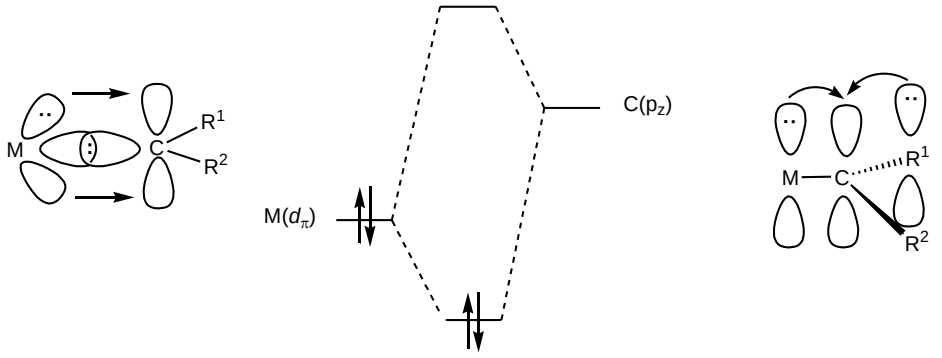


**Figure 1.1** Fischer carbenes

In a Schrock (triplet state) carbene, two covalent bonds are formed *via* the interaction of a triplet carbene with a metal with two unpaired electrons. Each M-C bond is polarised towards the carbon, because the carbon is more electronegative than the metal. In this case, the carbene acts as an $X_2$ ligand with nucleophilic character (Figure 1.2).

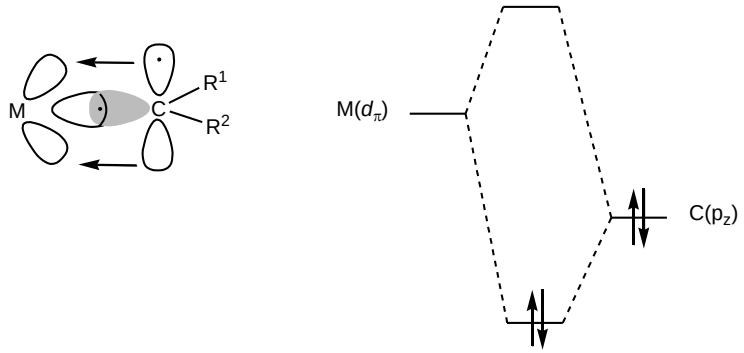


**Figure 1.2** Schrock carbenes

### 1.1.2 N-Heterocyclic carbenes: electronic and steric properties

N-heterocyclic carbenes (NHCs) are Fischer carbenes, where the carbene is embedded in an N-heterocycle, as the imidazol-2-ylidene shown in Scheme 1.1. The large number of monographic and review articles devoted to the study of the steric and electronic properties of NHC exemplifies the great interest in NHC-chemistry [3-10] Moreover, very recently, Bertrand has reported a comparative study of the different reactivity of carbenes with small organic molecules. This study illustrates the importance of the electrophilicity of stable singlet carbenes with respect to their reactivity.[11]


**Scheme 1.1** Imidazol-2-ylidene

In these ligands, an electronic stabilization of the singlet state is produced as a result of a combined influence of the inductive and the mesomeric effects of the nitrogen atoms ("push-pull" effect).[12] Because of the higher electronegativity of nitrogen compared to carbon, σ-electron density of the C-N bonds is withdrawn towards the nitrogen atoms resulting in a stabilization of the C(σ) orbital of the NHC carbon atom (inductive effect, Figure 1.3). Additionally, nitrogen is a good π-donor substituent and therefore, the donation of its non-bonding electron pair to the empty C($p_z$) orbital of the NHC carbon atom strongly disfavours the triplet carbene, because the occupation of the C($p_z$) orbital of the NHC carbon atom with an unpaired electron would interfere with the π-bonding of nitrogen atoms (mesomeric effect, Figure 1.3).[1, 13-14]

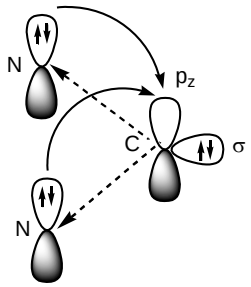


**Figure 1.3** Electronic stabilization ("push-pull" effect) of N-heterocyclic carbenes

Along this Ph.D. Thesis, NHCs are represented with a curved line between N-C-N bonds (or variations depending on substitution on the NHC frame) indicating the mesomeric effect of the nitrogen atoms, which donate their non-bonding electron pair into the C($p_z$) orbital of the carbene carbon atom (Scheme 1.1).

The nature of the metal-NHC bond has normally been considered as a pure σ-donation of a lone pair of electrons from the C(σ) orbital of the NHC carbon atom to the M($d_\sigma$) orbital, because the π-backbonding of the M($d_\pi$) electron density to the C($p_z$) orbital of the NHC carbon atom has not been seen as significant with respect to σ-bonding.[15-16] However, the relative contribution of π-bonding to the metal centre is considered as significant by some authors,[17] and some experimental and theoretical studies have shown greater involvement of π-bonding in the total metal-NHC attractive interaction.[6, 18-23] It is important to point out, that most of the times this π-backbonding contribution is not just a property associated with the ligand, but also with the metal, and this is why most of the cases in which a high π-contribution is observed are related to early transition metals in low oxidation states.

The electronic character of NHCs can be assessed by means of different metric techniques, such as, p*K*a measurements, nucleophilicity, IR and NMR spectroscopy, and electrochemical measurements, and all of them have been recently summarised by Nolan.[5] However, by far, the most commonly employed value is the Tolman electronic parameter (TEP),[24] which was originally developed for phosphines. NMR spectroscopy or electrochemical methods provide better resolution and precision in quantifying the electronic character of NHCs, but most NHCs can be evaluated using the TEP scale,[24] which refers to the IR C-O stretching frequency of [$Ni(CO)_3$(NHC)].[6] Although in most of the cases the Ni complexes cannot be obtained, and therefore their IR spectra are not accessible, the easy-to-obtain iridium and rhodium-carbonyl complexes, [$M(CO)_2X$(NHC)] (M = Ir or Rh; X = halide), can be used, and suitable IR correlations have been determined.[3, 9, 25-28] Another advantage of the aforementioned TEP metric is that values can be theoretically assessed. In this regard, Prof. Gusev recently reported the electron-donor and steric properties of a diverse group of representative NHC ligands quantified with the help of DFT calculations.[4] These studies showed excellent correlations between experimental and calculated values, demonstrating that DFT calculations are a useful method to evaluate the properties of new NHCs, even before they have been synthesised.

In general it is well established that NHCs are more electron-rich than trialkyl-phosphines and, furthermore, that aryl substituted imidazolylidene ligands are more electron-rich than their alkyl-substituted counterparts (Scheme 1.2). The nature of the heterocyclic ring also determines the electronic character of the NHC ligand and, in this regard, it is interesting to compare the different electronic properties of the ubiquitous imidazolylidenes with some other related NHCs, as those referred to as *abnormal* or mesoionic carbenes. A more detailed approach to this issue will be given in the introduction of Chapter 3.

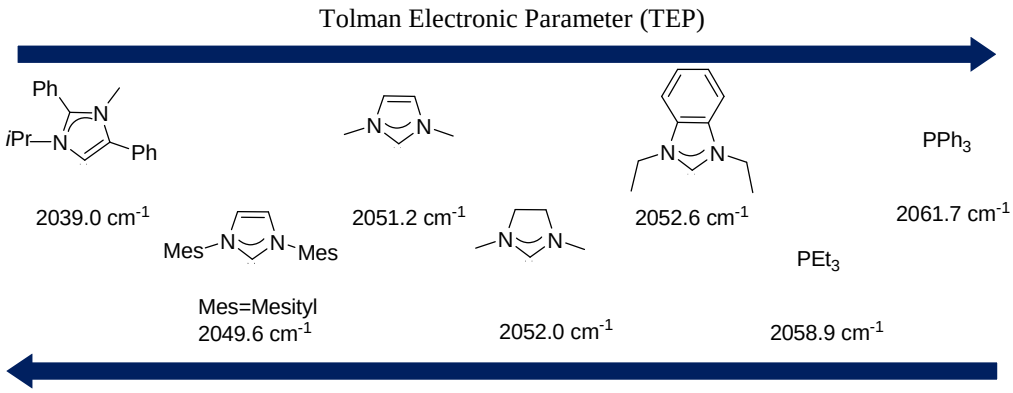


**Scheme 1.2** Tolman Electronic Parameter (TEP) *vs* electron-donating character of some NHCs

To synthesise tailor-made catalysts, it is helpful not only to use ligands with the proper electronic properties, but also to modulate its steric properties. A very useful approach to quantify the steric bulk of NHC ligands was made by Cavallo and co-workers,[10, 29] who defined the concept of the buried volume (% $V_{Bur}$) as the measure of the space occupied by an organometallic ligand in the first coordination sphere of the metal centre, as can be seen in Figure 1.4. The access to the % $V_{Bur}$ of any given NHC, is available for any author by simply use of web application for the calculation of the buried volume of NHCs.[29] The values may vary between 26.1% for the smallest NHCs, possessing methyl as N-substituents to 57.4% for the largest NHCs with bulkier N-substituents (Figure 1.4).[10, 30]

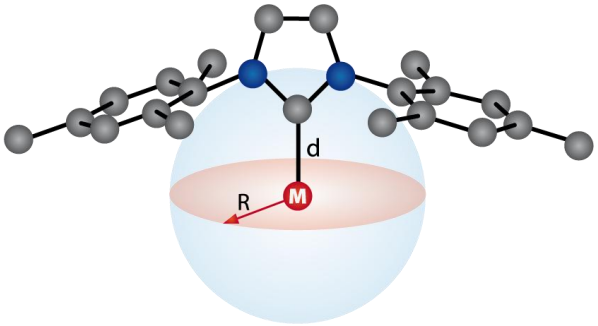


**Figure 1.4** Graphical representation of the sphere used to calculate % $V_{Bur}$ values

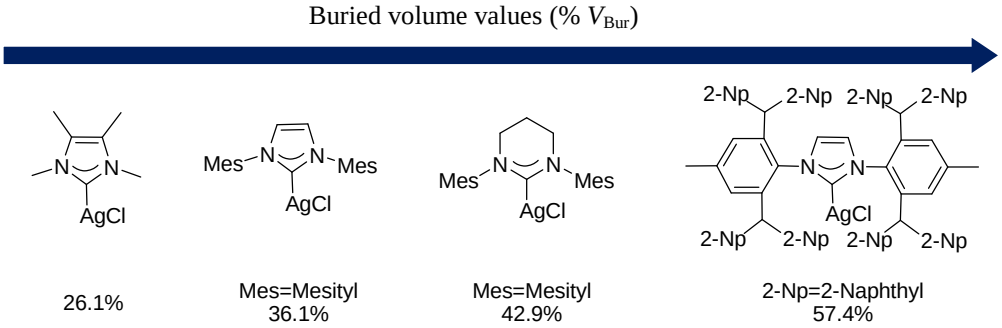


**Scheme 1.3** % $V_{Bur}$ for N-heterocyclic carbenes in [(NHC)AgCl] complexes

### 1.1.3 NHC-background chemistry in the Organometallic and Homogeneous Catalysis Group (QOMCAT) at the Universitat Jaume I

Since 2001, the research group of Organometallic Chemistry and Homogeneous Catalysis at the Universitat Jaume I, QOMCAT, directed by Prof. Eduardo Peris, focused the aim of its research on the development of "new and easy-to-make class of NHC ligands for the synthesis of improved metal catalysts". The earliest investigations in this field, were based on combining the strength of the M-C bond and the stabilizing *chelate* effect, to afford highly stable complexes that could provide improved catalytic applications under the harshest reaction conditions.[31] As a result, a

series of mono-, bi- an tridentate-NHC ligands were synthesised for the preparation of homogeneous catalysts,[32] which overcame the temperature thresholds of traditional catalysts and also facilitated the activation of traditionally inert bonds.[33]

More recently, the group reoriented the efforts in designing rigid poly-NHC frameworks for the preparation of homo- and heterometallic catalysts. Such types of poly-carbenes, especially those linked by rigid π-conjugated systems, enable electronic communication between the carbene units, which may allow for interesting applications in the fabrication of molecular electronic devices, as well as can provide interesting catalytic applications. The synthetic approach to rigid poly-NHCs also allowed the preparation of a series of heterometallic complexes, which were applied to the study of *tandem* catalytic processes. In this type of catalytic reactions, each metal facilitated a mechanistically distinct cycle, and therefore very sophisticated organic transformations were accomplished.[34-39]

Some of the more relevant achievements by the group are described in the next section.

#### 1.1.3.1 Mono-, bi- and tridentate-NHC ligands for the preparation of improved homogeneous catalysts

In 2001, the first example of a palladium *pincer*-NHC complex (compound **1.1**, Scheme 1.4) was described.[40] Complex **1.1** showed excellent activity in the Heck coupling reaction, mostly due to the stability conferred by the *pincer* ligand, allowing the complex to withstand higher reaction temperatures than those usually used for this type of reaction (160ºC versus 100-120ºC). Subsequently, the coordination of this *pincer* ligand was extended to other metals such as Ru[41] and Rh[56] (compounds **1.2** and **1.3**, Scheme 1.4). Depending on the reaction conditions used, the bridging coordination of the ligand could also be observed (**1.4**, Scheme 1.4).

Then a series of complexes with chelating di-NHCs were obtained, in which the topological and electronic properties of the ligands were modulated by changing the N-substituents, linkers and backbones. Several coordination modes were obtained, yielding complexes with *chelating*, *bridging* and *tripodal* di-NHCs (compounds **1.5**, **1.6** and **1.7**, and **1.8**, respectively, Scheme 1.4).

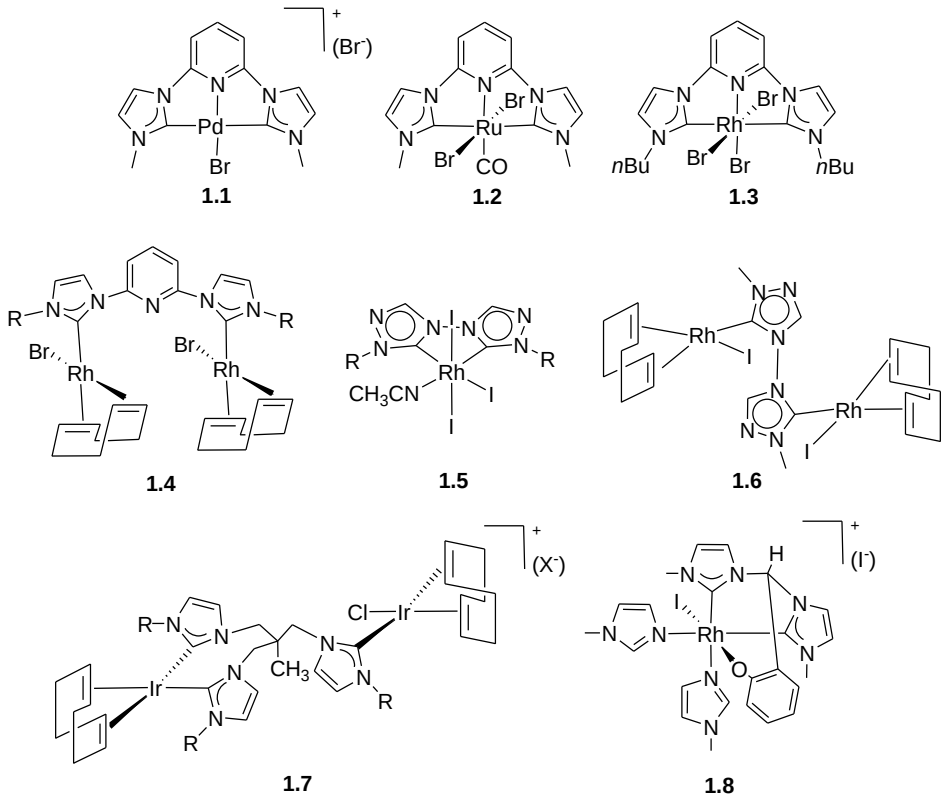


**1.1** **1.2** **1.3**

**1.4** **1.5** **1.6**

**1.7** **1.8**

**Scheme 1.4** Some of the di- and tri-NHC-based complexes synthesised in our group

The catalytic activities of the new complexes were tested in a number of organic transformations, such as: hydrosilylation, hydroformylation, olefin oxidation, C-C coupling reactions, hydro- and diboration, deuteration of organic substrates and *Borrowing-Hydrogen* processes. Most of the work developed by the group until 2009 was summarised in a micro-review.[32]

More recently, the QOMCAT group approached some newer research lines in close relation with *Green Chemistry*. In one of these lines, a series of M-NHC catalysts were prepared for the reduction of $CO_2$ to formate using *i*PrOH instead of $H_2$, through a transfer hydrogenation process. This new procedure for $CO_2$ reduction made the process safer and more environmentally friendly.[42] In this context, other *Green Chemistry* developments were achieved, such as the synthesis of mono- and bidentate NHC-based ligands with polar functionalities for the preparation of catalysts soluble in sustainable solvents (water and glycerol),[43-48] and also for the employment of other

alternative energy heating activation tools (MW or US).[46-47] Examples of these catalysts are shown in Scheme 1.5.

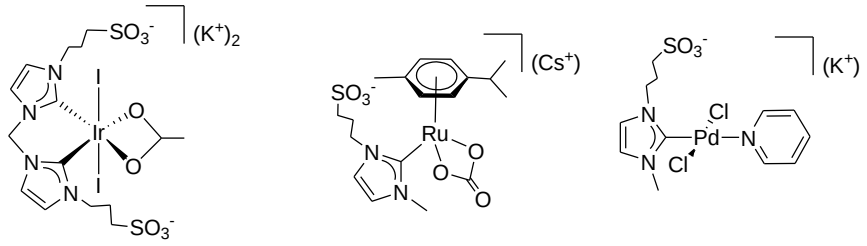


**1.9** **1.10** **1.11**

**Scheme 1.5** Some more recent mono- and bidentate-NHC-based complexes synthesised in our group

The catalysts shown in Scheme 1.5 were applied in the reduction of $CO_2$ to formate using $H_2$ or *i*PrOH,[44, 48] deuteration of arylpyridines[44] (compound **1.9**, Scheme 1.5), isomerization of allylic alcohols[45] (compound **1.10**, Scheme 1.5), Suzuki-Miyaura C-C coupling[43] (compound **1.11**, Scheme 1.5) and transfer hydrogenation processes[46-47] (compound **1.9**, Scheme 1.5), showing good catalytic performances.

### 1.1.3.2 Rigid poly-NHC frameworks for the preparation of homo- and heterometallic catalysts. Applications in *tandem* catalysis

As mentioned above, in recent years the QOMCAT group has directed its research interest in the design of poly-NHC metal complexes. By using a triazolylidene, which was found to be a very convenient *Janus-type* ligand, a wide variety of homo- and hetero-dimetallic complexes based on Ru(II),[49] Ir(I),[50] Rh(I)[50] and Ir(I)/Rh(I),[50] Ir(III)/Pd(II),[36] Ir(III)/Pt(II),[51] Ir(III)/Ir(I),[35] Ir(III)/Rh(I),[35] Ir(III)/Au(I),[52] Ir(III)/Ru(II)[53] and Ru(II)/Pd(II)[39] were obtained and characterised (Scheme 1.6).

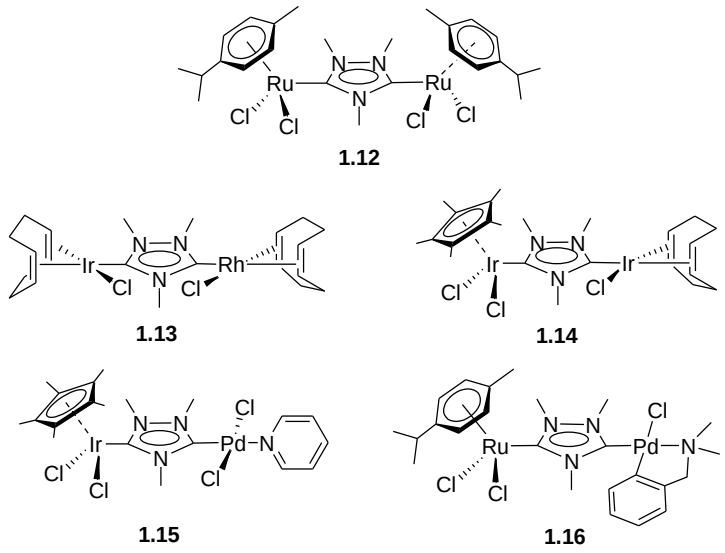


**Scheme 1.6** Some rigid (*Janus-head-type*) dimetallic complexes based on a triazolylidene ligand

The easy access to a wide variety of hetero-dimetallic complexes allowed for the study of *tandem* catalytic processes, in which each of the metal centres facilitated mechanistically independent cycles.[36-37, 52, 54] Interestingly, the presence of the two different metals furnished catalytic benefits compared to the cases in which mixtures of homodimetallic species were used,[53, 55] in a clear illustration of a synergistic behaviour between the metals present in the heterometallic unit. The *tandem* catalytic processes where these heterodimetallic catalysts were applied included cyclization of 2-aminophenyl ethyl alcohol/alkylation of the resulting indole,[35] dehalogenation/transfer hydrogenation of haloacetophenone,[36] Suzuki-Miyaura C-C coupling/transfer hydrogenation, and Suzuki-Miyaura C-C coupling/α-alkylation of haloacetophenones,[36] combined dehalogenation/transfer hydrogenation, and the Suzuki-Miyaura C-C coupling/transfer hydrogenation,[56] halo- and nitroarenes reduction/primary alcohols coupling,[37] isomerization/asymmetric hydrophosphination of 1,3-diphenylpropargyl alcohol,[38] and the hydrodefluorination of organic molecules.[39]

Another interesting asymmetric poly-NHC ligand that allows the preparation of heterodimetallic complexes is the recently described Y-shaped tri-NHC ligand, capable of bridging two metals in two different coordination environments (one

chelating, the other monodentate), therefore affording complexes with different reactivities at the two ends of the molecule, regardless whether the complexes are homo-[57] or heterometallic[56] (compounds **1.17** and **1.18**, respectively, Scheme 1.7).

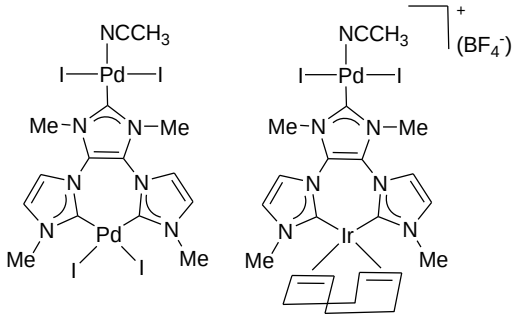


**1.17** **1.18**

**Scheme 1.7** Rigid tri-NHC-based complexes

The synthesis of poly-NHC ligands linked by rigid π-conjugated systems is one of the most recent aims of our research group. On this basis, a rigid, planar tri-NHC based on a triphenylene core was obtained and coordinated to Au(I),[58] Pd(II)[58] and Rh(I)[59] (Scheme 1.8).

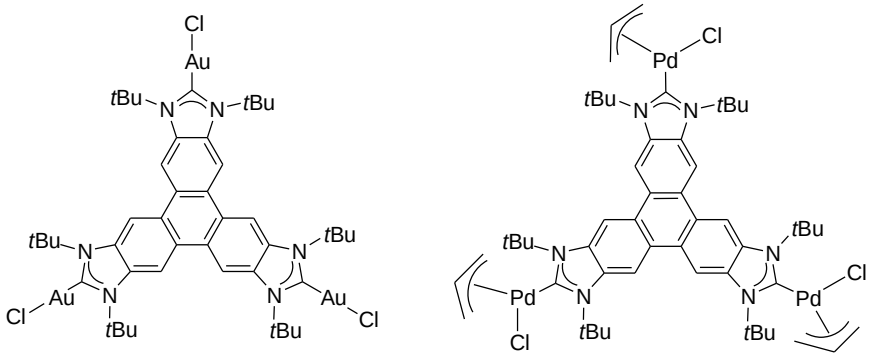


**1.19** **1.20**

**Scheme 1.8** $D_{3h}$-symmetrical tri-NHC-based complexes synthesised in our group

Tri-NHC Au(I) and Pd(II) complexes, **1.19** and **1.20**, respectively, (Scheme 1.8) experimentally proved to provide a significant catalytic benefit in the hydroamination of phenylacetylene, α-arylation of propiophenone with arylbromides and Suzuki-Miyaura C-C coupling, compared with the related trimetallic and monometallic complexes formally having the same stereoelectronic properties.[60] This observation

suggests that polyaromatic systems may facilitate the interaction between the catalyst and the substrate by means of π-stacking and therefore the catalytic response is increased, as has been previously reported.[61]

Along with the catalytic benefits provided by poly-NHCs, such types of ligands enable electronic communication between the carbene units, which may allow for interesting applications in molecular electronic devices. The idea of using unsaturated/aromatic polytopic NHCs as linkers in organometallic complexes is based on the possibility of the interaction between metal $d_\pi$ orbitals and the π-delocalised system of the NHC through M=C π-bonding.[62] In this context, a series of new pyrene-based-bisazoliums (**1.21**, PBIs) were obtained and were used for the preparation of dirhodium and diiridium complexes (Scheme 1.9).

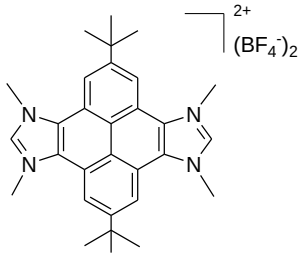


**1.21**

**Scheme 1.9** Pyrene-based-bisazolium (PBI)

The fluorescence properties of the PBIs were studied showing emissions in the range of 370-420 nm, and quantum yields ranging from 0.29-0.41.[63]

In the last year, other mono- and di-NHC based ligands decorated with π-extended polyaromatic rings or frameworks that minimise the metal-to-metal separation between the dimetallic complexes were synthesised.[64-66] These new complexes illustrated spectacular architectures and some of them are depicted in Scheme 1.10.

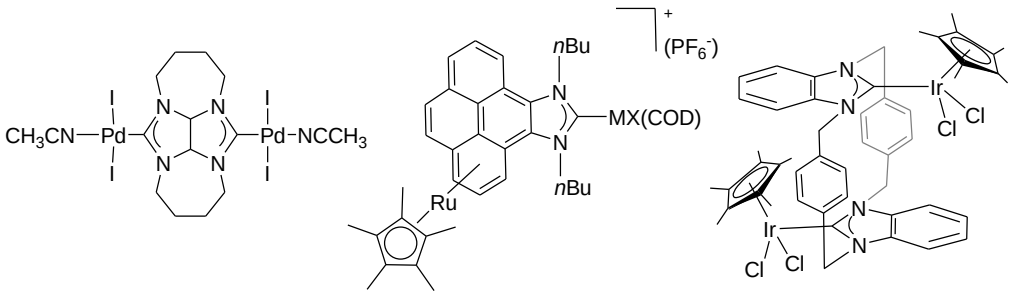


**1.22** **1.23** **1.24**

**Scheme 1.10** Recently developed mono- and di-NHC-based complexes with unusual architectures

## 1.2 OBJECTIVES

The general objective of this Thesis, in concordance with the lines of research developed by our group explained above, is the synthesis of improved homogeneous catalysts with novel stereoelectronic properties. In this sense, the work is focused on the synthesis and characterization of metal complexes bearing different nitrogen/carbon ligands, study of their reactivity and exploration of their catalytic properties. This general objective can be divided in the following more specific objectives:

- Synthesis of palladium and iridium complexes for the development of *Green Chemistry* processes. The main goal is to perform the catalytic reactions under the 'greenest' possible conditions, using non-toxic solvents, high atom-economy and minimum waste of energy.
- Systematic study of the reactivity of imidazolylidene-pyridylidene based ligands, by their coordination to rhodium and iridium precursors.
- Design, synthesis and coordination of poly-N-heterocyclic carbene ligands for the preparation of multimetallic complexes with unusually highly symmetrical structures, and study of their electronic properties.

## 1.3 REFERENCES


1. Bourissou, D.; Guerret, O.; Gabbai, F. P.; Bertrand, G., *Chem. Rev.* **2000**, *100*, 39-91.
2. Schrock, R. R., *Chem. Rev.* **2002**, *102*, 145-179.
3. Leuthausser, S.; Schwarz, D.; Plenio, H., *Chem.-Eur. J.* **2007**, *13*, 7195-7203.
4. Gusev, D. G., *Organometallics* **2009**, *28*, 6458-6461.
5. Nelson, D. J.; Nolan, S. P., *Chem. Soc. Rev.* **2013**, *42*, 6723-6753.
6. Dorta, R.; Stevens, E. D.; Scott, N. M.; Costabile, C.; Cavallo, L.; Hoff, C. D.; Nolan, S. P., *J. Am. Chem. Soc.* **2005**, *127*, 2485-2495.
7. de Fremont, P.; Marion, N.; Nolan, S. P., *Coord. Chem. Rev.* **2009**, *253*, 862-892.
8. Wuertz, S.; Glorius, F., *Acc. Chem. Res.* **2008**, *41*, 1523-1533.
9. Droege, T.; Glorius, F., *Angew. Chem. Int. Ed.* **2010**, *49*, 6940-6952.
10. Clavier, H.; Nolan, S. P., *Chem. Commun.* **2010**, *46*, 841-861.
11. Martin, D. C., Y.; Lavayo, V.; Bertrand, G., *J. Am. Chem. Soc.* **2014**, *136*, 5023-5030.
12. Pauling, L., *J. Chem. Soc. Chem. Comm.* **1980**, 688-689.
13. Herrmann, W. A., *Angew. Chem. Int. Ed.* **2002**, *41*, 1291-1309.
14. Weskamp, T.; Böhm, V. P. W.; Herrmann, W. A., *J. Organomet. Chem.* **2000**, *600*, 12-22.
15. Hu, X. L.; Castro-Rodriguez, I.; Olsen, K.; Meyer, K., *Organometallics* **2004**, *23*, 755-764.
16. Nemcsok, D.; Wichmann, K.; Frenking, G., *Organometallics* **2004**, *23*, 3640-3646.
17. Diez-Gonzalez, S.; Nolan, S. P., *Coord. Chem. Rev.* **2007**, *251*, 874-883.
18. Back, O.; Henry-Ellinger, M.; Martin, C. D.; Martin, D.; Bertrand, G., *Angew. Chem. Int. Ed.* **2013**, *52*, 2939-2943.
19. Comas-Vives, A.; Harvey, J. N., *Eur. J. Inorg. Chem.* **2011**, 5025-5035.

20. Jacobsen, H.; Correa, A.; Costabile, C.; Cavallo, L., *J. Organomet. Chem.* **2006**, *691*, 4350-4358.
21. Sanderson, M. D.; Kamplain, J. W.; Bielawski, C. W., *J. Am. Chem. Soc.* **2006**, *128*, 16514-16515.
22. Fantasia, S.; Petersen, J. L.; Jacobsen, H.; Cavallo, L.; Nolan, S. P., *Organometallics* **2007**, *26*, 5880-5889.
23. Khramov, D. M.; Lynch, V. M.; Bielawski, C. W., *Organometallics* **2007**, *26*, 6042-6049.
24. Tolman, C. A., *Chem. Rev.* **1977**, *77*, 313-348.
25. Chianese, A. R.; Li, X. W.; Janzen, M. C.; Faller, J. W.; Crabtree, R. H., *Organometallics* **2003**, *22*, 1663-1667.
26. Chianese, A. R.; Kovacevic, A.; Zeglis, B. M.; Faller, J. W.; Crabtree, R. H., *Organometallics* **2004**, *23*, 2461-2468.
27. Kelly, R. A., III; Clavier, H.; Giudice, S.; Scott, N. M.; Stevens, E. D.; Bordner, J.; Samardjiev, I.; Hoff, C. D.; Cavallo, L.; Nolan, S. P., *Organometallics* **2008**, *27*, 202-210.
28. Wolf, S.; Plenio, H., *J. Organomet. Chem.* **2009**, *694*, 1487-1492.
29. Poater, A.; Cosenza, B.; Correa, A.; Giudice, S.; Ragone, F.; Scarano, V.; Cavallo, L., *Eur. J. Inorg. Chem.* **2009**, 1759-1766.
30. Dierick, S.; Dewez, D. F.; Marko, I. E., *Organometallics* **2014**, *33*, 677-683.
31. Myers, R. T., *Inorg. Chem.* **1978**, *17*, 952-958.
32. Corberan, R.; Mas-Marza, E.; Peris, E., *Eur. J. Inorg. Chem.* **2009**, 1700-1716.
33. Peris, E.; Crabtree, R. H., *Coord. Chem. Rev.* **2004**, *248*, 2239-2246.
34. Mata, J. A.; Hahn, F. E.; Peris, E., *Chem. Sci.* **2014**, *5*, 1723-1732.
35. Zanardi, A.; Corberan, R.; Mata, J. A.; Peris, E., *Organometallics* **2008**, *27*, 3570-3576.
36. Zanardi, A.; Mata, J. A.; Peris, E., *J. Am. Chem. Soc.* **2009**, *131*, 14531-14537.
37. Zanardi, A.; Mata, J. A.; Peris, E., *Chem.-Eur. J.* **2010**, *16*, 10502-10506.
38. Sabater, S.; Mata, J. A.; Peris, E., *Eur. J. Inorg. Chem.* **2013**, 4764-4769.
39. Sabater, S.; Mata, J. A.; Peris, E., *Nat. Commun.* **2013**, *4*.

40. Peris, E.; Loch, J. A.; Mata, J.; Crabtree, R. H., *Chem. Commun.* **2001**, 201-202.
41. Poyatos, M.; Mata, J. A.; Falomir, E.; Crabtree, R. H.; Peris, E., *Organometallics* **2003**, *22*, 1110-1114.
42. Sanz, S.; Benitez, M.; Peris, E., *Organometallics* **2010**, *29*, 275-277.
43. Azua, A.; Mata, J. A.; Heymes, P.; Peris, E.; Lamaty, F.; Martinez, J.; Colacino, E., *Adv. Synth. Catal.* **2013**, *355*, 1107-1116.
44. Azua, A.; Sanz, S.; Peris, E., *Chem.-Eur. J.* **2011**, *17*, 3963-3967.
45. Azua, A.; Sanz, S.; Peris, E., *Organometallics* **2010**, *29*, 3661-3664.
46. Azua, A.; Mata, J. A.; Peris, E., *Organometallics* **2011**, *30*, 5532-5536.
47. Azua, A.; Mata, J. A.; Peris, E.; Lamaty, F.; Martinez, J.; Colacino, E., *Organometallics* **2012**, *31*, 3911-3919.
48. Sanz, S.; Azua, A.; Peris, E., *Dalton Trans.* **2010**, *39*, 6339-6343.
49. Viciano, M.; Sanau, M.; Peris, E., *Organometallics* **2007**, *26*, 6050-6054.
50. Mas-Marza, E.; Mata, J. A.; Peris, E., *Angew. Chem. Int. Ed.* **2007**, *46*, 3729-3731.
51. Zanardi, A.; Mata, J. A.; Peris, E., *Chem. Eur. J.* **2010**, *16*, 13109-13115.
52. Sabater, S.; Mata, J. A.; Peris, E., *Chem. Eur. J.* **2012**, *18*, 6380-6385.
53. Sabater, S.; Mata, J. A.; Peris, E., *Organometallics* **2012**, *31*, 6450-6456.
54. Zanardi, A.; Mata, J. A.; Peris, E., *Chem. Eur. J.* **2010**, *16*, 13109-13115.
55. Gusev, D. G.; Peris, E., *Dalton Trans.* **2013**, *42*, 7359-7364.
56. Gonell, S.; Poyatos, M.; Mata, J. A.; Peris, E., *Organometallics* **2012**, *31*, 5606-5614.
57. Gonell, S.; Poyatos, M.; Mata, J. A.; Peris, E., *Organometallics* **2011**, *30*, 5985-5990.
58. Gonell, S.; Poyatos, M.; Peris, E., *Angew. Chem. Int. Ed.* **2013**, *52*, 7009-7013.
59. Gonell, S.; Alabau, R. G.; Poyatos, M.; Peris, E., *Chem. Commun.* **2013**, *49*, 7126-7128.
60. Gonell, S.; Poyatos, M.; Peris, E., *Angew. Chem. Int. Ed.* **2013**, *52*, DOI: 10.1002/anie.201302686.

61. Carboni, S.; Gennari, C.; Pignataro, L.; Piarulli, U., *Dalton Trans.* **2011**, *40*, 4355-4373.

62. Schuster, O.; Mercs, L.; Albrecht, M., *Chimia* **2010**, *64*, 184-187.

63. Gonell, S.; Poyatos, M.; Peris, E., *Chem.-Eur. J.* **2014**, DOI: 10.1002/chem.201304952.

64. Valdes, H.; Poyatos, M.; Peris, E., *Organometallics* **2013**, *32*, 6445-6451.

65. Valdes, H.; Poyatos, M.; Peris, E., *Organometallics* **2014**, *33*, 394-401.

66. Ruiz-Botella, S.; Guisado-Barrios, G.; Mata, J. A.; Peris, E., *Organometallics* **2013**, *32*, 6613-6619.

# CHAPTER 2

# TWO GREEN PROCESSES: HOMOGENEOUS CATALYSIS IN WATER AND ACTIVATION OF AMMONIA BY *BORROWING-HYDROGEN*

## 2.1 INTRODUCTION

In 1998, Anastas and Warner formulated the principles of *Green Chemistry*.[1] Since then, chemical industry has notably focused on the design of chemical processes that reduce (or avoid) the use of hazardous substances. The commitment to apply the principles of *Green Chemistry*, using cleaner and more environmental-friendly technologies, has also centred the attention of the scientific community, as exemplified by the increase of new scientific journals and books exclusively devoted to *Green Chemistry*.[1-8]

The most important factors to consider for designing a green process are: prevention of waste, atom-efficiency, minimizing the use of auxiliary reagents and solvents (or use environmental-friendly solvents), and decrease of energy requirements.

Taking these premises into account, and considering the experience of our research group in the design of homogeneously catalysed processes, we decided to focus the first part of this investigation on two different catalytic transformations: the *Suzuki-Miyaura C-C cross coupling reaction in water*, and the *alkylation of ammonia with primary alcohols.* Each part of this chapter contains an introductory section of the catalytic transformation performed, followed by the design and synthesis of the catalysts used and their catalytic activities. The details regarding the characterization of every new species and all the experimental procedures are included in the Experimental Section (Chapter 5). Due to the fact that other groups published results related to this research, early after our studies were carried out, we will try to present a brief overview of the research developed in each catalytic transformation, as well as a short summary of the most recent outcomes published after our studies.

## 2.2 SUZUKI-MIYAURA C-C COUPLING IN WATER

### 2.2.1 Introduction

During the last two decades, there has been an increasing interest in the use of water as solvent for many homogeneously catalysed reactions.[9-12] Cost, environmental benefits and safety are among the reasons most often argued to justify the replacement of organic solvents by water in organic transformations. The design of a water-soluble catalyst requires the introduction of hydrophilic functional groups in the molecular structure of the catalyst. Detailed accounts on the design of hydrophilic ligands and their applications in aqueous-phase metal-catalysed reactions have been published,[12-14] and most devote a part to the use of hydrophilic N-heterocyclic carbene (NHC) ligands.

Metal-catalysed cross-coupling reactions constitute one of the most useful methods for C-C bond formation,[15] with Pd-catalysts being ubiquitous in such reactions. Among these processes, the Suzuki-Miyaura coupling, namely, the coupling between an arylboronic acid and an aryl halide,[16] is one of the most widely used protocols for the synthesis of biphenyls due to the good tolerance of a wide variety of functional groups. For this reason, the search for a way to perform such transformation in an environmentally benign manner is a challenge for researchers in the field of homogeneous catalysis.

The first example of Pd-catalysed cross-coupling reactions in water was reported by Calabrese and co-workers in 1990.[17] Since then, a number of water-soluble Pd-catalysts bearing hydrophilic ligands has been reported, and several reviews have been dedicated to this subject.[18-23] Although the introduction of NHC ligands to the coordination sphere of a metal complex has a series of advantages, such as stability and tolerance to a variety of functional groups, by the time that this research was initiated the number of NHC-palladium complexes for homogeneous catalysis in water was limited to very few examples,[24-30] and even fewer were related to highly stable chelate and *pincer* NHC-based complexes.[26,29]

Among the hydrophilic functional groups used in the preparation of water-soluble catalysts, sulfonate groups are very good candidates. They provide excellent solubilities in water and afford a minimum interference with the coordination sphere

of the metal, so they can be considered as an inert functionality from the catalytic point of view. By the time that this work was initiated, the number of sulfonate-NHC-palladium complexes was scarce, the main examples being those reported by Shaughnessy,[31] Pinel,[27] Nozaki[32] and our group.[33]

Since 2010, the number of publications regarding the use of water-soluble NHC-palladium complexes has enormously increased, and two recent reviews by Herrmann[13] and Verpoort[14] highlighted the increasing interest related to the synthesis and application of water-soluble NHC transition-metal complexes, especially in palladium-catalysed C-C coupling reactions.[13] Other interesting examples of Suzuki-Miyaura reactions in water catalysed by NHC-palladium complexes were not included in the above mentioned reviews since they have been reported more recently.[34-36] This fact shows the great interest of the scientific community to develop and improve processes in water as a way to work in a greener manner.

With all this in mind, in this section we focus our attention on the development of a rational series of sulfonate-functionalised-NHC-palladium complexes as catalysts for the Suzuki-Miyaura C-C coupling. The study gives a good opportunity to compare the catalytic outcomes of mono-, bis-chelating and *pincer*-NHC-based palladium complexes in aqueous media.

All the content of Section 2.2.2 was carried out in collaboration with Dr. Fernando Godoy during a short stay in our group as a visiting researcher.

### 2.2.2 Synthesis and characterization of Pd(II) complexes

The general aim of this work was to obtain a series of sulfonate-functionalised-NHC complexes of Pd(II), in which the ligands behave as monodentate-, bis-chelating and *pincer*-coordinated. We thought that the choice of this type of coordination modes should cover a wide set of topologies of NHC-palladium complexes that already had proved efficient catalytic properties in non-aqueous solvents.[37-38]

In this regard, we focused our attention on the compounds shown in Scheme 2.1. The di-NHC, **2.1**, and the chelating NHC complexes, **2.2**, were described by Herrmann and co-workers.[39] The *pincer*-coordinated Pd(II) complex, **2.3**, was described by our group in collaboration with Prof. Crabtree.[37] These three compounds are very active

in C-C coupling reactions, and constituted the reference compounds for the preparation of our hydrophilic Pd-complexes.

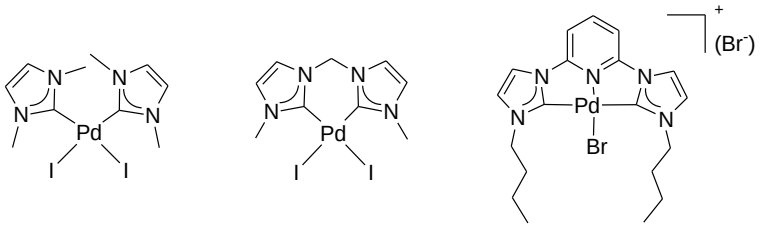


**2.1** **2.2** **2.3**

**Scheme 2.1** Reference NHC-based Pd compounds

### 2.2.2.1 Synthesis of sulfonate-functionalised-NHC ligand precursors

In order to prepare our hydrophilic NHC ligand precursors, we decided to prepare the sulfonate-functionalised-imidazoliums depicted in Scheme 2.2. (1-Methyl-3-propanesulfonate)imidazolium, **AH**, was prepared according to the literature method,[33] while bis(3-propanesulfonateimidazol-1-yl)methane, **$BH_2$**, and 2,6-bis(3-propanesulfonateimidazol-1-yl)pyridine, **$CH_2$**, were synthesised and characterised during the development of this research work.

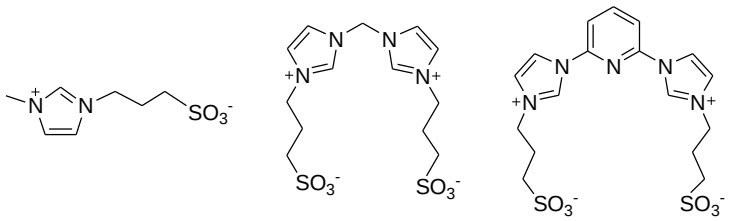


**AH** **$BH_2$** **$CH_2$**

**Scheme 2.2** Sulfonate-functionalised imidazoliums

The preparation of these sulfonate-imidazoliums was based on the use of 1,3-propanesultone as alkylating agent, as previously used for the preparation of other sulfonate-functionalised-NHC ligands.[31, 40] As depicted in Scheme 2.2, the three imidazoliums are zwitterionic, meaning that they contain separate positively and negatively charged parts.

*a) Synthesis of (1-methyl-3-propanesulfonate)imidazolium, **AH***

The synthesis of (1-methyl-3-propanesulfonate)imidazolium, **AH**, was performed according to the known literature method.[33] The reaction of commercially available 1-methylimidazole with 1,3-propanesultone in refluxing $CH_3CN$, gave **AH** in 95% yield (Scheme 2.3).

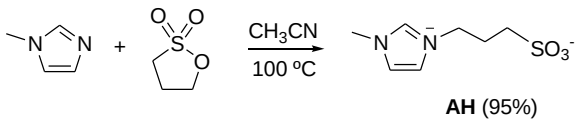


**AH** (95%)

**Scheme 2.3** Synthesis of **AH**

*b) Synthesis of bis(3-propanesulfonateimidazol-1-yl)methane, **$BH_2$***

The synthesis of bis(3-propanesulfonateimidazol-1-yl)methane, **$BH_2$**, was performed in two steps (Scheme 2.4). First, bis(imidazol-1-yl)methane was prepared by deprotonation of imidazole and subsequent reaction with $CH_2Cl_2$ (yield 75%).[41] Then, bis(imidazol-1-yl)methane reacted with 1,3-propanesultone in refluxing $CH_3CN$, to afford **$BH_2$** in 82% yield.

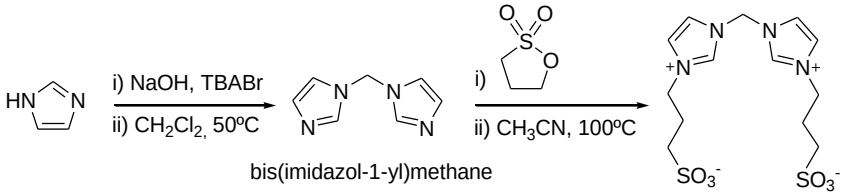


bis(imidazol-1-yl)methane

**$BH_2$** (82%)

**Scheme 2.4** Synthesis of **$BH_2$**

*c) Synthesis of 2,6-*bis*(3-propanesulfonateimidazol-1-yl)pyridine, **$CH_2$***

The synthesis of 2,6-bis(3-propanesulfonateimidazol-1-yl)pyridine, **$CH_2$**, was carried out following a similar procedure as the one for **$BH_2$** (Scheme 2.5). The deprotonation of imidazole with KOH, followed by reaction with 2,6-dibromopyridine formed 2,6-bis(imidazol-1-yl)pyridine[42] in 70% yield. Subsequent reaction with 1,3-propanesultone produced **$CH_2$** in 85% yield.

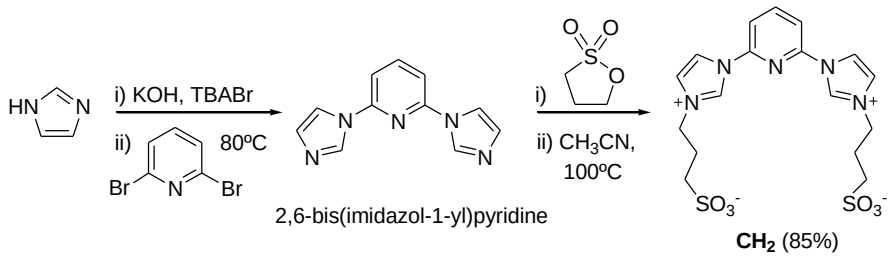


**Scheme 2.5** Synthesis of **$CH_2$**

The zwitterionic compounds **$BH_2$** and **$CH_2$** were fully characterised by NMR spectroscopy, mass spectrometry and elemental analysis. Full details about their characterization are given in the Experimental Section (Chapter 5).

### 2.2.2.2 Synthesis and characterization of Pd(II) sulfonate-functionalised-NHC complexes, 1A-4C

Once the sulfonate-functionalised imidazoliums were synthesised and characterised, the corresponding palladium complexes were obtained. In this section the preparation of complexes **1A**, **2B**, **3C** and **4C** will be discussed. All these Pd(II) compounds are new and have been prepared during the development of the present work.

As depicted in Scheme 2.6, the general preparation of complexes **1A**, **2B** and **3C** implied the reaction between $Pd(OAc)_2$, KI (as halide source) and the corresponding imidazolium compounds during 2-12h at 80ºC, and then during 3-12h at 140-160ºC, depending on the complex. After completion of the reaction, the solvent was removed under vacuum to yield a crude product that was purified by washing or by column chromatography. Compounds **1A**, **2B** and **3C** were obtained in 75, 29 and 18% yield, respectively.

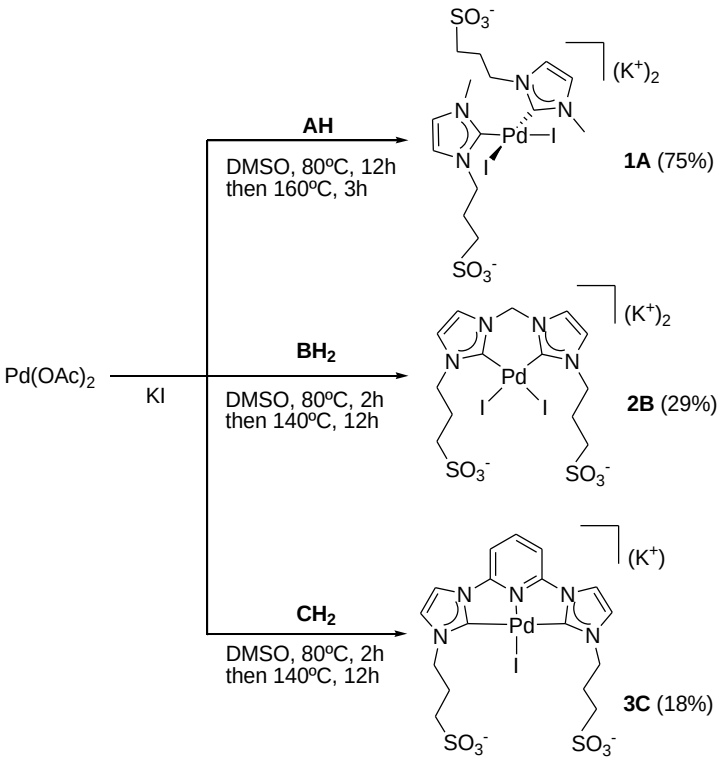


**Scheme 2.6** Synthesis of **1A**, **2B** and **3C**

All complexes were soluble in $H_2O$, partially soluble in alcohols ($CH_3OH$ and EtOH), and very insoluble in most common organic solvents such as $CH_2Cl_2$, $CHCl_3$, $Et_2O$, THF, or acetone.

Since the introduction of pyridine ligands has demonstrated to provide highly active catalysts for various Pd-mediated C-C reactions by the so-called PEPPSI effect (Pyridine Enhanced Precatalyst Preparation, Stabilization and Initiation),[43-45] we decided to prepare the pyridine substituted CNC-*pincer* complex **4C**. Compound **4C** was obtained by reaction of **3C** with pyridine in the presence of silver triflate in 98% yield (Scheme 2.7). Complex **4C** was soluble in $H_2O$ and in alcohols, and very insoluble in most common organic solvents.

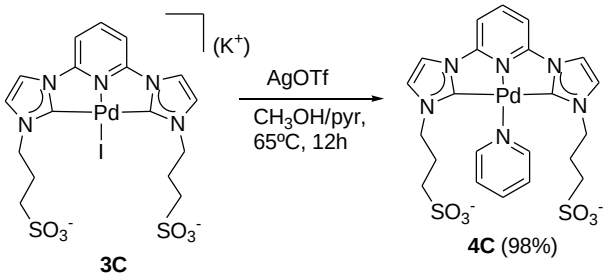


**Scheme 2.7** Synthesis of **4C**

All complexes were characterised by means of NMR spectroscopy and High Resolution Mass Spectrometry (ESI-TOF-MS). Complexes **1A** and **4C** were the only ones to give satisfactory elemental analysis. Several attempts to obtain satisfactory elemental analysis of **2B** and **3C** failed, probably because both species are highly hygroscopic. All the characterization details are given in the Experimental Section (Chapter 5). In this section, we will discuss in detail the NMR spectroscopic characterization of compounds **1A** and **3C**, as illustrative examples of all the complexes obtained.

*$^1$H NMR spectrum of **1A***

Figure 2.1 shows the $^1$H NMR spectrum of **1A**. The signals due to the proton of the C*H* groups of the imidazole ring are shown as two singlets at 7.18 and 7.13 ppm (a). The protons due to the C$H_3$ groups display a single resonance at 3.85 ppm (c), as a consequence of the twofold symmetry of the complex. The signals corresponding to the propanesulfonate groups, are depicted on the NMR spectrum shown in Figure 2.1.

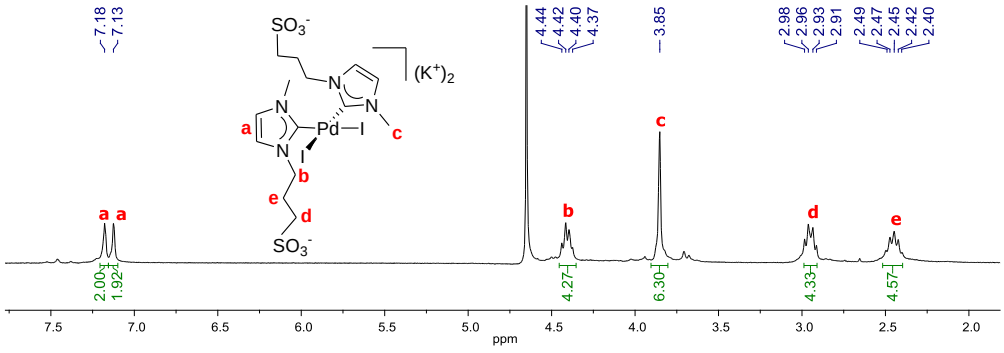


**Figure 2.1** $^1$H NMR spectrum of **1A** in $D_2O$

### *$^{13}C\{^1H\}$ NMR spectrum of **1A***

Figure 2.2 shows the $^{13}C\{^1H\}$ NMR spectrum of **1A**. The spectrum is consistent with the twofold symmetry of the complex, as seen by the low number of signals. The most characteristic signal is the one attributed to the metallated carbene carbons, at 163.9 ppm (1), in the typical region were other *cis* unbridged ylidenes of the type $PdX_2(NHC)_2$ appear[46-49] (*trans*-NHCs appear at higher frequencies ~ 180 ppm[46]). The signals due to the carbons of the *C*H groups of the imidazole ring appear at 124.0 and 122.4 ppm (2), respectively. The resonance corresponding to the carbon atom of the $CH_3$ groups is shown at 38.2 ppm (5). All the rest of the signals for the propanesulfonate carbon atoms are conveniently depicted on the spectrum shown in Figure 2.2, and are consistent with the structure proposed for the complex.

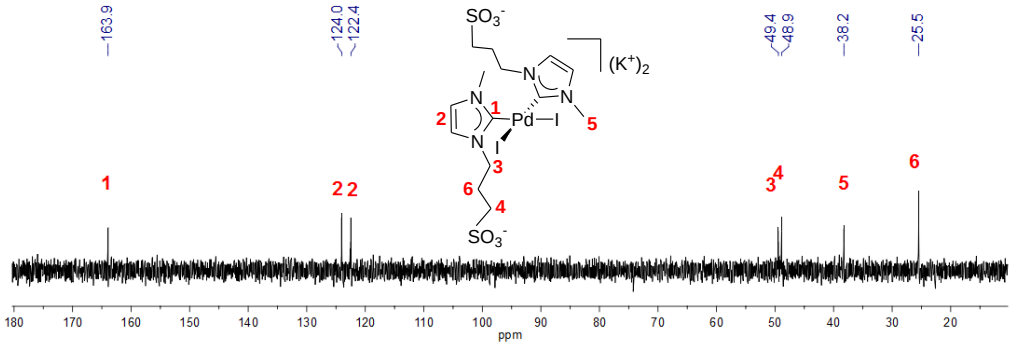


**Figure 2.2** $^{13}C\{^1H\}$ NMR spectrum of **1A** in $D_2O$

### *$^1H$ NMR spectrum of **3C***

Figure 2.3 shows the $^1H$ NMR spectrum of **3C**. The number of signals in the spectrum is consistent with the twofold symmetry of the molecule. The resonances due to the proton of the C*H* groups of the pyridine ring appear at 8.27 (triplet, a) and 7.54 (doublet, c) ppm. The signals attributed to the proton of the C*H* groups of the imidazole rings are seen as two doublets at 7.86 and 7.37 ppm (b). The three signals attributed to the protons of propanesulfonate are displayed at similar chemical shifts as those shown for **1A** (Figure 2.1).

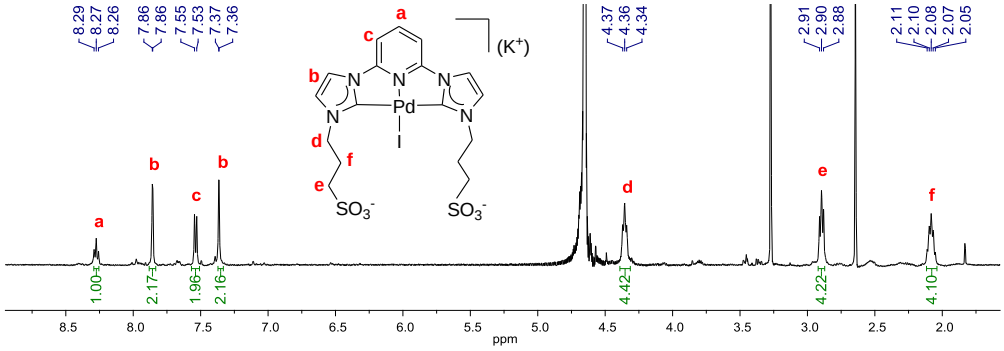


**Figure 2.3** $^{1}$H NMR spectrum of **3C** in $D_2O$

### *$^{13}C\{^{1}H\}$ NMR spectrum of **3C***

Figure 2.4 shows the $^{13}C\{^{1}H\}$ NMR spectrum of **3C**. The most characteristic signal is the one attributed to the metallated carbene carbons, at 166.5 ppm (1), which confirms the coordination of the NHC ligand to the metal centre. The signals attributed to the carbon of the $C_{ortho}$, $CH_{meta}$, and $CH_{para}$ groups of the pyridine ring appear at 149.7 ppm (2), 109.1 ppm (5) and 147.1 ppm (3), respectively. Due to the twofold symmetry of the compound, two signals corresponding to the carbon of the *C*H groups of the imidazole rings are shown at 124.7 ppm and 118.3 ppm (4). All the rest of the signals for the propanesulfonate carbons are conveniently displayed on the spectrum, and are consistent with the structure proposed for the complex.

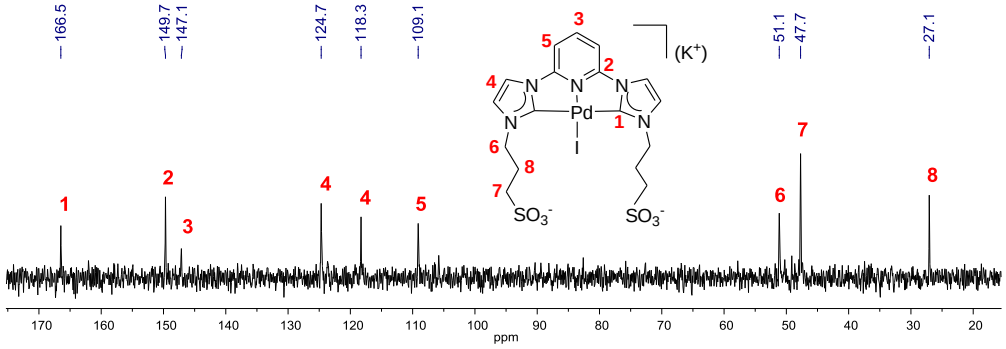


**Figure 2.4** $^{13}C\{^{1}H\}$ NMR spectrum of **3C** in $D_2O$

### 2.2.3 Catalytic activity of complexes, 1A-4C

In the following section, the catalytic results achieved with the palladium complexes described above will be described. It is advisable to use the table containing the different complexes attached to this manuscript in order to facilitate the reading of this section.

In order to accomplish the final objective of this section, we studied the catalytic activity of the water-soluble palladium complexes **1A**-**4C** in the Suzuki-Miyaura C-C coupling in water. In a typical Suzuki-Miyaura cross-coupling reaction an arylboronic acid reacts with an aryl halide to yield a biaryl compound, as shown in Scheme 2.8.

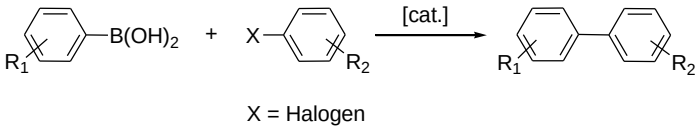


**Scheme 2.8** Biaryl synthesis *via* the transition-metal-catalysed Suzuki-Miyaura cross-coupling reaction

We first decided to carry out a catalyst screening of complexes **1A-4C** (Scheme 2.6, Scheme 2.7), by comparing their activities in the coupling of 4-bromoacetophenone and 4-chloroacetophenone with phenylboronic acid in water. The activation of 4-chloroacetophenone required the addition of tetrabutylammonium bromide (TBABr) as a phase transfer catalyst. The reactions were performed in a pyrex tube, in neat Milli-Q water, on a hot plate at 110ºC, with a 1 mol% catalyst loading in the presence of $K_2CO_3$. The choice of this base was done according to previous studies made by Chen and co-workers, in which the use of $K_2CO_3$ afforded the best catalytic results using triazole-based-NHC palladium catalysts.[26] The reactions were monitored by GC analysis after the appropriate intervals of time, using anisole as internal standard. Table 2.1 presents the results obtained in this first screening of complexes **1A-4C**.

**Table 2.1** Suzuki-Miyaura coupling of phenylboronic acid and aryl halides using **1A-4C**[a]

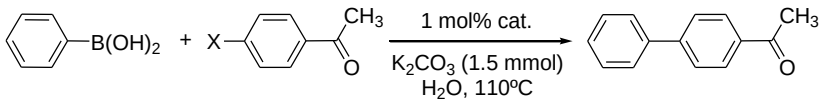


| Entry | Catalyst | X[b] | t(h) | Yield (%)[c] |
|---|---|---|---|---|
| 1 | **1A** | Cl | 12 | 87 |
| 2 | | Br | 4 | >99 |
| 3 | **2B** | Cl | 12 | 39 |
| 4 | | Br | 4 | 59 |
| 5 | **3C** | Cl | 12 | 58 |
| 6 | | Br | 4 | >99 |
| 7 | **4C** | Cl | 12 | 51 |
| 8 | | Br | 4 | 90 |

[a]**Reactions conditions**: aryl halide (1 mmol), phenylboronic acid (1.2 mmol), $K_2CO_3$ (1.5 mmol) and 1 mol% of catalyst in 5 mL of Milli-Q $H_2O$ at 110ºC. [b]All reactions with 4-chloroacetophenone were performed with addition of TBABr (1.5 mmol). [c]Yields determined by GC using anisole as internal standard.

As can be seen in Table 2.1, complexes **1A**, **3C** and **4C** were very active in the arylation of 4-bromoacetophenone (yields above 90%, entries 2, 6 and 8), while complex **2B** only afforded moderate yield (59%, entry 4). When the more inert 4-choloracetophenone was used, only compound **1A** afforded a high catalytic outcome (87%, entry 1), while **3C** and **4C** provided moderate yields of the final product (entries 5 and 7), and **2B** was inefficient. According to the activities shown for the coupling between 4-bromoacetophenone and phenylboronic acid, catalysts **1A** and **3C** were the most active ones. This observation implies that the presence of the pyridine ligand in **4C**, does not provide the expected enhancement of the catalytic activity by the PEPPSI effect, compared to catalyst **3C.**

To further analyze the catalytic activities of complexes **1A** and **3C**, we studied the reaction of 4-bromoacetophenone and 4-chloroacetophenone with different catalyst loadings ranging from $10^{-1}$ to $10^{-3}$ mol %. The results are listed in Table 2.2.

**Table 2.2** Aqueous Suzuki-Miyaura reaction of phenylboronic acid and aryl halides using catalysts **1A** and **3C**[a]

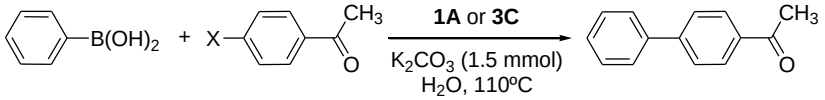


| Entry | Catalyst | Catalyst loading (%) | X[b] | t(h) | Yield (%)[c] | TON[c] |
|---|---|---|---|---|---|---|
| 1 | | $10^{-1}$ | | | 85 | 850 |
| 2 | **1A** | $10^{-2}$ | Cl | 12 | 76 | 7600 |
| 3 | | $10^{-3}$ | | | 37 | 37000 |
| 4 | | $10^{-1}$ | | | >99 | 1000 |
| 5 | **1A** | $10^{-2}$ | Br | 2 | >99 | 10000 |
| 6 | | $10^{-3}$ | | | >99 | 100000 |
| 7 | | $10^{-1}$ | | | 52 | 520 |
| 8 | **3C** | $10^{-2}$ | Cl | 12 | 31 | 3100 |
| 9 | | $10^{-3}$ | | | 18 | 18000 |
| 10 | | $10^{-1}$ | | | >99 | 1000 |
| 11 | **3C** | $10^{-2}$ | Br | 3 | >99 | 10000 |
| 12 | | $10^{-3}$ | | | 87 | 87000 |

[a]**Reaction conditions**: aryl halide (1 mmol), phenylboronic acid (1.2 mmol), $K_2CO_3$ (1.5 mmol) and catalyst in 5 mL of Milli-Q $H_2O$ at 110ºC. [b]All reactions with 4-chloroacetophenone were performed with addition of TBABr (1.5 mmol). [c]Yields determined by GC using anisole as internal standard. [c]TON = (mmol of product) / (mmol of catalyst)

As reflected in Table 2.2, both **1A** and **3C** showed excellent activities in the coupling of 4-bromoacetophenone when catalyst loadings as low as $10^{-3}$ mol % were used, although **1A** provided higher activity (compare entries 6 and 12). These data slightly improve previously published results for the coupling of 4-bromoacetophenone with phenylboronic acid using triazole-based-NHC palladium catalysts.[26] For the reactions carried out with 4-chloroacetophenone, **1A** afforded good activities when catalyst loadings of $10^{-1}$ or even $10^{-2}$ mol % were used (entries 1 and 2), but its activity dramatically decreased at lower catalyst loadings. For the same substrate, **3C** showed a moderate activity when a catalyst loading of $10^{-1}$ mol % was used (entry 7). The activity of **1A** in the coupling of 4-chloroacetophenone compares well with the results published by Çetinkaya and co-workers using *trans*-[$PdBr_2$(NHC)L] complexes

(NHC = benzimidazol-2-ylidene; L = pyridinecarboxylic acid or triphenylphosphine-3,3,3-trisulfonic acid trisodium salt), although in their case a catalyst loading of 1 mol% was used.[24, 50] It is worth mentioning that for the reactions carried out with 4-chloroacetophenone with both catalysts (**1A** and **3C**), the subsequent use of lower catalyst loadings results in an increase of the TON value, despite all yields lie below 100% (see entries 1-3 for **1A**, and 7-9 for **3C**). We think that this result indicates that some heterogeneous contribution to the catalytic outcome may be at play in these processes, and this may explain the rather strange variation of the catalytic efficiency upon decreasing the catalyst concentration. In fact, if palladium nanoparticles are formed during the reaction process, the reaction rate may well show a zero order variation on the initial concentration of the catalyst. An interesting review article about problems concerning the distinction between homogeneously and heterogeneously catalysed processes was recently published by Crabtree, in which a special emphasis was made to the case of palladium-catalysed processes, where many times heterogeneous processes are wrongly assumed to be homogeneous.[51] Further studies may be needed to clarify this point, but these are out of the scope of this research.

One of the most important problems in the use of neat water in the Suzuki-Miyaura C-C coupling is the poor solubility of most coupling partners. In order to circumvent this problem, mixtures of alcohol and water are often used.[25, 52-54] In order to widen the number of aryl halide substrates that we could use in the coupling reaction, we decided to perform the reaction in a 1:1 mixture of $H_2O$:*i*PrOH, using our most active catalysts **1A** and **3C**. Result are shown in Table 2.3.

**Table 2.3** Suzuki-Miyaura reaction of phenylboronic acid and aryl halides in $H_2O$/*i*PrOH[a]

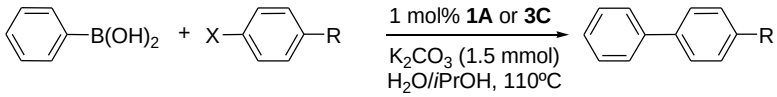


| Entry | Catalyst | X[b] | R | t(h) | Yield (%)[c] |
|---|---|---|---|---|---|
| 1 | **1A** | Cl | $COCH_3$ | 12 | >99 |
| 2 | | | $OCH_3$ | | 35 |
| 3 | | | H | | 73 |
| 4 | | | $CH_3$ | | 34 |
| 5 | **1A** | Br | $COCH_3$ | 4 | >99 |
| 6 | | | $OCH_3$ | | 86 |
| 7 | | | H | | 99 |
| 8 | | | $CH_3$ | | 94 |
| 9 | **3C** | Cl | $COCH_3$ | 12 | 84 |
| 10 | | | $OCH_3$ | | 12 |
| 11 | | | H | | 31 |
| 12 | | | $CH_3$ | | 12 |
| 13 | **3C** | Br | $COCH_3$ | 4 | >99 |
| 14 | | | $OCH_3$ | | 81 |
| 15 | | | H | | 92 |
| 16 | | | $CH_3$ | | 73 |

[a]**Reaction conditions:** aryl halide (1 mmol), phenylboronic acid (1.2 mmol), $K_2CO_3$ (1.5 mmol) and 1 mol% of catalyst. Reactions performed in a mixture of 2.5 mL of Milli-Q $H_2O$/2.5 mL $^i$PrOH at 110ºC. [b]All reactions with chloroarenes were performed with addition of TBABr (1.5 mmol). [c]Yields determined by GC using anisole as internal standard.

As can be seen from the data shown in Table 2.3, this mixture of $H_2O$:*i*PrOH as solvent allowed the effective coupling of a variety of bromoarenes, including non-activated ones. In the case of chloroarenes, both **1A** and **3C** were very active in the coupling of phenylboronic acid with 4-chloroacetophenone (entries 1 and 9), but only **1A** was capable of effectively activate other chloroarenes such as chorobenzene (entry 3).

These data were difficult to compare with previous results provided by other authors using the same substrates and reaction conditions, since conversions (generally based on substrates) are reported and our results are based on yields (based on products).[25, 54] *Yields* provide a more accurate representation of the catalytic activities, than those provided by *conversions*. In order to illustrate this point, we decided to study the time-course of the reactions between phenylboronic acid and two chloroarenes (Figure 2.5), by representing both, conversions and yields. As can be seen from the three plots depicted in Figure 2.5, the coupling of 4-chloroacetophenone with phenylboronic acid afforded almost quantitative yield to the final biphenyl product in just two hours. On the other hand, the maximum yield achieved for the coupling of 4-chlorotoluene was 35 %, after 12h. However, the conversion for this latter substrate was above 80%, as can be seen from the corresponding graphic, a result that was mainly attributed to the transformation of substrates into products other than the desired biphenyl compound. This simple experiment illustrates very well why the catalytic yields are always more convenient and scientifically more relevant than catalytic conversions. For this reaction, we also detected the formation of 1,1'-biphenyl as a consequence of the homocoupling of phenylboronic acid, as well as other minor unidentified products. These results are interesting because they suggest that the poor catalytic outcome of catalyst **1A** when deactivated chloroarenes were used was not due to the deactivation of the catalyst along the reaction course, but to the formation of other kinetically favoured products. These results suggest that probably a careful optimization of the reaction conditions may afford better outcomes.

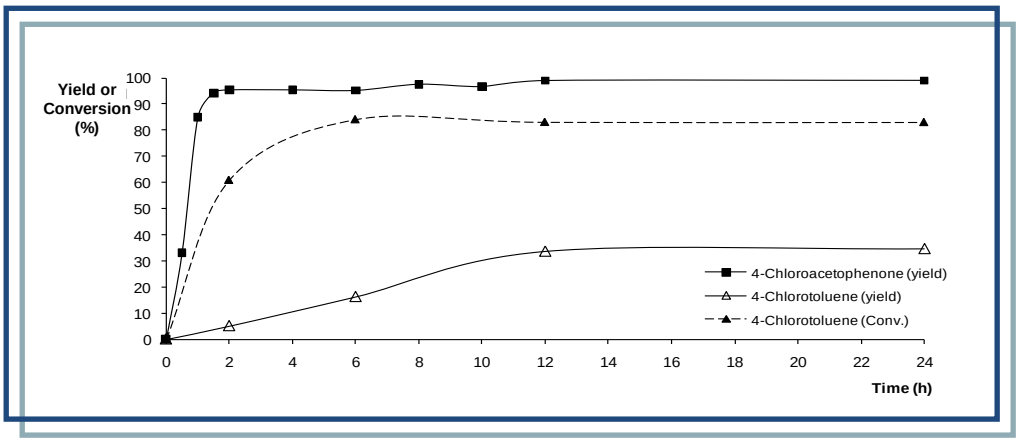


**Figure 2.5** Time-course for the Suzuki-Miyaura reaction of 4-chloroacetophenone and 4-chlorotoluene with phenylboronic acid using catalyst **1A** (1 mol%) in $H_2O$/*i*PrOH. Solid lines refer to yields. The dotted line is referred to conversion.

It is interesting to see that the complex containing the mono-NHC ligand, **1A**, showed higher catalytic activity than the *pincer* complex **3C**. When the first NHC-based-*pincer*-palladium complexes were reported,[37-38] one of their main achievements was precisely their capability to activate C-Cl bonds compared to other known Pd-NHC compounds, but this only happened at very high temperatures using high-temperature-boiling solvents, such as DMSO or DMF. For homogeneously catalysed reactions in water, we have a temperature limitation, so we believe that we may not be able to take advantage of the extraordinary high stability of *pincer*-type complexes **3C** and **4C**, by using them in reactions carried out at higher temperatures.

The most relevant results obtained so far for the Suzuki-Miyaura cross-coupling reactions in water were achieved by Karimi *et al*. just few months after our results were reported. At very low catalyst loadings, the "centipede-like" Pd catalyst **2.4** (Scheme 2.9), yielded 91-93% product when tolylboronic acid was reacted with 4-bromobenzaldehyde or 4-chlorobenzaldehyde in water, at room temperature after 24h. Remarkably, this "centipede-like" Pd catalyst was recycled 17 times without any observable loss in activity.[55] These results are notable, especially if we take into account that the effect of the temperature in the Suzuki-Miyaura reactions had previously been studied by Çetinkaya, observing that temperatures beyond 100ºC showed the generation of major amounts of the homocoupling products.

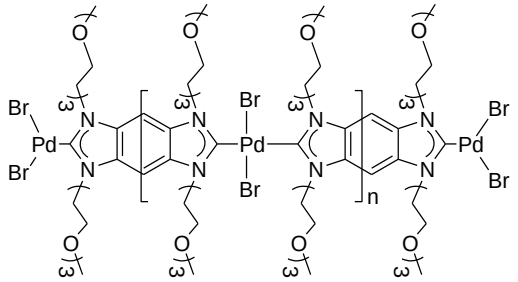

**2.4**

**Scheme 2.9** Triethylene glycol legged "centipede-like" Pd catalyst

## 2.2.4 Conclusions

In this section we prepared four new palladium complexes with NHC ligands decorated with sulfonate functionalities. The presence of the sulfonate fragment allows the solubility of these new palladium complexes in water, which in turn are insoluble in most organic solvents. Compounds **1A-4C** have been characterised by usual spectroscopic techniques.

All four palladium complexes were tested in the Suzuki-Miyaura coupling of a series of bromo- and chloroarenes with phenylboronic acid in water, showing that complex **1A**, containing two mutually *cis* NHC-sulfonate ligands, performs the best catalytic activity. The activity shown by complex **1A** is excellent and compares well with the best catalysts used in neat water reported by the time that this work was done.[24, 26] However, the efficiency of **1A** is lower than the best systems reported in the literature for non-aqueous Suzuki-Miyaura coupling reactions.[56] It is also important to point out that some heterogeneous catalytic contribution should be considered in all these processes, as can be deduced from the higher catalytic activities shown by upon decreasing the catalytic concentration, which suggests a zero order reaction rate on the catalyst. Although some further studies should be carried out in order to clarify this point (some further kinetic studies, or the mercury-drop test), these were not considered at the time that this research was developed.

## 2.3 *BORROWING-HYDROGEN* PROCESSES

### 2.3.1 Introduction

The reactions governed by the so-called *Borrowing-Hydrogen* mechanism are considered to fit the grounds of *Green Chemistry*, since they accomplish the principle of high atom-economy, where normally all the atoms from the substrates are incorporated in the products or in non-toxic by-products such as $H_2O$ or $NH_3$.[57] The search for efficient catalysts for *Borrowing-Hydrogen* reactions is an interesting issue, mainly because this type of reactions provides access to a wide variety of highly valuable organic molecules under environmental-friendly procedures. In 2011, Crabtree accentuated the important role of organometallic chemists in the development of green processes, highlighting the *Borrowing-Hydrogen*-governed activation of alcohols.[58]

In a *Borrowing-Hydrogen* process, a substrate (normally an alcohol) can be alkylated without the need of alkylating agents. Instead of activating the alcohol by conversion into an halide, the alcohol is dehydrogenated by means of an organometallic catalyst. The two hydrogens released are ‘taken’ by the organometallic catalyst, forming a dihydride species. The dehydrogenation of the alcohol gives the corresponding carbonyl compound (aldehyde or ketone) that can then undergo *in situ* transformations and form a wide range of products. As depicted in Scheme 2.10, this carbonyl compound can condensate with an amine, an alkane or an alcohol, to generate an imine, an alkene or a ketone, respectively. Finally, the metal-dihydride "gives" the two hydrogen atoms to the generated unsaturated compound, leading to the formation of amines **a**, alkanes **b** or functionalised alcohols **c**. In all cases there is, ideally, no net hydrogen loss or gain during the reaction sequence.

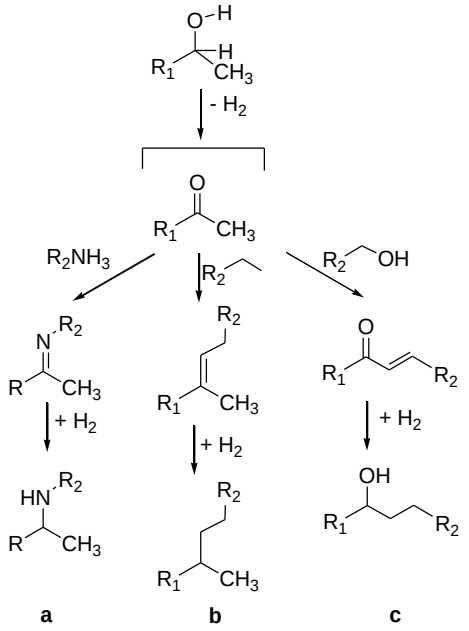


**Scheme 2.10** General schemes for *Borrowing-Hydrogen* processes involving an alcohol

The overall redox-neutral reaction is catalysed *via* a series of steps involving both oxidation and reduction. This route avoids both the toxicity issues associated with alkyl halides and waste formation in the form of a halide salt derived from the base, which is needed in the traditional synthesis.

The most active catalysts in *Borrowing-Hydrogen* processes refer to Ru(II)[59-64] and Ir(III)-based[63, 65-68] complexes. Specifically, Shvo's catalyst (Scheme 2.11) has exceptional features that make it one of the most effective catalysts for all kinds of transfer hydrogenations from alcohols to alkenes, alkynes, carbonyl groups and imines.[69-70] The mechanism of hydrogenation and dehydrogenation reactions catalysed by Shvo's catalyst is unique among transition-metal catalysts, as it involves simultaneous transfer of separate hydrogen atoms from (or to) the metal centre and the ligand. Thus, Shvo's catalyst is an example of a ligand-metal bifunctional catalyst where the redox activity is distributed between the metal centre and a cyclopentadienone ligand. The ubiquitous Shvo's catalyst, $[Ph_4(\eta^5\text{-}C_4CO)]_2H]Ru_2(CO)_4(\mu\text{-}H)$, is a dimeric precatalyst that forms monomeric oxidizing (**I**) and reducing (**II**) species upon dissociation in solution. The concentrations of these active forms are governed by equilibrium effects; species **I** and **II** can be inter-

converted through the gain or loss of "$H_2$" from hydrogen donors ($AH_2$) and acceptors (A), as shown in Scheme 2.11.

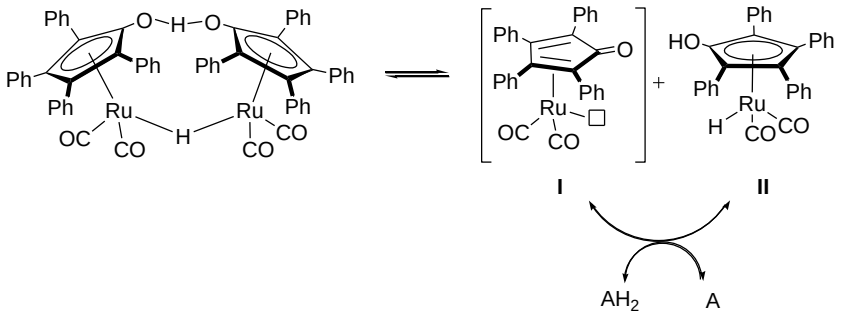


**Scheme 2.11** Shvo's catalyst. **I** and **II** interconvert in the presence of a hydrogen acceptor (A) or donor species ($AH_2$)

As will be discussed later, we have centred our interest in two catalytic reactions governed by a *Borrowing-Hydrogen* mechanism. The reactions studied imply the dehydrogenative activation of alcohols. Our initial aim was to study these reactions under the "greenest" possible conditions, thus using non-toxic solvents under the highest atom-economic conditions and minimum waste of energy.

During the last decade, our research group has been interested in the synthesis of new NHC ligand precursors for the design of improved homogeneous catalysts.[71-74] Specifically, a large amount of catalysts for efficient C-H bond activation processes were described. Among the reactions governed by *Borrowing-Hydrogen* processes, *β*-alkylation of secondary alcohols with primary alcohols was one of the most studied reactions in our group, and remarkable results using 'Ru($\eta^6$-arene)(NHC)[75] and 'IrCp*(NHC)'[76] complexes were obtained. In particular, catalysts **2.5**[76] and **2.6**[75] showed outcomes that lie among the best for this kind of transformation (Scheme 2.12).

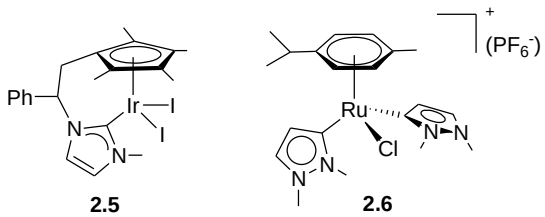


**Scheme 2.12** Highly efficient catalysts **2.5** and **2.6** for *β*-alkylation of secondary alcohols

In some systems, the presence of cooperating ligands is known to improve the catalytic efficiency *via* a metal-ligand bifunctional catalysis.[77-80] An elegant review by Crabtree focused on selected examples of ligands carrying a functional group that can change the properties of the ligand as a result of an external stimulus, or undergo catalytically-relevant ligand-based reactivity.[81]

Probably the most prominent example of bifunctional catalysis was reported by Noyori in 1995. Noyori demonstrated that the presence of a 'NH group' in the ligand can enhance the catalytic activity of the metal complexes, by the so-called 'NH effect', for the hydrogenation of ketones.[80, 82] Another interesting example was described by Fujita and Yamaguchi, who smartly reported the acceptorless oxidation of alcohols by 'IrCp*' complexes, using 2-hydroxopyridine as ligand (Scheme 2.13, **2.7**).[83] From their experimental results, the authors concluded that the efficiency of their catalyst in the oxidation of alcohols relied on a ligand-promoted dehydrogenation procedure, in which the dehydrogenation of the hydroxo group at the coordinated pyridine played a crucial role.

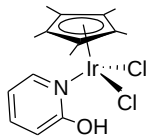


**2.7**

**Scheme 2.13** 'IrCp*' complex **2.7**

### 2.3.1.1 *β*-Alkylation of secondary alcohols with primary alcohols

The *β*-alkylation of secondary alcohols with primary alcohols consists of the alkylation of a secondary alcohol in the *beta* position using a primary alcohol as alkylating agent (Scheme 2.14). Most of the efforts dealing with the design of effective catalysts for this process concern the preparation of highly active catalysts that selectively afford the formation of the *β*-alkylated alcohols, with minimum production of the related ketones, which are often obtained as undesired side-products of the reaction.

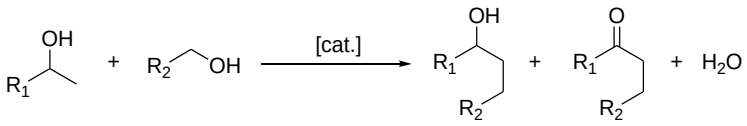


**Scheme 2.14** *β*-Alkylation of secondary alcohols with primary alcohols

The most widely accepted mechanism for this reaction is the one shown in Scheme 2.15.[84] In the first step of the process, both alcohols (primary and secondary) are oxidised to form an aldehyde (**i**) and a ketone (**ii**) together with the metal-dihydride [M]-$(H)_2$. Subsequently, the base catalyzes an aldol condensation between the aldehyde and the ketone to form an *α,β*-unsaturated ketone (**iii**). Finally, the dihydride [M]-$(H)_2$ reduces the C=C and C=O double bonds of the *α,β*-unsaturated ketone (**iii**) by donation of its two hydrogens, with subsequent formation of the final *β*-alkylated alcohol (**iv**).

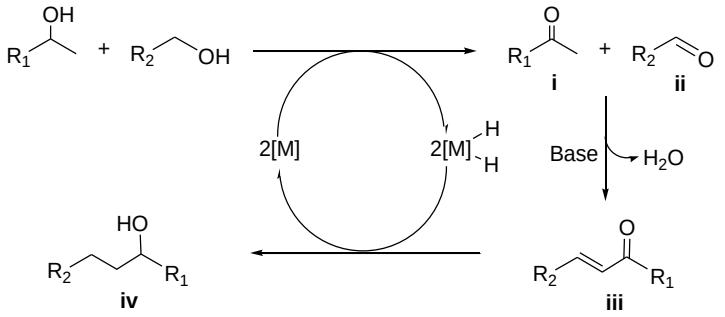


**Scheme 2.15** Mechanism of *β*-alkylation of secondary alcohols with primary alcohols

### 2.3.1.2 Alkylation of ammonia with primary alcohols

The inexpensive chemical ammonia is one of the most desirable substrates for the formation of nitrogen-containing organic molecules, despite its lack of reactivity in most catalytic reactions.[85]

A particular important class of nitrogen-containing molecules, amines, are produced in a 100,000 t/y worldwide scale, being of significant importance for bulk chemistry and also high-value intermediates in organic synthesis.[86] Other important applications of amines include their use in pharmaceutical industry, and the manufacture of solvents, plastics, surfactants, textiles, cosmetics, toiletries, hydrazines, dyes and agrochemicals.[87]

Traditionally, amines are synthesised by alkylation of ammonia or amines with conventional alkylating agents, such as alkyl halides. However, over-alkylations commonly lead to mixtures of primary, secondary, tertiary amines as well as quaternary ammonium salts (Scheme 2.16).[88] This over-alkylation makes the purification process tedious, expensive and far from being a green process due to the toxicity issues associated with alkyl halides and waste formation.

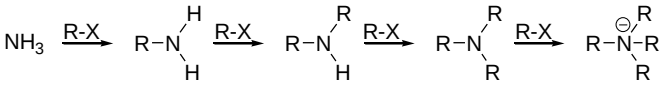


**Scheme 2.16** Over-alkylation of amines

Compared to the well-known classical N-alkylation of amines with alkyl halides, an atom economically and environmentally attractive method is the alkylation of amines with primary alcohols, which is governed by a *Borrowing-Hydrogen*[89] process. Scheme 2.17 shows the proposed general mechanism for this reaction.[67,90] The first step of the mechanism implies the *in situ* dehydrogenation of the primary alcohol to the corresponding aldehyde (**i**), generating a metal-dihydride [M]-$(H)_2$. Then, a nucleophilic attack of the amine to the carbonyl intermediate (**i**) takes place, forming the imine (**ii**) and releasing $H_2O$. Finally, the dihydride [M]-$(H)_2$ reduces the imine by donation of its two hydrogen atoms, achieving the corresponding alkylated amine (**iii**).

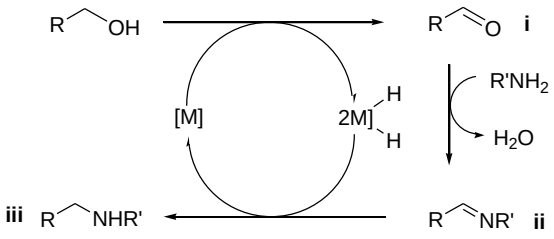


**Scheme 2.17** Alkylation of amines with primary alcohols

This is an attractive and promising alternative to traditional alkylating procedures due to several reasons: *a)* it is a safe and non-toxic procedure, *b)* water is generated as the only by-product, *c)* alcohols are inexpensive and more readily available than the corresponding toxic alkyl halides, and *d)* the selectivity of the reaction can be controlled by the catalyst. Moreover, this reaction also has the advantage of favouring the selective production of secondary amines, because a primary amine can more

easily react with the aldehyde. In contrast, traditional alkylation tends to give over-alkylation because the secondary amine is more reactive than the primary with the alkyl halide.

Considering the increasing attention given to *Green Chemistry* as well as to economic reasons, the use of ammonia as an alternative route to amines has gained attention in the scientific community. All the transformations using ammonia as substrate to produce nitrogen-containing molecules, have been extensively reviewed.[85, 91-92] In the case of the alkylation of ammonia with alcohols, many alkylamines are prepared on large scale by the reaction of an alcohol with ammonia, normally using heterogeneous catalysts under extreme conditions, such as high pressures and temperatures.[87,91] The use of homogeneous catalysts for this reaction is an interesting alternative, which should allow a more selective coupling of alcohols with ammonia under milder conditions.

The first alkylation of ammonia with alcohols catalysed by a homogeneous catalyst was reported by Fujita and co-workers in 2007.[93] The article showed that $[IrCp^*Cl_2]_2$ catalyzes the multiple alkylation of ammonium acetate with benzylic and aliphatic alcohols forming tertiary amines. Later, Milstein and Gunanathan achieved the alkylation of pressurised ammonia with alcohols using a ruthenium complex with a PNP *pincer* ligand (**2.8**, in Scheme 2.18).[94] In this case, the primary amines were obtained with high selectivity and good yields.

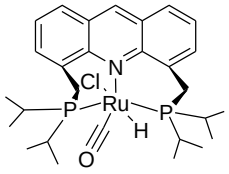


**2.8**

**Scheme 2.18** Ru-catalyst **2.8**

Shortly thereafter, Mizuno and co-workers reported that nitriles could also be obtained by a ruthenium catalysed reaction between alcohols and ammonia.[95] Beller[96-97] and Vogt[98] independently reported preparative procedures for the formation of primary amines by means of ruthenium-catalysed amination of secondary alcohols with ammonia. Although the efficiency and selectivity of these reactions were

excellent, the requirement of ammonia in the gaseous or liquid state limits the synthetic utility of these approaches.

Recently, exceptional results in *Borrowing-Hydrogen* processes have been achieved. For instance, *β*-alkylation of secondary alcohols with primary alcohols using copper[103] and iron[104] complexes as catalysts, have been reported. An efficient and green aldehyde-catalysed transition metal-free dehydrative C-alkylation method for preparation of useful long chain alcohols, using primary alcohols and methyl carbinols as substrates, has also been described.[105] Additionally, extraordinary outcomes for the N-alkylation of amines with alcohols by using *Borrowing-Hydrogen* methodology have recently been reported by Martín-Matute, based on an iridium complex with an alcohol/alkoxide-tethered NHC, which is able to catalyze the reaction at temperatures as low as 50ºC.[106] The most spectacular result achieved in this topic corresponds to the enantioselective amination of alcohols using a chiral Ir complex in cooperation with a chiral phosphoric acid, reported by Zhao and co-workers.[107]

Bearing in mind all these previous results, we focused our attention on the development of new challenging *Borrowing-Hydrogen* processes, using 'IrCp*' complexes as catalysts, with ligands that could participate in the catalytic cycle. As previously mentioned, our group has experience in *β*-alkylation of secondary alcohols with primary alcohols, hence we decided to start our studies by testing the efficiency of our catalysts in this reaction, to further extend our studies to a more challenging *Borrowing-Hydrogen* process, such as the alkylation of ammonia with primary alcohols.

In the next section, we will present firstly the synthesis of our new 'IrCp*' complexes with non-spectator ligands, followed by the catalytic results obtained in the *β*-alkylation of secondary alcohols with primary alcohols, and in the alkylation of ammonia with primary alcohols. The catalytic activity of our new 'IrCp*' compounds will be compared with that of $[IrCp^*Cl_2]_2$ and Shvo's catalyst.

### 2.3.2 Synthesis and characterization of Ir(III) complexes

As mentioned above, the presence of cooperating ligands in homogeneous catalysts can improve the catalytic efficiency through a metal-ligand bifunctional catalysis. In

this context, and taking into account that our aim is to improve catalysis based on *Borrowing-Hydrogen* processes, we decided to synthesise 'IrCp*' compounds bearing a formamidine ligand.

Formamidine ligands can act as two-electron donor ligands, *via* the more basic and less sterically crowded imino lone pair, by forming simple adducts where the formamidine is acting as a monodentate ligand (Scheme 2.19, **I**).[99] Deprotonation of the NH group with a strong base, may lead to the formation of a formamidinate, which can coordinate to the metal centre in a chelating form (Scheme 2.19, **II**). We believe that this conversion, between monodentate and chelating coordination, may have some implications on the catalytic activity of transition metal complexes bearing this type of ligands.

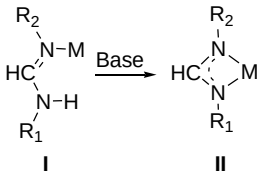


**I** **II**

**Scheme 2.19** Monodentate (**I**) and chelating (**II**) coordination of a formamidine

Moreover, the formamidine ligand possesses the structural properties to provide to our complexes a great efficiency in catalyst, because the NH group might participate in the catalytic cycle by a similar procedure to the so-called 'NH effect'.[80, 82] Thereby, the formamidine ligand can produce a metal-ligand bifunctional catalysis.

In this section, we will describe the synthesis of the formamidine ligand **D** and its coordination to iridium, achieving the two different coordination modes described above (Scheme 2.19), depending on the synthetic conditions.

### 2.3.2.1 Synthesis of the formamidine ligand

Aiming to prepare new 'IrCp*' catalysts supported by a formamidine ligand, we decided to synthesise a formamidine bearing mesityl groups (2,4,6-trimethylphenyl). It is known that mesityl-functionalised ligands, such as mesityl-based NHC, can enhance both the stability and activity of the metal centre, leading in some cases to the activation of the methyl groups of the mestyl ring.[100]

The formamidine ligand, 1,3-bis(2,4,6-trimethylphenyl)formamidine, **D**, was prepared according to the procedure described in the literature by Grubbs.[101] A

mixture of commercially available 2,4,6-trimethylaniline, triethyl orthoformate and a small amount of acetic acid was stirred at 140ºC overnight, providing **D** in 95% yield (Scheme 2.20). As mentioned above, the details about the characterization of **D** will be omitted, since it has previously been described.[101]

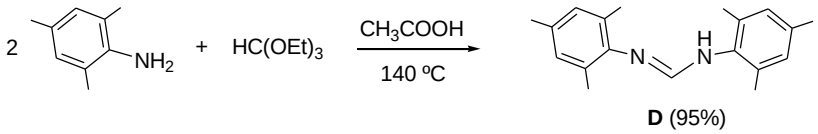


**D** (95%)

**Scheme 2.20** Synthesis of 1,3-bis(2,4,6-trimethylphenyl)formamidine, **D**

### 2.3.2.2 Synthesis and characterization of [IrCp*Cl$_2$(formamidine)], 5D, and [IrCp*Cl(formamidinate)], 6D

Once 1,3-bis(2,4,6-trimethylphenyl)formamidine, **D**, was synthesised, two different 'IrCp*' complexes were obtained, depending on whether the coordination mode adopted by the ligand **D** is monodentate (formamidine, **5D**) or chelate (formamidinate, **6D**), see Scheme 2.19. These two new complexes were prepared during the development of the present work.

*a) Synthesis and characterization of [IrCp*Cl$_2$(formamidine)], **5D***

As depicted in Scheme 2.21, the formamidine-Ir(III) complex **5D** was obtained by direct reaction of 1,3-bis(2,4,6-trimethylphenyl)formamidine, **D**, with [IrCp*Cl$_2$]$_2$ in a 2:1 molar ratio. The reaction mixture was stirred at room temperature under nitrogen atmosphere in dry $CH_2Cl_2$ for 2h. Then the solvent was evaporated under vacuum and the crude product was washed with hexane, collected by vacuum filtration and dried under vacuum, providing compound **5D** as a crystalline orange air stable solid, in 90% yield. Compound **5D** was characterised by means of NMR and mass spectrometry and gave satisfactory elemental analysis. Suitable crystals for X-Ray Diffraction studies were obtained by slow diffusion of hexane into a concentrated solution of compound **5D** in $CHCl_3$.


**D** **5D** (90%)

**Scheme 2.21** Synthesis of complex **5D**

Complex **5D**, constitutes one of the very few examples of this kind of formamidine-based compounds described in literature,[99] and to the best of our knowledge, the only iridium complex with this type of coordination mode reported in the literature thus far.

*$^{1}$H NMR spectrum of **5D***

Figure 2.6 shows the $^{1}$H NMR spectrum of **5D**. As a diagnostic of the monodentate coordination of **D**, the $^{1}$H NMR spectrum of **5D** shows two doublets ($^{3}J_{HH}$ = 13 Hz) due to the coupling between the protons (a) and (d) in the spectrum. The signals assigned to the proton of the C*H* group of the mesityl fragments appear as two singlets, at 7.01 and 6.78 ppm (c and b), and the signals attributed to the protons of the C$H_3$ groups of the mesityl fragments appear as singlets at 2.35, 2.32, 2.20 and 2.17 ppm (e, f, g and h). Finally, the resonances due to the protons of the C$H_3$ groups of the Cp* ring appear as a singlet at 1.3 ppm (i).

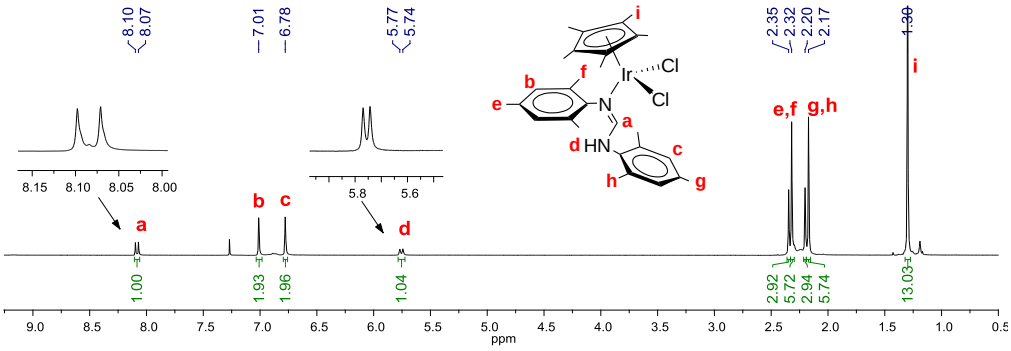


**Figure 2.6** $^{1}$H NMR spectrum of **5D** in $CDCl_3$

*$^{13}C\{^{1}H\}$ NMR spectrum of **5D***

Figure 2.7 shows the $^{13}C\{^{1}H\}$ NMR spectrum of compound **5D**. The signal due to the carbon of the *C*H group of the imine appears at 160.8 ppm (1). The signals corresponding to the six different quaternary carbons of the mesityl fragments are seen at 140.4, 136.8, 136.4, 133.9, 133.2 and 132.7 ppm. The two different carbons of the *C*H groups of the mesityl fragments display their signals at 129.6 and 129.4 ppm (2). The signals corresponding to the carbon of the $CH_3$ groups of the mesityl fragments appear at 21.0, 20.9, 19.1 and 17.8 ppm (4 and 5). Finally, the resonances due to the carbon of the $CH_3$ groups of the Cp* ring are observed at 85.6 and at 8.6 ppm.

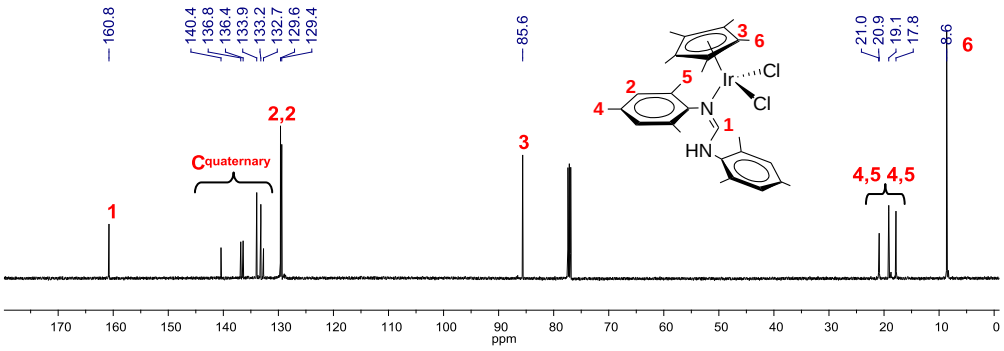


**Figure 2.7** $^{13}C\{^{1}H\}$ NMR spectrum of **5D** in $CDCl_3$

*Molecular structure of **5D***

Crystals of **5D** suitable for X-Ray Diffraction analysis were obtained by slow diffusion of hexane into a concentrated solution of **5D** in $CHCl_3$. Figure 2.8 shows the molecular diagram for complex **5D**. Table 2.4 summarises the most representative bond lenghts and angles of complex **5D**.

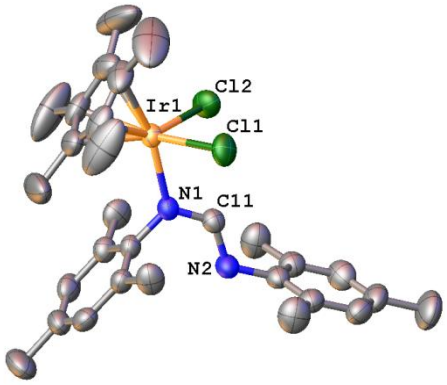


**Figure 2.8** Molecular diagram of complex **5D**. Ellipsoids are at the 50% probability level. Hydrogen atoms are omitted for clarity.

**Table 2.4** Selected bond lenghts and angles of complex **5D**

| **Bonds lenghts (Å)** | | **Bond Angles (º)** | |
|---|---|---|---|
| Ir(1)-N(1) | 2.126(3) | Cl(1)-Ir(1)-Cl(2) | 89.47(4) |
| Ir(1)-Cl(1) | 2.4199(10) | N(1)-Ir(1)-Cl(1) | 84.73(8) |
| Ir(1)-Cl(2) | 2.4113(10) | N(2)-Ir(1)-Cl(2) | 85.22(8) |
| N(1)-C(11) | 1.290(4) | | |
| N(2)-C(11) | 1.334 (5) | | |

The molecular diagram of complex **5D** confirms the coordination of the formamidine ligand **D** in a monodentate manner. Compound **5D** consists of an Ir(III) centre in a pseudo-three-legged-piano-stool environment, with one Cp*, two chlorides and one amidine ligands completing the coordination sphere about the Ir centre. The Ir-N bond distance is 2.126Å, and the mesityl group bound to N(1) is pointing out of the metal coordination sphere, in a quasi-parallel orientation with respect to the Cp* plane.

*b) Synthesis and characterization of [IrCp*Cl$_2$(formamidinate)], **6D***

The formamidinate-Ir(III) complex **6D** (Scheme 2.22), was obtained following the procedure described on the literature for the coordination of amidines in a chelating form.[99] 1,3-Bis(2,4,6-trimethylphenyl)formamidine, **D**, was dissolved under nitrogen atmosphere in dry THF and cooled to 0ºC, and then *n*BuLi was added. The resulting reaction mixture was stirred for 10 minutes at 0º C and transferred *via* cannula into a Schlenk flask containing [IrCp*Cl$_2$]$_2$ in dry THF. The resulting solution was stirred

for 10 minutes at 0º C, and then 2h at room temperature. After that time, the solvent was evaporated under vacuum and the crude product was extracted with benzene, washed with hexane, collected by vacuum filtration and dried under vacuum, providing compound **6D** as an air-stable yellow solid, in 70% yield. Compound **6D** was characterised by means of NMR and mass spectrometry, and gave satisfactory elemental analysis. Crystals suitable for X-Ray Diffraction studies were obtained by slow diffusion of hexane into a concentrated solution of compound **6D** in benzene.

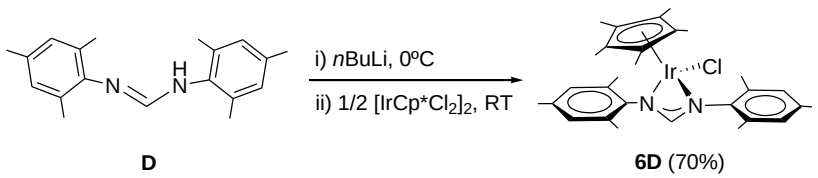


**D** **6D** (70%)

**Scheme 2.22** Synthesis of complex **6D**

*$^1$H NMR spectrum of **6D***

Figure 2.9 shows the $^1$H NMR spectrum of compound **6D**. The spectrum confirms the absence of the signal due to the NH group of the imine, thus providing the first evidence that the coordination of the amidinate ligand has taken place in a chelating form. The signal corresponding to the acidic proton of the C*H* group of the imine appears at 9.15 ppm as a singlet (a). The only resonance due to the proton of the C*H* groups of the mesityl fragments appears at 6.83 ppm as a singlet (b), suggesting that the complex has a "mirror plane", and therefore a twofold symmetry. Only two different singlets at 2.57 (c) and 2.17 (d) ppm, are observed due to the protons of the six C$H_3$ groups of the mesityl fragments, as a consequence of the symmetry of the complex. Finally, the resonances due to the protons of the C$H_3$ groups f the Cp* ring appear as a singlet at 1.21 ppm (e).

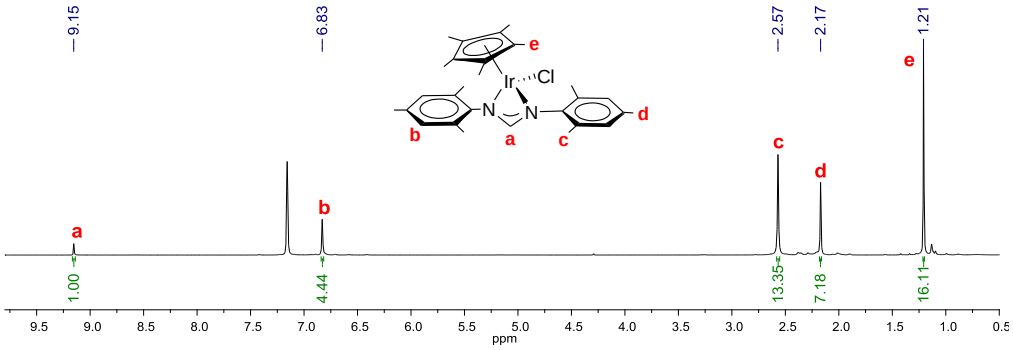


**Figure 2.9** $^{1}$H NMR spectrum of **6D** in $C_6D_6$

*$^{13}C\{^{1}H\}$ NMR spectrum of **6D***

Figure 2.10 shows the $^{13}C\{^{1}H\}$ NMR spectrum of **6D**. The signal due to the carbon of the *C*H group of the imine appears at 167.6 ppm (1). The signals corresponding to the three different quaternary carbons are seen at 140.4, 134.2, 133.1 ppm. The resonance due to the carbon of the four *C*H groups of the two mesityl fragments (two *C*H each mesityl fragment) appear as a singlet at 129.6 ppm (2), confirming the high symmetry of the compound. The signals corresponding to the carbon of the $CH_3$ groups of the mesityl fragments appear at 21.8 and 20.7 ppm (4 and 5). Finally, the resonances due to the carbon of the $CH_3$ groups of the Cp* ring were observed at 83.2 (3) and 9.0 ppm (6).

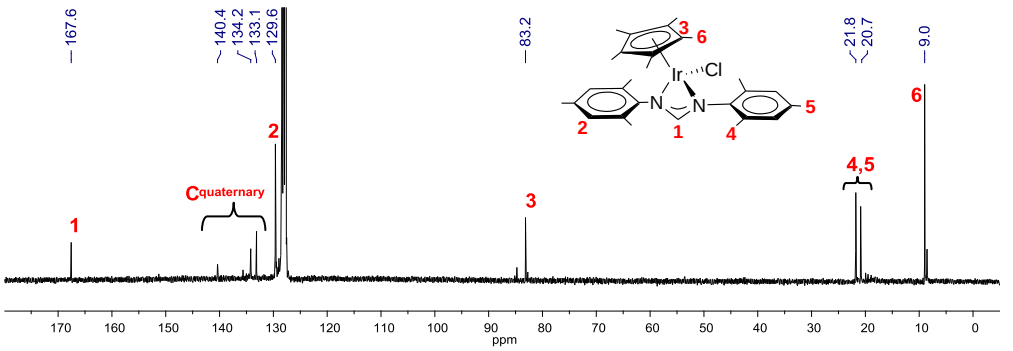


**Figure 2.10** $^{13}C\{^{1}H\}$ NMR spectrum of **6D** in $C_6D_6$

*Molecular structure of **6D***

Crystals of **6D** suitable for X-Ray Diffraction analysis were obtained by slow diffusion of hexane into a concentrated solution of **6D** in benzene. Figure 2.11 shows

the molecular diagram of complex **6D**. Table 2.5 presents the most representative bond lenghts and angles for complex **6D**.

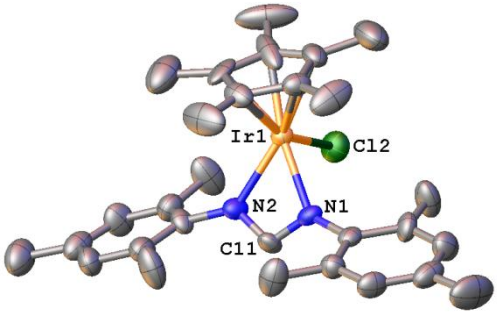


**Figure 2.11** Molecular diagram of complex **6D**. Ellipsoids are at the 50% probability level. Hydrogen atoms are omitted for clarity.

The molecular structure of this complex confirms the chelating coordination of the formamidinate ligand. One Cp* and one chloride complete the coordination sphere about the Ir(III) centre. The two Ir-N distances are virtually identical (2.140 and 2.149 Å), and the same happens with the two N-C bonds (1.292 and 1.332 Å), therefore affording a highly symmetric chelating coordination form. The N(1)-Ir(1)-N(2) chelate bite-angle is 60.4º.

**Table 2.5** Selected bond lenghts and angles of complex **6D**

| Bonds lenghts (Å) | | Bond Angles (º) | |
|---|---|---|---|
| Ir(1)-N(1) | 2.140(7) | N(1)-Ir(1)-Cl(2) | 89.6(2) |
| Ir(1)-N(2) | 2.149(8) | N(2)-Ir(1)-Cl(2) | 89.0(2) |
| Ir(1)-Cl(2) | 2.391(2) | N(1)-Ir(1)-N(2) | 60.4(3) |
| Ir(1)-Cl(2) | 2.391(2) | | |
| N(1)-C(11) | 1.292(11) | | |
| N(2)-C(11) | 1.332(11) | | |

### 2.3.3 Catalytic activity of complexes 5D and 6D

In the following section, the catalytic results achieved with the iridium complexes described above will be described. It is advisable to use the table containing the different complexes attached to this manuscript in order to facilitate the reading of this section.

Once the formamidine and the formamidinate-based iridium compounds **5D** and **6D** were synthesised and characterised, we decided to study their catalytic applications in the *β*-alkylation of secondary alcohols with primary alcohols. Then, we extended the studies on the catalytic activities of our complexes to a more challenging and much less studied reaction, such as the *alkylation of ammonia with primary alcohols*. The difference between the two coordination modes of **5D** and **6D** may have some implications on the catalytic activity. In principle, we expected that the NH group of the formamidine in **5D**, may enhance the catalytic activity of **5D** by means of a cooperative 'NH effect' or a metal-ligand bifunctional catalysis.

### 2.3.3.1 *β*-Alkylation of secondary alcohols with primary alcohols

We permormed the *β*-alkylation of 1-phenylethanol with primary alcohols in toluene at 100ºC, under aerobic conditions, using catalyst loadings of 1 or 0.1 mol% and KOH (100 mol%) (Table 2.6). Four different primary alcohols were used (benzyl alcohol, 1-butanol, 3-chlorobenzyl alcohol and 4-chlorobenzyl alcohol). The catalytic assays were monitored by $^{1}$H NMR using anisole as internal standard, in order to assess that there was no loss of substrates or products during the reaction. The advance of the reaction was monitored by comparing a reference signal of the $^{1}$H NMR spectrum of the starting material with reference signals due to the products. As an illustrative example, Scheme 2.23 shows the reference signals chosen in order to determine the advance of the reaction between 1-phenylethanol and benzyl alcohol. As the reaction progresses, the signals due to the proton of the -CH group of 1-phenylethanol (1H, q, 4.90 ppm) and to the protons of the -C$H_2$OH group of benzyl alcohol (2H, t, 4.71 ppm) decrease, while new signals corresponding to the products increase. The reference signals for the new products were those due to the proton of the -CH group of the generated *β*-alkylated alcohol (1H, t, 4.60 ppm) and to the protons of the -C$H_2$CO group of the generated ketone (2H, t, 3.31 ppm).

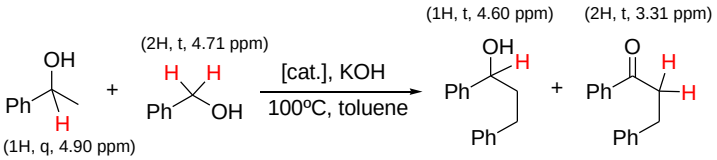


**Scheme 2.23** Reference signals used to evaluate the evolution of the reaction between 1-phenylethanol and benzyl alcohol

Table 2.6 shows the results obtained in the *β*-alkylation of 1-phenylethanol using compounds **5D** and **6D** as catalysts.

**Table 2.6** *β*-Alkylation of 1-phenylethanol with primary alcohols[a]

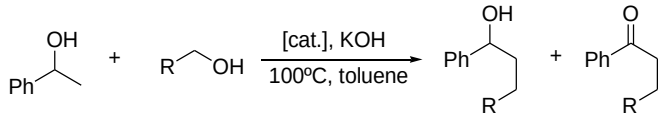


| Entry | Cat. loadings (mol %) | R | t(h) | Alcohol (%)[b] | Ketone (%)[b] |
|---|---|---|---|---|---|
| 1 | **5D** (1) | Ph | 3 | 90 | 9 |
| 2 | **6D** (1) | | 3 | 72 | 23 |
| 3[c] | **5D** (1) | | 8 | 75 | 0 |
| 4 | **5D** (0.1) | | 24 | 65 | 0 |
| 5 | **5D** (1) | *n*Pr | 6 | 62 | 25 |
| 6 | **6D** (1) | | 6 | 61 | 15 |
| 7[c] | **5D** (1) | | 8 | 91 | 8 |
| 8 | **5D** (0.1) | | 24 | 10 | 0 |
| 9 | **5D** (1) | 3-Cl($C_6H_4$) | 6 | 93 | 4 |
| 10 | **6D** (1) | | 6 | 60 | 7 |
| 11[c] | **5D** (1) | | 8 | 40 | 0 |
| 12 | **5D** (0.1) | | 24 | 40 | 0 |
| 13 | **5D** (1) | 4-Cl($C_6H_4$) | 3 | 91 | 8 |
| 14 | **6D** (1) | | 3 | 62 | 7 |
| 15[c] | **5D** (1) | | 3 | 80 | 0 |
| 16 | **5D** (0.1) | | 24 | 80 | 0 |
| 17[d] | **5D** (1) | Ph | 3 | 37 | 0 |

[a] **Reaction conditions**: 1-phenylethanol (1 mmol), primary alcohol (1 mmol), KOH (1 mmol), and 1 (or 0.1) mol % of catalyst in 0.3 mL of toluene at 100ºC, and anisole (1 mmol) as internal standard. [b] Yields determined by $^1$H NMR. [c] Primary alcohol (2 mmol). [d] *In situ* preparation of **5D** by addition of 0.5 mol % of $[IrCp^*Cl_2]_2$ and 1 mol % of **D**.

As can be seen from the data shown in Table 2.6, **5D** is far more efficient than **6D** (compare entries 1-2, 5-6, 9-10, and 13-14), both in terms of conversions to the final products and selectivity toward the corresponding *β*-alkylated alcohols. Catalyst **5D** is also active at catalyst loading of 0.1 mol %, (entries 4, 8, 12 and 16) especially when benzyl alcohol and 4-chlorobenzyl alcohol were used, although longer reaction times

were needed (24h) to achieve moderately high yields. Remarkably, the *in situ* preparation of **5D**, resulted in a much lower activity than that shown by the preformed catalyst (compare entries 1 and 17).

The reactions were performed trying to achieve the maximum atomic efficiency, so we used a molar ratio of 1:1 between the primary and secondary alcohols, and therefore avoided the use of any excess of reagent that inevitably would remain unreacted. In some cases, a 2:1 primary alcohol/1-phenylethanol ratio was used in order to achieve a major selectivity toward the corresponding *β*-alkylated alcohol (entries 3, 7, 11 and 15). Under these reaction conditions, we observed that, even when longer reaction times were used, the catalytic activity decreased and the selectivity was improved, comparing with those results when a 1:1 primary alcohol/1-phenylethanol ratio was used.

An interesting feature about the comparison of the results shown in Table 2.6 is that the different coordination mode of the formamidine ligand in complexes **5D** and **6D** provides different activities in a quite rational way. It seems that the NH group in the formamidine ligand of complex **5D** effectively provides a cooperative 'NH effect', which turns into a neat improvement of the catalytic activity of the complex.

It is worth mentioning that by the time that our work was being carried out, compound **5D** was among the most efficient iridium catalyst for this type of reaction. Our results improve the catalytic outcomes shown by other previously reported catalysts based on 'IrCp*(NHC)', reported by Crabtree[63] and us,[76] and Ru($\eta^6$-arene)(NHC)[102] complexes.

Once we proved that our new iridium compounds were highly active in the *β*-alkylation of secondary alcohols with primary alcohols, we proceeded a step further and tested them in the more challenging alkylation of ammonia with primary alcohols.[108]

### 2.3.3.2 Alkylation of ammonia with primary alcohols

We first carried out a catalyst screening by comparing the activity of $[IrCp^*Cl_2]_2$, Shvo's catalyst (Scheme 2.11) and our new reported compounds **5D** and **6D**. The alkylation of the different ammonium salts with benzyl alcohol was carried out in the absence of solvent, at 110 or 130ºC under nitrogen atmosphere, using different

catalyst loadings, and 3 mol % of $NaHCO_3$ (Table 2.7). We performed the reactions using 3:1 or 3.6:1 molar ratios between the benzyl alcohol and the source for ammonia. All the catalytic assays were monitored by GC, registering yields at fixed times and using anisole as internal standard.

Table 2.7 shows the results obtained using benzyl alcohol and three different sources for ammonia ($NH_4OAc$, $NH_4Cl$, $NH_4OH$), in the presence of $[IrCp^*Cl_2]_2$, **5D** and **6D**, and Shvo's catalyst.

**Table 2.7** Alkylation of ammonia with benzyl alcohol[a]

$$PhCH_2OH + NH_4X \xrightarrow[\Delta]{[cat.]/base} N(CH_2Ph)_3$$

| Entry | Cat. | Cat. loadings (mol%) | X | Base | Alcohol/$NH_4^+$ ratio | T (ºC) | Yield (%)[b] |
|---|---|---|---|---|---|---|---|
| 1 | $[IrCp^*Cl_2]_2$ | 3 | OAc | $NaHCO_3$ | 3 | 110 | 72 |
| 2 | $[IrCp^*Cl]_2$ | 0.5 | OAc | $NaHCO_3$ | 3.6 | 130 | 87 |
| 3 | $[IrCp^*Cl_2]_2$ | 0.5 | OAc | ------ | 3.6 | 130 | 44 |
| 4 | **5D** | 3 | OAc | $NaHCO_3$ | 3 | 110 | 97 |
| 5 | **5D** | 0.5 | OAc | $NaHCO_3$ | 3.6 | 130 | 99 |
| 6 | **5D** | 0.5 | OAc | ------ | 3.6 | 130 | 97 |
| 7 | **6D** | 3 | OAc | $NaHCO_3$ | 3 | 110 | 98 |
| 8 | **6D** | 0.5 | OAc | ------ | 3.6 | 130 | 60 |
| 9 | Shvo's | 3 | OAc | $NaHCO_3$ | 3 | 110 | 97 |
| 10 | Shvo's | 0.5 | OAc | $NaHCO_3$ | 3.6 | 130 | 99 |
| 11 | Shvo's | 0.5 | OAc | ------ | 3.6 | 130 | 99 |
| 12 | **5D** | 3 | Cl | $NaHCO_3$ | 3 | 110 | 51 |
| 13 | **6D** | 3 | Cl | $NaHCO_3$ | 3 | 110 | 18 |
| 14[c] | **5D** | 3 | OH | ------ | 3 | 110 | 44 |
| 15[d] | **5D** | 5 | Cl | KOH | 3.6 | 130 | 99 |
| 16[d] | Shvo's | 5 | Cl | KOH | 3.6 | 130 | 99 |

[a]**Reaction conditions**: benzyl alcohol (3 or 3.6 mmol), source for ammonia (1 mmol), $NaHCO_3$ (3 mol %) and 0.5, 3 or 5 mol % of catalyst at 110 or 130ºC for 17h. [b]Yields determined by GC, using anisole as internal standard.[c]$NH_4OH$, 30% in $H_2O$. [d]t = 39h; 1 mmol of KOH.

As can be seen from the data shown in Table 2.7, both **5D** and Shvo's catalyst displayed excellent catalytic outcomes for the reactions carried out using $NH_4OAc$

and $NaHCO_3$, specially when we compare these data with those provided by $[IrCp^*Cl_2]_2$ and **6D** under the same reaction conditions. As previously reported by Fujita and co-workers,[93] all catalysts provided excellent activities when the alcohol/source for ammonia ratio was increased from 3 to 3.6, even when the catalyst loading was reduced to 0.5 mol %. Both Shvo's catalyst and **5D** were also tested in the alkylation of other ammonium salts such as $NH_4Cl$ and $NH_4OH$, providing very similar activities in these cases. Remarkably, **5D** was moderately active in the alkylation of an aqueous solution of $NH_3$ (entry 14). For the reactions carried out in the absence of an extra amount of base, Shvo's and **5D** afforded excellent yields to the final product (entries 6 and 11) while $[IrCp^*Cl_2]_2$ and **6D** provided moderate-low outcomes (entries 3 and 8, respectively).

Taking all these data into account, we decided to widen the catalytic scope of **5D** and Shvo's catalyst by studying their activity with a variety of primary alcohols. Compound **6D** was also tested in some selected reactions for comparative purposes. The alkylation of ammonia with different primary alcohols was carried out at 130 or 140ºC, under inert conditions, using catalyst loadings of 1, 3 and 5 mol%, and 1 mol% of KOH or without base (Table 2.8). We performed the reactions using 3.6:1 or 6:1 molar ratio of primary alcohols and source for ammonia. All the catalytic assays were monitored by GC, registering yields at fixed times and using anisole as internal standard. Table 2.8 shows the results obtained using six different primary alcohols (4-chlorobenzyl alcohol, 3-chlorobenzyl alcohol, 4-methylbenzyl alcohol, 1-hexanol, 1-butanol and 1-cyclohexanol) and two different sources for ammonia ($NH_4OAc$ and $NH_4Cl$), in the presence of complexes **5D** and **6D**, and Shvo's catalyst.

**Table 2.8** Alkylation of ammonia with primary alcohols[a]

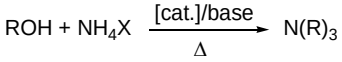


| Entry | Cat. loadings (mol%) | X | R | Base (1mol%) | Time (h) | Yield (%)[b] |
|---|---|---|---|---|---|---|
| 1 | **5D** (1) | OAc | | ---- | 17 | 76 |
| 2 | **6D** (1) | OAc | | ---- | 17 | 73 |
| 3 | Shvo's (1) | OAc | 4-Cl-benzyl | ---- | 17 | 99 |
| 4 | **5D** (5) | Cl | | KOH | 39 | 67 |
| 5 | Shvo's (5) | Cl | | KOH | 39 | 99 |

| | | | | | | |
|---|---|---|---|---|---|---|
| 6 | **5D** (1) | OAc | | ---- | 17 | 45[d] |
| 7 | **6D** (1) | OAc | | ---- | 17 | 20 |
| 8 | Shvo's (1) | OAc | 3-Cl-benzyl | ---- | 17 | 66 |
| 9 | **5D** (5) | Cl | | KOH | 39 | 87 |
| 10 | Shvo's (1) | Cl | | KOH | 39 | 90[d] |
| 11 | **5D** (1) | OAc | | ---- | 17 | 99 |
| 12 | **6D** (1) | OAc | | ---- | 17 | 70 |
| 13 | Shvo's (1) | OAc | 4-Me-benzyl | ---- | 17 | 99 |
| 14 | **5D** (5) | Cl | | KOH | 39 | 99 |
| 15 | Shvo's (5) | Cl | | KOH | 39 | 99 |
| 16 | **5D** (1) | OAc | | ---- | 17 | 51 |
| 17[c] | **5D** (3) | OAc | | ---- | 17 | 90 |
| 18[c] | Shvo's (3) | OAc | *n*-Hexyl | ---- | 17 | 99 |
| 19[c] | **5D** (5) | Cl | | KOH | 39 | 95 |
| 20[c] | Shvo's (5) | Cl | | KOH | 39 | 99 |
| 21 | **5D** (1) | OAc | | ---- | 17 | 15 |
| 22[c] | **5D** (3) | OAc | | ---- | 17 | 37 |
| 23[c] | Shvo's (3) | OAc | *n*-Butyl | ---- | 17 | 93 |
| 24[c] | **5D** (5) | Cl | | KOH | 39 | 26 |
| 25[c] | Shvo's (5) | Cl | | KOH | 39 | 99 |
| 26 | **5D** (1) | OAc | | ---- | 17 | 51[e] |
| 27[c] | **5D** (3) | OAc | | ---- | 17 | 78[e] |
| 28[c] | Shvo's (3) | OAc | Cyclohexyl | ---- | 17 | 99[e] |
| 29[c] | **5D** (5) | Cl | | KOH | 39 | 66[e] |
| 30[c] | Shvo's (5) | Cl | | KOH | 39 | 99[e] |

[a]**Reaction conditions:** alcohol (3.6 mmol), $NH_4X$ (1 mmol), at 130ºC. [b]Yields determined by GC, using anisole as internal standard. [c]6 mmol of alcohol and 1 mmol of $NH_4X$, at 140ºC. [d]Yield as a 1:1 mixture of trisalkylamine and bisalkylamine. [e]Only the bisalkylamine is observed.

As can be seen in Table 2.8, both **5D** and Shvo's catalyst afforded excellent yields for the coupling of several ammonium salts with a wide set of primary alcohols, including benzylic and aliphatic alcohols. Catalyst **6D** is less active than the other two catalysts under study. In general, catalyst **5D** affords excellent yields when benzylic alcohols are used, but its activity is moderate-high when alkylic primary alcohols are

employed. The activity of Shvo's catalyst is higher in most of the cases, thus illustrating the wide applicability of this exceptional catalyst. The reactions are very selective to the formation of the tertiary amines, except those where cyclohexanol is used, which selectively render biscyclohexyl amine (entries 26-30). Catalyst **5D** is more selective than Shvo's catalyst in the production of the tertiary amine when 3-chlorobenzyl alcohol is used (compare entries 9 and 10), since Shvo's catalyst produces the secondary and primary amine in a 1:1 ratio.

According to the results obtained, we believe that the presence of the NH group on the amidine ligand of catalyst **5D** is increasing the catalytic activity compared to that of $[IrCp^*Cl_2]_2$. This 'NH effect' may facilitate the dehydrogenation of the primary alcohol to an aldehyde in the first step of the catalytic cycle,[93] as Noyori's group showed for the reverse reaction implying the hydrogenation of ketones.[80, 82] However, we believe that the NH bond is not deprotonated during the process, because this would imply the formation of the chelating species **6D**, which we have proven that displays a much lower catalytic activity than **5D**, so its participation in the process can be discarded. In fact, the conversion of **5D** into **6D** needs the addition of a very strong base, such as *n*BuLi, so the formation of this species under the reaction conditions is rather unlikely.

Although detailed studies have not been carried out in order to elucidate the mechanism of the dehydrogenation of the primary alcohol to an aldehyde, we have proposed a mechanism that can explain the observed reactivity. To propose this mechanism, we have taken into account our previous proposed mechanism for the dehydrogenation of alcohols performed by 'IrCp*(NHC)' complexes.[109-111]

As can be seen in Scheme 2.24, the first step of the reaction implies an oxidative addition of the primary alcohol to the metallic fragment leading to a cationic Ir(V)-H species, **i**. Subsequently, a *β*-elimination takes places and a new dihydride Ir(V) species, **ii**, is formed along with a molecule of aldehyde. The Ir(V)-dihydride **ii** reductively eliminates a hydrogen molecule. We believe that the amidine ligand may stabilise the Ir(V) transition states **i** and **ii**, through a hydrogen bond between the NH and the oxygen of the alkoxide ligand in **i** and a NH-HIr dihydrogen bond in **ii**. As previously proposed by Fujita and Yamaguchi,[93, 95] once the aldehyde has been formed, its reaction with ammonia would facilitate the formation of the corresponding primary imine, which then is reduced to the corresponding amine by the primary

alcohol, in a metal-mediated transfer hydrogenation process. Subsequent alkylation of the resulting primary amine, affords the final tertiary amine.

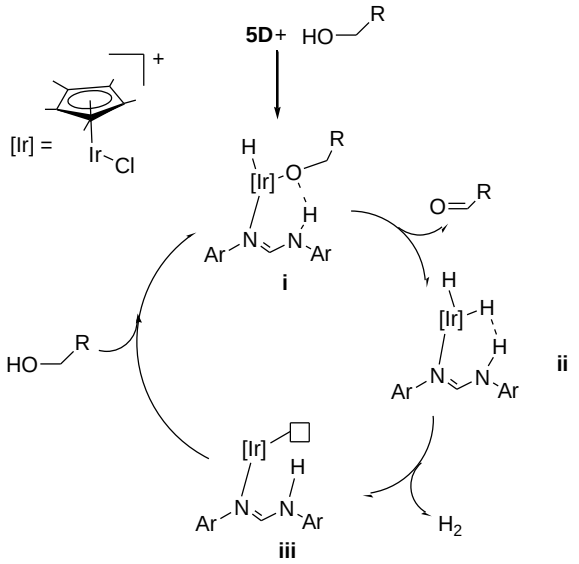


**Scheme 2.24** Dehydrogenation of alcohols catalysed by **5D**

Since the *β*-alkylation of secondary alcohols and the alkylation of ammonia are governed by a *Borrowing-Hydrogen* process, the first step of both reactions is the dehydrogenation of the primary alcohol to give an aldehyde. In order to prove that catalyst **5D** is able to oxidise primary alcohols under hydrogen-acceptorless conditions, we performed a reaction of benzyl alcohol in refluxing toluene in the presence of **5D** (5 mol %) and $Cs_2CO_3$. After 15h, we observed a 70% yield of aldehyde, although the conversion of the alcohol was complete.

## 2.3.4 Conclusions

In this section we have synthetised two new complexes, namely, [IrCp*(formamidine)], **5D**, and [IrCp*(formamidinate)], **6D**, which have been fully characterised by the standard spectroscopyc techniques. These compounds have been tested in two *Borrowing-Hydrogen* processes: *β*-alkylation of secondary alcohols and alkylation of ammonia with primary alcohols. For the latter reaction, the performances of **5D** and **6D** have been compared to those of Shvo's catalyst and $[IrCp^*Cl_2]_2$.

Compounds **5D** and **6D** have shown extraordinary catalytic activity toward the *β*-alkylation of secondary alcohols with primary alcohols comparing with other NHC-based metal complexes traditionally used for this reaction. In all cases, compound **5D** has been more efficient than compound **6D** in terms of activity and selectivity toward the generation of the corresponding *β*-alkylated alcohol.

Compound **5D** and Shvo's catalyst effectively have catalysed the alkylation of ammonia with primary alcohols in the absence of solvent. Interestingly, the alkylation of ammonia with primary alcohols has been highly selective to the generation of tertiary amines. The two catalysts add to the list of the very few metal complexes active in this type of reaction and clearly improve the catalytic outcomes of previously reported systems. Furthemore, we have added a new and extraordinary useful catalytic application of the ubiquitous Shvo's catalyst.

We believe that the high activity of the compound **5D** may be attributed to the presence of the NH group in the amidine ligand and based on that a catalytic cycle for the dehydrogenation of primary alcohols (main step in both catalytic processes studied) has been presented and discussed.

## 2.4 REFERENCES


1. Anastas, P. T.; Warner, J., *Green Chemistry: Theory and Practice*, Oxford University Press, Oxford, **1998**, ISBN 13 978-0-19-850698-0.
2. *Green chemistry*, RSC Publishing.
3. *Green Chemistry Letters and Reviews*, Taylor & Francis.
4. *International Journal of Green Chemistry and Bioprocess*, Universal Research Publications.
5. Lancaster, M., *Green Chemistry An introductory Text*, 3rd ed., RSC Publishing, **2010**, ISBN 978-1-84755-873-2.
6. Matlack, A., *Introduction to Green Chemistry*, 2nd ed., CRC Press, Newark, USA, **2010**, ISBN 9781420078114.
7. Rothenberg, G., Concepts and Green Applications. In *Catalyisis*, Wiley-VCH, **2008**, ISBN 978-3-527-31824-7.
8. Sinou, D., Metal catalysis in water. In *Modern Solvents in Organic Synthesis*, Springer-Verlag Berlin, Berlin, **1999**, ISBN 978-3-540-66213-6.
9. Lamblin, M.; Nassar-Hardy, L.; Hierso, J. C.; Fouquet, E.; Felpin, F. X., *Adv. Synth. Catal.* **2010**, *352*, 33-79.
10. Lindstrom, U. M., *Chem. Rev.* **2002**, *102*, 2751-2771.
11. Herrmann, W. A.; Kohlpaintner, C. W., *Angew. Chem. Int. Ed.* **1993**, *32*, 1524-1544.
12. Shaughnessy, K. H., *Chem. Rev.* **2009**, *109*, 643-710.
13. Schaper, L. A.; Hock, S. J.; Herrmann, W. A.; Kuhn, F. E., *Angew. Chem. Int. Ed.* **2013**, *52*, 270-289.
14. Velazquez, H. D.; Verpoort, F., *Chem. Soc. Rev.* **2012**, *41*, 7032-7060.
15. Diederich, F.; Stang, P. J., *Metal-Catalyzed Cross-Coupling Reactions*, Weinheim, Germany, **1998**.
16. Miyaura, N.; Yamada, K.; Suginome, H.; Suzuki, A., *J. Am. Chem. Soc.* **1985**, *107*, 972-980.
17. Casalnuovo, A. L.; Calabrese, J. C., *J. Am. Chem. Soc.* **1990**, *112*, 4324-4330.

18. Carril, M.; SanMartin, R.; Dominguez, E., *Chem. Soc. Rev.* **2008**, *37*, 639-647.
19. Shaughnessy, K. H., *Eur. J. Org. Chem.* **2006**, 1827-1835.
20. Bai, L.; Wang, J. X., *Curr. Org. Chem.* **2005**, *9*, 535-553.
21. Shaughnessy, K. H.; DeVasher, R. B., *Curr. Org. Chem.* **2005**, *9*, 585-604.
22. Franzen, R.; Xu, Y. J., *Can. J. Chem.-Rev. Can. Chim.* **2005**, *83*, 266-272.
23. Genet, J. P.; Savignac, M., *J. Organomet. Chem.* **1999**, *576*, 305-317.
24. Turkmen, H.; Can, R.; Cetinkaya, B., *Dalton Trans.* **2009**, 7039-7044.
25. Roy, S.; Plenio, H., *Adv. Synth. Catal.* **2010**, *352*, 1014-1022.
26. Gu, S. J.; Xu, H.; Zhang, N.; Chen, W. Z., *Chem.-Asian J.* **2010**, *5*, 1677-1686.
27. Mesnager, J.; Lammel, P.; Jeanneau, E.; Pinel, C., *Appl. Catal. A-Gen.* **2009**, *368*, 22-28.
28. Ohta, H.; Fujiharaa, T.; Tsuji, Y., *Dalton Trans.* **2008**, 379-385.
29. Tu, T.; Feng, X. K.; Wang, Z. X.; Liu, X. Y., *Dalton Trans.* **2010**, *39*, 10598-10600.
30. Yang, C.-C.; lin, P.-S.; Liu, F.-C.; Lin, I. J. B., *Organometallics* **2010**, *29*, 5959-5971.
31. Moore, L. R.; Cooks, S. M.; Anderson, M. S.; Schanz, H. J.; Griffin, S. T.; Rogers, R. D.; Kirk, M. C.; Shaughnessy, K. H., *Organometallics* **2006**, *25*, 5151-5158.
32. Nagai, Y.; Kochi, T.; Nozaki, K., *Organometallics* **2009**, *28*, 6131-6134.
33. Azua, A.; Sanz, S.; Peris, E., *Organometallics* **2010**, *29*, 3661-3664.
34. Wang, Y.; Luo, J.; Liu, Z., *Appl. Organomet. Chem.* **2013**, *27*, 601-605.
35. Schmid, T. E.; Jones, D. C.; Songis, O.; Diebolt, O.; Furst, M. R. L.; Slawin, A. M. Z.; Cazin, C. S. J., *Dalton Trans.* **2013**, *42*, 7345-7353.
36. Kolychev, E. L.; Asachenko, A. F.; Dzhevakov, P. B.; Bush, A. A.; Shuntikov, V. V.; Khrustalev, V. N.; Nechaev, M. S., *Dalton Trans.* **2013**, *42*, 6859-6866.
37. Loch, J. A.; Albrecht, M.; Peris, E.; Mata, J.; Faller, J. W.; Crabtree, R. H., *Organometallics* **2002**, *21*, 700-706.
38. Peris, E.; Loch, J. A.; Mata, J.; Crabtree, R. H., *Chem. Commun.* **2001**, 201-202.

39. Herrmann, W. A.; Elison, M.; Fischer, J.; Kocher, C.; Artus, G. R. J., *Angew. Chem. Int. Ed.* **1995**, *34*, 2371-2374.

40. Virboul, M. A. N.; Lutz, M.; Siegler, M. A.; Spek, A. L.; van Koten, G.; Gebbink, R., *Chem.-Eur. J.* **2009**, *15*, 9981-9986.

41. Diez Barra, E.; De la Hoz, A.; Sanchez Migallon, A.; Tejeda, J., *Heterocycles* **1992**, *34*, 1365-1373.

42. Caballero, A.; Diez-Barra, E.; Jalon, F. A.; Merino, S.; Rodriguez, A. M.; Tejeda, J., *J. Organomet. Chem.* **2001**, *627*, 263-264.

43. Organ, M. G.; Abdel-Hadi, M.; Avola, S.; Hadei, N.; Nasielski, J.; O'Brien, C. J.; Valente, C., *Chem.-Eur. J.* **2007**, *13*, 150-157.

44. Organ, M. G.; Avola, S.; Dubovyk, I.; Hadei, N.; Kantchev, E. A. B.; O'Brien, C. J.; Valente, C., *Chem.-Eur. J.* **2006**, *12*, 4749-4755.

45. O'Brien, C. J.; Kantchev, E. A. B.; Chass, G. A.; Hadei, N.; Hopkinson, A. C.; Organ, M. G.; Setiadi, D. H.; Tang, T. H.; Fang, D. C., *Tetrahedron* **2005**, *61*, 9723-9735.

46. Huynh, H. V.; Ho, J. H. H.; Neo, T. C.; Koh, L. L., *J. Organomet. Chem.* **2005**, *690*, 3854-3860.

47. Hahn, F. E.; Foth, M., *J. Organomet. Chem.* **1999**, *585*, 241-245.

48. Herrmann, W. A.; Schwarz, J.; Gardiner, M. G., *Organometallics* **1999**, *18*, 4082-4089.

49. Herrmann, W. A.; Elison, M.; Fischer, J.; Kocher, C.; Artus, G. R. J., *Chem.-Eur. J.* **1996**, *2*, 772-780.

50. Turkmen, H.; Pelit, L.; Cetinkaya, B., *J. Mol. Catal. A-Chem.* **2011**, *348*, 88-93.

51. Crabtree, R. H., *Chem. Rev.* **2012**, *112*, 1536-1554.

52. Pschierer, J.; Peschek, N.; Plenio, H., *Green Chem.* **2010**, *12*, 636-642.

53. Fleckenstein, C. A.; Plenio, H., *Green Chem.* **2007**, *9*, 1287-1291.

54. Fleckenstein, C.; Roy, S.; Leuthausser, S.; Plenio, H., *Chem. Commun.* **2007**, 2870-2872.

55. Karimi, B.; Akhavan, P. F., *Chem. Commun.* **2011**, *47*, 7686-7688.

56. Diebolt, O.; Braunstein, P.; Nolan, S. P.; Cazin, C. S. J., *Chem. Commun.* **2008**, 3190-3192.
57. Edwards, M. G. W., J. M. J., *Angew. Chem. Int. Ed.* **2002**, *41*, 4740.
58. Crabtree, R. H., *Organometallics* **2011**, *30*, 17-19.
59. Shvo, Y.; Czarkie, D.; Rahamim, Y.; Chodosh, D. F., *J. Am. Chem. Soc.* **1986**, *108*, 7400-7402.
60. Blum, Y.; Czarkie, D.; Rahamim, Y.; Shvo, Y., *Organometallics* **1985**, *4*, 1459-1461.
61. Hamid, M.; Slatford, P. A.; Williams, J. M. J., *Adv. Synth. Catal.* **2007**, *349*, 1555-1575.
62. Hollmann, D.; Bahn, S.; Tillack, A.; Beller, M., *Angew. Chem. Int. Ed.* **2007**, *46*, 8291-8294.
63. Gnanamgari, D.; Sauer, E. L. O.; Schley, N. D.; Butler, C.; Incarvito, C. D.; Crabtree, R. H., *Organometallics* **2009**, *28*, 321-325.
64. Hollmann, D.; Bahn, S.; Tillack, A.; Beller, M., *Chem. Commun.* **2008**, 3199-3201.
65. Kawahara, R.; Fujita, K.; Yamaguchi, R., *Adv. Synth. Catal.* **2011**, *353*, 1161-1168.
66. Fujita, K.; Li, Z. Z.; Ozeki, N.; Yamaguchi, R., *Tetrahedron Lett.* **2003**, *44*, 2687-2690.
67. Fujita, K. I.; Enoki, Y.; Yamaguchi, R., *Tetrahedron* **2008**, *64*, 1943-1954.
68. Fujita, K. I.; Fujii, T.; Yamaguchi, R., *Org. Lett.* **2004**, *6*, 3525-3528.
69. Karvembu, R.; Prabhakaran, R.; Natarajan, K., *Coord. Chem. Rev.* **2005**, *249*, 911-918.
70. Conley, B. L.; Pennington-Boggio, M. K.; Boz, E.; Williams, T. J., *Chem. Rev.* **2010**, *110*, 2294-2312.
71. Gonell, S.; Poyatos, M.; Peris, E., *Angew. Chem. Int. Ed.* **2013**, *52*, 7009-7013.
72. Mas-Marza, E.; Mata, J. A.; Peris, E., *Angew. Chem. Int. Ed.* **2007**, *46*, 3729-3731.
73. Zanardi, A.; Mata, J. A.; Peris, E., *J. Am. Chem. Soc.* **2009**, *131*, 14531-14537.

74. Sabater, S.; Mata, J. A.; Peris, E., *Nat. Commun.* **2013**, *4*.

75. Viciano, M.; Sanau, M.; Peris, E., *Organometallics* **2007**, *26*, 6050-6054.

76. Da Costa, A. P.; Viciano, M.; Sanau, M.; Merino, S.; Tejeda, J.; Peris, E.; Royo, B., *Organometallics* **2008**, *27*, 1305-1309.

77. Clapham, S. E.; Hadzovic, A.; Morris, R. H., *Coord. Chem. Rev.* **2004**, *248*, 2201-2237.

78. Ikariya, T.; Blacker, A. J., *Acc. Chem. Res.* **2007**, *40*, 1300-1308.

79. Zweifel, T.; Naubron, J. V.; Grutzmacher, H., *Angew. Chem. Int. Ed.* **2009**, *48*, 559-563.

80. Noyori, R.; Ohkuma, T., *Angew. Chem. Int. Ed.* **2001**, *40*, 40-73.

81. Crabtree, R. H., *New J. Chem.* **2011**, *35*, 18-23.

82. Ohkuma, T.; Ooka, H.; Hashiguchi, S.; Ikariya, T.; Noyori, R., *J. Am. Chem. Soc.* **1995**, *117*, 2675-2676.

83. Fujita, K.; Tanino, N.; Yamaguchi, R., *Org. Lett.* **2007**, *9*, 109-111.

84. Fujita, K.; Asai, C.; Yamaguchi, T.; Hanasaka, F.; Yamaguchi, R., *Org. Lett.* **2005**, *7*, 4017-4019.

85. Klinkenberg, J. L.; Hartwig, J. F., *Angew. Chem. Int. Ed.* **2011**, *50*, 86-95.

86. Magro, A. A. N. E., G. R.; Cole-Hamilton, D. J., *Chem. Commum.* **2007**, 3154.

87. Lawrence, S. A., *Amines: Synthesis, properties, and applications*, Cambridge University, Cambridge, **2004**.

88. Salvatore, R. N. Y., C. H.; Jung, K. W., *Tetrahedron* **2001**, *57*, 7785-7811.

89. Haniti, M.; Hamid, S. A.; Williams, J. M. J., *Tetrahedron Lett.* **2007**, *48*, 8263-8265.

90. Balcells, D.; Nova, A.; Clot, E.; Gnanamgari, D.; Crabtree, R. H.; Eisenstein, O., *Organometallics* **2008**, *27*, 2529-2535.

91. Roundhill, D. M., *Chem. Rev.* **1992**, *92*, 1-27.

92. Kim, J.; Kim, H. J.; Chang, S., *Eur. J. Org. Chem.* **2013**, 3201-3213.

93. Yamaguchi, R.; Kawagoe, S.; Asai, C.; Fujita, K. I., *Org. Lett.* **2008**, *10*, 181-184.

94. Gunanathan, C.; Milstein, D., *Angew. Chem. Int. Ed.* **2008**, *47*, 8661-8664.

95. Kawahara, R.; Fujita, K.; Yamaguchi, R., *J. Am. Chem. Soc.* **2010**, *132*, 15108-15111.

96. Imm, S.; Bahn, S.; Neubert, L.; Neumann, H.; Beller, M., *Angew. Chem. Int. Ed.* **2010**, *49*, 8126-8129.

97. Imm, S.; Bahn, S.; Zhang, M.; Neubert, L.; Neumann, H.; Klasovsky, F.; Pfeffer, J.; Haas, T.; Beller, M., *Angew. Chem. Int. Ed.* **2011**, *50*, 7599-7603.

98. Pingen, D.; Muller, C.; Vogt, D., *Angew. Chem. Int. Ed.* **2010**, *49*, 8130-8133.

99. Barker, J.; Kilner, M., *Coord. Chem. Rev.* **1994**, *133*, 219-300.

100. Jazzar, R. F. R.; Macgregor, S. A.; Mahon, M. F.; Richards, S. P.; Whittlesey, M. K., *J. Am. Chem. Soc.* **2002**, *124*, 4944-4945.

101. Kuhn, K. M.; Grubbs, R. H., *Org. Lett.* **2008**, *10*, 2075-2077.

102. Prades, A.; Viciano, M.; Sanau, M.; Peris, E., *Organometallics* **2008**, *27*, 4254-4259.

103. Liao, S.; Yu, K.; Li, Q.; Tian, H.; Zhang, Z.; Yu, X.; Xu, Q., *Org. Biomol. Chem.* **2012**, *10*, 2973-2978.

104. Yang, J.; Liu, X.; Meng, D.-L.; Chen, H.-Y.; Zong, Z.-H.; Feng, T.-T.; Sun, K., *Adv. Synth. Catal.* **2012**, *354*, 328-334.

105. Xu, Q.; Chen, J.; Liu, Q., *Adv. Synth. Catal.* **2013**, *355*, 697-704.

106. Bartoszewicz, A.; Marcos, R.; Sahoo, S.; Inge, A. K.; Zou, X.; Martin-Matute, B., *Chem.-Eur. J.* **2012**, *18*, 14510-14519.

107. Zhang, Y.; Lim, C.-S.; Sim, D. S. B.; Pan, H.-J.; Zhao, Y., *Angew. Chem. Int. Ed.* **2013**, *52*.

108. Agrawal, S.; Lenormand, M.; Martin-Matute, B., *Org. Lett.* **2012**, *14*, 1456-1459.

109. Peris, E.; Lee, J. C.; Crabtree, R. H., *J. Chem. Soc. Chem. Comm.* **1994**, 2573-2573.

110. Lee, J. C.; Peris, E.; Rheingold, A. L.; Crabtree, R. H., *J. Am. Chem. Soc.* **1994**, *116*, 11014-11019.

111. Patel, B. P.; Wessel, J.; Yao, W. B.; Lee, J. C.; Peris, E.; Koetzle, T. F.; Yap, G. P. A.; Fortin, J. B.; Ricci, J. S.; Sini, G.; Albinati, A.; Eisenstein, O.; Rheingold, A. L.; Crabtree, R. H., *New J. Chem.* **1997**, *21*, 413-421.

# CHAPTER 3

# SYNTHESIS AND "UNCONVENTIONAL" REACTIVITY OF IMIDAZOLYLIDENE-PYRIDYLIDENE COMPLEXES OF RHODIUM AND IRIDIUM

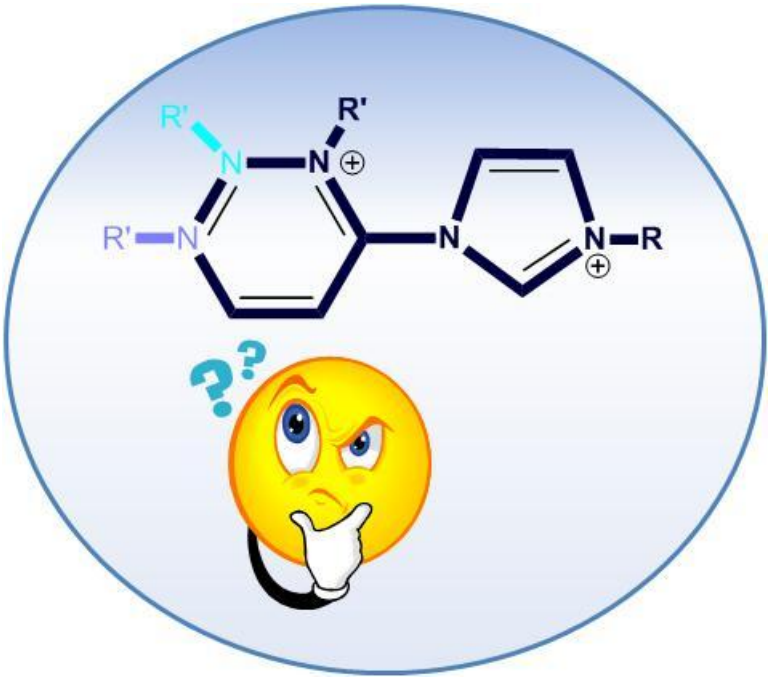

# 3.1 INTRODUCTION

## 3.1.1 *Classical* and *non-classical* N-heterocyclic carbenes

The coordination chemistry of N-heterocylic carbenes (NHCs) has experienced an explosive development in the last few years, not only due to the extremely large number of their catalytic applications,[1-6] but also due to the ready access to a large library of ligands with almost 'on-demand' stereoelectronic properties.[3, 7-8] Azolium salts are often found to be excellent NHC precursors because they are generally easy to make and provide a variety of topologies that may facilitate the preparation of metal complexes with different architectures. Apart from the most widely used NHCs that are stabilized by two adjacent heteroatoms (*normal*-NHCs), (**I** and **II**, Scheme 3.1), a wide set of other N-heterocyclic frameworks has allowed the preparation of carbenes, in which the electronic and steric parameters can differ from the *normal* ones. This new series includes heterocyclic carbenes that are not stabilized by two adjacent heteroatoms (*abnormal*-NHCs), (**III**, **IV** and **V**, Scheme 3.1). The term *abnormal*, was first proposed by Crabtree,[9-10] mostly attending to the differences shown compared to the most common imidazol-2-ylidenes (**I**, Scheme 3.1). It is now widely accepted, that *abnormal*-NHCs refer to any case where the free ligand is mesoionic. In a mesoionic ring system, no resonance form with all-neutral formal charges can be written (**III**, **IV** and **V**, Scheme 3.1), therefore one is obligated to assign positive and negative formal charges.

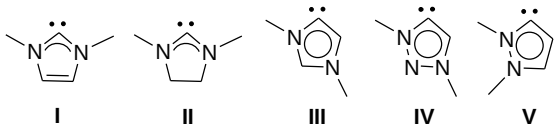


**Scheme 3.1** N-heterocyclic carbenes, including *normal*-NHC (**I** and **II**), *abnormal*- (or mesoionic-) NHC (**III**, **IV** and **V**)

Both types of NHC, *normal*-NHC (*n*NHC) and *abnormal*-NHC (*a*NHC) or mesoionic-NHC (MIC), form analogous compounds behaving similarly once bound to the metal centre. However, a fundamental property of a true carbene is divalency, and this holds true for $:CR^1R^2$ ($R^1$ and $R^2$ = H), as well as for *n*NHCs and *a*NHCs. Another carbene characteristic is its ability to dimerize to form an alkene, as in $C_2H_4$ ($CH_2$ dimer), and enetetraamines in the case of *n*NHCs. This type of dimerization

does not occur with *a*NHCs. Another property of a true carbene is the 6 valence electron on the carbene carbon, a property that holds true for $CH_2$ and free *n*NHCs, but may not be applied for *a*NHCs, for which the 'carbene' carbon always has 8 electrons. All these arguments have given rise to a full discussion about whether *a*NHCs should be considered as true carbenes or not. This type of discussion misrepresents the situation because as soon as any carbene binds to the metal, its six electron count turns into an octet character in the complex. When the *n*NHC or *a*NHC binds, several resonance forms are plausible, as shown for the *n*NHC in Scheme 3.2, but all of them feature a tetravalent carbon. So in all cases we are dealing with a tetravalent donor carbon atom in the complex and *a*NHCs and *n*NHCs behave very similarly. Many other ligands change their chemical character on binding, so the fact that carbenes behave in this way is not unexpected. We can therefore argue that to the extent that the NHC nomenclature is appropriate for *n*NHCs, it also holds for *a*NHCs, because it emphasizes the many factors that are common to both classes of ligands. The distinction between mesoionic and nonmesoionic carbenes in the free state is largely lost on binding.[11]

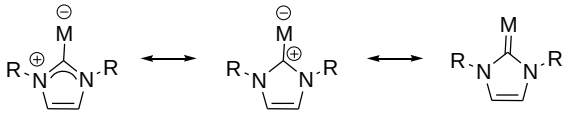


**Scheme 3.2** Several plausible resonance forms when a *n*NHC binds to a metal

Apart from *n*NHCs and *a*NHcs (or MICs), carbenes without α-heteroatoms related to the carbene carbon (*remote*-NHCs), are often seen in the recent literature (**VI** in Scheme 3.3). An interesting class of NHCs is the one with only one heteroatom present in the heterocycle, such as the pyridylidene family. For this type of ring, two types of carbenes can be formed: *normal* pyridylidene, with an α-heteroatom related to the carbene carbon (**VII**, Scheme 3.3), and *remote* pyridylidene, without an α-heteroatom (**VIII** and **IX**, Scheme 3.3). Along this PhD. Thesis, however, pyridylidenes of type **VIII** will be classified as "*abnormal*", and we will emphasize that this means that they are mesoionic in the free state, in order to avoid misunderstandings.

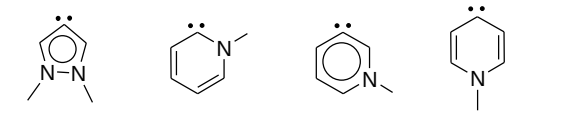


**Scheme 3.3** N-heterocyclic carbenes, including *remote*-NHC (**VI**) and pyridylidene family (**VII**, **VIII** and **IX**)

A simple way to selective obtain complexes with *abnormal* imidazolylidenes (coordinated by the C4(5) instead of the C2), is to use imidazolylidene ligand-precursors blocked at the C2 position by an appropriate group (alkyl or aryl group). The first example reported in the literature using this strategy was described by Crabtree and co-workers (**3.1**, Scheme 3.4).[12]

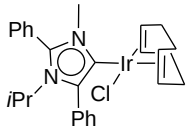


**3.1**

**Scheme 3.4** *a*NHC-based Ir(I) complex

Since Crabtree and co-workers reported the first *a*NHC-based complexes in 2001, the number and range of *abnormally*-bound carbenes has largely increased.[12-22] It has to be taken into account that direct metallation of the ligands derived from C2-blocked imidazolium salts must be used with caution, because selectivity towards *abnormal* position is not always guaranteed. In some cases, when the C2 position of the NHC ligand precursors is blocked with an alkyl group in order to achieve *a*NHCs, these ligands suffer unconventional reactivity and unexpected results.

For example, in 2004 Crabtree and co-workers reported the oxidative C-C cleavage in the metallation of the ligand derived from the C2-blocked imidazolium salt, **3.2** (Scheme 3.5) to $[Rh(COD)Cl]_2$ by transmetallation from the corresponding pre-formed silver-NHC complex.[19] The expected *abnormal*-NHC complex was not isolated; in contrast, the *normal* carbene-complex **3.3**, was formed, implying that a C2-$CH_3$ bond cleavage at the azolium had taken place.

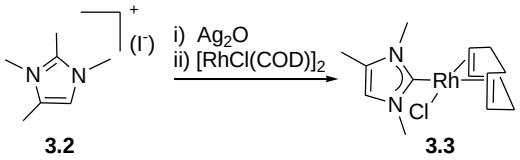


**3.2** **3.3**

**Scheme 3.5** C-C bond cleavage at the $CH_3$ group blocking the C2 position of the imidazolium salt **3.2**

Another unexpected C-H bond activation was reported in our group for the reaction of the bisimidazolium salt **3.4** with $[IrCp^*Cl_2]_2$ (Scheme 3.6).[22] In this particular case, C-H bond activation at the $CH_3$ group of the C2 position of salt **3.4** was observed, and complex **3.5** was obtained.

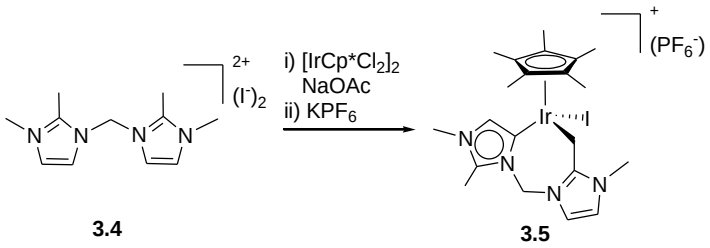


**3.4** **3.5**

**Scheme 3.6** C-H bond activation at the $CH_3$ group blocking the C2 position of bisimidazolium salt **3.4**

The electronic parameters of many *abnormal* carbenes have been determined based on the IR carbonyl stretching frequencies of complexes containing the $[M(NHC)(CO)_n]$ fragment, and correlating with the data for the $[LNi(CO)_3]$ benchmark that would translate into the TEP (Tolman Electronic Parameter) value, as mentioned in Chapter 1. These correlations were first established by Crabtree,[23] and then improved by Nolan,[24-25] based on the corresponding [IrCl(CO)(COD)] complexes. As a result of these studies, imidazole-based *a*NHCs are known to be stronger σ-donors than their C2-bound analogues.[12, 24, 26-27] The theoretical studies carried out by Gusev confirm this point.[28] Albrecht, also demonstrated the much higher *trans* influence of an *a*NHC versus *n*NHCs from crystallographic data, and proposed that this property enhances the catalytic activity of Rh(III) complexes in transfer hydrogenation.[29]

### 3.1.2 Pyridylidene-based complexes

Although the coordination of pyridine-based NHC (pyr-NHC) ligands is known since 1974 (Scheme 3.7),[30] there are still very few examples of complexes bearing this type of ligands. Common methods to obtain pyr-NHC complexes include: *a)* C-halogen oxidative addition of 2- or 4-halopyridiniums when treated with low valent transition metals such as Pd[31-34] or Pt,[35] *b)* quaternization of iridium or rhodium pyridyl complexes,[36] *c)* deprotonation of pyridinium ions by strong bases and metallation of *in situ* generated pyridylidene carbenes,[37] and *d)* C-H oxidative addition of functionalised pyridinium ions.[38] Together with these 'classical' forms to obtain pyridylidenes, which may be related to the most common forms to obtain all other coordinated NHCs, Conejero and Carmona proposed a very innovative approach to the preparation of pyridine-based NHCs, consisting of *e)* the isomerization/tautomerization of 2-substituted pyridines and polypyridines, a process which is known to be induced by some iridium (III) complexes.[39-43] Also, Conejero and co-workers have successfully coordinated pyridylidenes *f)* by reacting pyridinium-2-carboxylates with a variety of late transition metal precursors,[44] by adapting Crabtree's method for the preparation of imidazolylidenes from imidazolium-carboxylates.[45-46]

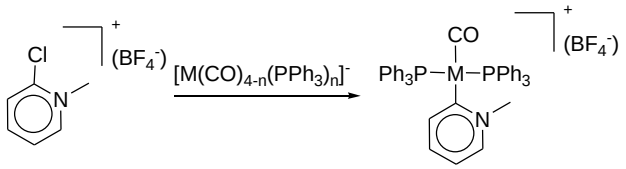


**3.6** **3.7a** M=Ir, n=1 **3.7b** M=Rh, n=2

**Scheme 3.7** First pyridylidene-type transition-metal complexes obtained by Stone in 1974

Pyridylidenes can coordinate to the metal through their *ortho*, *meta*, and *para* positions affording *normal* (**X**), *abnormal/remote* (**XI**), and *remote* (**XII**) pyridylidene complexes, respectively, as previously shown in Scheme 3.3. Analogous to all other *abnormal*-NHCs, pyr-NHC complexes are also stabilized by only one nitrogen atom and, consequently, are generally stronger σ-donors and better π-acceptors than the more common imidazol-2-ylidenes, as proved by experimental and theoretical studies.[37] In addition, crystallographic studies based on bond lengths of a series of Pd

and Ni complexes with different pyridylidenes and imidazolylidenes, stated that *remote*-pyridylidenes exhibit larger *trans* influence than imidazolylidenes.[47-48]

Taking into account that the chemical functionalization of imidazoles and pyridines is very well established, both imidazolylidenes and pyridylidenes can be connected to a variety of functionalities that allow them to be embedded in chelating environments.[13, 49-50] With NHC chemistry in continuous growth, and with the increasing interest in finding new coordination modes that can facilitate ligands with novel stereoelectronic properties, we found intriguing that just very few examples of linked imidazolylidene- (or triazolylidene-) pyridylidenes were described until the moment that our investigations started (Scheme 3.8).[51-54] In 2010, Albrecht and co-workers reported an interesting example of an iridium (III) complex bearing a linked triazolylidene-pyridylidene ligand, **3.8**, Scheme 3.8. Complex **3.8** was a very active water oxidation catalyst,[54] thus exemplifying the interesting potential applications of these ligands.

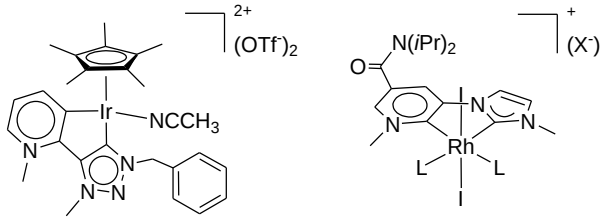


**3.8** **3.9**

**Scheme 3.8** Triazolylidene-pyridylidene complex, **3.8** and imidazolylidene-pyridylidene complex, **3.9**

Later, in 2012, Colbran and co-workers described the first linked imidazolylidene-pyridylidene complexes, **3.9** (Scheme 3.8).[51]

With all this in mind, in this Chapter we aimed to focus our attention on the development of a rational series of Ir and Rh complexes with a full set of chelate imidazolylidene-pyridylidene (*C,C'*-imz-pyr) ligands. As will be detailed in the next sections, together with the expected bis(NHC) complexes, we obtained a series of metal complexes arising from unusual ligand rearrangements, including C-C couplings, C-C and C-N bond cleavages and C-H activations. The study of these new *C,C'*-imz-pyr complexes gives a good opportunity to compare the structural and

reactivity differences of these compounds depending on the carbene type (*normal*, *abnormal* or *remote*), related to both the imidazolylidene and the pyridylidene.

# 3.2 RESULTS AND DISCUSSION

## 3.2.1 Synthesis and characterization of imidazolium-pyridinium salts

As mentioned above, the general aim of this work was to investigate the chemistry of transition metal complexes incorporating linked imidazolylidene-pyridylidene (*C*,*C*'-imz-pyr) ligands, in which the relative configuration of the imidazolium-pyridinium ligand precursors facilitated the systematic coordination of the chelate ligand in all possible combinations of *normal*, *abnormal* and *remote* modes.

In this regard, we focused our attention on the development of the (*C*,*C*'-imz-pyr) ligand precursors shown in Scheme 3.9. All these salts were synthesised and characterised for the first time during the development of this research work.

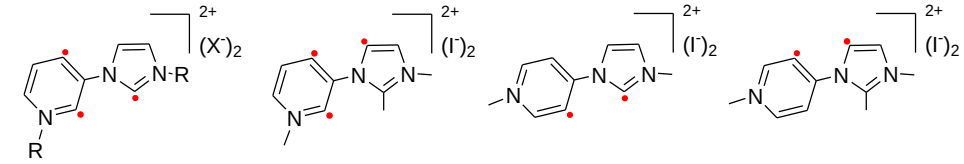


R=Me, X=I; **[EH$_2$]I$_2$** **[GH$_2$]I$_2$** **[IH$_2$]I$_2$** **[JH$_2$]I$_2$**

R=Me, X=$PF_6$; **[EH$_2$](PF$_6$)$_2$**

R=*n*Bu, X=I; **[FH$_2$]I$_2$**

**Scheme 3.9** Imidazolium-pyridinium salts used in this work. Red dots indicate the expected coordination sites.

*a) General protocol for the synthesis of the imidazolium-pyridinium salts* ***[EH$_2$]I$_2$, [FH$_2$]I$_2$, [GH$_2$]I$_2$*** *and* ***[EH$_2$](PF$_6$)$_2$***

As depicted in Scheme 3.10, the general protocol for the preparation of salts **[EH$_2$]I$_2$**, **[FH$_2$]I$_2$** and **[GH$_2$]I$_2$** consisted of a two-step procedure. The first step is an Ullmann coupling between the corresponding imidazole and 3-bromopyridine in the presence of $CuSO_4 \cdot 5H_2O$ and $K_2CO_3$. The second step involves the reaction of the neutral imidazole-pyridine with the corresponding alkyl halide to yield the imidazolium-pyridinium salts **[EH$_2$]I$_2$**, **[FH$_2$]I$_2$** and **[GH$_2$]I$_2$** in 71%, 50% and 35% yield, respectively.

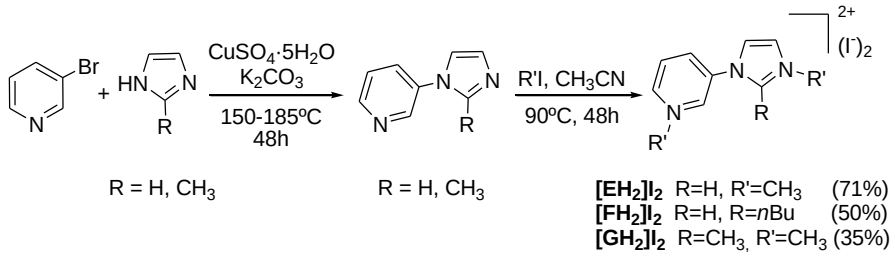


**Scheme 3.10** Synthesis of **[EH$_2$]I$_2$**, **[FH$_2$]I$_2$** and **[GH$_2$]I$_2$**

Salt **[EH$_2$](PF$_6$)$_2$** was prepared by anion metathesis of **[EH$_2$](I)$_2$** with ammonium hexafluorophosphate in $CH_3OH$. After purification, **[EH$_2$](PF$_6$)$_2$** was obtained in 77% yield (Scheme 3.11).

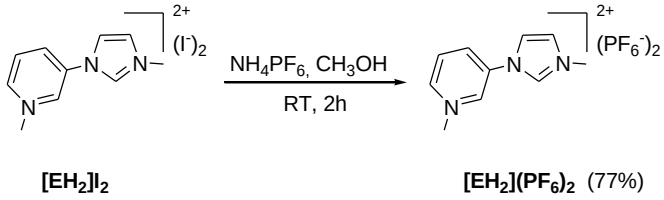


**Scheme 3.11** Synthesis of **[EH$_2$](PF$_6$)$_2$**

*b) General protocol for the synthesis of the imidazolium-pyridinium salts **[IH$_2$]I$_2$** and **[JH$_2$]I$_2$***

The synthesis of salts **[IH$_2$]I$_2$** and **[JH$_2$]I$_2$** was carried out following the above described procedures but using 4-bromopyridine hydrochloride. In order to neutralize the HCl it was necessary to use two equivalents of $K_2CO_3$ (Scheme 3.12).

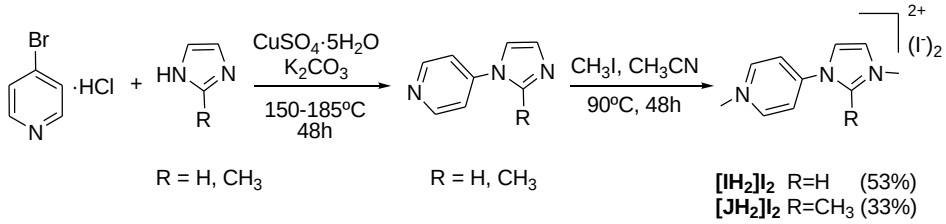


**Scheme 3.12** Synthesis of **[IH$_2$]I$_2$** and **[JH$_2$]I$_2$**

The new imidazolium-pyridinium salts, **[EH$_2$]I$_2$-[JH$_2$]I$_2$**, were fully characterised by means of NMR spectroscopy, mass spectrometry and elemental analysis. As an example, the NMR spectroscopic characterization of salt **[EH$_2$]I$_2$** is discussed below

in detail. $^{1}$H-$^{13}$C gHSQC and $^{1}$H-$^{13}$C gHMBC NMR experiments were carried out in order to confirm the assignment of the signals displayed in the $^{1}$H and $^{13}$C NMR spectra of **[EH$_2$]I$_2$** (see Experimental Section in Chapter 5). All the details of the spectroscopic data for the rest of imidazolium-pyridinium salts can be found in the Experimental Section (Chapter 5).

*$^{1}$H NMR spectrum of **[EH$_2$]I$_2$***

Figure 3.1 shows the $^{1}$H NMR spectrum of **[EH$_2$]I$_2$**. The signals due to the proton of the C*H* groups of the pyridinium ring (b, c, d and e) are observed at 9.76, 9.19, 8.99 and 8.46 ppm, respectively. The resonances due to the proton of the NC*H*N (a) and C*H* groups of the imidazolium ring (f and g) appear at 9.99, 8.39 and 8.07 ppm, respectively. The signals assigned to the protons of the C*H*$_3$ groups of the pyridinium (h) and imidazolium (i) are displayed at 4.46 and 4.03 ppm, respectively.

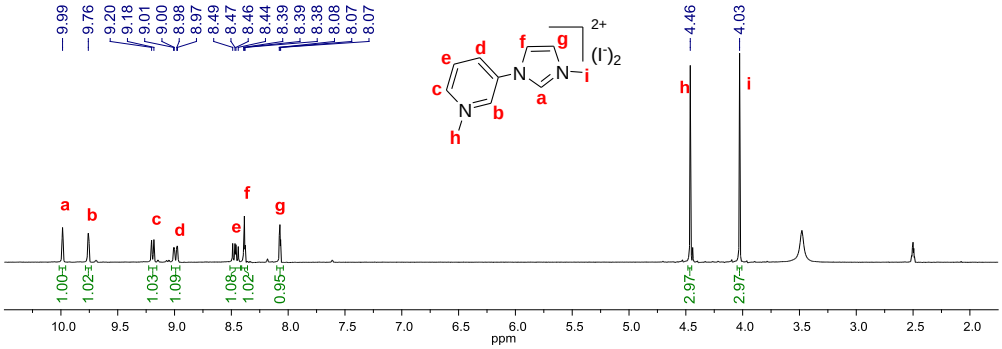


**Figure 3.1** $^{1}$H NMR spectrum of **[EH$_2$]I$_2$** in DMSO-$d_6$

*$^{13}$C{$^{1}$H} NMR spectrum of **[EH$_2$]I$_2$***

Figure 3.2 shows the $^{13}$C{$^{1}$H} NMR spectrum of **[EH$_2$]I$_2$**. The signals due to the carbon of the C*H* groups and the quaternary carbon of the pyridinium ring (1, 2, 3, 5 and 6) appear at 145.9, 140.5, 138.0, 133.6 and 128.1 ppm, respectively. The resonances corresponding to the carbon of the NC*H*N (4) and C*H* groups of the imidazolium ring (7) and (8) are seen at 137.3, 124.9 and 121.1 ppm, respectively. The signals assigned to the carbon of the C*H*$_3$ groups of the pyridinium (9) and imidazolium (10) are displayed at 48.7 and 36.7 ppm, respectively.

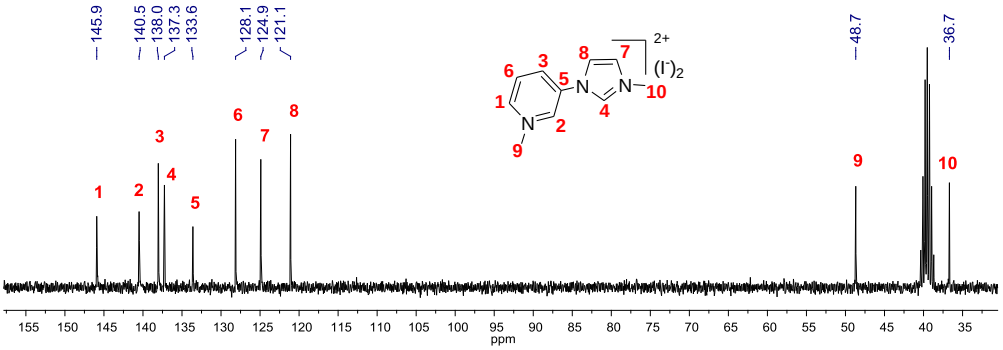


**Figure 3.2** $^{13}C\{^{1}H\}$ NMR spectrum of **[EH$_2$]I$_2$** in DMSO-$d_6$

## 3.2.2 Synthesis and characterization of [MI$_2$(*C,C'*-imz-pyr)(CH$_3$CN)$_2$]$^+$ (M = Rh, Ir) complexes

Once the imidazolium-pyridinium salts, **[EH$_2$]I$_2$-[JH$_2$]I$_2$**, were synthesised and characterised, their coordination to [MCl(COD)]$_2$ (M = Rh, Ir) was studied, and a series of [MI$_2$(*C,C'*-imz-pyr)(CH$_3$CN)$_2$]$^+$ (M = Rh, Ir) complexes, **7E-16I**, were obtained. In this section the synthesis and characterization of these complexes will be discussed. All complexes **7E-16I**, are new and have been prepared during the development of the present work.

### 3.2.2.1 Synthesis of [MI$_2$(*C,C'*-imz-pyr)(CH$_3$CN)$_2$]$^+$ (M = Rh, Ir) complexes

The synthesis of complexes **7E-16I**, has been divided in three parts depending on the imidazolium-pyridinium salt employed for their synthesis, and the coordination form that they are expected to provide, according to Scheme 3.9. In this regard, the first part will include the compounds obtained from salts **[EH$_2$]I$_2$**, **[EH$_2$](PF$_6$)$_2$** and **[FH$_2$]I$_2$**. The second part will describe the compound synthesised from **[GH$_2$]I$_2$**. Finally, compounds formed from salts **[IH$_2$]I$_2$-[JH$_2$]I$_2$** will be discussed.

*a) Coordination of **[EH$_2$]I$_2$**, **[EH$_2$](PF$_6$)$_2$** and **[FH$_2$]I$_2$**. Synthesis of [MI$_2$(C,C'-imz-pyr)(CH$_3$CN)$_2$]$^+$ (M = Rh, Ir) complexes, **7E-13E** and **11F***

In principle, it was expected that the imidazolium-pyridinium salts **[EH$_2$]I$_2$**, **[EH$_2$](PF$_6$)$_2$** and **[FH$_2$]I$_2$** might give rise to metal complexes with the corresponding *C,C'*-imz-pyr ligands, in which the pyridylidene part of the chelating ligand should coordinate to the metal through either the *ortho* or *para* carbons, achieving *normal* o *remote* coordination modes, respectively (Scheme 3.9).

As seen in Scheme 3.13, the reaction of **[EH$_2$]I$_2$**, **[EH$_2$](PF$_6$)$_2$** and **[FH$_2$]I$_2$** with [MCl(COD)]$_2$ (M = Rh, Ir) in $CH_3CN$ at 65ºC for 12h in the presence of an excess of KI (as halide source), afforded the corresponding [M(*C*,*C'*-imz-pyr) $(CH_3CN)_2I_2]^+$ (M = Rh, Ir) complexes, **7E-10E** and **11F**. All these complexes were obtained in more than 50%, and the pyridylidene unequivocally coordinated to the metal centre through the *para* carbon atom, thus affording the *remote* coordination mode. However, when **[EH$_2$]I$_2$** and **[EH$_2$](PF$_6$)$_2$** reacted with [RhCl(NBD)]$_2$, under exactly the same reaction conditions as those used for the preparation of **7E-10E** and **11F**, two new Rh(III) complexes, **12E** and **13E**, were obtained in 66% and 54% yield, respectively. Interestingly, in these two complexes the pyridylidene coordinated to the metal centre through the *ortho* carbon atom, affording the *normal* coordination mode (Scheme 3.13).

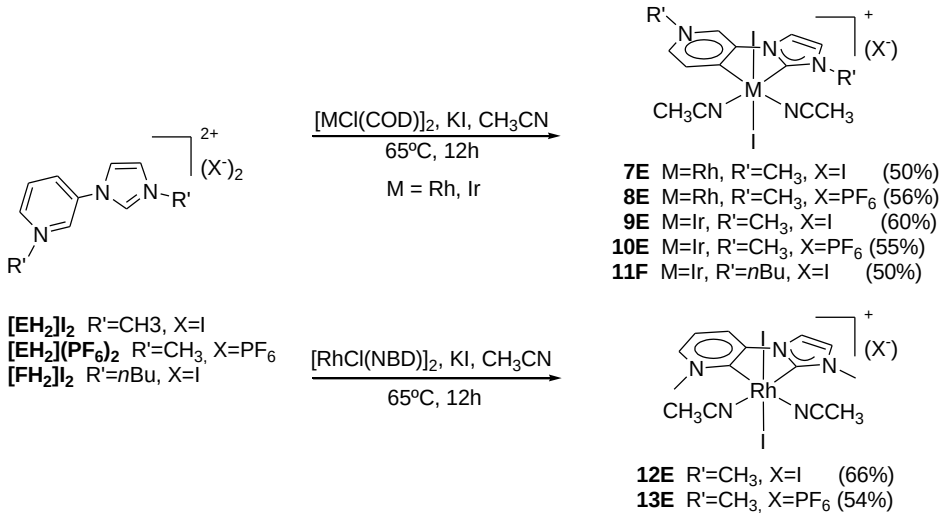


**Scheme 3.13** Synthesis of **7E-13E**

All complexes were characterised by means of NMR spectroscopy, mass spectrometry and elemental analysis. The molecular structure of **11F** was confirmed by means of X-Ray Diffraction studies. As an example, the spectroscopic characterization of compound **11F** is discussed in detail in section 3.2.2.2. A $^1$H-$^1$H gCOSY NMR experiment was carried out in order to confirm the assignment of the signals displayed on the $^1$H NMR spectrum of **11F** (see Experimental Section in Chapter 5). All the details of the spectroscopic data for the rest of compounds can be found in the Experimental Section (Chapter 5).

*b) Coordination of* ***[GH$_2$]I$_2$****. Synthesis of [IrI$_2$(C,C'-imz-pyr)(CH$_3$CN)$_2$]$^+$ complex,* ***14G***

In the case of **[GH$_2$]I$_2$**, we expected the formation of a metal complex with the pyridylidene coordinated through either the *ortho* or *para* carbons, therefore yielding the *normal* or *remote* coordination modes, respectively. The imidazolylidene was expected to coordinate through C4(5) position, affording an *abnormal* coordination mode (Scheme 3.9).

As depicted in Scheme 3.14, salt **[GH$_2$]I$_2$** was reacted with [MCl(COD)]$_2$ (M = Rh, Ir) in CH$_3$CN at 90ºC during 18h in the presence of an excess of KI (as halide source). When the reaction was performed using, [RhCl(COD)]$_2$ a mixture of compounds, which we were unable to identify, was obtained. On the contrary, the reaction with [IrCl(COD)]$_2$ afforded complex **14G** in 65% yield. For this complex the chelate ligand is coordinated through the pyridylidene in the *remote* mode and through a methylene group resulting from the C-H activation at the CH$_3$ group of the C2 position of the imidazolium ring (Scheme 3.14).

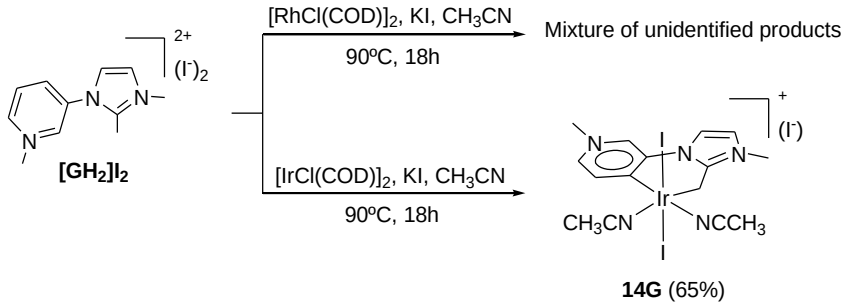


**Scheme 3.14** Synthesis of **14G**

As mentioned above, our initial aim when we decided to synthesise **[GH$_2$]I$_2$**, with the C2 position of the imidazolium ring blocked with one CH$_3$ group, was to facilitate the coordination of the imidazolylidene through the C4(5) position, therefore facilitating an *abnormal* coordination mode of the imidazole ring. This strategy for the preparation of C4-bound imidazolylidenes has proved to be successful previously. [21, 26-31] Nevertheless, a C-H activation at the CH$_3$ group of the C2 position of the imidazolium ring took place, and as mentioned above, compound **14G** was obtained instead.

Although this was not our expected result, we may rationalize this result as a consequence of the kinetic preference of the aliphatic ($CH_3$) C-H activation over the aromatic (imidazole). We have previously observed the preference for the formation of methylene-bound versus *abnormally*-bound imidazoles.[22] In this new case, this observation may also be supported by the kinetic preference for the formation of a six-membered iridacycle *versus* the themodynamic preference for the formation of a five-membered iridacycle, as previously described for the reactions of $[IrCl(COD)]_2$ with C2-substituted imidazoliums.[55]

Compound **14G** was characterised by means of NMR spectroscopy, mass spectrometry and elemental analysis. The molecular structure of **14G** was confirmed by means of X-Ray Diffraction. The spectroscopic characterization is discussed in detail in section 3.2.2.2. A $^{1}H$-$^{13}C$ gHMBC NMR experiment was carried out in order to confirm the assignment of the signals displayed on the $^{1}H$ and $^{13}C$ NMR spectra of **14G** (see Experimental Section in Chapter 5).

*c) Coordination of* ***[IH$_2$]I$_2$*** *and* ***[JH$_2$]I$_2$****. Synthesis of* $[MI_2(C,C'\text{-imz-pyr})(CH_3CN)_2]^+$ *(M = Rh, Ir) complexes,* ***15I*** *and* ***16I***

Salts **[IH$_2$I$_2$]** and **[JH$_2$I$_2$]**, were chosen in order to prepare metal complexes with the corresponding *C,C'*-imz-pyr ligands *abnormal/normally and* bis-*abnormally* coordinated, respectively (Scheme 3.9).

As depicted in Scheme 3.15, **[IH$_2$]I$_2$** was reacted with $[MCl(COD)]_2$ (M = Rh, Ir) in $CH_3CN$ at 65ºC during 12h in the presence of an excess of KI (as halide source), affording the corresponding $[MI_2(C,C'\text{-imz-pyr})(CH_3CN)_2]^+$ (M = Rh, Ir) complexes, **15I** and **16I** (Scheme 3.15). These two complexes, with the *abnormal* coordination of the pyridylidene, were obtained in moderate-high yields (above 50%). When the reaction was performed with **[JH$_2$I$_2$]**, under similar reaction conditions to those described for the coordination of **[IH$_2$I$_2$]**, the same compounds **15I** and **16I** were obtained as the only isolable products (Scheme 3.15), although this time the yields were lower (20−24%). This result is surprising, if we take into account that **[JH$_2$I$_2$]** was especially designed for the preparation of the *abnormal* coordination of the imidazolylidene, by blocking the C2 position of the imidazolium with the $CH_3$ group.

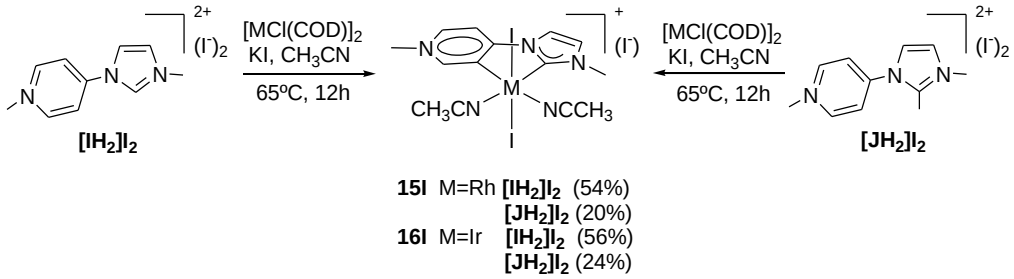


**Scheme 3.15** Synthesis of **15I** and **16I**

As can be seen in Scheme 3.15, an unexpected C-C bond cleavage took place instead of the expected bis-*abnormal* coordination of the *C,C'*-imz-pyr ligand derived from **[JH$_2$I$_2$]**. This unforeseen C-C cleavage in the metallation of C2-substituted imidazoliums was first described by Crabtree for reactions employing silver oxide,[19] (see Section 3.1.1) and we are unaware of any other similar examples of such type of process regarding rhodium, iridium or any other transition metal. Very recently Albrecht and co-workers have described that the demethylation of a C2-$CH_3$-substituted imidazolium may take place in the presence of CsOH, forming a cyclic urea,[56] which actually supports the idea previously reported by Crabtree that this demethylation may take place *via* an initial four-electron oxidation of the imidazolium C2-$CH_3$ to give a 2-formyl ion, followed by the hydrolytic cleavage to give the NHC,[19] which in our case is trapped by the rhodium or iridium centres. Although we have not studied the fate of the leaving $CH_3$ group, we believe that these two previous studies may give some important mechanistic clues.[19, 56] For this reason, Crabtree suggested that C2-$CH_3$ can be an unreliable blocking group for imidazolium/$Ag_2O$,[19] (Scheme 3.5) but our results widen the warning to other transition metals such as Rh and Ir.

A common feature about all the reactions described above, is that the addition of an external base is not needed to afford the coordination of the ligands, thus a double C-H activation of the imidazolium-pyridinium salt is assumed in order to justify the formation of complexes **7E-13E**, **11F**, **14G** and **15I** and **16I**. Although we did not perform any detailed studies in order to elucidate the reaction pathway of these complexes, we did look for the formation of any hydride intermediates by monitoring the reaction profiles by $^1$H NMR spectroscopy, but we did not observe any evidence of hydride formation. Another possibility was that 1,5-cyclooctadiene (COD) was

acting as hydrogen acceptor, but the analysis by GC while the reactions took place did not show any evidence of cyclooctene (COE) or cyclooctane (COA) formation. In an additional experiment, we carried out the formation of the above mentioned complexes with the addition of 5 equivalents of COD in the reaction medium, but this modification of the synthetic protocol did not improve the yields obtained, and evolution to COE or COA was not observed. These two observations discard that 1,5-cycloocadiene is implied in the reaction mechanism.

Interestingly, during the reaction pathway, in all cases the Rh(I) and Ir(I) precursors were oxidized to Rh(III) and Ir(III). This fact is in agreement with previous experimental and theoretical studies made in our group, regarding the C-H oxidative addition of bisimidazolium salts to Rh(I) and Ir(I) complexes.[57] In these studies, the metallation of bisimidazolium salts gave different products depending on the length of the alkylic $(CH_2)_n$ linker that connected the two imidazolium rings. In general, long linkers (n=2-4) facilitated the formation of square planar M(I) species, while short linkers (n=1) allowed the formation of pseudo-octahedral M(III) species. In our case, salts **$[EH_2]I_2$-$[JH_2]I_2$**, where the pyridinium rings are directly connected to the imidazolium ring (n=0), gave in all the cases the formation of the corresponding pseudo-octahedral M(III) species.

Because pyridiniums are considered to be less acidic than imidazoliums, we reasoned that salts **$[EH_2]I_2$-$[JH_2]I_2$** should first coordinate to the metal *via* the imidazole ring through a C-H activation on the imidazolium, and then facilitate the pyridinium C-H activation at the *ortho, meta* or *para* position, depending on the metal precursor used, by a chelate-assisted process.

Complexes **15I** and **16I** were characterised by means of NMR spectroscopy, mass spectrometry and elemental analysis. The molecular structure of **15I** was confirmed by means of X-Ray Diffraction studies. Due to the similarity of these two compounds, only the spectroscopic characterization of compound **15I** is discussed in detail in section 3.2.2.2. All the details of the spectroscopic data for compound **16I** can be found in the Experimental Section (Chapter 5).

### 3.2.2.2 Characterization of $[MI_2(C,C'\text{-imz-pyr})(CH_3CN)_2]^+$ (M = Rh, Ir) complexes

*a) NMR spectroscopic characterization of $[MI_2(C,C'\text{-imz-pyr})(CH_3CN)_2]^+$ (M = Rh, Ir) complexes, **11F**, **14G** and **15I***

*$^1$H NMR spectrum of **11F***

Figure 3.3 shows the $^1$H NMR spectrum of **11F**. The confirmation of the *remote* coordination of the pyridylidene can be easily determined by the evaluation of the signals attributed to the proton of the C*H* groups of the pyridylidene. These signals are depicted as three resonances at 8.54 (singlet, a), 8.23 (doublet, b) and 7.80 ppm (doublet, b), respectively. The signals attributed to the proton of the C*H* groups of the imidazolylidene appear as two doublets at 7.83 and 7.34 ppm (c). All the rest of the signals regarding the protons of the *n*-butyl groups, are conveniently assigned on the NMR spectrum shown in Figure 3.3.

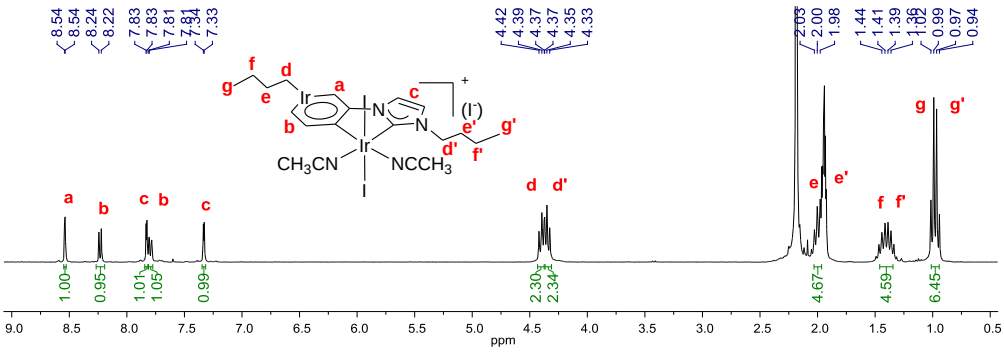


**Figure 3.3** $^1$H NMR spectrum of **11F** in $CD_3CN$

*$^{13}C\{^1H\}$ NMR spectrum of **11F***

Figure 3.4 shows the $^{13}C\{^1H\}$ NMR spectrum of **11F**. The most characteristic signals are the ones attributed to the metallated carbene carbons at 164.8 (1) and 149.4 ppm (2), from the pyridylidene and imidazolylidene, respectively. The signal due to the quaternary carbon of the pyridylidene appears at 146.8 ppm (3). The signals corresponding to the carbon of the *C*H groups of the pyridylidene are displayed at 137.1, 133.7 and 123.4 ppm (4). The resonances due to the carbon of the *C*H groups of the imidazolylidene are observed at 124.8 and 117.3 ppm (5). All the rest of the signals for the carbons of the *n*-butyl groups are conveniently displayed on the

spectrum shown in Figure 3.4, and are consistent with the structure assigned to the complex.

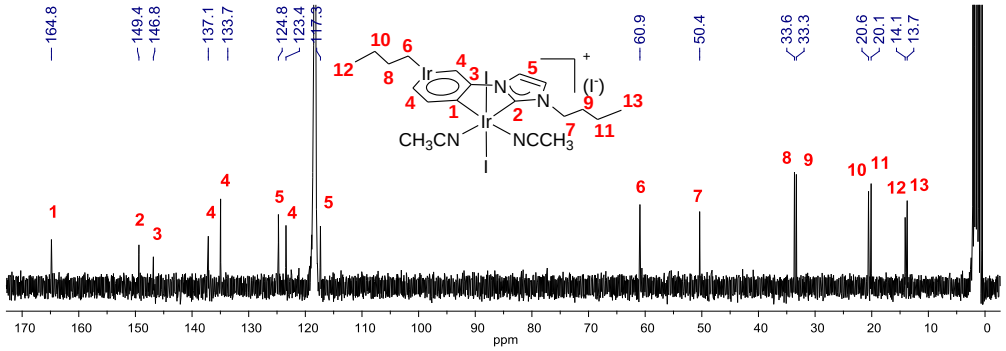


**Figure 3.4** $^{13}C\{^{1}H\}$ NMR spectrum of **11F** in $CD_3CN$

The assignment of *normal* or *remote* coordination of the pyridylidene in complexes **7E-13E** could be unambiguously assigned by the evaluation of the structure of the signals attributed to the protons of the pyridine ring in the corresponding $^{1}H$ NMR spectra, as can be seen for **11F** in Figure 3.3, and from the spectra of compounds that are shown in the Experimental section (Chapter 5). This selective formation of only one possible carbene type is remarkable, especially if we consider that previous studies with *n*-butyl-3-(2-pyridyl)pyridinium iodide (*N*,*C*-pyr-pyr) showed that the reactions with $[Ir(COD)_2]SbF_6$ afforded a mixture of two complexes, presumably due to the presence of the two possible carbene types, *normal* and *remote*.[58]

In the $^{13}C$ NMR spectra of complexes **7E-13E**, the most representative signals are probably the ones attributed to the metallated carbons. For the rhodium complexes described in this section, **7E**, **8E**, **12E** and **13E**, the $^{13}C\{^{1}H\}$ NMR chemical shifts attributed to the carbene carbon of the pyridylidene could be observed only for the $PF_6^-$ derivatives, (**8E** and **13E**) and not for the $I^-$ ones, (**7E** and **12E**), as described in the Experimental Section (Chapter 5). We attribute this observation to the high *trans* effect provided by the pyridylidene, which may facilitate the rapid exchange between the $CH_3CN$ ligand *trans* to the metallated pyridine and the iodide counterion, an effect that cannot be produced with a non-coordinating anion such as hexafluorophosphate ($PF_6^-$). This effect can also explain why the signals of coordinated $CH_3CN$ are not observed in $^{1}H$ and $^{13}C\{^{1}H\}$ NMR spectra when $CD_3CN$

is used as deuterated solvent. However, when the NMR spectra are recorded on DMSO-$d_6$, the signals corresponding to $CH_3CN$ are observed.

It is important to point out that, signals due to the pyridylidene carbene carbons display a big difference depending on whether the *remote* pyridylidene is coordinated to rhodium or iridium. For example, in the case of the the rhodium complex **8E** this signal appears at 183.9 ppm (d, $^1J_{RhC}$ = 28 Hz) (1, Figure 3.5), whereas the analogous iridium compound **10E** displays the signal at 164.6 ppm **(**1', in Figure 3.6). This almost 20 ppm shift is also displayed for the signals attributed to the carbene carbons of the imidazolylidene, which appear at 167.4 ppm (d, $^1J_{RhC}$ = 43 Hz) for **8E** (2, Figure 3.5) and at 149.3 ppm for **10E** (2', Figure 3.6). These observations are in accordance with similar chemical shift differences for the same type of previously described imidazolylidene-(or triazolylidene)-pyridylidene complexes of rhodium[43, 52] and iridium.[54, 59]

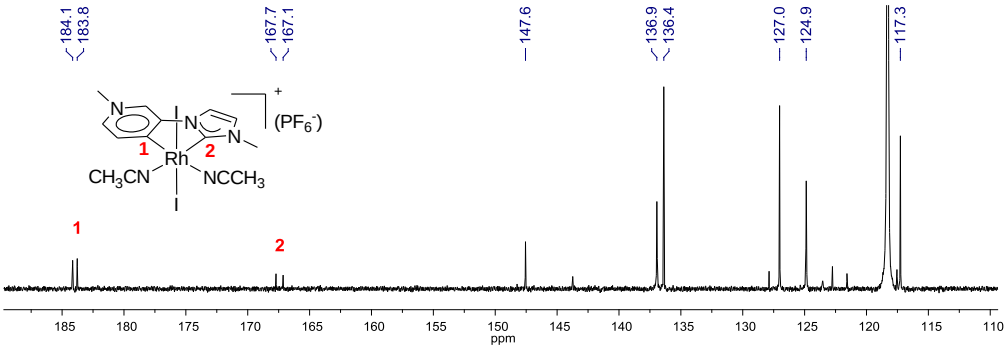


**Figure 3.5** $^{13}C\{^1H\}$ NMR spectrum of **8E** in $CD_3CN$

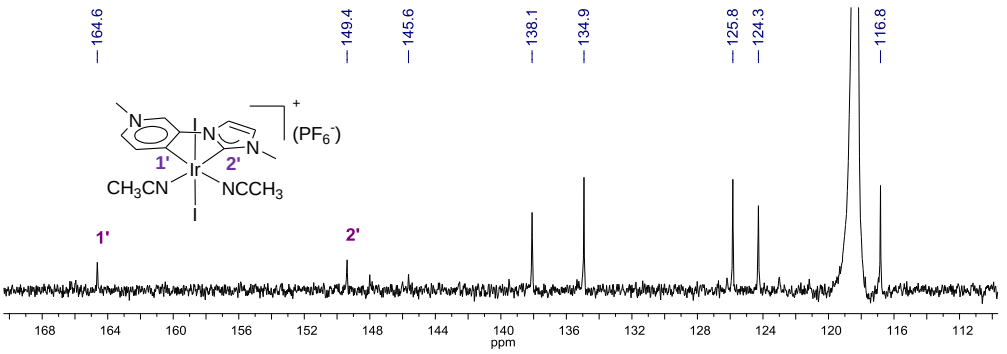


**Figure 3.6** $^{13}C\{^1H\}$ NMR spectrum of **10E** in $CD_3CN$

In the case of the *normal* coordination of the pyridylidene, the $^{13}C$ NMR spectrum of **13E** shows the signal due to the carbene carbon of the pyridylidene as a doublet at 175.7 ppm (d, $^{1}J_{RhC}$ = 36 Hz), while the doublet due to the carbene carbon of the imidazolylidene appears at 162.7 ppm (d, $^{1}J_{RhC}$ = 42 Hz) (1" in and 2" in Figure 3.7).

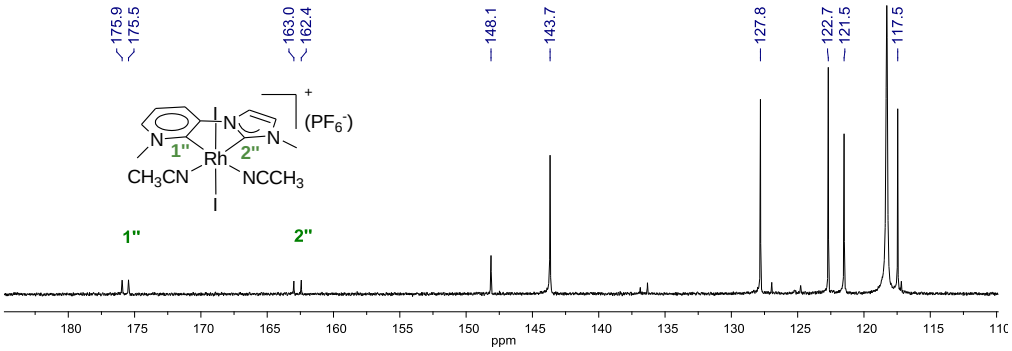


**Figure 3.7** $^{13}C\{^{1}H\}$ NMR spectrum of **13E** in $CD_3CN$

*$^{1}H$ NMR spectrum of **14G***

Figure 3.8 shows the $^{1}H$ NMR spectrum of **14G**. The assignment of the *remote* coordination of the pyridylidene can be unambiguously determined by the evaluation of the signals attributed to the proton of the C*H* groups of the pyridylidene. These signals are shown as two doublets at 8.51 ppm and 7.64 ppm (a), and a singlet at 8.21 ppm (b). The signals attributed to the proton of the C*H* groups of the imidazole ring appear as two doublets at 7.52 ppm and 7.15 ppm (c). The signal due to the protons of the metallated methylene is displayed as a singlet at 3.98 ppm (e), as a consequence of the symmetry of the molecule. The signals assigned to the protons of the C$H_3$ groups, are observed at 4.09 ppm (d) and 3.71 ppm (f).

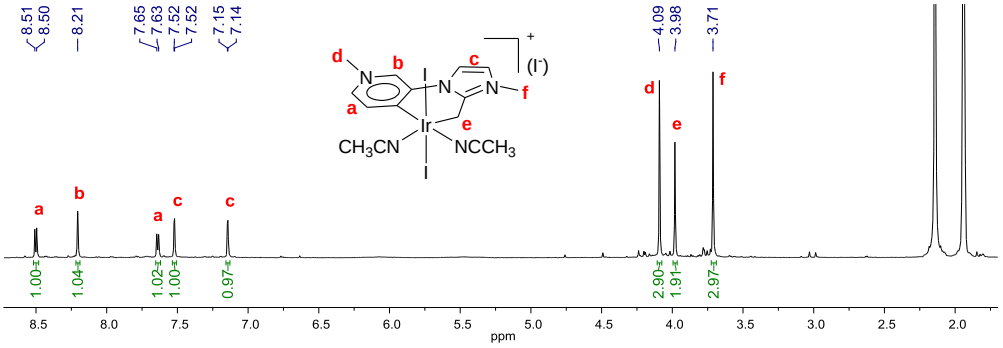


**Figure 3.8** $^{1}$H NMR spectrum of **14G** in $CD_3CN$

*$^{13}C\{^{1}H\}$ NMR spectrum of **14G***

Figure 3.9 shows the $^{13}C\{^{1}H\}$ NMR spectrum of **14G**. The characteristic signal attributed to the metallated methylene carbon appears at -25.5 ppm (8). The signal corresponding to the metallated carbene carbon is observed at 168.9 ppm (1). The signals due to the quaternary carbons of the imidazole ring and the pyridylidene appear at 163.5 (2) and 144.9 ppm (3), respectively. The signals corresponding to the *C*H groups of the pyridylidene appear at 145.8, 135.2 and 130.0 ppm (4). The resonances due to the *C*H groups of the imidazolylidene are displayed at 122.2 and 121.9 ppm (5). The signals regarding the carbon of the *C*$H_3$ groups appear at 46.9 (6) and 35.9 ppm (7).

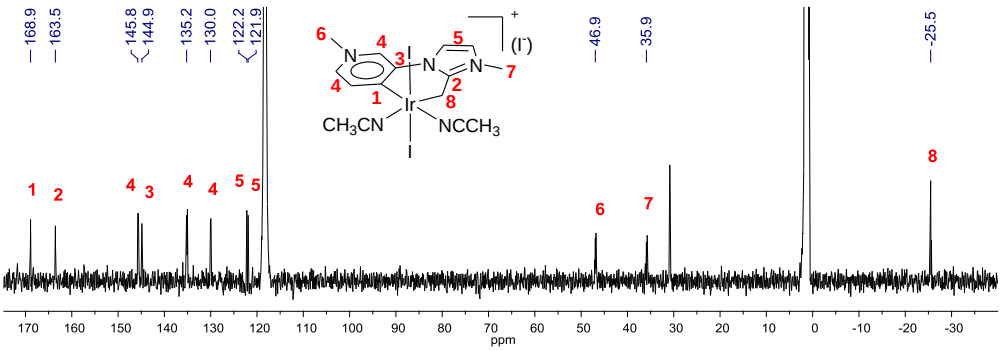


**Figure 3.9** $^{13}C\{^{1}H\}$NMR spectrum of **14G** in $CD_3CN$

*$^{1}H$ NMR spectrum of **15I***

Figure 3.10 shows the $^{1}$H NMR spectrum of **15I**. The assignment of the *abnormal* coordination of the pyridylidene can be readily assigned by the evaluation of the

signals attributed to the protons of the C*H* groups of the pyridylidene. These signals are shown as a singlet at 8.60 ppm (a) and as two doublets at 8.24 and 7.77 ppm (b). The signals corresponding to the proton of the C*H* groups of the imidazolylidene appear as two doublets at 7.99 and 7.39 ppm (c). The signals regarding the protons of the C$H_3$ groups, display their resonances at 4.26 (d) and 4.01 ppm (e), respectively.

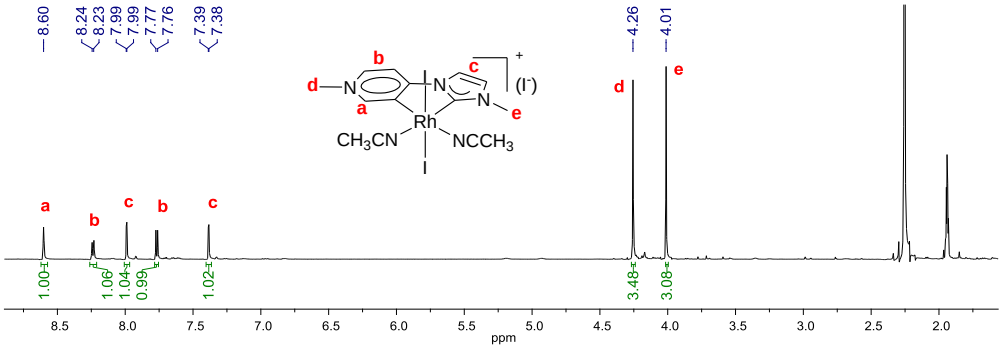


**Figure 3.10** $^{1}$H NMR spectrum of **15I** in $CD_3CN$

*$^{13}C\{^{1}H\}$ NMR spectrum of **15I***

Figure 3.11 shows the $^{13}C\{^{1}H\}$ NMR spectrum of **15I**. Probably, the most characteristic signals are the doublets attributed to the metallated carbene carbon at 169.3 (d, $^{1}J_{RhC}$ = 47 Hz) (1) and 139.6 ppm (d, $^{1}J_{RhC}$ = 34 Hz) (4), from the pyridylidene and imidazolylidene, respectively. The signal due to the quaternary carbon of the pyridylidene appears at 157.9 ppm (2). The signals corresponding to the carbon of the *C*H groups of the pyridylidene display their resonances at 153.5, 143.1 ppm and 127.0 (3). The resonances due to the carbons of the *C*H groups of the imidazolylidene appear at 117.5 and 109.0 ppm (5). The signals corresponding to the carbon of the *C*$H_3$ groups appear at 47.3 (6) and 36.0 ppm (7), respectively. The signals due to the carbons of the $CH_3CN$ are observed at 118.0 (*C*N) and 1.2 (*C*$H_3$) ppm.

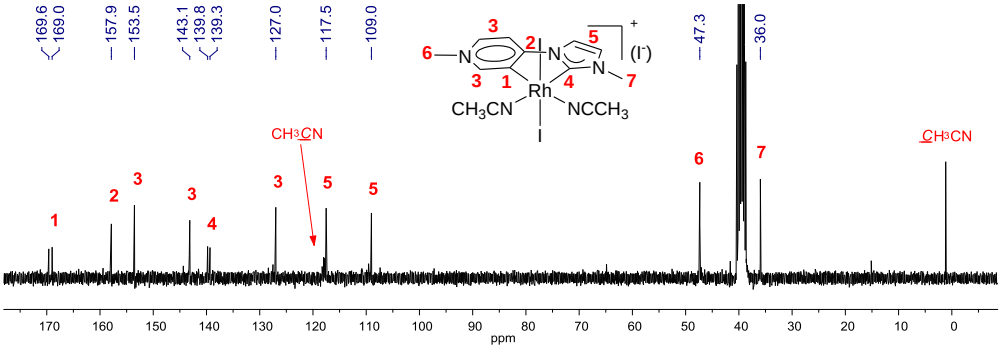


**Figure 3.11** $^{13}C\{^{1}H\}$ NMR spectrum of **15I** in DMSO-$d_6$

The evaluation of the NMR spectra of the complexes described in this section, **7E-16I**, reveals some features that are worth mentioning. With regard to the $^{13}C\{^{1}H\}$ NMR spectroscopy, we observed that the shifts due to the carbene carbons of the pyridylidenes decrease in the order: *remote*, *normal*, *abnormal*, for rhodium, *and remote*, *abnormal* for iridium.

Rhodium: *remote* ($\delta_c$ = 183.9) > *normal* ($\delta_c$ = 175.7) > *abnormal* ($\delta_c$ = 169.3)

Iridium: *remote* ($\delta_c$ = 164.7) > *abnormal* ($\delta_c$ = 160.8)

This trend is in agreement with the findings by Albrecht and co-workers for a series of palladium complexes with *normal*, *abnormal*, and *remote* pyridylidenes.[60] When the $^{13}C$ NMR resonances of the coordinated carbenes are compared to the corresponding resonances in the pyridinium salt precursors, it is observed that *abnormal* bonding induces the smallest chemical shift difference.

*b) X-Ray Diffraction of $[MI_2(C,C'\text{-imz-pyr})(CH_3CN)_2]^+$ (M = Rh, Ir) complexes,* ***11F****,* ***14G*** *and* ***15I***

*Molecular structure of* ***11F***

Crystals of **11F** suitable for X-ray Diffraction analysis were obtained by slow evaporation of a concentrated solution of the compound in $CH_3CN$.

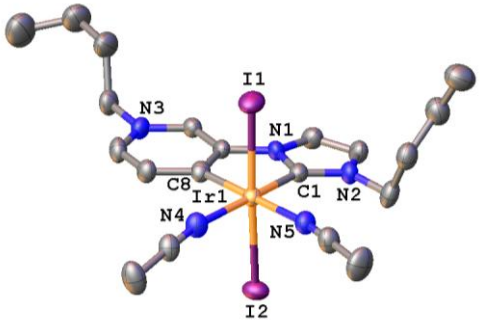


**Figure 3.12** Molecular diagram of complex **11F**. Ellipsoids are at the 50% probability level. Hydrogen atoms and counterion (iodide) are omitted for clarity.

The molecular structure of compound **11F** (Figure 3.12) confirms the chelate coordination of *C,C'*-imz-pyr ligand, where the pyridylidene is coordinated to the metal *via* the *remote* position and forms a five-membered iridacycle. The molecule displays a pseudo-octahedral arrangement about the iridium centre. Two iodide ligands, in a relative *trans* configuration, and two $CH_3CN$ complete the coordination sphere about the metal.

Table 3.1 shows the most representative bond lengths (Å) and angles (º) in complex **11F**. The chelate bite angle (C(1)-Ir(1)-C(8)) is 79.7º. The Ir-$C_{imz}$ (Ir(1)-C(1)) and Ir-$C_{pyr}$ (Ir(1)-C(8)) distances are 1.981 and 1.989 Å, respectively. The structure provides an excellent opportunity to evaluate the relative *trans* influence of the two different carbene ligands within the same molecule, by comparing the Ir-N distances of the $CH_3CN$ *trans* to the imidazolylidene (Ir(1)-N(4)) 2.086 and to the pyridylidene (Ir(1)-N(5)) 2.122 Å, therefore suggesting the stronger *trans* influence of the latter one.

**Table 3.1** Selected bond lengths and angles of complex **11F**

| Bonds lengths (Å) | | Bond angles (º) | |
|---|---|---|---|
| Ir(1)-I(1) | 2.6585(4) | I(1)-Ir(1)-I(2) | 117.548(14) |
| Ir(1)-C(1) | 1.981(5) | C(1)-Ir(1)-C(8) | 79.7(2) |
| Ir(1)-I(2) | 2.6610(4) | | |
| Ir(1)-N(4) | 2.086(4) | | |
| Ir(1)-N(5) | 2.122(5) | | |
| Ir(1)-C(8) | 1.989(5) | | |

*Molecular structure of **14G***

Crystals of **14G** suitable for X-ray Diffraction analysis were obtained by slow diffusion of $Et_2O$ into a concentrated solution of the compound in $CH_3CN$.

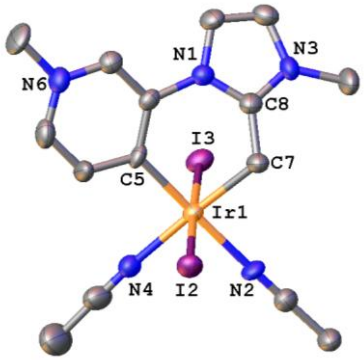


**Figure 3.13** Molecular diagram of complex **14G**. Ellipsoids are at the 50% probability level. Hydrogen atoms and counterion (iodide) are omitted for clarity.

The molecular structure of **14G** (Figure 3.13) confirms that the chelate ligand is coordinated through the *remote* position of the pyridylidene and the methylene group at the C2 position of the imidazolylidene, forming a distorted six-membered iridacycle. The molecule consists of a distorted octahedral structure. Two iodides occupying a *transoid* disposition and two $CH_3CN$ complete the coordination sphere.

Table 3.2 shows the most representative bond lengths (Å) and angles (º) of complex **14G**. The chelate bite angle (C(5)-Ir(1)-C(7)) is 89.0°. The Ir-N distance of the $CH_3CN$ *trans* to the *remote* pyridylidene (Ir(1)-N(2)) is 2.102 Å, similar to that found for the analogous bond in **11F** (Table 3.1).

**Table 3.2** Selected bond lengths and angles of complex **14G**

| Bond lengths (Å) | | Bond angles (º) | |
|---|---|---|---|
| Ir(1)-I(2) | 2.6608(7) | I(2)-Ir(1)-I(3) | 178.00(2) |
| Ir(1)-I(3) | 2.6881(6) | C(5)-Ir(1)-C(7) | 89.0(3) |
| Ir(1)-N(2) | 2.102(6) | | |
| Ir(1)-N(4) | 2.111(8) | | |
| Ir(1)-C(5) | 2.003(7) | | |
| Ir(1)-C(7) | 2.083(8) | | |

*Molecular structure of **15I***

Crystals of **15I** suitable for X-ray Diffraction analysis were obtained by slow diffusion of $Et_2O$ into a concentrated solution of the compound in $CH_3CN$.

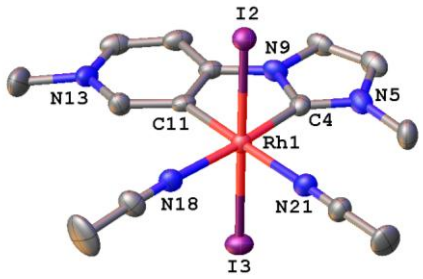


**Figure 3.14** Molecular diagram of complex **15I**. Ellipsoids are at the 50% probability level. Hydrogen atoms and counterion (iodide) are omitted for clarity.

The molecular structure of complex **15I** (Figure 3.14) confirms the chelate coordination of *C,C'*-imz-pyr ligand, where the pyridylidene is coordinated through the *abnormal* position and forms a five-membered rhodacycle. The molecule displays a pseudo-octahedral arrangement about the rhodium centre. Two *transoid* iodides and two *cisoid* $CH_3CN$ complete the coordination sphere about the rhodium centre.

Table 3.3 shows the most representative bond lengths (Å) and angles (º) of complex **15I**. The chelate bite angle is (C(4)-Rh(1)-C(11)) 79.6º. The Rh-$C_{imz}$ (Rh(1)-C(4)) and Rh-$C_{pyr}$ (Rh(1)-C(11)) distances are 1.962 and 1.995 Å, respectively. Again, the structure offers a good opportunity to evaluate the relative *trans* influence of the two types of carbenes, by comparing the Rh-N distances of the $CH_3CN$ *trans* to the imidazolylidene (Rh(1)-N(18)) 2.096 Å and pyridylidene (Rh(1)-N(21)) 2.127 Å, therefore confirming the stronger *trans* influence of the latter one.

**Table 3.3** Selected bond lengths and angles of complex **15I**

| Bond lengths (Å) | | Bond angles (º) | |
|---|---|---|---|
| Rh(1)-I(2) | 2.6666(6) | I(3)-Rh(1)-I(2) | 177.99(2) |
| Rh(1)-I(3) | 2.6504(6) | C(4)-Rh(1)-C(11) | 79.6(2) |
| Rh(1)-N(18) | 2.096(5) | | |
| Rh(1)-C(11) | 1.995(6) | | |
| Rh(1)-C(4) | 1.962(6) | | |
| Rh(1)-N(21) | 2.127(5) | | |

On the basis of bond length analyses of the crystal structures that we have described in this section, we can clearly state that pyridylidenes provide a greater *trans* influence than imidazolylidenes, as previously suggested by other research groups.[47-48] However, we did not find any studies in which a clear comparison between *remote*- and *abnormal*-pyridylidenes was made. By evaluating the bond distances of complexes **11F** and **15I**, we can now confirm that both *abnormal*- and *remote*-pyridylidenes provide a stronger *trans* influence than *normal*-imidazolylidenes (Scheme 3.16). Although the *remotely*-bound complex **11F** and the *abnormally*-bound compound **15I** contain different metals (iridium and rhodium, respectively), we can estimate the relative *trans* influence between these two types of pyridylidenes by comparing with the *trans* influence provided by the imidazolylidene in each complex. In this regard, the Ir-N bond distance of the $CH_3CN$ *trans* to the *remote*-pyridylidene is longer by 1.7% than the Ir-N distance of the $CH_3CN$ *trans* to the imidazolylidene in complex **11F**. The analogue comparison for the Rh-N distances in complex **15I** affords a similar bond length increase (1.5%), which may be interpreted as a consequence of a similar *trans* influence provided by the *remote*- and *abnormal*-pyridylidenes.

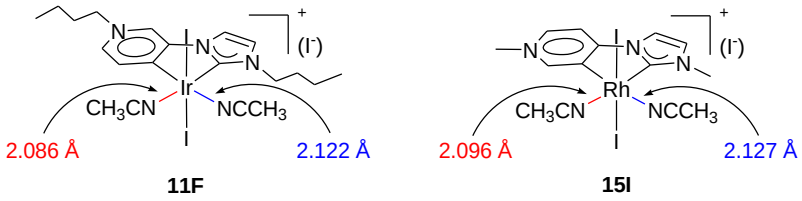


**Scheme 3.16** M-N bond distance of the $CH_3CN$ *trans* to the imidazolylidene and pyridylidene (Å) of complex **11F** and **15I**

### 3.2.3 Synthesis and characterization of [MCp*I(*C,C'*-imz-pyr)]$^+$ (M = Rh, Ir) complexes

Once the coordination of the (*C,C'*-imz-pyr) ligands derived from salts, **[EH$_2$]I$_2$**-**[JH$_2$]I$_2$**, to $[MCl(COD)]_2$ (M = Rh, Ir) was studied, we decided to extend their coordination to M(III) metal precursors, such as $[MCp^*Cl_2]_2$ (M = Rh, Ir). In this section the synthesis, characterization and reactivity of a new family of [MCp*I(*C,C'*-imz-pyr)]$^+$ (M = Rh, Ir) complexes, **17E-24I**, will be discussed. All complexes are new and have been prepared during the development of the present work.

### 3.2.3.1 Synthesis of [MCp*I(*C,C'*-imz-pyr)]$^+$ (M = Rh, Ir) complexes

The synthesis of complexes **17E**-**24I**, has been divided in three parts, in a similar manner as for Section 3.2.2.1. First, compounds obtained from salt **[EH$_2$]I$_2$** will be described. The second part will include the compound synthesised from **[GH$_2$]I$_2$**. Finally, compounds formed from salt **[IH$_2$]I$_2$** will be presented.

*a) Coordination of* **[EH$_2$]I$_2$**. *Synthesis of [MCp*I(C,C'-imz-pyr)]$^+$ (M = Rh, Ir) complexes,* ***17E-20E***

Salt **[EH$_2$]I$_2$** presented different coordination behaviour depending on the metal precursor employed. The reaction of this salt with [IrCp*Cl$_2$]$_2$ in refluxing $CH_3CN$, in the presence of $Cs_2CO_3$ and KI, cleanly led to the formation of the corresponding [IrCp*I(*C,C'*-imz-pyr)]$^+$ complex **17E** in 75% yield, after precipitation from $CH_2Cl_2$/$Et_2O$ (Scheme 3.17). In complex **17E** the pyridylidene coordinates to the metal through the *para*-carbon atom, thus affording a *remote* coordination mode. When the reaction was performed using [RhCp*Cl$_2$]$_2$ in the presence of NaOAc, a mixture of three different complexes was obtained. The three complexes were separated by column chromatography. Elution with $CH_2Cl_2$/acetone (1:1) afforded the separation of a major orange band that contained two [RhCp*I(*C,C'*-imz-pyr)]$^+$ isomers in which the pyridylidene is bound to the metal through the expected *remote* and *normal* coordination modes, **18E** (38%) and **19E** (16%), respectively (Scheme 3.17). Further elution using acetone and a small amount of $KPF_6$ allowed the separation of complex **20E** in 25% yield. In this new complex the imidazolylidene is bound to the metal, while the pyridinium ring is coupled to the Cp* ring, thus affording a Cp* functionalised with a pendant imidazolylidene. All Cp*-functionalised NHCs reported to date have been obtained through the prior preparation of the hybrid Cp*/NHC ligands,[61] so this intramolecular coupling in complex **20E** constitutes the first example of the formation of a NHC-cyclopentadienyl ligand through the post-coupling of previously coordinated ligands.

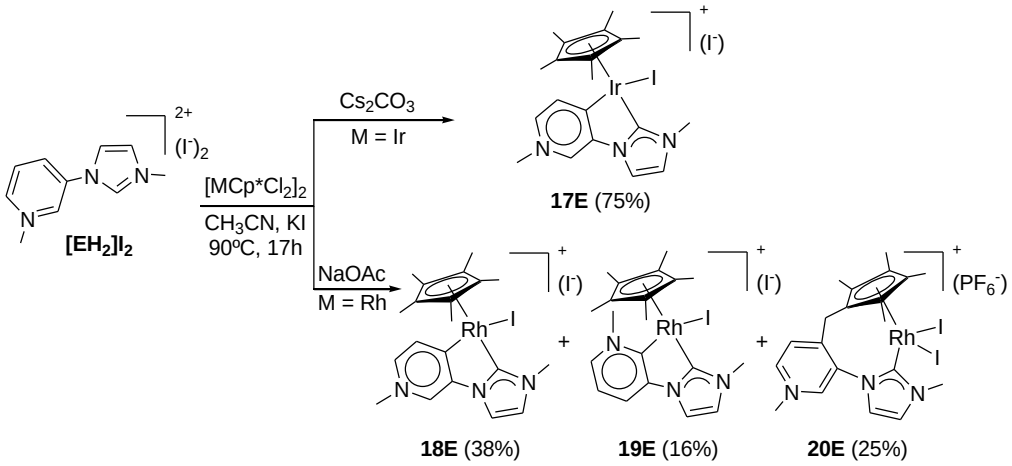


**Scheme 3.17** Synthesis of **17E**-**20E**

We believe that **20E** is formed *via* the formation of tetramethylfulvene-Rh intermediates. It has been reported that while $\eta^4$-tetramethylfulvene complexes react with nucleophiles,[62-66] $\eta^6$-tetrafulvene complexes are more prone to react with electrophiles.[67] The possible reaction pathways leading to complexes **20E** is depicted in Scheme 3.18.

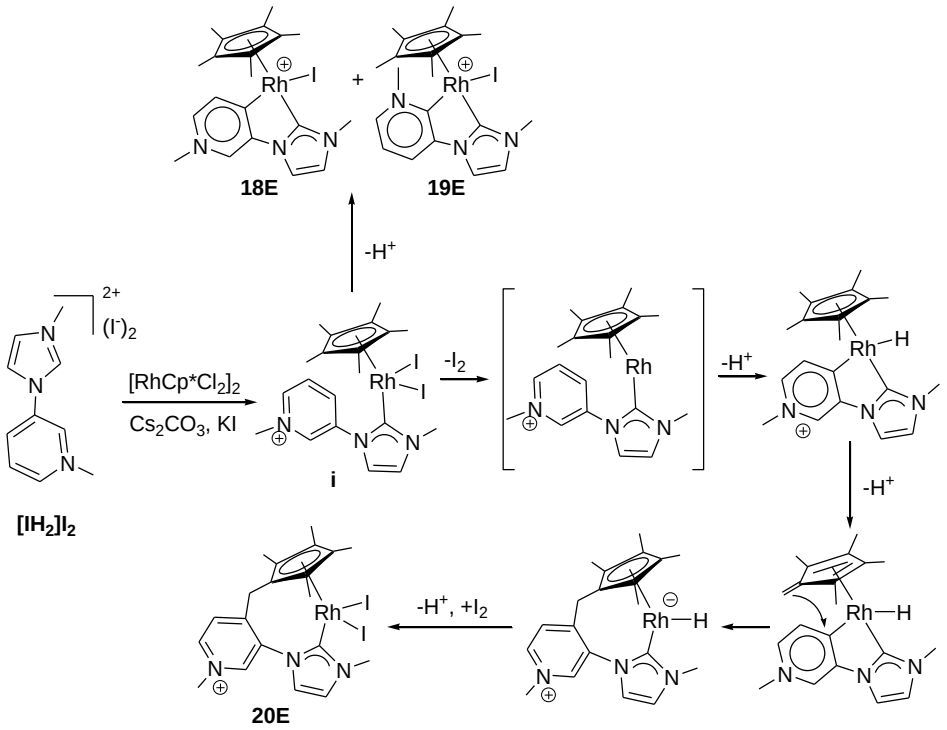


**Scheme 3.18** Proposed reaction pathway for the formation of **18E**, **19E** and **20E**

We initially thought that **20E** could be formed by a rearrangement of complexes **18E** and **19E**. In this regard, several reactions implying the reflux of **18E** and **19E** in $CH_3CN$ in the presence of KI and/or $I_2$ did not produce any change in the starting compounds, so we believe that these two compounds are formed through an irreversible metal-mediated C-H activation of the pyridinium ring and subsequent deprotonation of the metal hydride intermediate with a base. These hypothesis is supported by our previous experimental and theoretical studies on the mechanisms of the formation of bis-NHC complexes of Cp*M (M = Rh and Ir).[22, 57] The formation of complex **20E** may occur through the reductive elimination of diiodine from the reaction intermediate **i** (Scheme 3.18), followed by the oxidative addition of the pyridinium ring to form a Rh(III) hydride with a imidazolylidene-pyridylidene ligand. The deprotonation of the Cp* ligand may induce a nucleophilic attack of the fulvene on the pyridylidene carbon, affording the C-C coupling between the Cp* and the pyridinium rings. Finally, the oxidative addition of diiodine and deprotonation of the hydride would allow the formation of the final product. In the course of the

purification of complex **20E** by column chromatography we observed the separation of a first band containing a small amount of diiodine. We have performed control experiments in order to discard that the diiodine may come from the oxidation of the KI present in the reaction medium, therefore we believe that it may be formed from the reductive elimination from species **i**.

All complexes were characterised by means of NMR spectroscopy, mass spectrometry and elemental analysis. Satisfactory elemental analysis of **20E** could not be obtained probably because it was too hygroscopic. The molecular structure of **18E** and **20E** were confirmed by means of X-Ray Diffraction. The spectroscopic characterization of compounds **18E**, **19E** and **20E** is discussed in detail in section 3.2.3.2. All the details of the spectroscopic data for compound **17E** can be found in the Experimental Section (Chapter 5).

*b) Coordination of* ***[GH$_2$]I$_2$****. Synthesis of [MCp*I(C,C'-imz-pyr)]$^+$ (M = Rh, Ir) complexes,* ***21G*** *and* ***22G***

Aiming to corroborate the tendency of our salt **[GH$_2$]I$_2$** to undergo a C-H activation of the $CH_3$ group at the C2 position of the imidazolium ring, as previously observed in compound **14G**, we decided to react **[GH$_2$]I$_2$** with $[IrCp^*Cl_2]_2$. The reaction of this salt with $[IrCp^*Cl_2]_2$ in refluxing $CH_3CN$, in the presence of $Cs_2CO_3$ and KI, afforded the expected chelate complex **21G** (Scheme 3.19), where the C-H activation of the $CH_3$ group blocking the C2 took place. However, when the reaction was carried out using $[RhCp^*Cl_2]_2$, we obtained the unexpected complex, **22G**, where along with the expected C-H activation, a reductive coupling between the Cp* and the pyridinium rings took place.

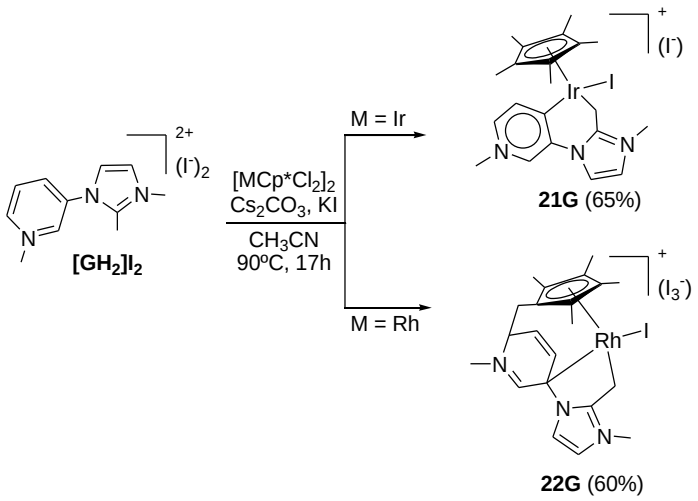


**Scheme 3.19** Synthesis of **21G** and **22G**

As previously explained for complex **20E** (Scheme 3.18), we believe that **22G** is formed *via* the formation of tetramethylfulvene-Rh intermediate. The possible reaction pathway leading to complex **22G** is depicted in Scheme 3.20.

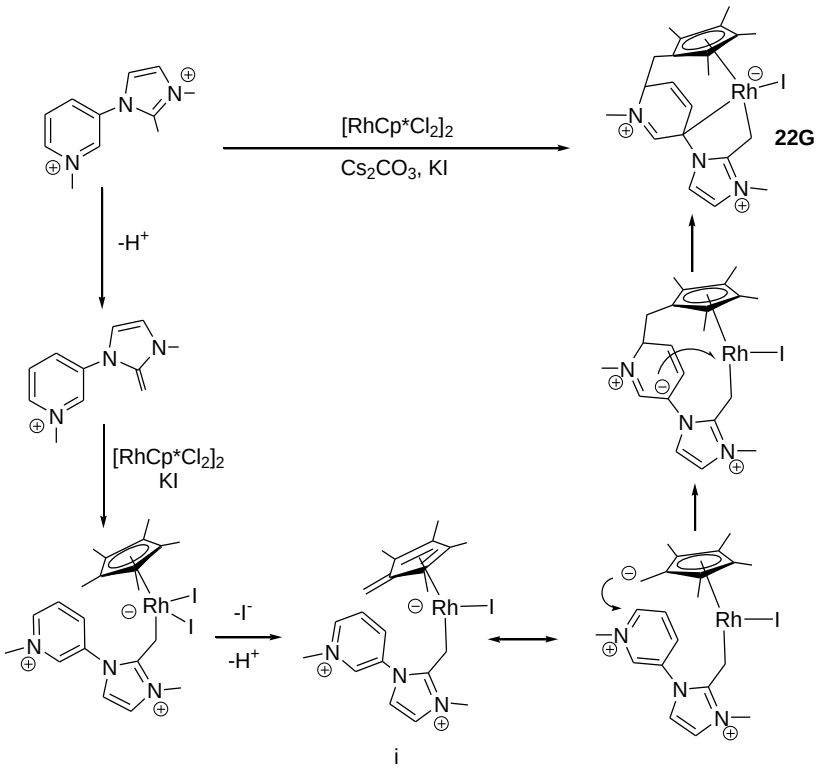


**Scheme 3.20** Reaction pathway for the formation of **22G**

In the formation of complex **22G**, we may first have the coordination through the methylene resulting from the C-H activation of the $CH_3$ group at the C2 position of the imidazolium ring (Scheme 3.20). Deprotonation of this new species results in the formation of the tetramethylfulvene intermediate **i**, which can undergo a nucleophilic attack at the carbon atom adjacent to the nitrogen of the pyridinium ring. The selectivity on this nucleophilic attack may be explained as a consequence of the relative perpendicular disposition of the two heterocycles (as shown in the molecular structure of complex **22G**, Figure 3.25), which leaves the carbon next to the nitrogen close to the fulvene ligand. The nucleophilic attack of the carbon bound to the imidazolylidene on the rhodium centre generates a Rh-C bond in compound **22G**. The overall process implies the dearomatization of the pyridinium ring through consecutive nucleophilic and electrophilic attacks on the ring.

Complexes **21G** and **22G** were characterised by means of NMR spectroscopy, mass spectrometry and elemental analysis. The molecular structure of **22G** was confirmed

by means of X-Ray Diffraction. The spectroscopic characterization of compound **22G** is discussed in detail in section 3.2.3.2 due to its particularity. A $^{1}$H-$^{1}$H gCOSY NMR experiment was carried out in order to confirm the assignment of the signals displayed in the $^{1}$H NMR spectrum of **22G** (see Experimental Section in Chapter 5). All the details of the spectroscopic data for compound **21G** can be found in the Experimental Section (Chapter 5).

*c) Coordination of* ***[IH$_2$]I$_2$****. Synthesis of [MCp*I(C,C'-imz-pyr)Cp*I]$^{+}$ (M = Rh, Ir) complexes,* ***23I*** *and* ***24I***

As seen in Scheme 3.15 (Section 3.2.2), the preparation of the rhodium and iridium complexes with the chelate *C,C'*-imz-pyr ligands in which the pyridylidene is bound by the *abnormal* position, could be achieved by using salt **[IH$_2$]I$_2$**.[68] The reaction of **[IH$_2$]I$_2$** with [IrCp*Cl$_2$]$_2$ in refluxing $CH_3CN$ in the presence of $Cs_2CO_3$ and KI, allowed the formation of the expected [IrCp*I(*C,C'*-imz-pyr)]$^{+}$ complex **24I**, in which the pyridylidene ligand is coordinated to iridium in an *abnormal* coordination mode (Scheme 3.21). This result is consistent with our previous findings in which **[IH$_2$]I$_2$** reacted with [IrCl(COD)]$_2$, affording the same type of coordination of the ligand (**15I**, Scheme 3.15). Along with complex **24I**, we could also isolate a small amount of a dimetallic species, **23I**, in which a ring-opening of the imidazole ring has occurred (Scheme 3.21). These two compounds were separated by column chromatography. Elution with $CH_2Cl_2$/acetone (8:2) afforded the separation of a yellow band that contained compound **23I**. Further elution with acetone separated an orange band that contained compound **24I**.

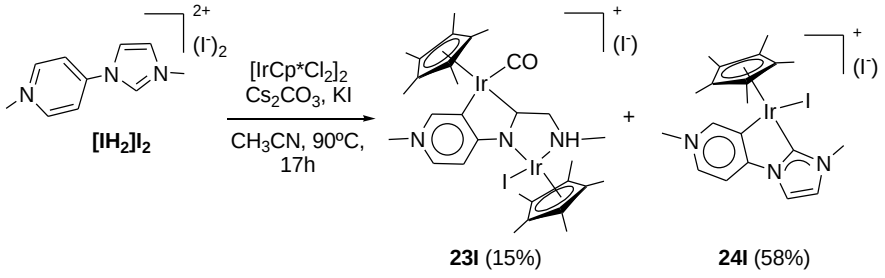


**Scheme 3.21** Synthesis of **23I** and **24I**

We believe that the formation of **23I** occurs *via* the hydrolysis of the imidazolylidene fragment. Imidazole-2-ylidenes can be hydrolyzed under basic conditions in the

presence of small amounts of $H_2O$, allowing the formation of iminoformamides,[69-71] although this is a very slow process for aromatic imidazolium derivatives,[69, 71] implying that it may be of minor importance in all the reactions pursuing the coordination of NHCs to metals that are carried out at low temperatures and with short-time reactions. In fact, in a very recent study, it has been reported that the attempt to coordinate one bisimidazolium salt to $[IrCl(COD)]_2$ in the presence of $Cs_2CO_3$ (9 hours of reaction in refluxing $CH_3CN$), afforded a mono-NHC-Ir(I) species with a iminoformamide branch formed by hydrolysis of the formed free carbene.[72] In our case, the hydrolysis of the imidazolylidene should afford the formation of **[IH]I** (Scheme 3.22), which in the presence of $[IrCp^*Cl_2]_2$ might lead to the ring-opened product **23I**. In addition to hydrolysis, further rearrangements involving a decarbonylation of the aldehyde to generate the carbonyl ligand and the amine branch took place during the reaction. In order to prove the participation of **[IH]I** in the formation of **23I**, we added an equimolecular amount of $Cs_2CO_3$ to a solution of **$[IH_2]I_2$** in $CD_3CN$ (Scheme 3.22). After 5 minutes of stirring at room temperature, we observed the formation of **[IH]I** (30%, estimated by $^1H$ NMR), but the reaction became quantitative only after 3h at 80ºC.

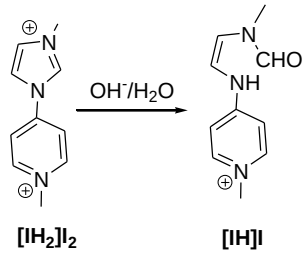


**Scheme 3.22** Formation of **[IH]I**

In order to give further support to the possible involvement of **[IH]I** in the process of formation of the dimetallic complex **23I**, we performed a reaction in which we first hydrolysed salt **$[IH_2]I_2$** to form **[IH]I** in $CH_3CN$ in the presence of $Cs_2CO_3$. Only after we confirmed that **[IH]I** was formed, we added the corresponding amount of $[IrCp^*Cl_2]_2$, and we observed that the yield in the formation of **23I** increased up to 40 %. Under these reaction conditions we did not detect the formation of complex **24I.**

Complexes **23I** and **24I** were characterised by means of NMR spectroscopy, mass spectrometry and elemental analysis. The molecular structures of **23I** and **24I** were

confirmed by means of X-Ray Diffraction. The spectroscopic characterization of compound **23I** is discussed in detail in section 3.2.3.2. All the details of the spectroscopic data for compound **24I** can be found in the Experimental Section (Chapter 5).

### 3.2.3.2 Characterization of [MCp*I(*C,C'*-imz-pyr)]$^+$ (M = Rh, Ir) complexes

*a) Spectroscopic characterization of [MCp*I(C,C'-imz-pyr)]$^+$ (M = Rh, Ir) complexes, **18E**, **19E**, **20E**, **22G** and **23I***

*$^1$H NMR spectrum of **18E** and **19E***

Figure 3.15 shows the $^1$H NMR spectrum of a mixture of compounds **18E** and **19E**. The assignment of the *remote* and *normal* coordination of the pyridylidene for **18E** and **19E** can be easily determined by the evaluation of the signals attributed to the proton of the C*H* groups of the pyridylidene. For **18E**, the signals due to the pyridylidene protons appear as two doublets at 9.93 (a) and 8.22 ppm (c), and as a doublet of doublets at 8.06 ppm (c). The signals of the proton of the C*H* groups due to the imidazolylidene are shown, as two doublets at 8.55 and 7.26 ppm (b). For **19E**, the three resonances due to the pyridylidene protons are shown as a doublet of doublets at 8.74 (a'), a doublet at 8.50 (a') and a doublet of doublets at 7.51 ppm (c'). The protons of the imidazolylidene display their resonances as two doublets at 8.32 and 7.39 ppm (b'). All the rest of the signals due to the protons of the C$H_3$ groups of the pyridylidene, imidazolylidene and Cp* ring, of both **18E** and **19E**, are conveniently assigned in the $^1$H NMR spectrum shown in Figure 3.15.

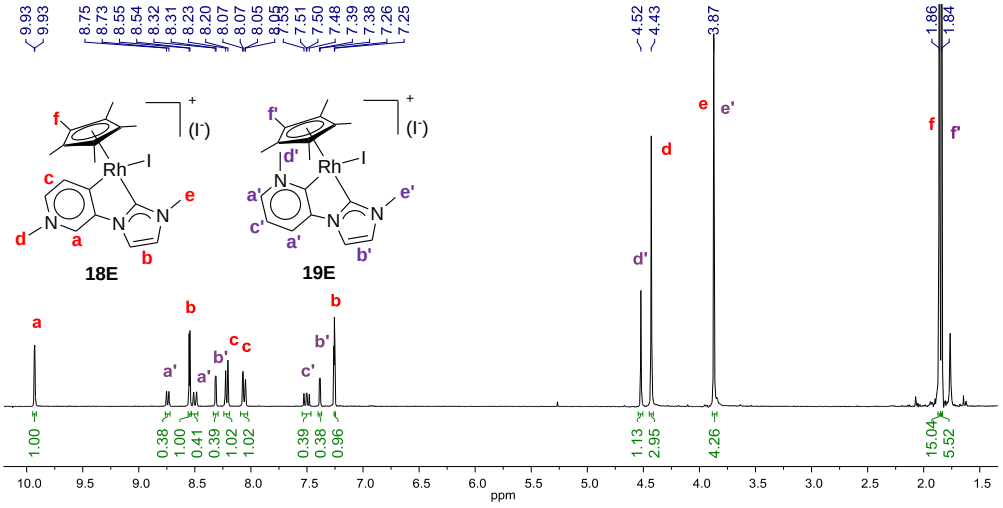


**Figure 3.15** $^{1}$H NMR spectrum of **18E** and **19E** in $CDCl_3$

*$^{13}C\{^{1}H\}$ NMR spectrum of* **18E** and **19E**

Figure 3.16 shows the $^{13}C\{^{1}H\}$ NMR spectrum of the mixture of **18E** and **19E**. Probably, the most characteristic signals are the two doublets attributed to the metallated carbene carbon of the pyridylidene and the imidazolylidene. For **18E** these two doublets are observed at 194.8 (d, $^{1}J_{RhC}$ = 37 Hz) (1), and 181.7 ppm (d, $^{1}J_{RhC}$ = 55 Hz) (2), respectively. The signals due to the quaternary carbons of pyridylidene and Cp* ring appear at 147.3 (3) and 100.1 ppm (d, $^{1}J_{RhC}$ = 5 Hz) (6), respectively. The signals corresponding to the carbon of the *C*H groups of the pyridylidene are shown at 136.5, 135.0 and 125.0 ppm (4). The resonances due to the carbon of the *C*H groups of the imidazolylidene are displayed at 124.2 and 118.4 ppm (5). For **19E**, the related signals corresponding to the two doublets attributed to the metallated carbene carbon are displayed at 192.6 (d, $^{1}J_{RhC}$ = 45 Hz) (1') and 179.9 ppm (d, $^{1}J_{RhC}$ = 54 Hz) (2'). The signals due to the quaternary carbon of pyridylidene and Cp* ring are shown at 146.9 (3') and 101.0 ppm (d, $^{1}J_{RhC}$ = 5 Hz) (6'), respectively. The signals corresponding to the carbon of the *C*H groups of the pyridylidene display their resonance at 141.0, 125.6 and 122.0 ppm (4'). The resonances due to the carbon of the *C*H groups of the imidazolylidene appear at 120.6 and 119.1 ppm (5'). All the rest of the signals due to the carbon of the *C*$H_3$ groups of the pyridylidene, imidazolylidene and Cp* ring, of both **18E** and **19E**, are conveniently assigned on the $^{13}C$ NMR spectrum shown in Figure 3.16.

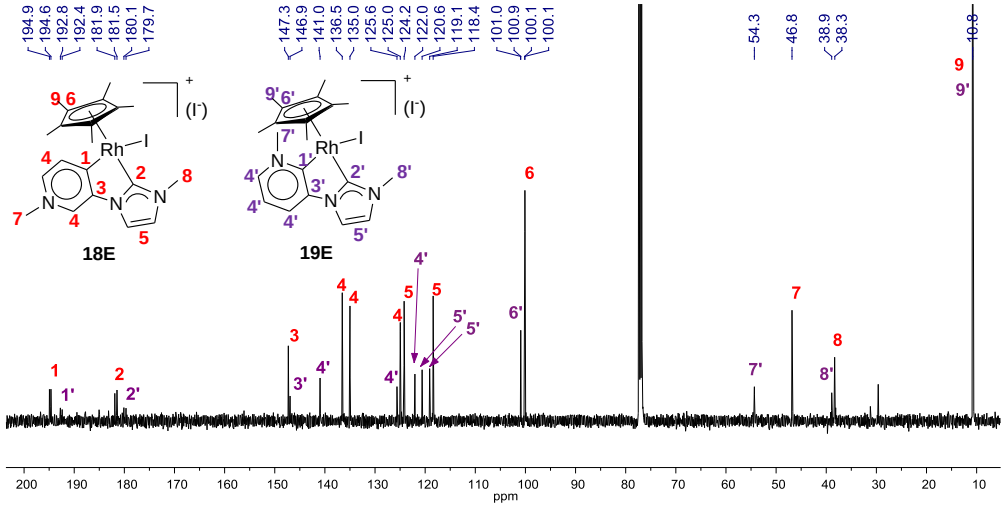


**Figure 3.16** $^{13}C\{^{1}H\}$ NMR spectrum of **18E** and **19E** in $CDCl_3$

*$^{1}H$ NMR spectrum of **20E***

Figure 3.17 shows the $^{1}H$ NMR spectrum of **20E**. The first evidence that the activation of the Cp* ligand has been produced is shown by the characteristic signals resulting from the protons of the four inequivalent Cp*C*H*$_3$ groups at 2.25, 2.21, 1.84, 1.35 ppm (g) and the two diastereotopic protons of the C*H*$_2$ linker at 3.62 (d, $^{3}J_{HH}$ = 15 Hz) and 3.44 ppm (d, $^{3}J_{HH}$ = 15 Hz) (f). The signals due to the protons of the C*H* groups of the pyridine ring appear as a singlet at 8.77 (a) and as two doublets at 8.59 and 8.12 ppm (b). The signals attributed to the proton of the C*H* groups of the imidazolylidene are shown as two doublets at 7.56 and 7.52 ppm (c). Finally, the protons of the C*H*$_3$ groups of the pyridine ring and imidazolylidene display their resonances at 4.25 (d) and 4.18 ppm (e).

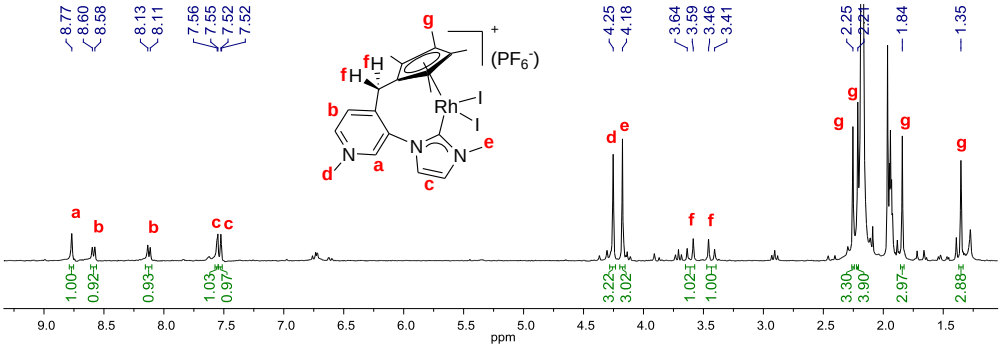


**Figure 3.17** $^{1}$H NMR spectrum of **20E** in $CD_3CN$

*$^{13}C\{^{1}H\}$ NMR spectrum of* **20E**

Figure 3.18 shows the $^{13}C\{^{1}H\}$ NMR spectrum of **20E**. Probably, the most characteristic signals are attributed to the metallated carbon of the imidazolylidene at 170.1 ppm (d, $^{1}J_{RhC}$ = 57 Hz) (1), and the five inequivalent quaternary carbons of the Cp* (d, $^{1}J_{RhC}$ = 7 Hz) at 113.3, 108.1, 97.4, 94.6 and 80.6 ppm (6). The signals due to the quaternary carbon of pyridylidene are shown at 152.1 (2) and 142.7 ppm (4). The rest of the signals corresponding to the carbon of the *C*H and *C*H$_3$ groups of the pyridine ring, and imidazolylidene, as well as for the *C*H$_2$ linker and the *C*H$_3$ groups of the Cp* ring, are conveniently displayed in the spectrum.

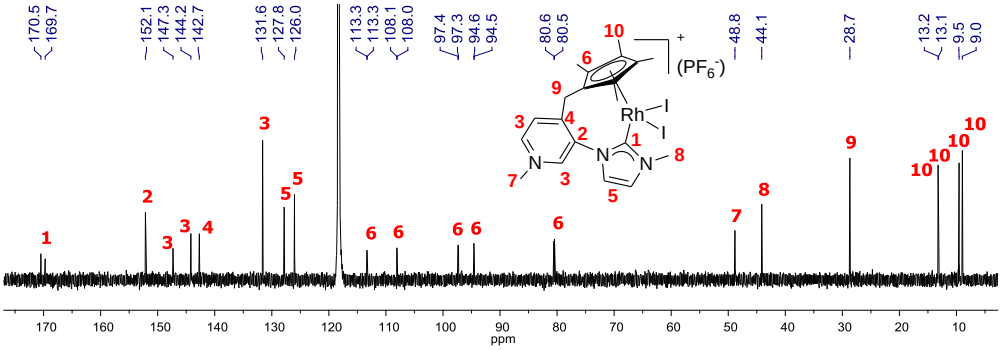


**Figure 3.18** $^{13}C\{^{1}H\}$ NMR spectrum of **20E** in $CD_3CN$

*$^{1}H$ NMR spectrum of* ***22G***

Figure 3.19 shows the $^{1}$H NMR spectrum of **22G**. The first evidence that the coupling between the Cp* and the pyridinium rings has been produced is indicated by the four

distinct signals corresponding to the inequivalent C$H_3$ groups at 2.15, 1.82, 1.74 and 1.12 ppm (i), and the two diastereotopic protons of the $CH_2$ linker at 1.97 (dd, $^3J_{HH}$ = 1.5 Hz, $^2J_{HH}$ = 14 Hz) and 1.68 ppm (dd, $^3J_{HH}$ = 2 Hz, $^2J_{HH}$ = 14 Hz) (j). The signals due to the protons of the metallated methylene appear as two diastereotopic protons at 3.46 (dd, $^2J_{RhH}$ = 3 Hz, $^2J_{HH}$ = 14 Hz) and 2.71 ppm (dd, $^2J_{RhH}$ = 3 Hz, $^2J_{HH}$ = 14 Hz) (g). All the rest of the signals are conveniently displayed on the spectrum shown in Figure 3.19, and are consistent with the structure assigned to the complex.

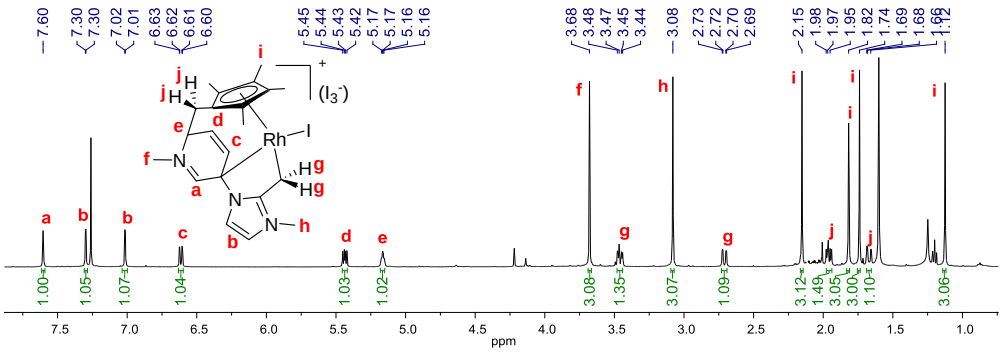


**Figure 3.19** $^1$H NMR spectrum of **22G** in $CDCl_3$

*$^{13}C\{^1H\}$ NMR spectrum of **22G***

Figure 3.20 shows the $^{13}C\{^1H\}$ NMR spectrum of **22G**. The most characteristic signals are probably the ones attributed to the five inequivalent quaternary carbons of the Cp*, at 106.0, 101.0, 99.1, 89.8 and 87.4 ppm (6) and two doublets at 64.6 (d, $^1J_{RhC}$ = 15.1 Hz) (7) and 2.0 ppm (d, $^1J_{RhC}$ = 26.9 Hz) (13), which correspond to the two metallated carbon atoms of the pyridine and $CH_3$ groups, respectively. The rest of the signals corresponding to the pyridine ring, imidazole ring and Cp* $CH_3$ carbons, are conveniently displayed in the spectrum.

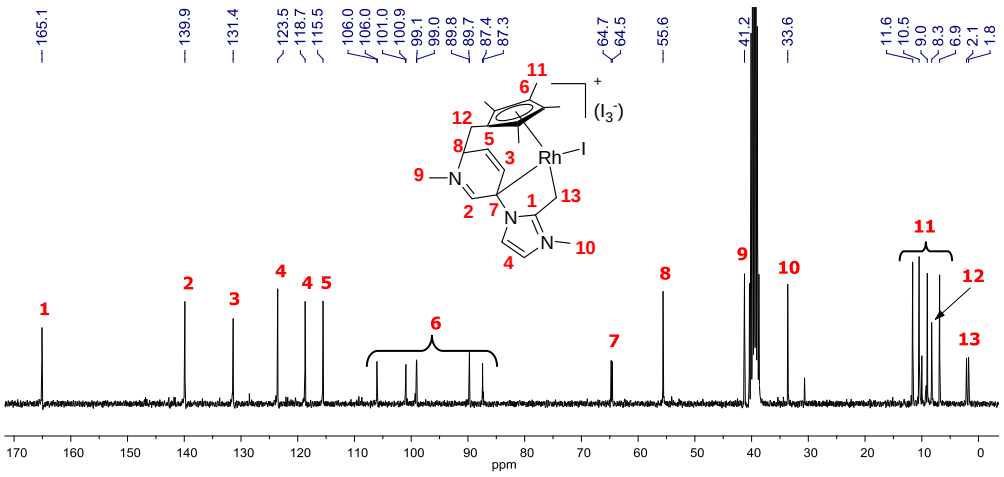


**Figure 3.20** $^{13}C\{^{1}H\}$ NMR spectrum of **22G** in DMSO-$d_6$

*$^{1}H$ NMR spectrum of **23I***

Figure 3.21 shows the $^{1}H$ NMR spectrum of **23I**. The first evidence that the compound **23I** is an 'IrCp*' dimer is shown by the two different signals due to the protons of the C$H_3$ groups of two different Cp* rings at 2.01 and 1.91 ppm (g). All the rest of the signals are conveniently displayed on the spectrum shown in Figure 3.21, and are consistent with the structure assigned to the complex.

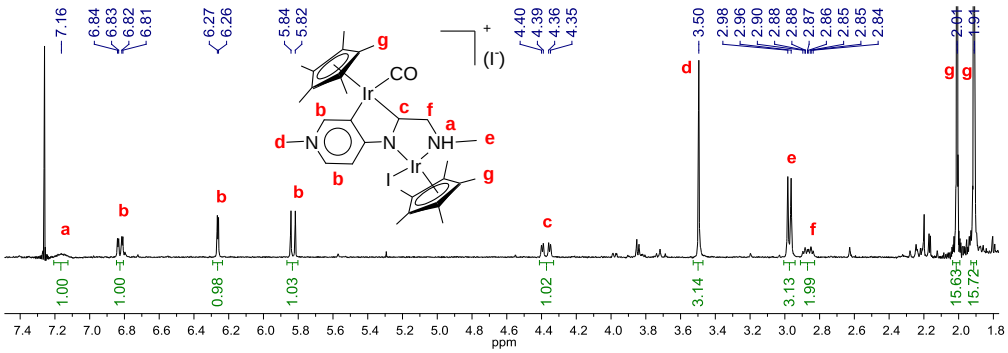


**Figure 3.21** $^{1}H$ NMR spectrum of **23I** in $CDCl_3$

*$^{13}C\{^{1}H\}$ NMR spectrum of **23I***

Figure 3.22 shows the $^{13}C\{^{1}H\}$ NMR spectrum of **23I**. The most characteristic signals are attributed to the metallated carbon of the pyridylidene at 171.8 ppm (1) and to the carbon of the carbonyl ligand at 170.4 ppm. Two different signals due to the

quaternary carbons of the two different Cp* rings are shown at 99.5 and 86.6 ppm (5). The signals corresponding to the carbons of the *C*$H_3$ groups of the two different Cp* rings appear at 10.6 and 9.7 ppm (10). The rest of the signals are conveniently displayed in the spectrum.

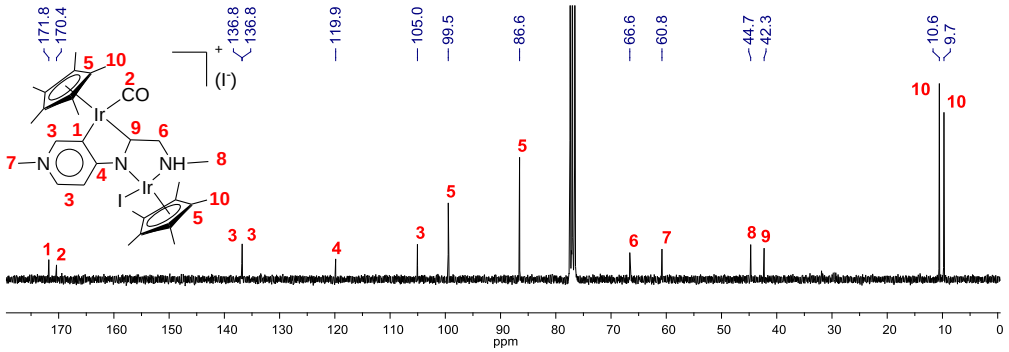


**Figure 3.22** $^{13}C\{^{1}H\}$ NMR spectrum of **23I** in $CDCl_3$

*b) X-Ray Diffraction of [MCp*I(C,C'-imz-pyr)]$^+$ (M = Rh, Ir) complexes,* ***18E****,* ***19E****,* ***20E****,* ***22G*** *and* ***23I***

*Molecular structure of* ***18E***

Slow diffusion of $Et_2O$ into a concentrated solution of the mixture of compounds **18E** and **19E** in $CH_3CN$ gave crystals of **18E**, suitable for X-ray Diffraction analysis.

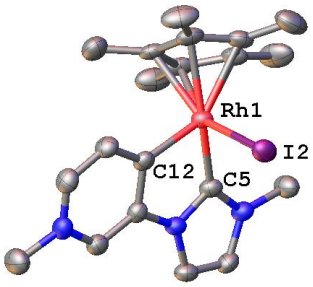


**Figure 3.23** Molecular diagram of complex **18E**. Ellipsoids at 50% probability level. Hydrogen atoms, counterion (iodide) and solvent ($CH_2Cl_2$) are omitted for clarity. Only one of the two molecules in the asymmetric unit is represented.

The molecular structure of compound **18E** (Figure 3.23) confirms that the pyridylidene is coordinated to the metal *via* the *remote* form. The molecule can be

regarded as a three-legged piano stool. Along with chelate *C,C'*-imz-pyr ligand, an iodide and a pentamethylcyclopentadienyl ligand complete the coordination sphere about the rhodium atom.

Table 3.4 shows the most representative bond lengths (Å) and angles (º) of complex **18E**. The chelate bite angle C(5)-Rh(1)-C(12) is 78.8º. The Rh-$C_{imz}$ (Rh(1)-C(5)), Rh-$C_{pyr}$ (Rh(1)-C(12)) and Rh-$C_{centroid}$ (Rh(1)-$C_{centroid}$) distances are 2.025, 2.009 and 1.866 Å, respectively.

**Table 3.4** Selected bond lengths and angles of complex **18E**

| Bond lengths (Å) | | Bond angles (º) | |
|---|---|---|---|
| Rh(1)-I(2) | 2.6932(5) | C(5)-Rh(1)-C(12) | 78.8(2) |
| Rh(1)-C(5) | 2.025(5) | | |
| Rh(1)-C(12) | 2.009(5) | | |
| Rh(1)-$C_{centroid}$ | 1.866(5) | | |

*Molecular structure of **20E***

Slow diffusion of $Et_2O$ into a concentrated solution of compound **20E** in $CH_3CN$ gave crystals suitable for X-ray Diffraction analysis.

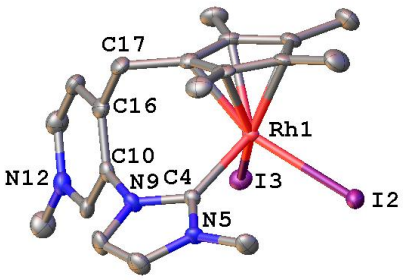


**Figure 3.24** Molecular diagram of complex **20E**. Only one enantiomer of the two present in the structure is displayed. Ellipsoids at 50% probability level. Hydrogen atoms and counterion (iodide) omitted for clarity.

The molecular structure of compound **20E** (Figure 3.24) verifies the C-C coupling between the pyridinium ring and one of the $CH_3$ groups of the Cp* ligand, therefore a chelating $\eta^5$-(tetramethylcyclopentadienyl)/NHC ligand has been formed. Two iodides complete the coordination sphere about the Rh(III) centre.

Table 3.5 shows the most representative bond lengths (Å) and angles (º) of complex **20E**. The Rh-$C_{imz}$ (Rh(1)-C(4)) and Rh-$C_{centroid}$ (Rh(1)-$C_{centroid}$) distances are 2.032 and 1.823 Å, respectively. All other distances and angles are unexceptional and compare well with related compounds reported by our group.[73-75] The two Cp* carbons *trans* to the imidazolylidene ligand display a larger Rh-$C_{imz}$ distance, than that shown for the three other carbon atoms (compare 2.245 and 2.240, with 2.132-2.191 A˚, respectively) as a consequence of the *trans* influence of the NHC ligand. This effect is also observed in related compounds reported by our group.[73-75]

**Table 3.5** Selected bond lengths of complex **20E**

| Bond lengths (Å) | |
|---|---|
| Rh(1)-I(2) | 2.7063(4) |
| Rh(1)-I(3) | 2.7020(4) |
| Rh(1)-C(4) | 2.032(3) |
| Rh(1)-$C_{centroid}$ | 1.823(3) |

*Molecular structure of **22G***

Slow diffusion of hexane into a concentrated solution of compound **22G** in $CH_2Cl_2$ gave crystals suitable for X-ray Diffraction analysis.

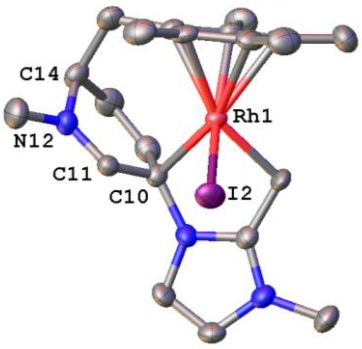


**Figure 3.25** Molecular diagram of complex **22G**. Only one enantiomer is displayed. Ellipsoids at 50% probability level. Hydrogen atoms and counterion (triiodide) omitted for clarity.

The molecular structure of compound **22G** (Figure 3.25) confirms the coupling of the pyridinium ring to one of the $CH_3$ groups of the Cp* ligand. In this case, the

pyridinium has been dearomatized and contains two $sp^3$ carbon atoms, at the 2 and 5 positions of the ring (carbons labelled as C(10) and C(14) in the molecular diagram). The C2 position of the pyridinium ring (labelled as C(14) in the molecular structure) is directly bound to the methylene group of the cyclopentadienyl ligand. The C5 carbon (labelled as C(10) in the molecular structure) and the carbon of the $CH_3$ group of the C2 position of the imidazolium ring (labelled as C(3) in the molecular structure), are bound to the rhodium centre. One iodide complete the coordination sphere about the Rh(III) centre. The compound crystallized with a $I_3^-$ counteranion, an indication of the existence of residual $I_2$ present in the reaction media.

Table 3.6 shows the most representative bond lengths (Å) and angles (º) of complex **22G**. The Rh(1)-C(10), Rh(1)-C(3) and Rh-$C_{centroid}$ (Rh(1)-$C_{centroid}$) distances are 2.191, 2.112 and 1.832 Å, respectively. The presence of the C=N double bond (N(12)-C(11)) 1.316 Å confirms the iminium character of the ring, which adopts a boat-conformation with the carbons labelled as C(10) and C(14) out of the plane formed by the other four atoms of the pyridinium.

**Table 3.6** Selected bond lengths and angles of complex **22G**

| Bond lengths (Å) | | Bond angles (º) | |
|---|---|---|---|
| Rh(1)-I(2) | 2.7256(5) | C(3)-Rh(1)-C(10) | 78.85(19) |
| Rh(1)-C(3) | 2.112(5) | | |
| Rh(1)-C(10) | 2.191(5) | | |
| Rh(1)-$C_{centroid}$ | 1.832(5) | | |
| N(12)-C(11) | 1.316(6) | | |

*Molecular structure of **23I***

Slow diffusion of $Et_2O$ into a concentrated solution of compound **23I** in $CHCl_3$ gave crystals suitable for X-ray crystallography.

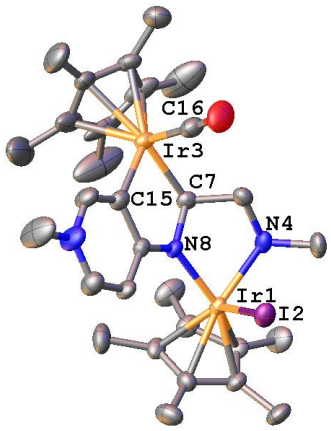


**Figure 3.26** Molecular diagram of complex **23I**. Ellipsoids at 50% probability level. Hydrogen atoms, counterion (iodide), and solvent ($CH_2Cl_2$ and $Et_2O$) omitted for clarity.

The molecular structure of compound **23I** (Figure 3.26) confirms the dimetallic nature of the molecule. The bis-heterocyclic ligand has been transformed into one pyridylidene-amino-amido ligand. The pyridylidene is bound to one iridium fragment through an *abnormal* coordination form, and the amino-amido part of the ligand is *N,N'*-chelating a second iridium fragment. The ethylene linker between the amino-amido functionalities is metallated to the first iridium fragment by the α-carbon relative to the amido group, so in the same molecule we have a *C,C'* and a *N,N'* chelating ligands binding the two different iridium fragments. The iridium fragment with the *C,C'* chelating ligand is bound to a carbonyl group.

Table 3.7 shows the most representative bond lengths (Å) and angles (º) of complex **23I**. The Ir(1)-N(4), Ir(1)-N(8) and Ir-$C_{centroid}$ Ir(1)-$C_{centroid}$ distances are 2.153, 2.078 and 1.798 Å, respectively. The Ir(3)-C(7), Ir-$C_{pyr}$ Ir(3)-C(15) and Ir-$C_{centroid}$ Ir(3)-$C_{centroid}$ distances are 2.099, 2.056 and 1.903 Å, respectively.

**Table 3.7** Selected bond lengths and angles of complex **23I**

| Bond lengths (Å) | | Bond angles (º) | |
|---|---|---|---|
| Ir(1)-I(2) | 2.7208(5) | N(8)-Ir(1)-N(4) | 78.8(2) |
| Ir(1)-N(4) | 2.153(5) | C(7)-Ir(3)-C(15) | 78.1(2) |
| Ir(1)-N(8) | 2.078(5) | | |
| Ir(1)-$C_{centroid}$ | 1.798(5) | | |
| Ir(3)-C(7) | 2.099(6) | | |
| Ir(3)-C(15) | 2.056(7) | | |
| Ir(3)-C(16) | 1.837(8) | | |
| Ir(3)-$C_{centroid}$ | 1.903(5) | | |

## 3.3 CONCLUSIONS

In this work we have shown the systematic preparation of the series of imidazolylidene-pyridylidene complexes of rhodium- and iridium(III) with the three possible types of coordination of the pyridylidene (*normal*, *abnormal*, and *remote*). Attempts to obtain analogous complexes with the *abnormal* coordination of the imidazolylidene by using a C2-$CH_3$-substituted imidazolium resulted in the aliphatic C-H activation of the $CH_3$ group, affording the methylene-bound imidazolium, or C-C bond cleavage, yielding the demethylated products, which are similar to the products obtained when non-substituted imidazoliums were used. Although the aliphatic C-H activation of the $CH_3$ group in C2-$CH_3$-substituted imidazoliums has already been described for iridium and rhodium complexes,[22, 55] this is the first time that the demethylation is observed for these two metals. In any case, the difficulties in achieving the *abnormal* coordination of the imidazolylidene when a pyridylidene is bound to the metal are remarkable. The evaluation of the crystal structures of complexes **11F**, **14G**, and **15I** allowed us to evaluate the relative *trans* influence of the pyridylidene and the imidazolylidene. Both *remote* and *abnormal* coordinations of the pyridylidene provide similar *trans* influence, this being larger than the one provided by the imidazolylidene.

Our work regarding the coordination of the same type of imidazolylidene-pyridylidene ligands to $[MCp^*Cl_2]_2$ (M = Rh, Ir), provides three different pieces of evidence of the non-conventional behaviour of a series of imidazolylidene-pyridylidene ligands, by describing three unprecedented new reactivities. The formation of the Cp*-functionalised NHC through the intramolecular coupling of two existing ligands in the molecule constitutes an interesting alternative to the methods that have been reported to date, implying the use of pre-formed Cp*-NHC precursors.[61] The reductive coupling of the Cp* and the pyridine opens the possibility for the use of 'M(III)Cp*' (M = Rh, Ir) complexes in the reduction of pyridiniums. Finally, the formation of the dimetallic complex **23I** underlines the importance of the hydrolysis of free carbenes in the synthesis of metal complexes; a reaction that is most of the times underestimated and should be taken under serious consideration in all reactions involving the use imidazolylidenes in long-time reactions when traces of water may be present.

## 3.4 REFERENCES


1. Herrmann, W. A.; Kocher, C., *Angew. Chem. Int. Ed.* **1997**, *36*, 2163-2187.
2. Herrmann, W. A.; Elison, M.; Fischer, J.; Kocher, C.; Artus, G. R. J., *Angew. Chem. Int. Ed.* **1995**, *34*, 2371-2374.
3. Hahn, F. E., *Angew. Chem. Int. Ed.* **2006**, *45*, 1348-1352.
4. de Fremont, P.; Marion, N.; Nolan, S. P., *Coord. Chem. Rev.* **2009**, *253*, 862-892.
5. Poyatos, M.; Mata, J. A.; Peris, E., *Chem. Rev.* **2009**, *109*, 3677-3707.
6. Crabtree, R. H., *Coord. Chem. Rev.* **2007**, *251*, 595-595.
7. Diez-Gonzalez, S.; Nolan, S. P., *Coord. Chem. Rev.* **2007**, *251*, 874-883.
8. Hahn, F. E.; Jahnke, M. C., *Angew. Chem. Int. Ed.* **2008**, *47*, 3122-3172.
9. Kovacevic, A.; Grundemann, S.; Miecznikowski, J. R.; Clot, E.; Eisenstein, O.; Crabtree, R. H., *Chem. Commun.* **2002**, 2580-2581.
10. Appelhans, L. N.; Zuccaccia, D.; Kovacevic, A.; Chianese, A. R.; Miecznikowski, J. R.; Macchioni, A.; Clot, E.; Eisenstein, O.; Crabtree, R. H., *J. Am. Chem. Soc.* **2005**, *127*, 16299-16311.
11. Crabtree, R. H., *Coord. Chem. Rev.* **2013**, *257*, 755-766.
12. Chianese, A. R.; Kovacevic, A.; Zeglis, B. M.; Faller, J. W.; Crabtree, R. H., *Organometallics* **2004**, *23*, 2461-2468.
13. Schuster, O.; Yang, L. R.; Raubenheimer, H. G.; Albrecht, M., *Chem. Rev.* **2009**, *109*, 3445-3478.
14. Albrecht, M., *Chimia* **2009**, *63*, 105-110.
15. Albrecht, M., *Chem. Commun.* **2008**, 3601-3610.
16. Arnold, P. L.; Pearson, S., *Coord. Chem. Rev.* **2007**, *251*, 596-609.
17. Bacciu, D.; Cavell, K. J.; Fallis, I. A.; Ooi, L. L., *Angew. Chem. Int. Ed.* **2005**, *44*, 5282-5284.
18. Heckenroth, M.; Kluser, E.; Neels, A.; Albrecht, M., *Angew. Chem. Int. Ed.* **2007**, *46*, 6293-6296.
19. Chianese, A. R.; Zeglis, B. M.; Crabtree, R. H., *Chem. Commun.* **2004**, 2176-2177.

20. Heckenroth, M.; Albrecht, M., *Chimia* **2008**, *62*, 253-255.
21. Alcarazo, M.; Roseblade, S. J.; Cowley, A. R.; Fernandez, R.; Brown, J. M.; Lassaletta, J. M., *J. Am. Chem. Soc.* **2005**, *127*, 3290-3291.
22. Viciano, M.; Feliz, M.; Corberan, R.; Mata, J. A.; Clot, E.; Peris, E., *Organometallics* **2007**, *26*, 5304-5314.
23. Chianese, A. R.; Li, X. W.; Janzen, M. C.; Faller, J. W.; Crabtree, R. H., *Organometallics* **2003**, *22*, 1663-1667.
24. Kelly, R. A., III; Clavier, H.; Giudice, S.; Scott, N. M.; Stevens, E. D.; Bordner, J.; Samardjiev, I.; Hoff, C. D.; Cavallo, L.; Nolan, S. P., *Organometallics* **2008**, *27*, 202-210.
25. Nelson, D. J.; Nolan, S. P., *Chem. Soc. Rev.* **2013**, *42*, 6723-6753.
26. Leuthausser, S.; Schwarz, D.; Plenio, H., *Chem.-Eur. J.* **2007**, *13*, 7195-7203.
27. Song, G. Y.; Zhang, Y.; Li, X. W., *Organometallics* **2008**, *27*, 1936-1943.
28. Gusev, D. G., *Organometallics* **2009**, *28*, 6458-6461.
29. Yang, L.; Kruger, A.; Neels, A.; Albrecht, M., *Organometallics* **2008**, *27*, 3161-3171.
30. Fraser, P. J.; Roper, W. R.; Stone, F. G. A., *J. Chem. Soc. Dalton* **1974**, 760-764.
31. Raubenheimer, H. G.; Cronje, S., *Dalton Trans.* **2008**, 1265-1272.
32. Meyer, W. H.; Deetlefs, M.; Pohlmann, M.; Scholz, R.; Esterhuysen, M. W.; Julius, G. R.; Raubenheimer, H. G., *Dalton Trans.* **2004**, 413-420.
33. Schuster, O.; Raubenheimer, H. G., *Inorg. Chem.* **2006**, *45*, 7997-7999.
34. Isobe, K.; Kai, E.; Nakamura, Y.; Nishimoto, K.; Miwa, T.; Kawaguchi, S.; Kinoshita, K.; Nakatsu, K., *J. Am. Chem. Soc.* **1980**, *102*, 2475-2476.
35. Canovese, L.; Visentin, F.; Uguagliati, P.; DiBianca, F.; Fontana, A.; Crociani, B., *J. Organomet. Chem.* **1996**, *525*, 43-48.
36. Fanizzi, F. P.; Sunley, G. J.; Wheeler, J. A.; Adams, H.; Bailey, N. A.; Maitlis, P. M., *Organometallics* **1990**, *9*, 131-136.
37. Gomez-Bujedo, S.; Alcarazo, M.; Pichon, C.; Alvarez, E.; Fernandez, R.; Lassaletta, J. M., *Chem. Commun.* **2007**, 1180-1182.

38. Owen, J. S.; Labinger, J. A.; Bercaw, J. E., *J. Am. Chem. Soc.* **2004**, *126*, 8247-8255.

39. Alvarez, E.; Conejero, S.; Lara, P.; Lopez, J. A.; Paneque, M.; Petronilho, A.; Poveda, M. L.; del Rio, D.; Serrano, O.; Carmona, E., *J. Am. Chem. Soc.* **2007**, *129*, 14130.

40. Alvarez, E.; Conejero, S.; Paneque, M.; Petronilho, A.; Poveda, M. L.; Serrano, O.; Carmona, E., *J. Am. Chem. Soc.* **2006**, *128*, 13060-13061.

41. Conejero, S.; Lara, P.; Paneque, M.; Petronilho, A.; Poveda, M. L.; Serrano, O.; Vattier, F.; Alvarez, E.; Maya, C.; Salazar, V.; Carmona, E., *Angew. Chem. Int. Ed.* **2008**, *47*, 4380-4383.

42. Conejero, S.; Lopez-Serrano, J.; Paneque, M.; Petronilho, A.; Poveda, M. L.; Vattier, F.; Alvarez, E.; Carmona, E., *Chem.-Eur. J.* **2012**, *18*, 4644-4664.

43. Conejero, S.; Maya, C.; Paneque, M.; Petronilho, A.; Poveda, M. L.; Vattier, F.; Alvarez, E.; Carmona, E.; Laguna, A.; Crespo, O., *Dalton Trans.* **2012**, *41*, 14126-14136.

44. Rosello-Merino, M.; Diez, J.; Conejero, S., *Chem. Commun.* **2010**, *46*, 9247-9249.

45. Voutchkova, A. M.; Appelhans, L. N.; Chianese, A. R.; Crabtree, R. H., *J. Am. Chem. Soc.* **2005**, *127*, 17624-17625.

46. Voutchkova, A. M.; Feliz, M.; Clot, E.; Eisenstein, O.; Crabtree, R. H., *J. Am. Chem. Soc.* **2007**, *129*, 12834-12846.

47. Schneider, S. K.; Julius, G. R.; Loschen, C.; Raubenheimer, H. G.; Frenking, G.; Herrmann, W. A., *Dalton Trans.* **2006**, 1226-1233.

48. Herde, J. L.; Lambert, J. C.; Senoff, C. V., *Inorg. Synth.* **1974**, *14*, 18-20.

49. Corberan, R.; Mas-Marza, E.; Peris, E., *Eur. J. Inorg. Chem.* **2009**, 1700-1716.

50. Normand, A. T.; Cavell, K. J., *Eur. J. Inorg. Chem.* **2008**, 2781-2800.

51. McSkimming, A.; Ball, G. E.; Bhadbhade, M. M.; Colbran, S. B., *Inorg. Chem.* **2012**, *51*, 2191-2203.

52. McSkimming, A.; Bhadbhade, M.; Colbran, S. B., *Dalton Trans.* **2010**, *39*, 10581-10584.

53. Lalrempuia, R.; Muller-Bunz, H.; Albrecht, M., *Angew. Chem. Int. Ed.* **2011**, *50*, 9969-9972.

54. Lalrempuia, R.; McDaniel, N. D.; Muller-Bunz, H.; Bernhard, S.; Albrecht, M., *Angew. Chem. Int. Ed.* **2010**, *49*, 9765-9768.

55. Song, G. Y.; Li, X. W.; Song, Z. C.; Zhao, J.; Zhang, H. J., *Chem.-Eur. J.* **2009**, *15*, 5535-5544.

56. Petronilho, A.; Müller-Bunz, H.; Albrecht, M., *Chem. Commun.* **2012**, DOI: 10.1039/c2cc32843g.

57. Viciano, M.; Poyatos, M.; Sanau, M.; Peris, E.; Rossin, A.; Ujaque, G.; Lledos, A., *Organometallics* **2006**, *25*, 1120-1134.

58. Song, G. Y.; Zhang, Y.; Su, Y.; Deng, W. Q.; Han, K. L.; Li, X. W., *Organometallics* **2008**, *27*, 6193-6201.

59. Lalrempuia, R.; McDaniel, N. D.; Müller-Bunz, H. ç., S.; Albrecht, M., *Angew. Chem. Int. Ed.* **2010**, *49*, 9765-9768.

60. Stander-Grobler, E.; Schuster, O.; Heydenrych, G.; Cronje, S.; Tosh, E.; Albrecht, M.; Frenking, G.; Raubenheimer, H. G., *Organometallics* **2010**, *29*, 5821-5833.

61. Royo, B.; Peris, E., *Eur. J. Inorg. Chem.* **2012**, 1309-1318.

62. Fujita, K.; Nakamura, M.; Yamaguchi, R., *Organometallics* **2001**, *20*, 100-105.

63. Klahn, A. H.; Oelckers, B.; Godoy, F.; Garland, M. T.; Vega, A.; Perutz, R. N.; Higgitt, C. L., *J. Chem. Soc. Dalton* **1998**, 3079-3086.

64. Fan, L.; Turner, M. L.; Adams, H.; Bailey, N. A.; Maitlis, P. M., *Organometallics* **1995**, *14*, 676-684.

65. Kolle, U.; Grub, J., *J. Organomet. Chem.* **1985**, *289*, 133-139.

66. Fairchild, R. M.; Holman, K. T., *Organometallics* **2008**, *27*, 1823-1833.

67. Gusev, O. V.; Sergeev, S.; Saez, I. M.; Maitlis, P. M., *Organometallics* **1994**, *13*, 2059-2065.

68. Segarra, C.; Mas-Marzá, E.; Mata, J. A.; Peris, E., *Organometallics* **2012**, *31*, 5169-5176.

69. Bonnette, F.; Kato, T.; Destarac, M.; Mignani, G.; Cossio, F. P.; Baceiredo, A., *Angew. Chem. Int. Ed.* **2007**, *46*, 8632-8635.

70. Denk, M. K.; Rodezno, J. M.; Gupta, S.; Lough, A. J., *J. Organomet. Chem.* **2001**, *617*, 242-253.

71. Holloczki, O.; Terleczky, P.; Szieberth, D.; Mourgas, G.; Gudat, D.; Nyulaszi, L., *J. Am. Chem. Soc.* **2011**, *133*, 780-789.

72. Zuo, W. W.; Braunstein, P., *Dalton Trans.* **2012**, *41*, 636-643.

73. da Costa, A. P.; Sanau, M.; Peris, E.; Royo, B., *Dalton Trans.* **2009**, 6960-6966.

74. da Costa, A. P.; Mata, J. A.; Royo, B.; Peris, E., *Organometallics* **2010**, *29*, 1832-1838.

75. Da Costa, A. P.; Viciano, M.; Sanau, M.; Merino, S.; Tejeda, J.; Peris, E.; Royo, B., *Organometallics* **2008**, *27*, 1305-1309.

# CHAPTER 4

# N-HETEROCYLIC CARBENE-BASED MULTITOPIC LIGANDS FOR THE DESIGN OF MULTIMETALLIC COMPLEXES

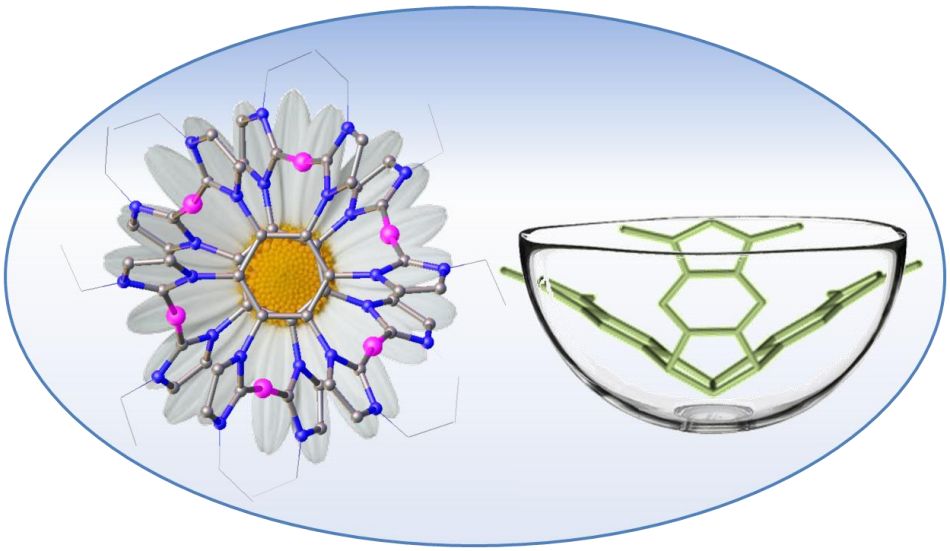

## 4.1 INTRODUCTION

During the last few years, there has been an increasing interest in the design of sophisticated ligands that do far more than fulfil their traditional spectator role, because they may provide additional functions that can be useful in catalysis[1] and in material science.[2-4] In this sense, poly-NHC ligands have emerged as a good example of such type of ligands, because they may give access to a wide variety of topologies which may provide unusual reactivity patterns.[5-8] Poly-NHCs have given rise to a plethora of homo- and hetero-multimetallic complexes,[9-21] which have sometimes led to interesting applications in cooperative or *tandem* catalysis.[22-30] As mentioned in Chapter 1, our group has recently described the interesting benefits provided by di- and tri-NHC ligands with extended conjugated π-electron systems.[31-32] In particular, the triphenylene-based tri-NHC ligand **4.2** has allowed us the preparation of palladium and gold complexes.[31] These compounds showed significant catalytic benefits compared with related trimetallic and monometallic complexes with formally the same stereoelectronic properties, as those afforded by the trypticene-based tri-NHC **4.1**,[22] previously reported by Williams and Bielawski (Scheme 4.1).[33] While both ligands, **4.1** and **4.2**, display a $D_{3h}$-symmetrical arrangement and dispose the metals at a similar metal-to-metal distance, **4.2** benefits from having a π-delocalized system, to which the higher catalytic activities were attributed.

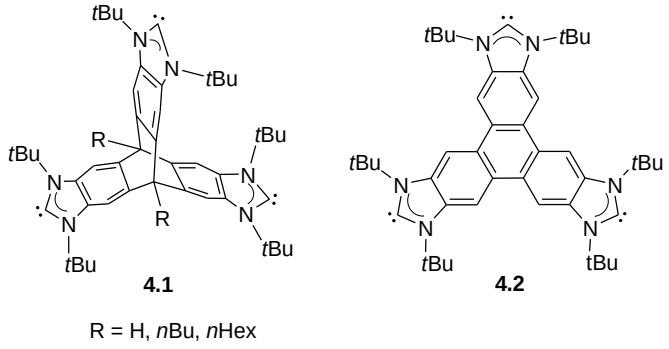


**Scheme 4.1** Poly-NHCs, displaying $D_{3h}$-symmetrical arrangement, **4.1** and **4.2**

As a modification of the topology of these tri-NHC ligands, we envisaged that the polycyclic core structure of tribenzotriquinacene, **TBTQ**, offered the possibility of enforcing a bowl-shaped polycondensed aromatic ligand (**K**, in Scheme 4.2),[34-41]

therefore adding a new structural asset to the construction of rigid $C_3$-symmetrical tri-carbenes.

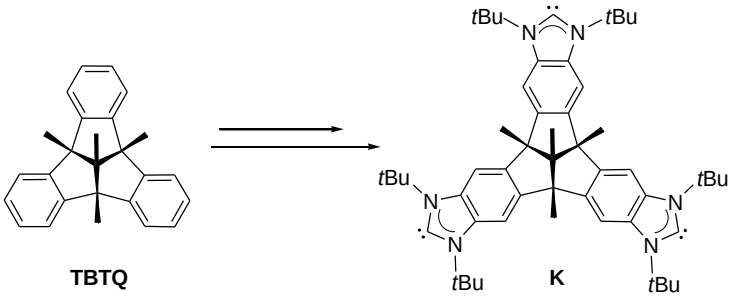


**Scheme 4.2** Poly-NHC **K** based on **TBTQ**, displaying $C_{3v}$-symmetrical arrangement

Bowl-shaped ligands for the construction of metal catalysts may affect the selectivity and specificity based on the global size and shape of substrate molecules, mimicking some of the features of enzyme catalysis. This proof-of-concept was elegantly applied to NHCs in 2009 by Chianese and co-workers, who described a series of iridium complexes with flexible bowl-shaped mono-NHC ligands that showed moderate specificity in the competitive hydrosilylation of ketones.[42]

Functionalised tribenzotriquinacenes (**TBTQ**) have been widely studied by Kuck and co-workers, who developed a full detailed chemistry of this type of threefold-symmetry scaffold. Their chemical versatility combined with their convex/concave molecular surfaces render these compounds highly versatile building blocks for application in molecular and material design. The preparation of **TBTQ**-derived structures requires from complicated multistep synthetic procedures, which may be out of the scope of this research work. We were very fortunate to count with the collaboration of Prof. Kuck (Bielefeld University-Germany) who kindly provided us with the necessary amounts of the **TBTQ** derivatives, which we used for the development of the work described in this chapter.

### 4.1.1 Poly-NHC ligands and supramolecular chemistry

Metal-directed self-assembly of supramolecular structures has attracted great attention in the last two decades, after the first report of double-helical complex formation by J. M. Lehn starting from 2,2´-bipyridine and copper(I).[43] Soon after, a huge number of self-assembled metallohelicates[44-45] and other three-dimensional

supramolecular structures[46-48] were described by variation of the metal complexes and the ligands. The use of N-heterocyclic carbene ligands as building blocks for the formation of these types of supramolecular structures did not get much attention at these early stages, although some examples of such structures with bridging bisisocyanides,[49] acyclic diaminocarbenes[50] or *remote* NHC ligands[51] are known today.

Hahn and co-workers pioneered the synthesis of the first three-dimensional metallosupramolecular structure containing exclusively M-NHC bonds from two hexa-NHC ligands and six silver(I) ions (**4.3**, Scheme 4.2).[16] Complex **4.3** was synthesised by the direct reaction of lutidine-bridged hexaimidazolium salt with $Ag_2O$. Following the same procedure, other metallosupramolecular assemblies, based on cylindrical polynuclear Ag(I) carbene complexes from tetra-, tris- and bisimidazolium salts (**4.4**, **4.6** and **4.10**, respectively, Scheme 4.3) were synthesised by the same group. These tetra-, tri- and dinuclear silver complexes were used as carbene-transfer agents, and were employed for the preparation of homonuclear Au(I) (**4.5**, **4.7** and **4.11**, Scheme 4.3), Cu(I) (**4.8**, Scheme 4.3) and Hg(I) (**4.9**, Scheme 4.3) complexes with retention of the three-dimensional structure.[14, 52-53]

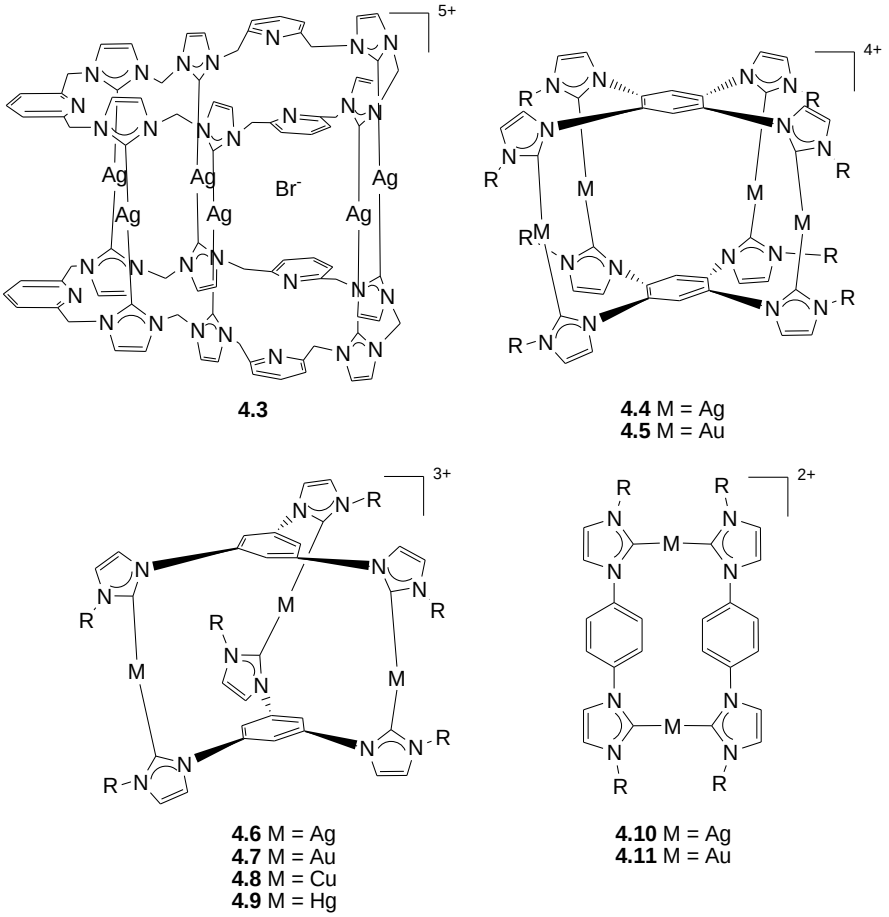


**4.3**

**4.4** M = Ag
**4.5** M = Au

**4.6** M = Ag
**4.7** M = Au
**4.8** M = Cu
**4.9** M = Hg

**4.10** M = Ag
**4.11** M = Au

**Scheme 4.3** Metallosupramolecular structures containing exclusively M-NHC bonds synthesised by Hahn

With all these precedents in mind, we thought that we could apply our expertise in the preparation of rigid poly-NHCs for the design of novel metallo-organic macromolecular cylinders with unusual chemical properties. In principle, such type of structures may be used for the development of new chemical behaviours, in which the reactivity of selected fragments may be confined to the interior of the macromolecular cage, or even be used for the selective recognition of small neutral of ionic molecules.[54-59] This chapter deals with the preparation of two types of poly-NHCs, and the study of their coordination properties. First, we centred our efforts on the synthesis and coordination of the $C_{3v}$-symmetrical threefold tribenzotriquinacene-based tri-NHC ligand **K** (Scheme 4.1) to Rh(I). The Tolman Electronic Parameter

(TEP) and the electrochemical studies of the compound obtained were also described. The second part of the chapter deals to the synthesis of new hexaimidazolium salts and their coordination to Ag(I), affording the self-assembly formation of cylindrical hexasilver dodecarbene complexes, which may be considered higher nuclearity relatives of complexes **4.4** and **4.6** (Scheme 4.3). The transmetallation of these new hexanuclear complexes to Au(I) was also studied.

# 4.2 RESULTS AND DISCUSSION

## 4.2.1 Synthesis and characterization of a $C_{3v}$-symmetrical threefold tribenzotriquinacene-based tri-NHC complex

The general aim of this work was to investigate the chemistry of transition metal complexes incorporating poly-NHC ligands with rigid highly symmetric geometries. As previously mentioned, we found bowl-shaped $C_{3v}$-symmetrical **TBTQ** core to be an excellent starting material for the preparation of the tri-NHC ligand **K** shown in Scheme 4.2. Once the ligand was prepared, our aim was to extend its coordination to transition metal fragments and study the properties of the resulting tri-NHC complexes. For the development of this part of the work, we collaborated with Prof. Dietmar Kuck (Bielefeld University-Germany), who provided us with the necessary amounts of the **TBTQ** derivatives that we used as starting materials. Although the preparation of these materials has already been published in the literature,[39-40, 60] all the synthetic procedures imply multistep processes that would undoubtedly make the development of this work much more difficult.

In general, the synthetic procedure of the more recent poly-NHCs prepared in our research group starts with the multifold Buchwald-Hartwig amination of polyaromatic molecules with adjacent bromides. This methodology was extensively employed by Bielawski and co-workers and we thought that this approach could be used starting from hexabromotribenzotriquinacene **4.12**[39] (Scheme 4.4), which may constitute an excellent starting material for the preparation of our new ligand.

*a) Synthesis and characterization of salt* ***[KH$_3$](BF$_4$)$_3$***.

As depicted in Scheme 4.4, the general protocol for the preparation of salt **[KH$_3$](BF$_4$)$_3$** consisted of a two-step procedure. The first step implies the hexa-amination of **4.12**[39] with *tert*-butylamine (*t*BuNH$_2$) in the presence of [Pd(OAc)$_2$], IPr·HCl and NaO*t*Bu in toluene at 115ºC, to afford the hexaaminotribenzotriquinacene, **HexaNH$_2$-TBTQ**, in 99% yield. The second step involves the trisannulation of **HexaNH$_2$-TBTQ** with triethylorthoformate (HC(OEt)$_3$) in the presence of HBF$_4$ at 80ºC to give salt **[KH$_3$](BF$_4$)$_3$** in 95% yield.

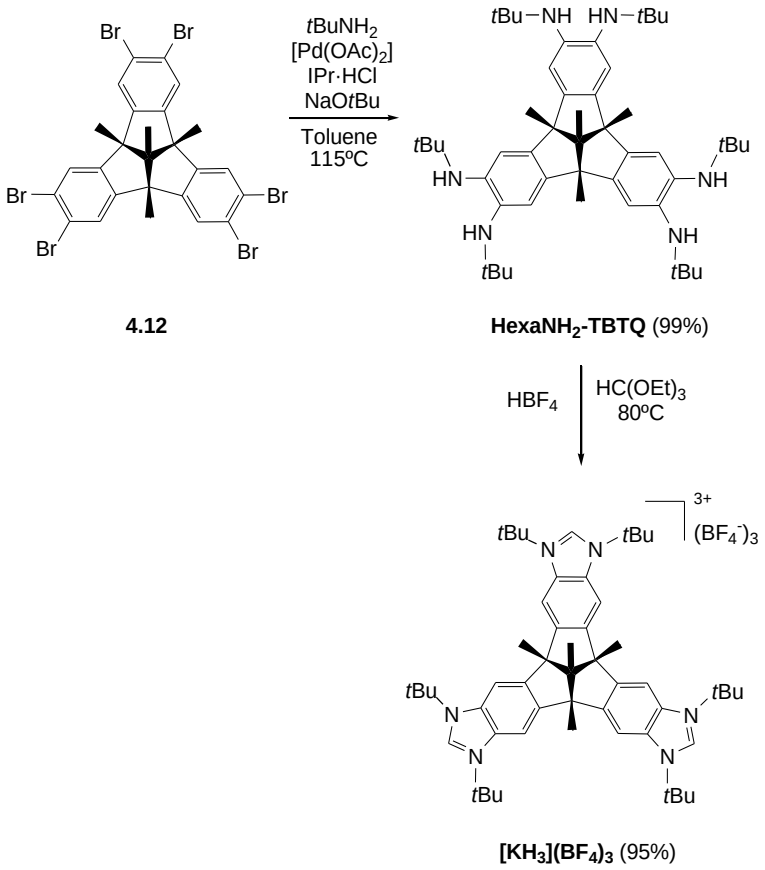


**Scheme 4.4** Synthesis of **HexaNH$_2$-TBTQ** and **[KH$_3$](BF$_4$)$_3$**

**HexaNH$_2$-TBTQ** and salt **[KH$_3$](BF$_4$)$_3$** were characterised by means of NMR spectroscopy and High Resolution Mass Spectrometry (ESI-TOF-MS). The molecular structure of **[KH$_3$](BF$_4$)$_3$** was confirmed by means of X-Ray Diffraction. As an example, the NMR spectroscopic characterization of **[KH$_3$](BF$_4$)$_3$** is described below. All the details regarding the spectroscopic data for compound **HexaNH$_2$-TBTQ** can be found in the Experimental Section (Chapter 5).

*$^1$H NMR spectrum of **[KH$_3$](BF$_4$)$_3$***

Figure 4.1 shows the $^1$H NMR spectrum of **[KH$_3$](BF$_4$)$_3$**. The signal due to the acidic proton of the NC*H*N groups appears at 8.49 ppm (a). Due to the high symmetry of the molecule, the resonance corresponding to the six aromatic protons of the three benzimidazolium units is shown as a single peak at 8.21 ppm (b). The signals

assigned to the protons of the C$H_3$ groups of the triquinacene core and *tert*-butyl groups appear at 1.99 (c), 1.58 (e) and 1.84 ppm (d), respectively.

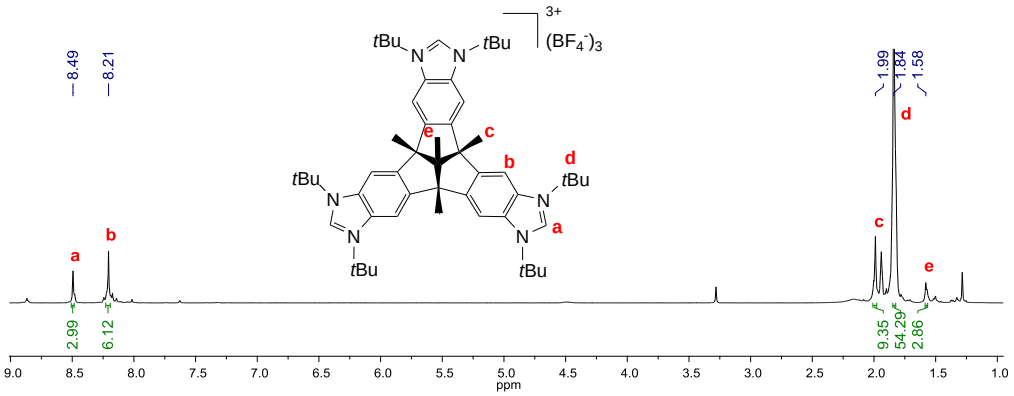


**Figure 4.1** $^{1}$H NMR spectrum of **[KH$_3$](BF$_4$)$_3$** in $CD_3CN$

*$^{13}C\{^1H\}$ NMR spectrum of **[KH$_3$](BF$_4$)$_3$***

Figure 4.2 shows the $^{13}C\{^1H\}$ NMR spectrum of **[KH$_3$](BF$_4$)$_3$**. The resonances due to the aromatic $C_{quaternary}$ and *C*H groups of the benzimidazolium units are shown at 149.0, 139.5 (1) and 111.8 ppm (3), respectively. The signal assigned to the carbon of the N*C*HN groups appears at 133.3 ppm (2). The signals due to the quaternary carbons of the triquinacene core and *tert*-butyl groups are displayed at 72.4 (4), 64.3 (5) and 62.5 ppm (6), respectively. The signals assigned to the carbon of the *C*H$_3$ groups of the *tert*-butyl groups and triquinacene core appear at 28.9 (7), 26.9 (8) and 16.8 ppm (9), respectively.

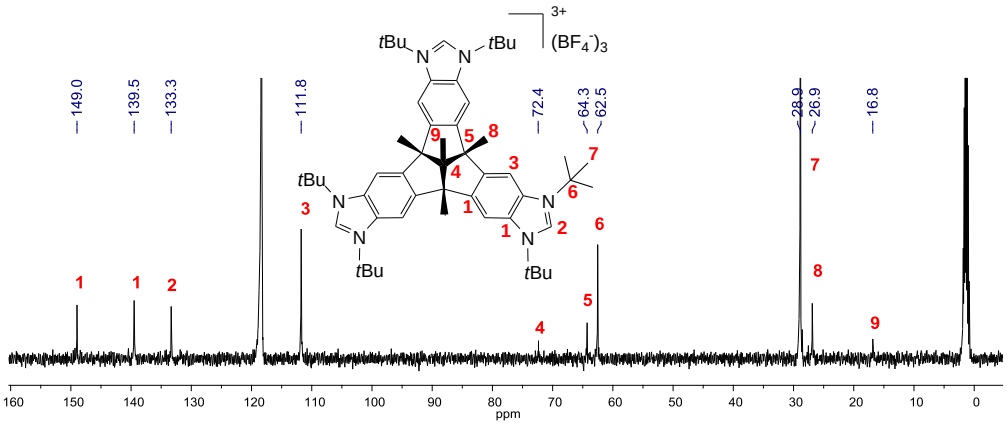


**Figure 4.2** $^{13}C\{^{1}H\}$ NMR spectrum of **$[KH_3](BF_4)_3$** in $CD_3CN$

*Molecular structure of **$[KH_3](BF_4)_3$***

Crystals of **$[KH_3](BF_4)_3$** suitable for X-Ray Diffraction analysis were obtained by slow evaporation of a concentrated solution of the compound in acetonitrile.

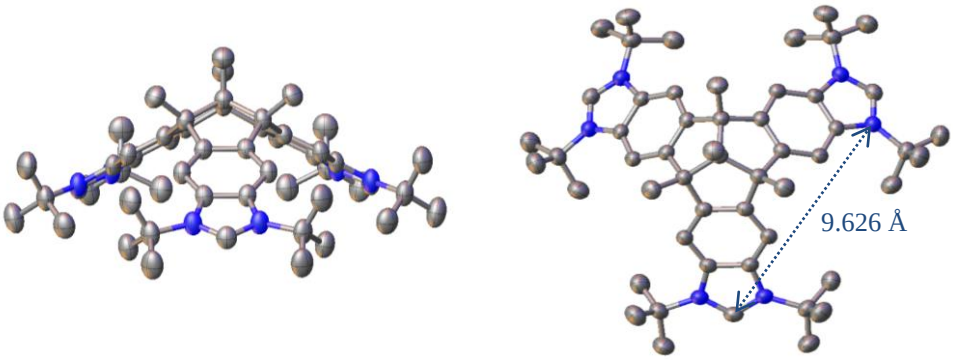


**Figure 4.3** Two perspectives of the molecular structure of **$[KH_3](BF_4)_3$**. Ellipsoids are at the 30% probability level. Hydrogen atoms and counteranions ($3BF_4^-$) are omitted for clarity.

The molecular structure of compound **$[KH_3](BF_4)_3$** (Figure 4.3) confirms that three benzimidazolium units are connected to the triquinacene core in a strictly planar orientation within a $C_{3v}$-symmetrical framework. As a consequence, the distances between the three N*C*HN carbons are equal (9.626 Å), and the corresponding distances between the metal atoms coordinated to a potential tri-NHC derived from **$[KH_3](BF_4)_3$** can be estimated to be in the range of 11.5-11.8 Å. This distance would be smaller than the metal-to-metal distances displayed by the coordinated related tri-NHCs **4.1** and **4.2** (Scheme 4.1), which is approximately 13.5 Å in both cases.[11, 22]

*b) Synthesis and characterization of tri-NHC **K**.*

To prepare the free tri-NHC **K**, deprotonation of **[KH$_3$](BF$_4$)$_3$** was carried out in $C_6D_6$ in the presence of three equivalents of potassium bis(trimethylsilylamide) (KHMDS) and a catalytic amount of NaO*t*Bu, as shown in Scheme 4.5.

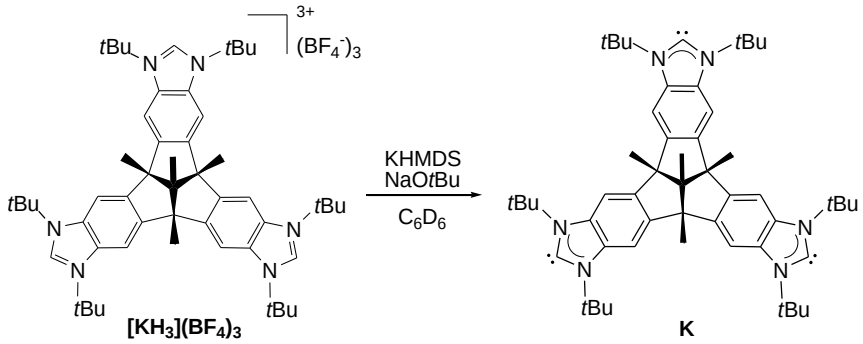


**Scheme 4.5** Synthesis of **K**

The tri-NHC **K** was characterised by means of NMR spectroscopy and High Resolution Mass Spectrometry (ESI-TOF-MS). The $^1$H NMR spectrum of **K** revealed that the signal due to the NC*H*N proton disappeared, and that all other resonances were high-field shifted, while reflecting the threefold symmetry of the product (for further details see Experimental Section (Chapter 5)). The $^{13}$C{$^1$H} NMR spectrum and HRMS of **K** is discussed below in detail.

*$^{13}$C{$^1$H} NMR spectrum of **K***

Figure 4.4 shows the $^{13}$C{$^1$H} NMR spectrum of **K**. The spectrum exhibits a distinctive single resonance due to the three equivalent carbene carbons at 225.8 ppm (1), in the same region as shown by other previously published benzimidazole-based carbenes.[19, 33, 61-64] The resonances corresponding to the aromatic $C_{quaternary}$ and *C*H groups of the benzimidazolium units are shown at 142.8, 136.4 (2) and 107.4 ppm (3), respectively. The signals due to the quaternary carbons of the triquinacene core and *tert*-butyl groups are displayed at 72.6 (4), 61.8 (5) and 57.3 ppm (6), respectively. The signals assigned to the carbon of the *C*H$_3$ groups of the *tert*-butyl groups and triquinacene core appear at 30.8 (7), 27.4 (8) and 17.0 ppm (9), respectively.

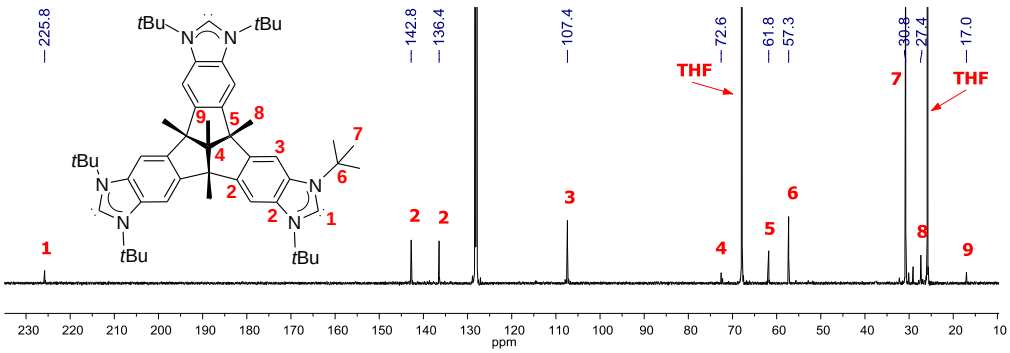


**Figure 4.4** $^{13}C\{^{1}H\}$ NMR spectrum of **K** in $C_6D_6$

*HRMS of **K***

The accurate molecular mass of the compound determined by HRMS (Figure 4.5) showed a main peak at m/z 793.5903, which may be assigned to $[M + H]^+$.

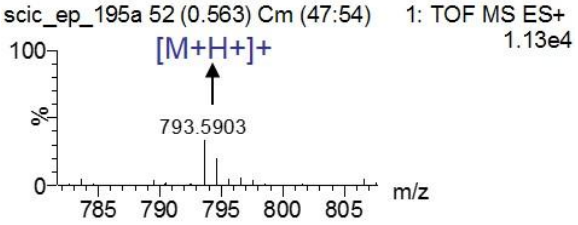


**Figure 4.5** High Resolution Mass Spectrum of **K**

*b) Synthesis and characterization of complex **25K***

The coordination of **K** to rhodium was performed by sequential deprotonation of **$[KH_3](BF_4)_3$** with KHMDS in THF at 0ºC, and further addition of $[RhCl(COD)]_2$ at room temperature (Scheme 4.6), yielding the desired compound **25K** in moderate yield (32%), after purification by column chromatography.

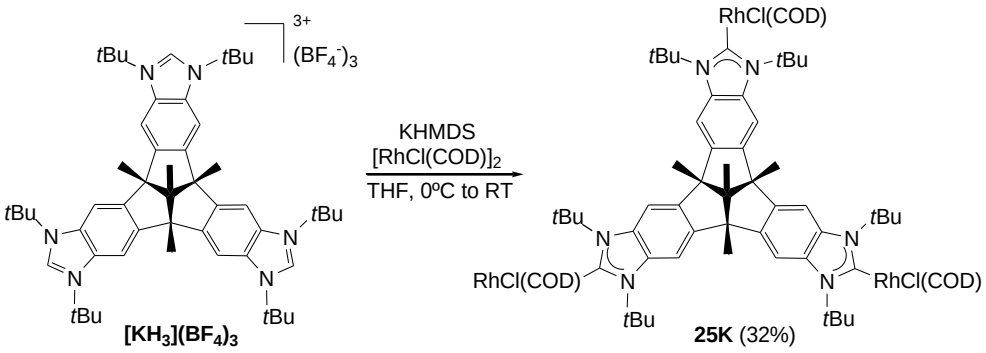


**Scheme 4.6** Synthesis of **25K**

Compound **25K** was characterised by means of NMR spectroscopy and mass spectrometry. Repeated attempts to obtain satisfactory elemental analysis and to grow single crystals of **25K** for X-Ray Diffraction analysis were unsuccessful due to the slow decomposition of the complex, both in solution and in the solid state. In this regard, it is important to recall that some benzimidazolylidenes of rhodium(I) are known to be unstable and able to transfer N-heterocyclic carbenes.[65] In our case, the trirhodium complex may also be unstable due to steric reasons. The steric bulk of the tricarbene ligand **K**, measured as its percent of buried volume (%$V_{Bur}$), was determined to be 40.4% (calculated using the data from the crystal structure of the trisazolium **[KH$_3$](BF$_4$)$_3$**), while the % $V_{Bur}$ of **4.2** was estimated to be 36.1% (calculated using the CIF file of the tri-AuCl complex[22]). The spatial occupation values were determined using the Sambvca software developed by Cavallo and co-workers.[66]

The NMR spectroscopic characterization of **25K** is discussed below in detail.

*$^1$H NMR spectrum of **25K***

Figure 4.6 shows the $^1$H NMR spectrum of **25K**. The signal due to the proton of the NC*H*N groups has disappeared, providing a preliminary indication that the coordination of **K** to [RhCl(COD)]$_2$ has occurred. The resonances due to the aromatic protons of the benzimidazolium units are shown at 7.61 and 7.58 ppm (a). The signals assigned to the protons of the C$H_3$ groups of the *tert*-butyl N-substituents and triquinacene core are seen at 2.37 and 2.36 (b), 1.97 (c) and 1.83 ppm (d),

respectively. The rest of the signals corresponding to the COD protons are conveniently displayed on the NMR spectrum shown in Figure 4.6.

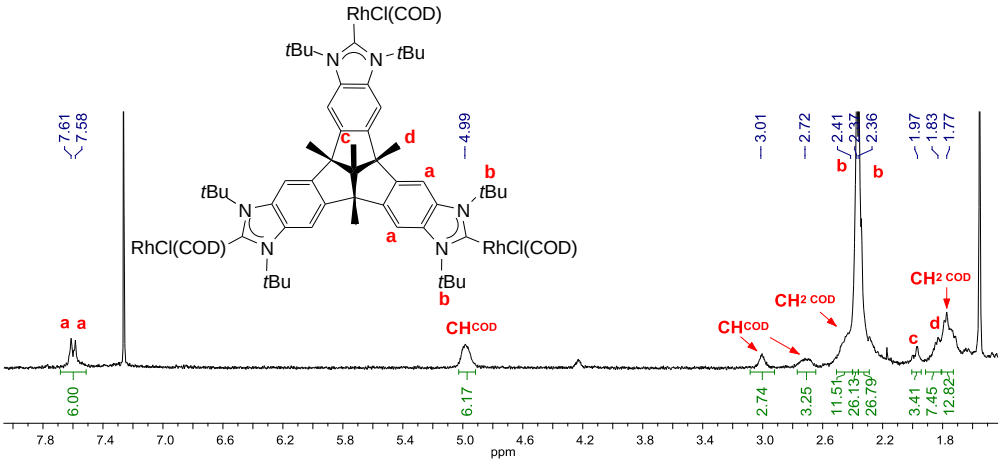


**Figure 4.6** $^{1}$H NMR spectrum of **25K** in $CDCl_3$

*$^{13}C\{^{1}H\}$ NMR spectrum of **25K***

Figure 4.7 shows the $^{13}C\{^{1}H\}$ NMR spectrum of **25K**. The most characteristic signals are the ones attributed to the metallated carbene carbon that are shown as two doublets at 195.9 and 195.7 ppm ($^{1}J_{RhC}$ = 49 Hz) (1), revealing that the rhodium fragments may exhibit different local environments. The resonances due to the aromatic $C_{quaternary}$ and *C*H groups of the benzimidazolium units are shown at 142.5, 136.1 (2) and 108.3 ppm (3), respectively. The signals assigned to the quaternary carbons of the triquinacene core and *tert*-butyl groups are displayed at 72.2 (4), 61.7 (5) and 60.2 ppm (6), respectively. The signals assigned to the carbon of the $CH_3$ groups of the *tert*-butyl groups and triquinacene core appear at 32.5 and 32.4 (7), 27.2 (8) and 16.7 ppm (9). The rest of signals corresponding to the COD carbons are conveniently displayed in the spectrum shown in Figure 4.7.

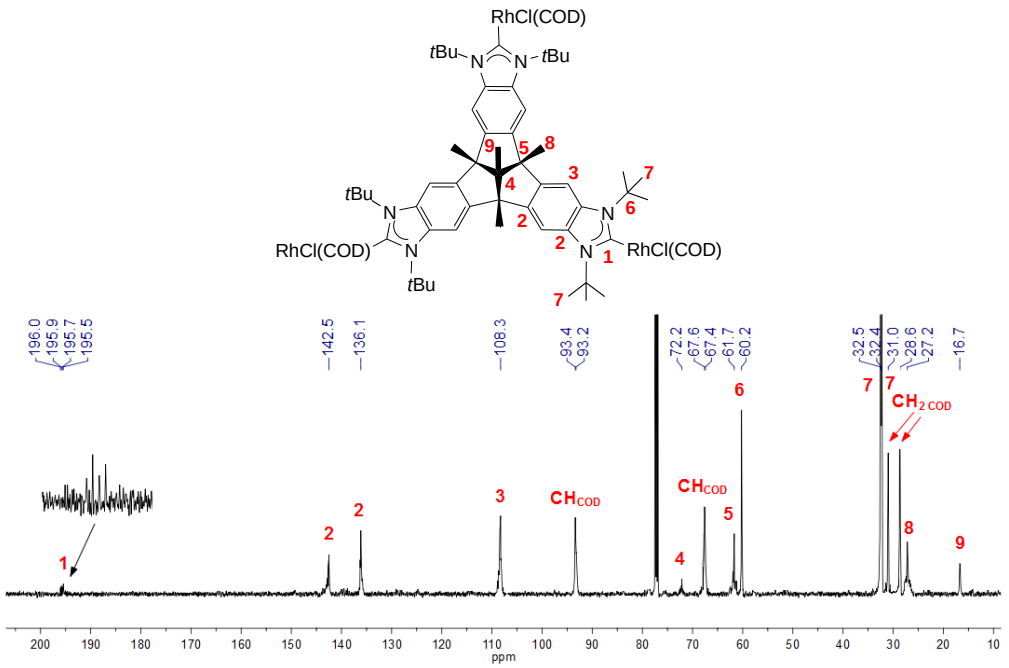


**Figure 4.7** $^{13}C\{^{1}H\}$ NMR spectrum of **25K** in $CDCl_3$

The asymmetric arrangement of the tri-NHC **K** should allow the rhodium fragment to adopt two possible conformations, one with the chloride ligand pointing into the inner cavity of the bowl-shaped ligand, and another with the chlorine pointing out of the cavity. These two situations may yield a maximum of four different atropisomers that may be present in **25K** (**25Ka-25Kd**, Scheme 4.7). Given the high steric repulsion provided by the N-*t*Bu groups, we believe that free rotation about the C-Rh bond is highly unlikely[67] and therefore, these four isomers do not interconvert. This is corroborated by VT NMR experiments; low temperature experiments do not reveal any sharpening or splitting of the $^{1}H$ NMR signals, while high temperature (60ºC) NMR experiments reveal that the two sets of $^{13}C\{^{1}H\}$ NMR signals remain unmodified. Despite the fact that the metallated carbene atom gives rise to two different $^{13}C$ NMR signals, the rest of the spectrum does not seem to be affected by this loss of symmetry, therefore displaying a pattern that may suggest a pseudo-$C_{3v}$ symmetry. All our attempts to separate the atropisomers of **25K** by column chromatography or by slow crystallization were unsuccessful.

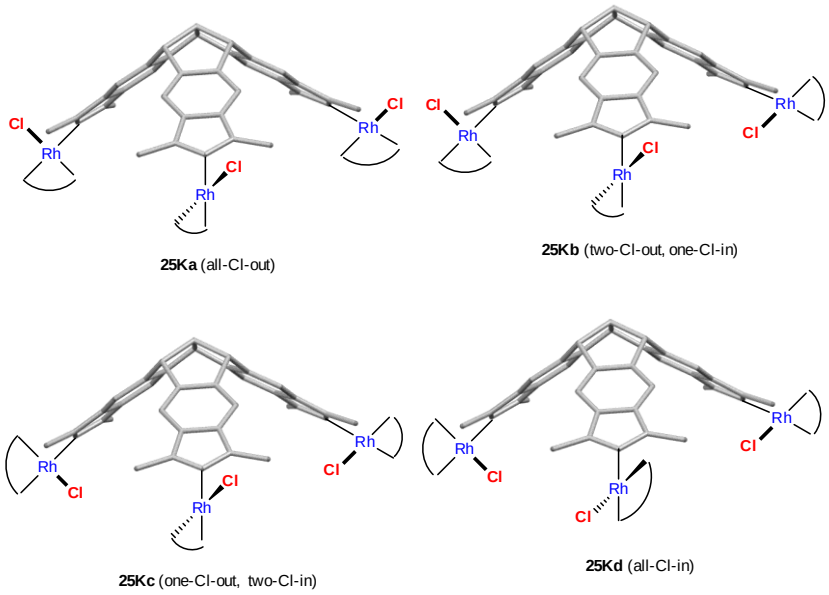


**Scheme 4.7** The four possible atropisomers of complex **25K** (in and out are with respect to the inner cavity of the ligand)

### 4.2.1.1 Determination of the Tolman Electronic Parameter (TEP), and Cyclic Voltammetry (CV) studies

For the determination of the electron-donating character of **K**, we estimated its Tolman Electronic Parameter (TEP) by DFT calculations of the $IR_{C-O}$ stretching frequencies of the ligand coordinated to a single $Ni(CO)_3$ fragment at one of the donor sites (**I**, Scheme 4.8; Note that N-methyl groups have been used for simplification of the calculations). The resulting TEP value for this species is 2055.8 $cm^{-1}$, slightly lower than the calculated value for our recently described triphenylene-based tri-NHC **4.2** (2057.2 $cm^{-1}$, also with Me instead of *t*Bu groups)[11] and to the one shown by the mono-carbene $BimMe_2$ (1,3-dimethylbenzimidazolylidene, 2057.0 $cm^{-1}$).[68] Subsequent addition of one and two $Ni(CO)_3$ fragments, leading to **II** and **III** (Scheme 4.8), resulted in a slight increase of the TEP values to 2056.7 and 2057.6 $cm^{-1}$, respectively. These shifts were due to the inductive effect provided by the $Ni(CO)_3$ fragments, which are withdrawing electron-density from the ligand, and therefore are reducing the overall electron-donating power of the tri-NHC. All TEP values were determined by Prof. Gusev (Wilfrid Laurier University-Canada), who

carried out the appropriate calculations. In a collaborative work with our group, Gusev recently suggested that the estimation of the variation of the TEP values associated to the coordination of different metal fragments to rigid poly-NHCs may be related to the electronic communication between the metals across the ligand.[69] In our case, the small variation in the TEP value indicates that the three carbene units are basically disconnected. A similar trend was observed for our previously reported triphenylene-based tri-NHC, **4.2** (Scheme 4.1).[11]

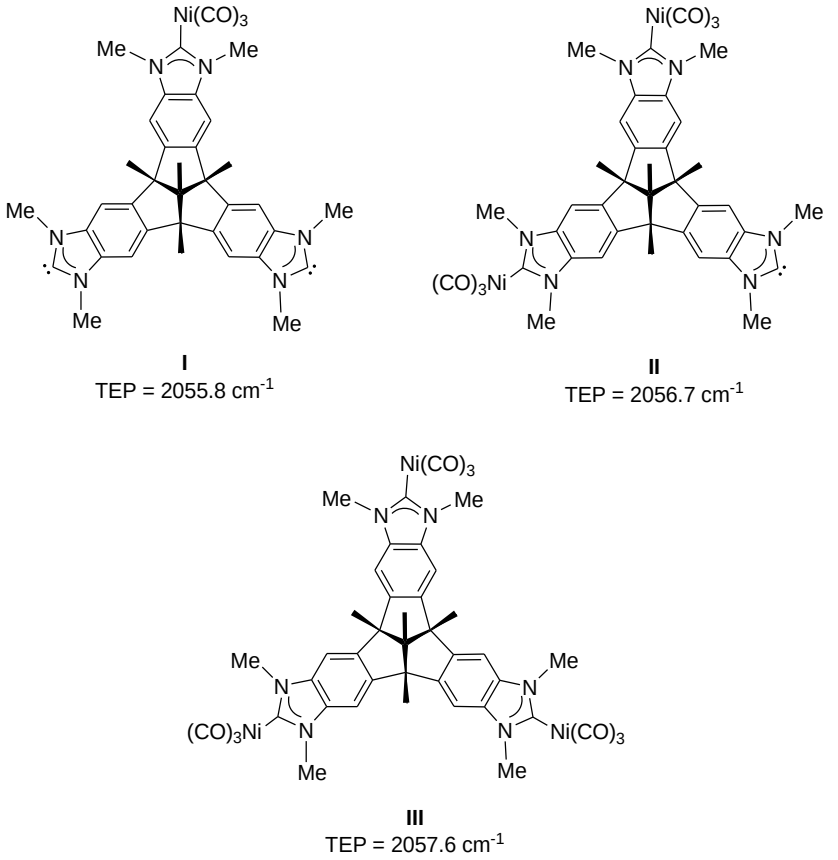


**Scheme 4.8** TEP values for **K** coordinated to one (**I**), two (**II**) and three (**III**) fragments of $Ni(CO)_3$

Cyclic voltammetry studies of the $Rh_3$-complex **25K** were also performed (Figure 4.8). The trinuclear complex displays a quasi-reversible three-electron oxidation at $E_{1/2}$ = 0.66 V, which is higher than the redox potential of the monometallic complex [RhCl(BimN*t*Bu$_2$)(COD)] (0.56 V), thus suggesting a lower electrondonating power

of the tri-carbene ligand **K**. Differential pulse voltammetry (DPV) analysis shows a single peak which displays a bandwidth similar to that observed for the Rh-monocarbene complex [RhCl(BimN*t*Bu$_2$)(COD)] (dotted line in Figure 4.8). This observation implies that complex **25K** corresponds to a decoupled system, as expected due to the presence of the triquinacene core, which seems to disrupt the communication between the metal centres. At this point, it is interesting to note that the triphenylene-based tri-NHC **4.2** also provided a essentially decoupled trimetallic systems, although the electrochemical studies revealed a weak but not negligible coupling of 42 mV.[11]

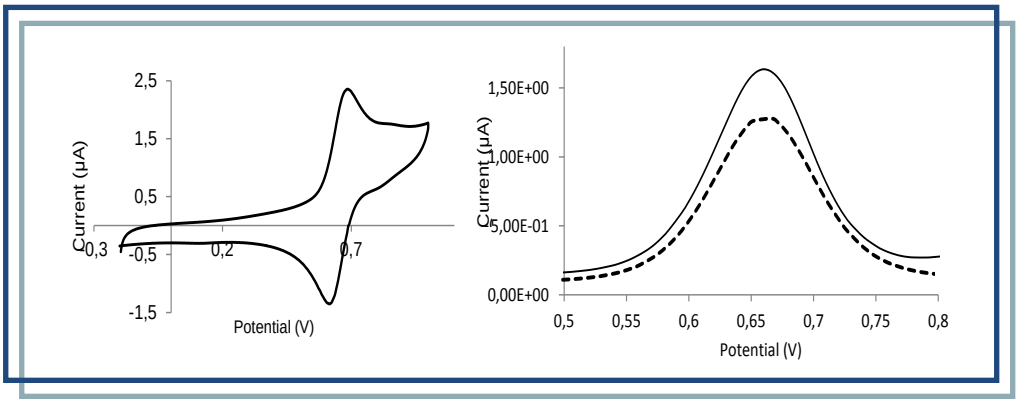


**Figure 4.8** Cyclic voltammetry diagram of complex **25K** (left) and relevant section of the differential pulse voltammetry (DPV) (right). The dashed line was obtained by adding a potential-shifted and weighted signal of the monometallic complex [RhCl(BimN*t*Bu$_2$)(COD)] (BimN*t*Bu$_2$ = 1,3-di(*tert*-butyl)benzimidazolylidene). Measurements performed on a 10mM analyte in $CH_2Cl_2$ with 0.1mM [$NBu_4$]$PF_6$, at a scan rate of 100 mV $s^{-1}$ and referenced to SCE by shifting ferrocene to 445 mV.

## 4.2.2 Synthesis and characterization of cylindrical transition metal poly-NHC complexes

As stated in Section 4.1.1, metallosupramolecular structures derived from ubiquitous NHC ligands are still rare. Hahn and co-workers have contributed to the development of this field thanks to their studies and design of new metallosupramolecular assemblies featuring only M-NHC bonds from poly-NHC ligands and multimetallic ions.[14, 16, 52, 70-71] Because we wanted to contribute to the field, in this last part of our work we focused our attention on the syntheses of a new type of hexa-NHC ligand,

which should provide access to sixfold symmetry molecules. This new type of ligands, together with their coordination compounds, was initiated during a stay at the *Institut für Anorganische und Analytische Chemie* (Münster, Germany) under the supervision of Prof. Dr. F. Ekkehardt Hahn.

*a) Synthesis and characterization of poly-imidazolium salts* ***[LH$_6$](OTf)$_6$*** *and* ***[MH$_6$](BF$_4$)$_6$.***

The synthesis of the 1,2,3,4,5,6-hexa(*N*-alkylimidazolium)benzene salts **[LH$_6$](OTf)$_6$** and **[MH$_6$](BF$_4$)$_6$** (alkyl = Me and Et, respectively), were performed as described in Scheme 4.9. First, hexa(imidazol-1-yl)benzene was prepared according to the known literature method,[72] by deprotonation of imidazole and subsequent reaction with hexafluorobenzene (yield 75%). Then, hexa(imidazol-1-yl)benzene reacted with both, methyl trifluoromethanesulfonate to afford **[LH$_6$](OTf)$_6$** in 93% yield, or triethyloxonium tetrafluoroborate to afford **[MH$_6$](BF$_4$)$_6$** in 78% yield.

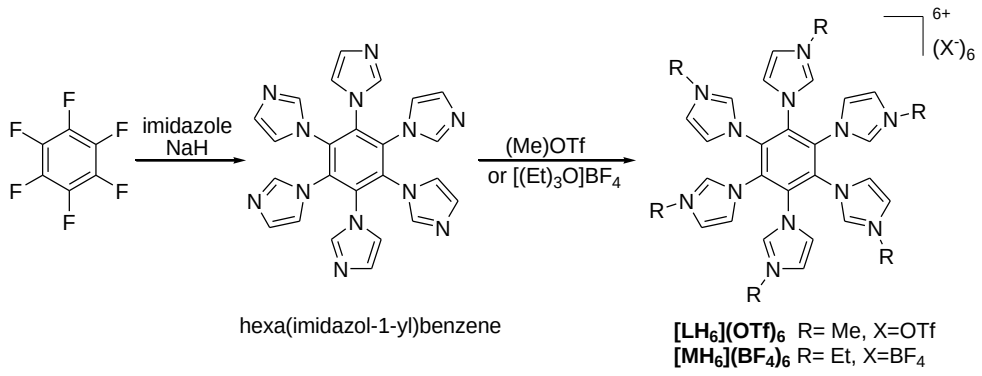


**Scheme 4.9** Synthesis of **[LH$_6$](OTf)$_6$** and **[MH$_6$](BF$_4$)$_6$**

Both **[LH$_6$](OTf)$_6$** and **[MH$_6$](BF$_4$)$_6$** are soluble in polar solvents such as DMSO, $CH_3CN$ and $CH_3OH$, while rather insoluble in THF, $Et_2O$ or $CH_2Cl_2$. Both salts were fully characterised by means of NMR spectroscopy, mass spectrometry and elemental analysis. The NMR spectroscopic characterization of salt **[LH$_6$](OTf)$_6$** is discussed below in detail. A $^1$H-$^{13}$C gHSQC NMR experiment was carried out in order to confirm the assignation of the signals displayed in the $^1$H and $^{13}$C{$^1$H} NMR spectra of **[LH$_6$](OTf)$_6$** (see Experimental Section in Chapter 5). All the details of the spectroscopic data of **[MH$_6$](BF$_4$)$_6$** can be found in the Experimental Section (Chapter 5).

### *$^{1}$H NMR spectrum of* ***[LH$_6$](OTf)$_6$***

Figure 4.9 shows the $^{1}$H NMR spectrum of **[LH$_6$](OTf)$_6$**. The characteristic acidic signal of the proton of the NC*H*N groups appears at 9.14 ppm (a). The resonances due to the proton of the C*H* groups of the six imidazolium rings are shown at 7.95 and 7.61 ppm (b). The signals corresponding to the protons of the C$H_3$ groups appear at 3.94 ppm (c).

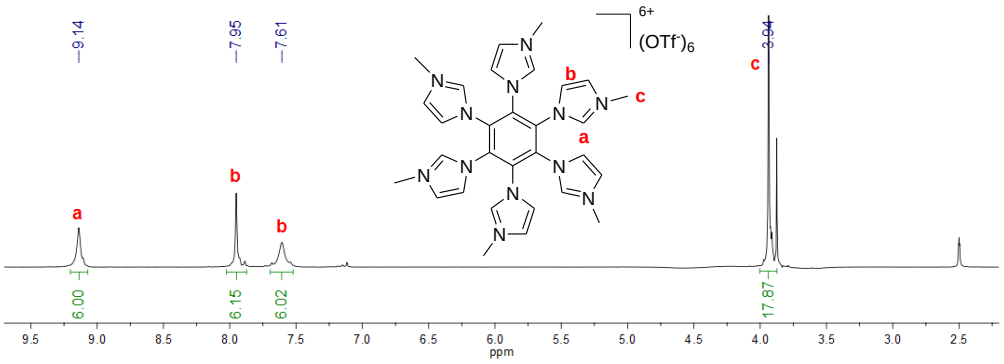


**Figure 4.9** $^{1}$H NMR spectrum of **[LH$_6$](OTf)$_6$** in DMSO-$d_6$

Due to the rotation of the imidazolium rings around the $C_{phenyl}$-$N_{imz}$ bond in solution, an average conformation is observed rather than a particular conformation, as may be inferred from the observation of only one type of NC*H*N proton signal. The observation of only two signals due to the two C*H* groups of the six imidazolium rings supports the formation of a highly symmetrical structure in solution. This observation supports the possibility that this NHC precursor may be used for the preparation of a sandwich-like carbene complex, as previously observed for the related complexes (**4.4** and **4.6**) shown in Scheme 4.3.

### *$^{13}$C{$^{1}$H} NMR spectrum of* ***[LH$_6$](OTf)$_6$***

Figure 4.10 shows the $^{13}$C{$^{1}$H} NMR spectrum of **[LH$_6$](OTf)$_6$**. Probably, the most characteristic signal is the one due to the NC*H*N carbons, which provide a single resonance at 138.2 ppm (1). The resonances due to the aromatic $C_{quaternary}$, and C*H* groups of the imidazolium rings are shown at 133.6 (2), 126.8 and 122.8 ppm (3), respectively. The signal assigned to the carbon of the C$H_3$ groups appears at 37.5 ppm (4). The signal of the carbon of the counteranion $CF_3SO_3^-$ ($OTf^-$), is observed as a consequence of the coupling with the three fluorines.

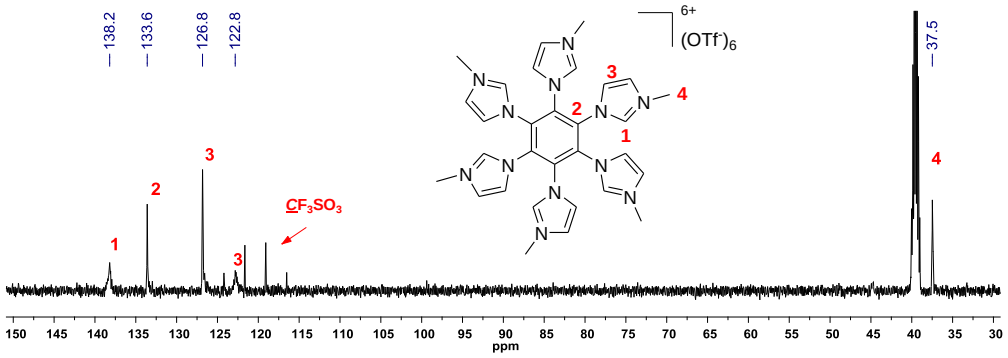


**Figure 4.10** $^{13}C\{^{1}H\}$ NMR spectrum of **[LH$_6$](OTf)$_6$** in DMSO-$d_6$

*b) Synthesis and characterization of hexanuclear dodecarbene complexes **26L-29M***

Once the hexaimidazolium salts, **[LH$_6$](OTf)$_6$** and **[MH$_6$](BF$_4$)$_6$**, were synthesised and fully characterised, the coordination of the ligands derived from them to Ag(I) and Au(I) was carried out. In this section we will give details about the coordination and the characterization of the resulting products.

For the coordination of the ligands derived from **[LH$_6$](OTf)$_6$** and **[MH$_6$](BF$_4$)$_6$**, we used the well-known reaction of the azolium salts with $Ag_2O$. The method used is inspired in the pioneer work reported by Lin et al[73] for the preparation of Ag-NHC complexes, and has been extensively applied by Hahn and co-workers for the synthesis of compounds **4.3**, **4.4**, **4.6** and **4.10** (Scheme 4.3).[16, 14, 50-51]

The reaction of **[LH$_6$](OTf)$_6$** (or **[MH$_6$](BF$_4$)$_6$**) with $Ag_2O$ in $CH_3OH$ at 50ºC afforded the corresponding cylinder-type complexes, **26L** and **27M**, (Scheme 4.10) consisting of six Ag(I) centres bridged by two benzene-hexaimidazolylidenes. The good solubility of the complexes obtained in organic solvents, suggested that discrete molecular structures were formed, rather than polymeric structures that should have provided materials with low solubility. The assumption that the cylinder-type Ag complexes, **26L** and **27M**, were formed, was made based on the characterization of the resulting products (*vide infra*).

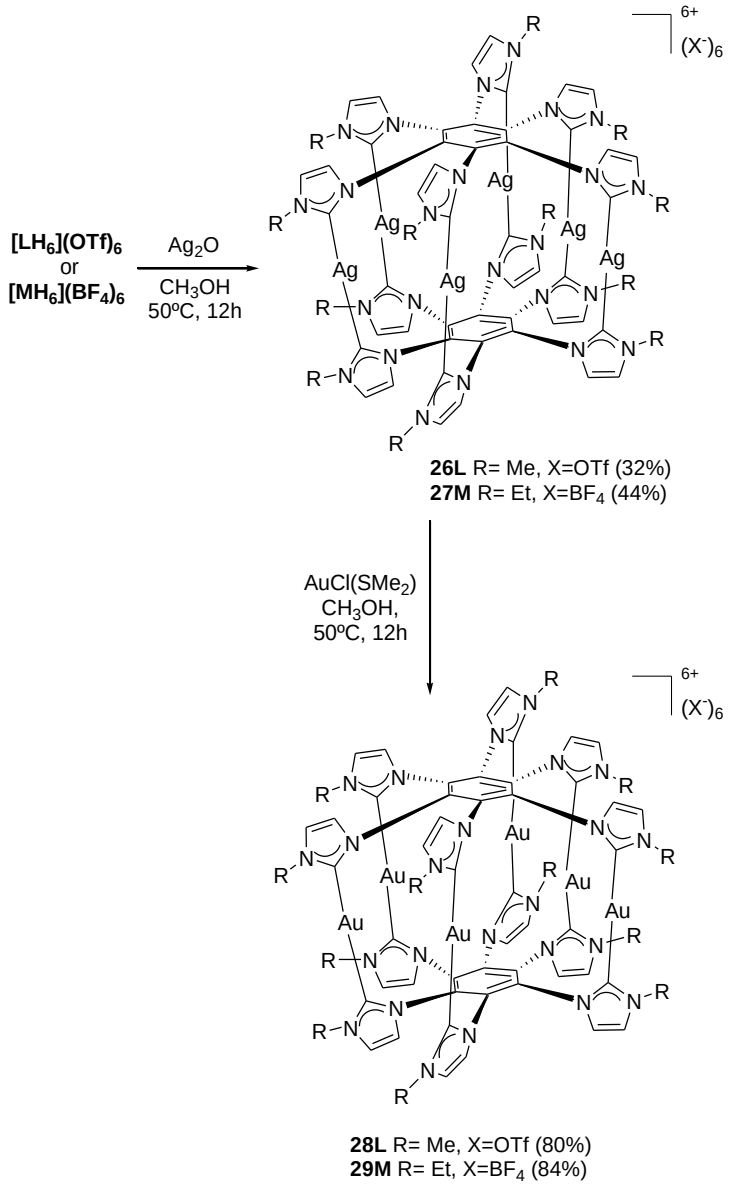


**Scheme 4.10** Synthesis of **26L, 27M**, **28L** and **29M**

The silver(I)-NHC complexes **26L** and **27M** were found to be excellent carbene transfer agents. All six silver atoms in **26L** and **27M** can be replaced by Au(I) to yield the corresponding homohexa-gold(I) carbene complexes **28L** and **29M** in 80 and 84% yield, respectively, without destruction of the three-dimensional metallosupramolecular assembly (Scheme 4.10). Transmetallation of Ag(I) to Au(I)

carbene complexes could be visually monitored from the precipitation of AgCl. Although AgCl started to precipitate immediately, the reaction mixtures were left stirring for 12h at 50ºC in $CH_3OH$, in order to allow the reactions to reach completion.

The new hexametallic dodecarbene compounds, **26L**, **27M**, **28L** and **29M**, were characterised by means of NMR spectroscopy and High Resolution Mass Spectrometry (ESI-TOF-MS). As an example, the NMR spectroscopic characterization of **26L** is discussed below in detail. All the details of the spectroscopic data for compounds **27M**, **28L** and **29M** can be found in the Experimental Section (Chapter 5).

*$^1$H NMR spectrum of **26L***

Figure 4.11 shows the $^1$H NMR spectrum of **26L**. The first indication suggesting the formation of the carbene complex is the disappearance of the signal attributed to the proton of the NC*H*N group. The resonances due to the protons of the C*H* groups of the imidazolium units are shown at 7.47 and 7.37 ppm (a). The signal corresponding to the protons of the C$H_3$ groups appears at 3.88 ppm (b). The observation of only two resonances for the C*H* groups of the imidazolium units indicates the formation of a highly symmetrical structure in solution.

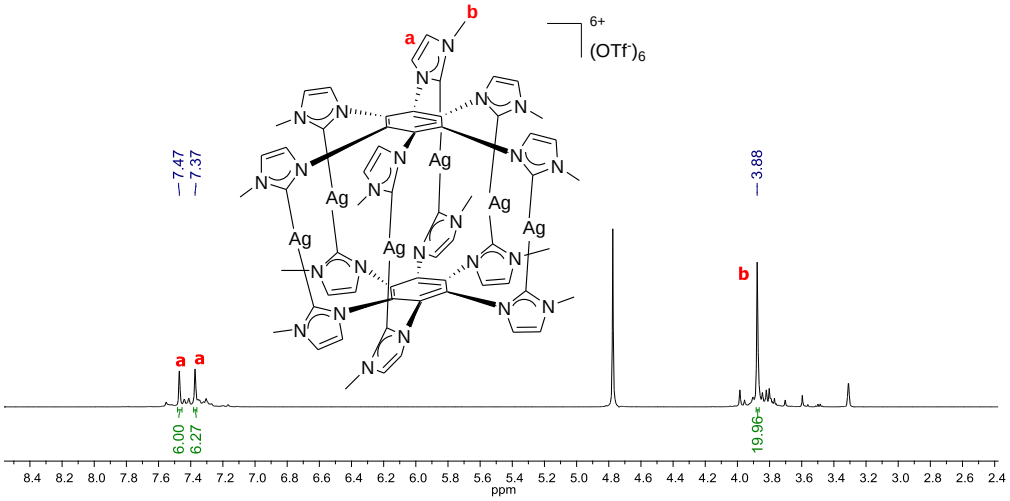


**Figure 4.11** $^1$H NMR spectrum of **26L** in $CD_3OD$

*$^{13}C\{^{1}H\}$ NMR spectrum of **26L***

Figure 4.12 shows the $^{13}C\{^{1}H\}$ NMR spectrum of **26L**. Probably, the most characteristic signal is the one that corresponds to the metallated carbene carbons, at 181.4 ppm (1), exhibiting the rarely observed coupling to both silver isotopes (dd, $^{1}J_{107AgC}$ = 182.0 Hz, $^{1}J_{109AgC}$ = 210.1 Hz). The observed chemical shifts and $^{1}J_{107/109AgC}$ coupling constants fall in the range previously described for similar compounds such as **4.3**, **4.4**, **4.6** and **4.10** (Scheme 4.3). [16, 14, 50-51] The resonances due to the aromatic $C_{quaternary}$ and *C*H groups of the imidazolium units are shown at 138.1 (2), 126.7 and 124.7 ppm (3), respectively. The signal assigned to the carbon of the $CH_3$ groups appears at 40.1 ppm (4). In this case, the signal assigned to the carbon of the $CF_3SO_3^-$ ($OTf^-$) counteranion, is observed as a quartet, as a consequence of coupling with the three fluorine atoms.

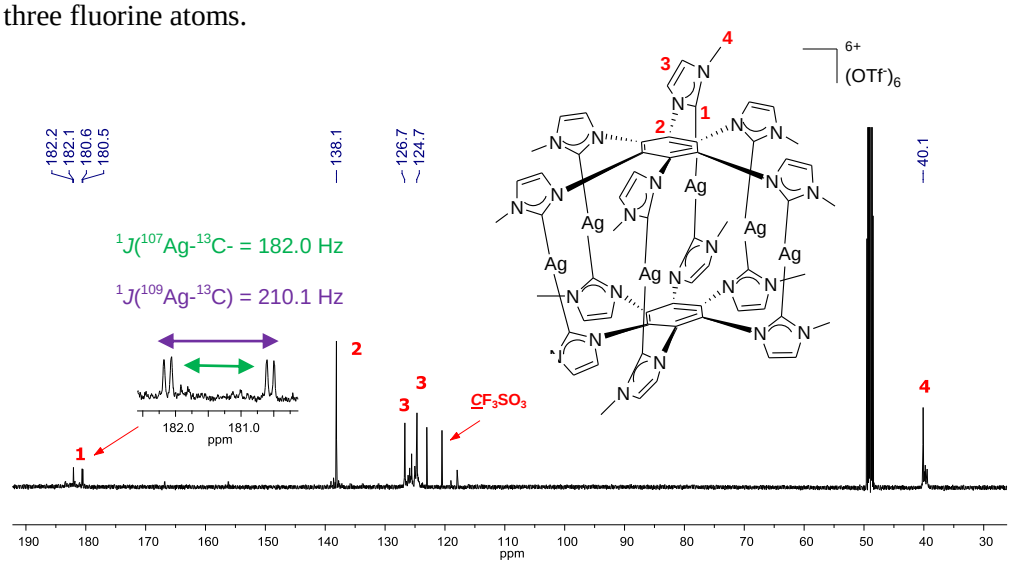


**Figure 4.12** $^{13}C\{^{1}H\}$ NMR spectrum of **26L** in $CD_3OD$

*Molecular structure of **27M***

Crystals of **27M** suitable for X-Ray Diffraction analysis were obtained by slow diffusion of diethyl ether into a concentrated solution of the compound in acetonitrile. Low thermal stability and high light sensitivity was observed. Several data sets were collected with different crystals. In all cases the same molecular structure was found. Data refinement, however, proved to be difficult due to a poor diffraction along with an important disorder of the $BF_4^-$ counteranions, which could not be fully resolved.

The best refinement (R= 0.0873) was obtained only after three $BF_4^-$ counteranions of the asymmetric unit were removed prior application of SQUEEZE methodology. However, we believe that the structure may be used to unambiguously confirm the geometry of the molecule, although a detailed analysis of the metric parameters should be done with care.

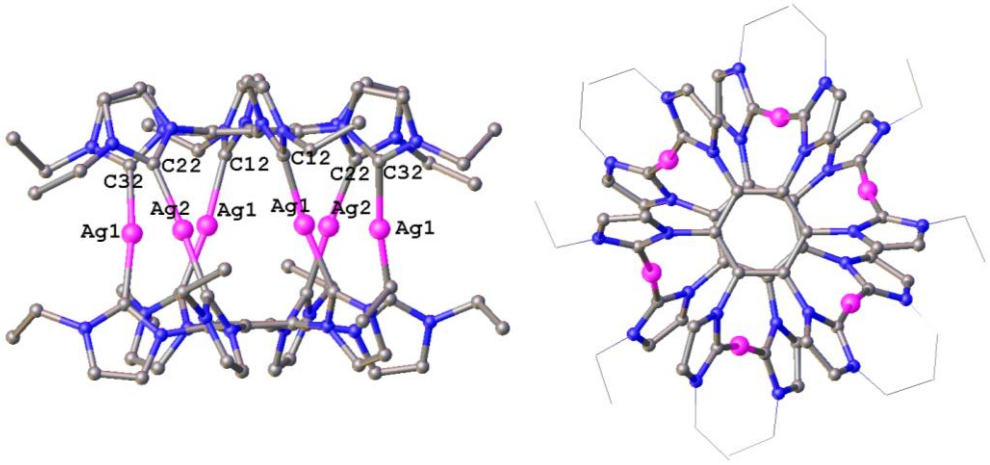


**Figure 4.13** Two perspectives of the molecular structure of **27M**. Thermal ellipsoids are at the 20% probability level. Hydrogen atoms and counterions ($6BF_4^-$) are omitted for clarity.

The molecular structure of the complex (Figure 4.13), is built from six silver(I) ions sandwiched in between two hexacarbene ligands related to each other by a pseudo-inversion centre. For the formation of **27M**, the plane of the NHC donor must rotate out of the plane of the central phenyl ring. For steric reasons, the six imidazol-2-ylidene rings of both ligands rotate from an imaginary perpendicular orientation relative to the central phenyl ring in an anticlockwise direction. The relative orientation of the two benzene-hexaimidazolylidene ligands is staggered, as can be seen from the top-view of the molecule.

Table 4.1 shows the most representative bond lengths (Å) and angles (º) of complex **27M**. The six silver ions form a quasi-regular hexagon, with Ag-Ag distances ranging between 3.416 and 3.569 Å, with the shortest distances being slightly shorter than the sum of the *van der Waals* radii of two silver atoms,[74] and very similar to the shortest Ag-Ag distance established in the related tetrasilver complex derived from complex **4.4** (Scheme 4.2).[14] Each Ag(I) ion is coordinated by two NHC donors from two

different hexacarbene ligands in an almost linear fashion ($C_{imz}$-Ag-$C_{imz}$ range: 173.4-171.1°). The Ag-$C_{imz}$ bond lengths range from 2.054 to 2.078 Å, and fall within the limits for related silver-carbenes in cylinder-like structures **4.4** and **4.6** (Scheme 4.3).[50-51] The separation between the two phenyl ring centroids is 5.387 Å, therefore any type of non-covalent interaction can be discarded.

**Table 4.1** Selected bond lengths and angles of complex **27M**

| Bond lengths (Å) | | Bond angles (º) | |
|---|---|---|---|
| Ag(2)-C(22) | 2.060(11) | C(22)-Ag(2)-C(22) | 173.4(6) |
| Ag(1)-C(12) | 2.078(10) | C(12)-Ag(1)-C(32) | 171.1(4) |
| Ag(1)-C(32) | 2.054(7) | | |
| Ph($C_{centroid}$(1))-Ph($C_{centroid}$(2)) | 5.387(7) | | |

## 4.3 CONCLUSIONS

In this chapter we have prepared and characterised a novel tribenzotriquinacene-based tri-NHC, **K**. Ligand **K** possesses a rigid, $C_{3v}$-symmetrical framework, which provides a unique bowl-shaped topology to the ligand, and spans the versatility of NHCs to a potential new family of metal complexes with unusual properties. The **TBTQ**-based tri-NHC, **K**, has been coordinated to [RhCl(COD)], generating a new tri-Rh(I) complex, **25K**, in which the three metal centres are essentially electronically disconnected. The electronic disconnection of the metal centres in the complex suggests that the scaffold may be used to support different types of metal complexes without detriment to their potential catalytic activity, and therefore, the ligand may be an excellent support for the study of cooperative effects.

On the other hand, we have developed the preparation and coordination of a new benzene-hexa-imidazolylidene, that we have used for the self-assembly formation of a series of cylinder-like complexes of silver and gold, **26L**-**29M**. The new complexes constitute unique examples of discrete molecular arrangements in which six metals atoms are sandwiched between two hexacarbene ligands, thus affording a very singular type of molecule, which can only be related to other existing cylinder-shaped NHC-based complex of lower nuclearity.[50-51] The formation of these type of supramolecular complexes may open the door to the preparation of high-nuclearity complexes with well defined cavities, which in turn may be modulated by the choice of the ligand. Further studies may imply the developing of methods to prepare poly-NHC-based ligands that can give rise to larger cavities, in order to explore their capabilities in the selective recognition of ions and neutral small molecules.

## 4.4 REFERENCES


1. Crabtree, R. H., *New J. Chem.* **2011**, *35*, 18-23.
2. Kurth, D. G., *Science and Technology of Advanced Materials* **2008**, *9*.
3. Braga, D.; Grepioni, F., *Coord. Chem. Rev.* **1999**, *183*, 19-41.
4. Keene, F. R., *Coord. Chem. Rev.* **1997**, *166*, 121-159.
5. Peris, E.; Crabtree, R. H., *Coord. Chem. Rev.* **2004**, *248*, 2239-2246.
6. Mata, J. A.; Poyatos, M.; Peris, E., *Coord. Chem. Rev.* **2007**, *251*, 841-859.
7. Poyatos, M.; Mata, J. A.; Peris, E., *Chem. Rev.* **2009**, *109*, 3677-3707.
8. Corberan, R.; Mas-Marza, E.; Peris, E., *Eur. J. Inorg. Chem.* **2009**, 1700-1716.
9. Gonell, S.; Poyatos, M.; Mata, J. A.; Peris, E., *Organometallics* **2012**, *31*, 5606-5614.
10. Gonell, S.; Poyatos, M.; Mata, J. A.; Peris, E., *Organometallics* **2011**, *30*, 5985-5990.
11. Gonell, S.; Alabau, R. G.; Poyatos, M.; Peris, E., *Chem. Commun.* **2013**, *49*, 7126-7128.
12. Maity, R.; Koppetz, H.; Hepp, A.; Hahn, F. E., *J. Am. Chem. Soc.* **2013**, *135*, 4966-4969.
13. Brinke, C. S. T.; Pape, T.; Hahn, F. E., *Dalton Trans.* **2013**, *42*, 7330-7337.
14. Rit, A.; Pape, T.; Hepp, A.; Hahn, F. E., *Organometallics* **2011**, *30*, 334-347.
15. Maity, R.; Brinke, C. S. T.; Hahn, F. E., *Dalton Trans.* **2013**, *42*, 12857-12860.
16. Hahn, F. E.; Radloff, C.; Pape, T.; Hepp, A., *Chem.-Eur. J.* **2008**, *14*, 10900-10904.
17. Maity, R.; Rit, A.; Brinke, C. S. T.; Daniliuc, C. G.; Hahn, F. E., *Chem. Commun.* **2013**, *49*, 1011-1013.
18. Mercs, L.; Neels, A.; Albrecht, M., *Dalton Trans.* **2008**, 5570-5576.
19. Er, J. A. V.; Tennyson, A. G.; Kamplain, J. W.; Lynch, V. M.; Bielawski, C. W., *Eur. J. Inorg. Chem.* **2009**, 1729-1738.
20. Prades, A.; Peris, E.; Alcarazo, M., *Organometallics* **2012**, *31*, 4623-4626.

21. Prades, A.; Poyatos, M.; Mata, J. A.; Peris, E., *Angew. Chem. Int. Ed.* **2011**, *50*, 7666-7669.
22. Gonell, S.; Poyatos, M.; Peris, E., *Angew. Chem. Int. Ed.* **2013**, *52*, 7009-7013.
23. Zanardi, A.; Mata, J. A.; Peris, E., *Chem. Eur. J.* **2010**, *16*, 13109-13115.
24. Zanardi, A.; Mata, J. A.; Peris, E., *Organometallics* **2009**, *28*, 4335-4339.
25. Zanardi, A.; Mata, J. A.; Peris, E., *J. Am. Chem. Soc.* **2009**, *131*, 14531-14537.
26. Zanardi, A.; Corberan, R.; Mata, J. A.; Peris, E., *Organometallics* **2008**, *27*, 3570-3576.
27. Sabater, S.; Mata, J. A.; Peris, E., *Chem.-Eur. J.* **2012**, *18*, 6380-6385.
28. Guisado-Barrios, G.; Hiller, J.; Peris, E., *Chem.-Eur. J.* **2013**, 10405-10411.
29. Sabater, S.; Mata, J. A.; Peris, E., *Nat. Commun.* **2013**, *4*.
30. Mata, J. A.; Hahn, F. E.; Peris, E., *Chem. Sci*. **2014**, *5*, 1723-1732.
31. Gonell, S.; Poyatos, M.; Peris, E., *Angew. Chem. Int. Ed.* **2013**, *52*, 7009-7013.
32. Gonell, S.; Alabau, R. G.; Poyatos, M.; Peris, E., *Chem. Commun.* **2013**, *49*, 7126-7128.
33. Williams, K. A.; Bielawski, C. W., *Chem. Commun.* **2010**, *46*, 5166-5168.
34. Niu, W. X.; Yang, E. Q.; Shi, Z. F.; Cao, X. P.; Kuck, D., *J. Org. Chem.* **2012**, *77*, 1422-1434.
35. Mughal, E. U.; Kuck, D., *Eur. J. Org. Chem.* **2012**, 3416-3423.
36. Wang, T.; Hou, Q. Q.; Teng, Q. F.; Yao, X. J.; Niu, W. X.; Cao, X. P.; Kuck, D., *Chem.-Eur. J.* **2010**, *16*, 12412-12424.
37. Mughal, E. U.; Kuck, D., *Org. Bio. Chem.* **2010**, *8*, 5383-5389.
38. Zhou, L.; Zhang, T. X.; Li, B. R.; Cao, X. P.; Kuck, D., *J. Org. Chem.* **2007**, *72*, 6382-6389.
39. Kuck, D.; Schuster, A.; Krause, R. A.; Tellenbroker, J.; Exner, C. P.; Penk, M.; Bogge, H.; Muller, A., *Tetrahedron* **2001**, *57*, 3587-3613.
40. Tellenbroker, J.; Kuck, D., *Angew. Chem. Int. Ed.* **1999**, *38*, 919-922.
41. Kirchwehm, Y.; Damme, A.; Kupfer, T.; Braunschweig, H.; Krueger, A., *Chem. Commun.* **2012**, *48*, 1502-1504.
42. Chianese, A. R.; Mo, A.; Datta, D., *Organometallics* **2009**, *28*, 465-472.

43. Lehn, J. M.; Rigault, A.; Siegel, J.; Harrowfield, J.; Chevrier, B.; Moras, D., *Proc. Natl. Acad. Sci. U. S. A.* **1987**, *84*, 2565-2569.
44. Albrecht, M., *Chem. Rev.* **2001**, *101*, 3457-3497.
45. Piguet, C.; Bernardinelli, G.; Hopfgartner, G., *Chem. Rev.* **1997**, *97*, 2005-2062.
46. Boyer, J. L.; Kuhlman, M. L.; Rauchfuss, T. B., *Acc. Chem. Res.* **2007**, *40*, 233-242.
47. Therrien, B.; Suess-Fink, G.; Govindaswamy, P.; Renfrew, A. K.; Dyson, P. J., *Angew. Chem. Int. Ed.* **2008**, *47*, 3773-3776.
48. Kreickmann, T.; Hahn, F. E., *Chem. Commun.* **2007**, 1111-1120.
49. Yamamotoa, Y.; Suzuki, H.; Tajima, N.; Tatsumi, K., *Chem.-Eur. J.* **2002**, *8*, 372-379.
50. Lai, S. W.; Cheung, K. K.; Chan, M. C. W.; Che, C. M., *Angew. Chem. Int. Ed.* **1998**, *37*, 182-184.
51. Han, Y.; Lee, L. J.; Huynh, H. V., *Chem.-Eur. J.* **2010**, *16*, 771-773.
52. Rit, A.; Pape, T.; Hahn, F. E., *J. Am. Chem. Soc.* **2010**, *132*, 4572-4573.
53. Rit, A.; Pape, T.; Hahn, F. E., *Organometallics* **2011**, *30*, 6393-6401.
54. Han, Y.-F.; Jia, W.-G.; Lin, Y.-J.; Jin, G.-X., *Angew. Chem. Int. Ed.* **2009**, *48*, 6234-6238.
55. Yoon, J.; Kim, S. K.; Singh, N. J.; Kim, K. S., *Chem. Soc. Rev.* **2006**, *35*, 355-360.
56. Birkmann, B.; Froehlich, R.; Hahn, F. E., *Chem.-Eur. J.* **2009**, *15*, 9325-9329.
57. Wong, W. W. H.; Vickers, M. S.; Cowley, A. R.; Paul, R. L.; Beer, P. D., *Org. Biomol. Chem.* **2005**, *3*, 4201-4208.
58. Pluth, M. D.; Bergman, R. G.; Raymond, K. N., *Science* **2007**, *316*, 85-88.
59. Yoshizawa, M.; Tamura, M.; Fujita, M., *Science* **2006**, *312*, 251-254.
60. Kuck, D.; Lindenthal, T.; Schuster, A., *Chem. Ber.-Recl.* **1992**, *125*, 1449-1460.
61. Hahn, F. E.; Wittenbecher, L.; Le Van, D.; Frohlich, R., *Angew. Chem. Int. Ed.* **2000**, *39*, 541.

62. Khramov, D. M.; Boydston, A. J.; Bielawski, C. W., *Angew. Chem. Int. Ed.* **2006**, *45*, 6186-6189.

63. Wang, Y.-T.; Chang, M.-T.; Lee, G.-H.; Peng, S.-M.; Chiu, C.-W., *Chem. Commun.* **2013**, *49*, 7258-7260.

64. Hahn, F. E.; Wittenbecher, L.; Boese, R.; Blaser, D., *Chem.-Eur. J.* **1999**, *5*, 1931-1935.

65. Bittermann, A.; Herdtweck, E.; Harter, P.; Herrmann, W. A., *Organometallics* **2009**, *28*, 6963-6968.

66. Poater, A.; Cosenza, B.; Correa, A.; Giudice, S.; Ragone, F.; Scarano, V.; Cavallo, L., *Eur. J. Inorg. Chem.* **2009**, 1759-1766.

67. Chianese, A. R.; Li, X. W.; Janzen, M. C.; Faller, J. W.; Crabtree, R. H., *Organometallics* **2003**, *22*, 1663-1667.

68. Gusev, D. G., *Organometallics* **2009**, *28*, 6458-6461.

69. Gusev, D. G.; Peris, E., *Dalton Trans.* **2013**, 7359-7364.

70. Hahn, F. E.; Langenhahn, V.; Lugger, T.; Pape, T.; Le Van, D., *Angew. Chem. Int. Ed.* **2005**, *44*, 3759-3763.

71. Radloff, C.; Weigand, J. J.; Hahn, F. E., *Dalton Trans.* **2009**, 9392-9394.

72. Henrie, R. N.; Yeager, W. H., *Heterocycles* **1993**, *35*, 415-426.

73. Wang, H. M. J.; Lin, I. J. B., *Organometallics* **1998**, *17*, 972-975.

74. Ray, L.; Shaikh, M. M.; Ghosh, P., *Inorg. Chem.* **2008**, *47*, 230-240.

# CHAPTER 5

# EXPERIMENTAL SECTION

# 5.1 ANALYTICAL TECHNIQUES

### Nuclear Magnetic Resonance (NMR)

$^{1}$H, $^{1}$H-$^{1}$H gCOSY, $^{1}$H-$^{1}$H gNOESY, $^{13}$C{$^{1}$H}, $^{1}$H-$^{13}$C gHSQC and $^{1}$H-$^{13}$C gHMBC NMR spectra were recorded at 303-333 K on a Bruker AC 200 ($^{1}$H 200 MHz, $^{13}$C 50 MHz), a Varian Mercury 300 MHz and a Bruker ARX 300 ($^{1}$H 300 MHz, $^{13}$C 75 MHz), a Bruker AMX 400 ($^{1}$H 400 MHz, $^{13}$C 100 MHz), and a Varian NMR System 500 MHz ($^{1}$H 500 MHz, $^{13}$C 125 MHz) spectrometers. Chemical shifts are given in ppm (δ) and referenced to the residual peak of the deuterated solvent ($^{1}$H, $^{13}$C) as follows: $CDCl_3$ (δ 7.26, 77.16), $CD_2Cl_2$ (δ 5.32, 53.84), $CD_3CN$ (δ 1.94, 1.32), $C_6D_6$ (δ 7.16, 128.06), DMSO-$d_6$ (δ 2.50, 39.52) and $D_2O$ (δ 4.79).

### Electrospray Mass Spectra (ESI-MS)

Electrospray mass spectra (ESI-MS) were recorded on a Micromass Quatro LC instrument; $CH_3OH$ or $CH_3CN$ were used as mobile phase and nitrogen was employed as drying and nebulizing gas. Accurate mass measurements (HRMS) were performed by use of a Q-TOF Premier mass spectrometer with electrospray source (Waters, Manchester, UK) operating at a resolution of ca. 16 000 (fwhm).

### Elemental Analysis (EA)

Elemental analyses were carried out on a EuroEA3000 Eurovector Analyzer.

### Gas Chromatography (GC)

GC analyses were obtained on a Shimadzu GC-2010 apparatus equipped with a FID and a Technokroma (TRB-5MS, 30 m x 0.25 mm x 0.25 μm) column and on a Shimadzu GCMS-QP2010 apparatus equipped with a Technokroma (TRB-5MS, 30 m x 0.25 mm x 0.25 μm) column.

### Infrared Spectroscopy (IR)

Infrared spectra (FT-IR) were performed on a Bruker EQUINOX 55 spectrometer with a spectral window of 4000-600 $cm^{-1}$. Liquid samples were placed between KBr windows.

**Electrochemical Measurements**

The measurements were carried out using a GPES equipped PGSTAT-30 potentiostat from Autolab at room temperature. A three-electrode configuration was used, where two Pt microelectrodes were connected to the working electrode and counter electrode and a Ag wire was used as the pseudo-reference electrode. Redox potential of $Fe(C_2H_5)_2^+/Fe(C_2H_5)_2$ (445 mV) was used to calibrate the potential scale. Measurements were performed on 10 mM analyte in $CH_2Cl_2$ with 0.1 mM $[NBu_4]PF_6$ as supporting electrolyte, at a 100 mV $s^{-1}$ scan rate.

# 5.2 SYNTHESIS OF COMPLEXES

All operations were carried out by using standard Schlenk techniques under nitrogen atmosphere unless otherwise stated. Solvents were purified on a MBraun SPS or purchased from Aldrich and degassed prior to use by purging with nitrogen and kept over molecular sieves. All other reagents were used as received from commercial suppliers. Column chromatrography was performed on silica gel (*Merk* 60, 63-200 µm) using the solvents or mixture of solvents indicated. Metal precursors: $[IrCl(COD)]_2$,[1] $[IrCp^*Cl_2]_2$,[2] $[RhCl(COD)]_2$,[3] $[RhCp^*Cl_2]_2$,[4] $[RhCl(NBD)]_2$,[5] $[AuCl(SMe_2)]$;[6] ligands or ligand precursors: (1-methyl-3-propanesulfonate)imidazolium, **AH**,[7] bis(imidazol-1-yl)methane,[8] 2,6-bis(imidazol-1yl)pyridine,[9] 1,3-bis(2,4,6-trimethylphenyl)formamidine, **D**,[10] hexabromotribenzotriquinacene,[11] 1,3-bis(2,6-diisopropylphenyl)imidazolium chloride (IPr·HCl),[12] hexa(imidazol-1-yl)benzene;[13] and organometallic compound $[RhCl(BimNtBu_2)(COD)]$[14] (BimN*t*Bu = 1,3-di(*tert*-butyl)benzimidazolylidene), were prepared according to literature procedures.

## 5.2.1 Synthesis of azolium ligand precursors

### Synthesis of bis(3-propanesulfonateimidazol-1-yl)methane, $BH_2$

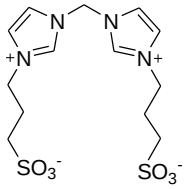

Preparation of compound **$BH_2$** was carried out by reaction of bis(imidazol-1-yl)methane and 1,3-propanesultone, under different reaction conditions than those reported in the literature.[15] A suspension of bis(imidazol-1-yl)methane (500 mg, 3.37 mmol) and 1,3-propanesultone (2.06 g, 16.9 mmol) in $CH_3CN$, was heated at 100ºC for 12h under aerobic conditions. After this time, the reaction mixture was cooled to room temperature and the generated solid was collected by filtration and washed with $CH_2Cl_2$ and $CH_3OH$. Compound **$BH_2$** was isolated as a white, air and moisture stable solid. Yield: 1.09 g (82 %). Compound **$BH_2$** was identified according to reported spectroscopic data.[15]

**Synthesis of 2,6-bis(3-propanesulfonateimidazol-1-yl)pyridine, $CH_2$**

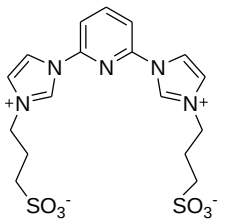

A suspension of 2,6-bis(imidazol-1-yl)pyridine (530 mg, 2.51 mmol) and 1,3-propanesultone (1.53 g, 12.6 mmol) in $CH_3CN$, was heated at 100ºC for 12h under aerobic conditions. After this time, the reaction mixture was cooled to room temperature and the generated solid was collected by filtration and washed with $CH_2Cl_2$ and $CH_3OH$. Compound **$CH_2$** was isolated as a white, air and moisture stable solid. Yield: 972 mg (85 %). $^1$H NMR (300 MHz, $D_2O$, 303 K): δ = 9.94 (s, 2H, NC*H*N), 8.50 (t, $^3J_{HH}$ = 8.1 Hz, 1H, C$H_{pyr}$), 8.42 (s, 2H, C$H_{imz}$), 8.07 (d, $^3J_{HH}$ = 8.1 Hz, 2H, C$H_{pyr}$), 7.90 (s, 2H, C$H_{imz}$), 4.62 (t, $^3J_{HH}$ = 7.2 Hz, 4H, NC$H_2$), 3.08 (t, $^3J_{HH}$ = 7.2 Hz, 4H, $CH_2CH_2SO_3$), 2.51 (t, $^3J_{HH}$ = 7.2 Hz, 4H, $CH_2CH_2SO_3$). $^{13}$C{1H} NMR (75 MHz, $D_2O$, 303 K): δ 145.8 (s, N*C*HN), 145.0 (s, $C_{qpyr\text{-}ortho}$), 135.3 (s, *C*H$_{pyr\text{-}para}$), 123.9 (s, *C*$_{imz}$), 120.1 (s, *C*$_{imz}$), 115.1 (s, *C*H$_{pyr\text{-}meta}$), 49.0 (s, N*C*$H_2$), 47.5 (s, $CH_2CH_2SO_3$), 25.2 (s, $CH_2CH_2SO_3$). ESI-MS (20 V, $CH_3OH$): *m/z* 334.2 [M-$C_3H_6SO_3$]$^+$. Anal. calcd. for $C_{17}H_{21}N_5S_2O_6$ (mol. wt. 455.51): C, 44.83; H, 4.65; N, 15.37. Found: C, 44.64; H, 4.32; N, 14.21.

**Synthesis of [1-(1'-methylpyridinium-3'-yl)-3-methyl]imidazolium diiodide, $[EH_2]I_2$**

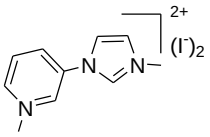

A mixture of imidazole (2.18 g, 32 mmol), 3-bromopyridine (1.54 mL, 16 mmol), $CuSO_4 \cdot 5H_2O$ (100 mg, 0.60 mmol), and $K_2CO_3$ (2.95 g, 21 mmol) was heated at 150ºC for 48h under nitrogen atmosphere. After this time, the reaction mixture was cooled to room temperature and the generated brown solid was dissolved in 50 mL of $H_2O$ and extracted with EtOAc, to obtain 1-(3'-pyridyl)imidazole and unreacted imidazole. This mixture, without further purification, was refluxed with iodomethane (3 mL, 48 mmol) in $CH_3CN$ (20 mL) for 24h, during this time **$[EH_2]I_2$** precipitated in the reaction medium which was collected by filtration and washed with $Et_2O$. Compound **$[EH_2]I_2$** was isolated as a pale yellow, air and moisture stable solid. Yield: 4.90 g (71%). For 1-(3'-pyridyl)imidazole: $^1$H NMR (500 MHz, DMSO-$d_6$, 303 K): δ = 8.95 (s, 1H, C$H_{pyr}$), 8.57 (d, $^3J_{HH}$ = 4 Hz, 1H, C$H_{pyr}$), 8.35 (s, 1H, C$H_{imz}$), 8.11 (d, $^3J_{HH}$ = 8 Hz, 1H, C$H_{pyr}$), 7.84 (s, 1H, C$H_{imz}$), 7.57 (dd, $^3J_{HH}$ = 4 Hz, $^3J_{HH}$ = 8 Hz, 1H, C$H_{pyr}$), 7.16 (s, 1H, C$H_{imz}$). For **$[EH_2]I_2$**: $^1$H NMR (500 MHz, DMSO-$d_6$, 303 K): δ = 9.99 (s, 1H, NC*H*N), 9.76 (d, $^3J_{HH}$ = 1 Hz, 1H, C$H_{pyr}$), 9.19 (d, $^3J_{HH}$ = 10 Hz, 1H, C$H_{pyr}$), 8.99

(dd, $^{4}J_{HH}$ = 2.5 Hz, $^{3}J_{HH}$ = 14 Hz, 1H, C$H_{pyr}$), 8.46 (dd, $^{3}J_{HH}$ = 10 Hz, $^{3}J_{HH}$ = 14 Hz, 1H, C$H_{pyr}$), 8.39 (t, $^{3}J_{HH}$ = 3 Hz, 1H, C$H_{imz}$), 8.07 (t, $^{3}J_{HH}$ = 3 Hz, 1H, C$H_{imz}$), 4.46 (s, 3H, C$H_{3pyr}$), 4.03 (s, 3H, C$H_{3imz}$). $^{13}C\{^{1}H\}$ NMR (125 MHz, DMSO-$d_6$, 303 K): δ = 145.9 (s, *C*H$_{pyr}$), 140.5 (s, *C*H$_{pyr}$), 138.0 (s, *C*H$_{pyr}$), 137.3 (s, N*C*HN), 133.6 (s, *C*$_{pyr}$), 128.1 (s, *C*H$_{pyr}$), 124.9 (s, *C*H$_{imz}$), 121.1 (s, *C*H$_{imz}$), 48.7 (s, *C*H$_{3pyr}$), 36.7 (s, *C*H$_{3imz}$). ESI-MS (20V, $CH_3OH$): *m/z* 174.1 $[M\text{-}2I\text{-}H]^{+}$, *m/z* 87.8 $[M\text{-}2I]^{2+}$. Anal. calcd for $C_{10}H_{13}N_3I_2$ (mol wt. 429.04): C, 27.99; H, 3.05; N, 9.79. Found: C, 28.43; H, 2.75; N, 9.50.

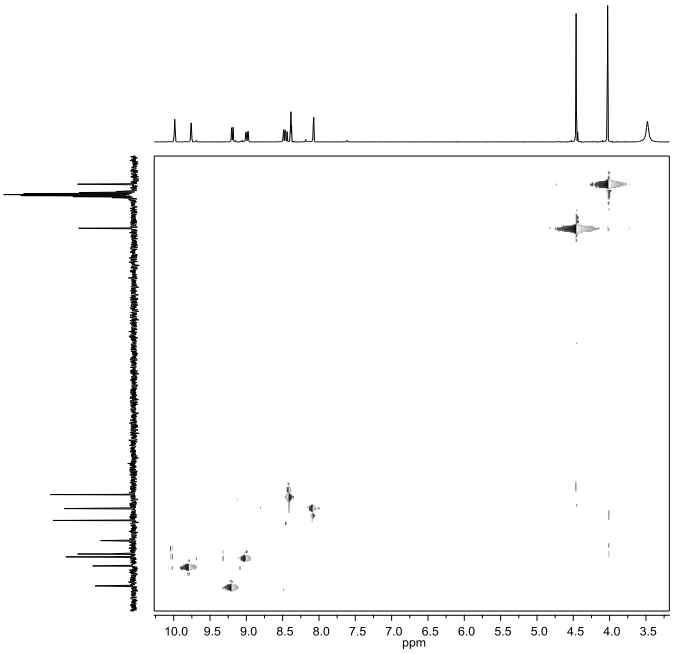


**Figure 5.1** $^{1}H$-$^{13}C$ gHSQC spectrum of **[EH$_2$]I$_2$** in DMSO-$d_6$

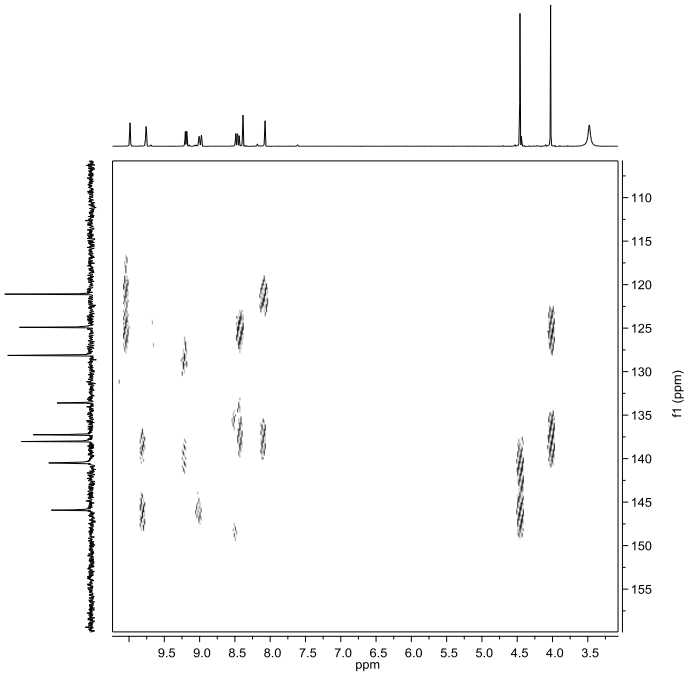


**Figure 5.2** $^{1}$H-$^{13}$C gHMBC spectrum of **[EH$_2$]I$_2$** in DMSO-$d_6$

**Synthesis of [1-(1'-methylpyridinium-3'-yl)-3-methyl] imidazolium di(hexafluorophosphate), [EH$_2$](PF$_6$)$_2$**

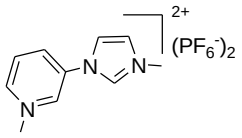


$NH_4PF_6$ (1.14 g, 7 mmol) was added slowly to a solution of **[EH$_2$]I$_2$** (1.00 g, 2.33 mmol) in $CH_3OH$ (25 mL). The mixture was stirred at room temperature for 2h, during this time **[EH$_2$](PF$_6$)$_2$** precipitated in the reaction medium which was collected by filtration and washed with cold $CH_3OH$ and $Et_2O$. Compound **[EH$_2$](PF$_6$)$_2$** was isolated as a colourless, air and moisture stable solid. Yield: 0.83 g (77%). $^{1}$H NMR (500 MHz, DMSO-$d_6$, 303 K): δ = 9.95 (s, 1H, C$H_{pyr}$), 9.73 (s, 1H, NC*H*N), 9.18 (d, $^{3}J_{HH}$ = 6 Hz, 1H, C$H_{pyr}$), 8.97 (d, $^{3}J_{HH}$ = 8 Hz, 1H, C$H_{pyr}$), 8.45 (dd, $^{3}J_{HH}$ = 6 Hz, $^{3}J_{HH}$ = 8 Hz, 1H, C$H_{pyr}$), 8.35 (s, 1H, C$H_{imz}$), 8.05 (s, 1H, C$H_{imz}$), 4.45 (s, 3H, C$H_{3pyr}$), 4.02 (s, 3H, C$H_{3imz}$). $^{13}$C{$^{1}$H} NMR (125 MHz, DMSO-$d_6$, 303 K): δ = 146.1, 140.6, 138.2, 137.4, 133.9, 128.3, 125.1, 121.2 (s, *C*H$_{imz}$, *C*$_{pyr}$ and *C*H$_{pyr}$), 48.7 (s, *C*H$_{3pyr}$), 36.7 (s, *C*H$_{3imz}$). ESI-MS (20V, $CH_3OH$): *m/z* 174.1 [M-2(PF$_6$)-H]$^{+}$, *m/z*

87.7 [M-2($PF_6$)]$^{2+}$. Anal. calcd. for $C_{10}H_{13}N_3P_2F_{12}$ (mol wt. 465.16): C, 25.82; H, 2.82; N, 9.03. Found: C, 26.13; H, 2.93; N, 9.31.

**Synthesis of [1-(1'-*n*-butylpyridinium-3'-yl)-3-*n*-butyl]imidazolium diiodide, $[FH_2]I_2$.**

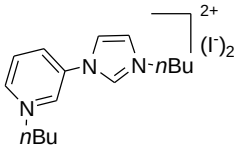

Compound **$[FH_2]I_2$** was obtained using the same procedure and quantities as for **$[EH_2]I_2$**, in this case, 1-iodobutane (5.5 mL, 48 mmol) was employed as alkylating agent. Yield: 4.0 g (50%). $^1$H NMR (500 MHz, DMSO-$d_6$, 303 K): δ = 10.06 (s, 1H, C*H*$_{pyr}$), 9.84 (s, 1H, NC*H*N), 9.31 (d, $^3J_{HH}$ = 6 Hz, 1H, C*H*$_{pyr}$), 9.04 (d, $^3J_{HH}$ = 8 Hz, 1H, C*H*$_{pyr}$), 8.50 (dd, $^3J_{HH}$ = 6 Hz, $^3J_{HH}$ = 8 Hz, 1H, C*H*$_{pyr}$), 8.45 (s, 1H, C*H*$_{imz}$), 8.18 (s, 1H, C*H*$_{imz}$), 4.72 (t, $^3J_{HH}$ = 7 Hz, 2H, NC*H*$_{2pyr}$), 4.35 (t, $^3J_{HH}$ = 7 Hz, 2H, NC*H*$_{2imz}$), 2.01 (m, 2H, $CH_2CH_{2pyr}CH_2$), 1.90 (m, 2H, $CH_2CH_{2imz}CH_2$), 1.36 (m, 4H, $CH_2CH_3$), 0.94 (t, $^3J_{HH}$ = 7 Hz, 6H, $CH_3$). $^{13}$C{$^1$H} NMR (125 MHz, DMSO-$d_6$, 303 K): δ = 145.0, 139.6, 138.4, 136.7, 134.4, 128.5, 123.7, 121.5 (s, *C*H$_{imz}$, *C*$_{pyr}$ and *C*H$_{pyr}$), 61.4 (s, N*C*H$_{2pyr}$), 49.5 (s, N*C*H$_{2imz}$), 32.2 (s, $CH_2CH_{2pyr}CH_2$), 30.9 (s, $CH_2CH_{2imz}CH_2$), 18.7 (s, *C*H$_{2pyr}$CH$_3$), 18.6 (s, *C*H$_{2imz}$CH$_3$), 13.3 (s, *C*H$_{3pyr}$), 13.2 (s, *C*H$_{3imz}$). ESI-MS (20V, $CH_3OH$): *m/z* 202.1 [M-2I-*n*Bu]$^+$, *m/z* 258.0 [M-2I-H]$^+$. Anal. calcd. for $C_{16}H_{25}N_3I_2$ (mol wt. 513.20): C, 37.45; H, 4.91; N, 8.19. Found: C, 37.67; H, 5.02; N, 8.03.

**Synthesis of [1-(1'-methylpyridinium-3'-yl)-2,3-dimethyl]imidazolium diiodide, $[GH_2]I_2$**

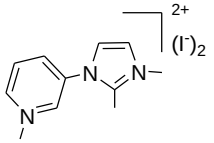

A mixture of 2-methylimidazole (1.04 g, 12.66 mmol), 3-bromopyridine (0.61 mL, 6.33 mmol), $CuSO_4 \cdot 5H_2O$ (40 mg, 0.25 mmol), and $K_2CO_3$ (1.31 g, 9.49 mmol) was heated for 48h at 185ºC under nitrogen atmosphere. After this time, the reaction mixture was cooled to room temperature and the generated brown solid was dissolved in 50 mL of $H_2O$ and extracted with EtOAc, to obtain 1-(3'-pyridyl)-2-methylimidazole and unreacted 2-methylimidazole. This mixture, without further purification, was refluxed with iodomethane (1.18 mL, 19 mmol) in $CH_3CN$ (20 mL) for 24h, during this time **$[GH_2]I_2$** precipitated in the reaction medium which was collected by filtration and washed with $Et_2O$. Compound **$[GH_2]I_2$** was isolated as a pale yellow, air and moisture stable solid. Yield: 1.12 g (35%). For 1-(3'-pyridyl)-2-

methylimidazole: $^{1}$H NMR (300 MHz, $CDCl_3$, 303 K): δ = 8.67 (m, 1H, C$H_{pyr}$), 8.62 (m, 1H, C$H_{pyr}$), 7.65 (m, 1H, C$H_{pyr}$), 7.45 (m, 1H, C$H_{pyr}$), 7.07 (d, $^{3}J_{HH}$ = 1.5 Hz, 1H, C$H_{imz}$), 7.02 (d, $^{3}J_{HH}$ = 1.5 Hz, 1H, C$H_{imz}$), 2.37 (s, 3H, C-C$H_{3imz}$). For **[$GH_2$]$I_2$**: $^{1}$H NMR (300 MHz, DMSO-$d_6$, 303 K): δ = 9.54 (s, 1H, C$H_{pyr}$), 9.24 (d, $^{3}J_{HH}$ = 6 Hz, 1H, C$H_{pyr}$), 8.86 (d, $^{3}J_{HH}$ = 8 Hz, 1H, C$H_{pyr}$), 8.43 (dd, $^{3}J_{HH}$ = 8 Hz, $^{3}J_{HH}$ = 6 Hz, 1H, C$H_{pyr}$), 8.01 (d, $^{3}J_{HH}$ = 2.4 Hz, 1H, C$H_{imz}$), 7.95 (d, $^{3}J_{HH}$ = 2.4 Hz, 1H, C$H_{imz}$), 4.44 (s, 3H, C$H_{3pyr}$), 3.90 (s, 3H, C$H_{3imz}$), 2.67 (s, 3H, C-C$H_{3imz}$). $^{13}$C{$^{1}$H} NMR (75 MHz, DMSO-$d_6$, 303 K): δ = 146.7, 146.5, 144.3, 142.6, 133.6, 128.4, 123.4, 122.0 (s, $C_{imz}$, C$H_{imz}$ , $C_{pyr}$ and C$H_{pyr}$), 48.6 (s, C$H_{3pyr}$), 35.5 (s, C$H_{3imz}$), 11.1 (s, C-C$H_{3imz}$). ESI-MS (20V, $CH_3OH$): *m/z* 94.5 $[M\text{-}2I]^{2+}$. Anal. calcd. for $C_{11}H_{15}N_3I_2$ (mol wt. 443.07): C, 29.82; H, 3.41; N, 9.48. Found: C, 29.67; H, 3.19; N, 9.42.

**Synthesis of [1-(1'-methylpyridinium-4'-yl)-3-methyl]imidazolium diiodide, [$IH_2$]$I_2$**

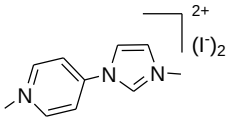


A mixture of imidazole (0.70 g, 10.28 mmol), 4-bromopyridine hydrochloride (1.00 g, 5.14 mmol), $CuSO_4 \cdot 5H_2O$ (32.8 mg, 0.21 mmol), and $K_2CO_3$ (2.13 g, 15.43 mmol) was heated for 72h at 185ºC under nitrogen atmosphere. After this time, the reaction mixture was cooled to room temperature and the generated brown solid was dissolved in 50 mL of $H_2O$ and extracted with EtOAc, to obtain 1-(4'-pyridyl)imidazole and unreacted imidazole. This mixture, without further purification, was refluxed with 1-iodomethane (1 mL, 15.42 mmol) in $CH_3CN$ (20 mL) for 24h, during this time **[$IH_2$]$I_2$** precipitated in the reaction medium which was collected by filtration and washed with $Et_2O$. Compound **[$IH_2$]$I_2$** was isolated as a yellow, air and moisture stable solid. Yield: 1.17 g (53%). For 1-(4'-pyridyl)imidazole: $^{1}$H NMR (300 MHz, $CDCl_3$, 303 K): δ = 8.68 (m, 2H, C$H_{pyr}$), 8.01 (s, 1H, C$H_{imz}$), 7.38 (s, 1H, C$H_{imz}$), 7.33 (m, 2H, C$H_{pyr}$), 7.23 (s, 1H, C$H_{imz}$). For **[$IH_2$]$I_2$**: $^{1}$H NMR (300 MHz, DMSO-$d_6$, 303 K): δ = 10.28 (s, 1H, NC*H*N), 9.33 (d, $^{3}J_{HH}$ = 6.5, 2H, C$H_{pyr}$), 8.62 (s, 1H, C$H_{imz}$), 8.57 (d, $^{3}J_{HH}$ = 6.5 Hz, 2H, C$H_{pyr}$), 8.09 (s, 1H, C$H_{imz}$), 4.40 (s, 3H, C$H_{3pyr}$), 4.01 (s, 3H, C$H_{3imz}$). $^{13}$C{$^{1}$H} NMR (75 MHz, DMSO-$d_6$, 303 K): δ = 148.0, 146.1, 138.2, 125.4, 120.0, 118.1 (s, C$H_{imz}$, $C_{pyr}$ and C$H_{pyr}$), 47.9 (s, C$H_{3pyr}$), 36.9 (s, C$H_{3imz}$). Anal. calcd. for $C_{10}H_{13}N_3I_2$ (mol wt. 429.04): C, 27.99; H, 3.05; N, 9.79. Found: C, 27.89; H, 2.98; N, 9.70.

**Synthesis of [1-(1'-methylpyridinium-4'-yl)-2,3-dimethyl]imidazolium diiodide, $[JH_2]I_2$**

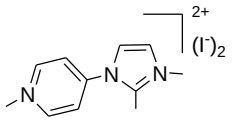

Compound $[JH_2]I_2$ was obtained using the same procedure and quantities as for $[IH_2]I_2$, in this case, 2-methylimidazole (0.84 g, 10.28 mmol) was employed. Yield: 0.757 g (33%). For 1-(4'-pyridyl)-2-methylimidazole: $^1$H NMR (300 MHz, $CDCl_3$, 303 K): δ = 8.66 (m, 2H, C$H_{pyr}$), 7.20 (m, 2H, C$H_{pyr}$), 7.02 (d, $^3J_{HH}$ = 1.5 Hz, 1H, C$H_{imz}$), 6.98 (d, $^3J_{HH}$ = 1.5 Hz, 1H, C$H_{imz}$), 2.39 (s, 1H, C-C$H_{3imz}$). For $[JH_2]I_2$: $^1$H NMR (300 MHz, DMSO-$d_6$, 303 K): δ = 9.32 (d, $^3J_{HH}$ = 6 Hz, 2H, C$H_{pyr}$), 8.44 (d, $^3J_{HH}$ = 6 Hz, 2H, C$H_{pyr}$), 8.13 (s, 1H, C$H_{imz}$), 7.99 (s, 1H, C$H_{imz}$), 4.46 (s, 3H, C$H_{3pyr}$), 3.91 (s, 3H, C$H_{3imz}$), 2.72 (s, 3H, C-C$H_{3imz}$). $^{13}$C{$^1$H} (75 MHz, DMSO-$d_6$, 303 K): δ = 148.0, 146.9, 146.4, 124.1, 123.9, 121.2 (s, $C_{imz}$, $C$H$_{imz}$, $C_{pyr}$ and $C$H$_{pyr}$), 48.2 (s, $C$H$_{3pyr}$), 35.6 (s, $C$H$_{3imz}$), 11.8 (s, C-$C$H$_{3imz}$). Anal. calcd. for $C_{11}H_{15}N_3I_2$ (mol wt. 443.07): C, 29.82; H, 3.41; N, 9.48. Found: C, 29.73; H, 3.06; N, 9.24.

**Synthesis of 2,3,6,7,8b,10,11-hexakis(*tert*-butylamine)-4b,8b,12b,12d-tetramethyl-4b,8b,12b,12d-tetrahydrodibenzo[2,3:4,5]pentaleno[1,6-*ab*]indene, HexaNH$_2$-TBTQ**

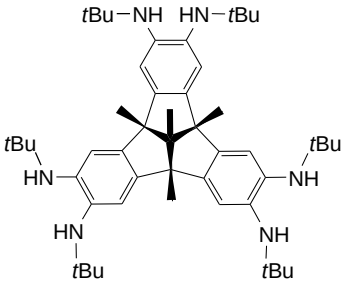

A supension of $Pd(OAc)_2$ (4.8 mg, 0.022 mmol), 1,3-bis(2,6-diisopropylphenyl) imidazolium chloride (IPr·HCl, 18 mg, 0.043 mmol), NaO*t*Bu (6 mg, 0.065 mmol) in dry toluene (10 mL), was stirred at room temperature for 30 minutes under nitrogen atmosphere. After this time, the solution was added via oven dried cannula into a Schlenk containing hexabromotribenzotriquinacene (250 mg, 0.31 mmol) and NaO*t*Bu (214 mg, 2.22 mol) in dry toluene (10 mL). *Tert*-butylamine (*t*BuNH$_2$, 0.233 mL, 2.22 mmol) was added and the resulting mixture was heated at 115 ºC for 12h. After this time, the reaction mixture was cooled to room temperature, filtered through Celite and concentrated under reduced pressure. Compound **HexaNH$_2$-TBTQ** was isolated as a dark brown, air and moisture sensitive solid. Yield: 232 mg (99%). $^1$H NMR (500 MHz, $CDCl_3$, 303 K): δ = 6.81 (s, 6H, C$H_{arom}$), 2.36 (s, 3H, C$H_{3central}$), 1.52 (s, 9H, C$H_3$), 1.26 (s, 54H, C(C$H_3$)$_3$). $^{13}$C{$^1$H} NMR (125 MHz, $CDCl_3$, 303 K): δ = 141.5 (s, $C_{qarom}$), 138.0 (s, $C_{qarom}$), 114.7 (s, $C$H$_{arom}$), 71.1 (s, $C$CH$_{3central}$), 61.7 (s, $C$CH$_3$), 51.9

(s, *C*$(CH_3)_3$), 30.3 (s, C(*C*$H_3)_3$), 26.3 (s, *C*$H_3$), 16.6 (s, *C*$H_{3central}$). ESI-MS (20 V, $CH_3OH$): m/z 763.5 $[M+H]^+$. HRMS (+)-ESI-TOF-MS of $[M+H]^+$, monoisotopic peak 763.6363, calcd. 763.6366, $\varepsilon_r$ = 1.5 ppm. Several attempts to obtain satisfactory elemental analysis of **HexaNH$_2$-TBTQ** failed, probably because this species is highly hygroscopic.

**Synthesis of trisimidazolium tribenzotriquinacene tris tetrafluoroborate, [KH$_3$](BF$_4$)$_3$**

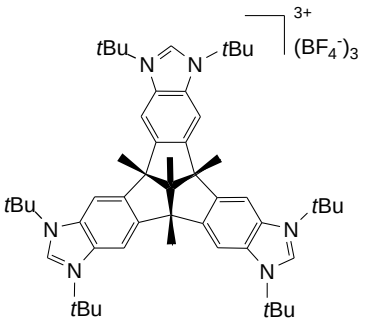


A mixture of compound **HexaNH$_2$-TBTQ** (232 mg, 0.3 mmol) and $HBF_4$ (0.138 mL, 1.0 mmol, 54% in $Et_2O$) in degassed triethylorthoformate (40 mL), was heated at 80 ºC for 4h under nitrogen atmosphere. After this time, the reaction mixture was cooled to room temperature and the generated solid was collected by filtration and washed with $CH_3OH$. Compound **[KH$_3$](BF$_4$)$_3$** was isolated as a beige, air and moisture stable solid. Slow evaporation of a concentrated solution of compound **[KH$_3$](BF$_4$)$_3$** in $CH_3CN$ gave crystals suitable for X-Ray crystallography. Yield: 322 mg (95 %). $^1$H NMR (500 MHz, $CD_3CN$, 303 K): δ = 8.49 (s, 3H, NC*H*N) 8.21 (s, 6H, C*H*$_{arom}$), 1.99 (s, 9H, C*H*$_3$), 1.84 (s, 54H, C(C*H*$_3)_3$), 1.58 (s, 3H, C*H*$_{3central}$). $^{13}$C{$^1$H} NMR (125 MHz, $CD_3CN$, 303 K): δ = 149.0 (s, *C*$_{qarom}$), 139.5 (s, *C*$_{qarom}$), 133.3 (s, N*C*HN), 111.8 (s, *C*H$_{arom}$), 72.4 (s, *C*CH$_{3central}$), 64.3 (s, *C*CH$_3$), 62.5 (s, *C*$(CH_3)_3$), 28.9 (s, C(*C*$H_3)_3$), 26.9 (s, *C*$H_3$), 16.8 (s, *C*$H_{3central}$). ESI-MS (20 V, $CH_3CN$): m/z 265.4 $[M]^{3+}$. HRMS (+)-ESI-TOF-MS of $[M]^{3+}$, monoisotopic peak 265.2014, calcd 265.2018, $\varepsilon_r$ = 1.5 ppm.

**Synthesis of trisimidazolylidene tribenzotriquinacene, K**

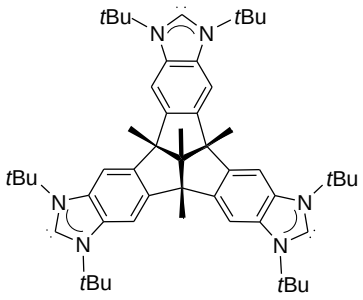


A Wilmad® (LPV) NMR tube with a Teflon-lined cap was charged with **[KH$_3$](BF$_4$)$_3$** (20 mg, 0.019 mmol), NaO*t*Bu (1.8 mg, 0.019 mmol) and dry $C_6D_6$ (0.6 mL). To this suspension, NaHMDS (1M in THF, 0.074 mL, 0.074 mmol, 3.9 equiv.) was added and the reaction mixture was stirred at room temperature for 2h under nitrogen atmosphere.

Formation of carbene **K** was identified by NMR and HRMS techniques. $^{1}$H NMR (300 MHz, $C_6D_6$, 303 K): δ = 7.65 (s, 6H, C$H_{arom}$), 1.79 (s, 3H, C$H_{3central}$), 1.77 (s, 54H, C(C$H_3$)$_3$), 1.74 (s, 9H, C$H_3$). $^{13}$C{$^{1}$H} NMR (125 MHz, $C_6D_6$, 303 K): δ = 225.8 (s, $C_{carbene}$) 142.8 (s, $C_{qarom}$), 136.4 (s, $C_{qarom}$), 107.4 (s, $C$H$_{arom}$), 72.6 (s, $C$CH$_{3central}$), 61.8 (s, $C$CH$_3$), 57.3 (s, $C$(CH$_3$)$_3$), 30.8 (s, C($C$H$_3$)$_3$), 27.4 (s, $C$H$_3$), 17.0 (s, $C$H$_{3central}$). HRMS (+)-ESI-TOF-MS of $[M+H]^+$, monoisotopic peak 793.5903, calcd 793.5897, $\varepsilon_r$ = 0.8 ppm.

**Synthesis of hexa(3-methylimidazol-1-yl)benzene hexa trifluoromethanesulfonate, [LH]$_6$(OTf)$_6$**

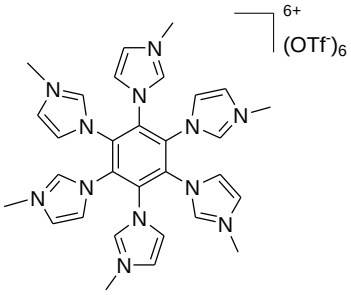


A suspension of hexa(imidazol-1-yl)benzene[13] (234 mg, 0.5 mmol) and methyl trifluoromethanesulfonate (0.68 mL, 6.0 mmol) in degassed 1,2-dichloroethane (20 mL), was heated at 100 ºC for 48h under nitrogen atmosphere. After this time, the reaction mixture was cooled to room temperature and the generated solid was filtered and washed with $Et_2O$. Compound **[LH]$_6$(OTf)$_6$** was isolated as a white, air and moisture stable solid. Yield: 678 mg (93%). $^{1}$H NMR (500 MHz, DMSO-$d_6$, 333 K): δ 9.14 (s, 6H, NC$H$N), 7.95 (s, 6H, C$H_{imz}$), 7.61 (s, 6H, C$H_{imz}$), 3.94 (s, 18H, C$H_3$). $^{13}$C{$^{1}$H} NMR (125 MHz, DMSO-$d_6$, 333 K): δ 138.2 (s, N$C$HN), 133.6 (s, $C_{qarom}$), 126.8 (s, $C$H$_{imz}$), 122.8 (s, $C$H$_{imz}$), 37.5 (s, CH$_3$). ESI-MS (20 V, CH$_3$OH): m/z 225.9 $[M\text{-}4(CF_3SO_3)+CH_3CN]^{4+}$. Anal. calcd. for $C_{36}H_{36}N_{12}F_{18}S_6O_{18}\cdot 2H_2O$ (mol wt. 1495.14): C, 28.92; H, 2.70; N, 11.24. Found: C, 28.77; H, 2.67; N, 10.95.

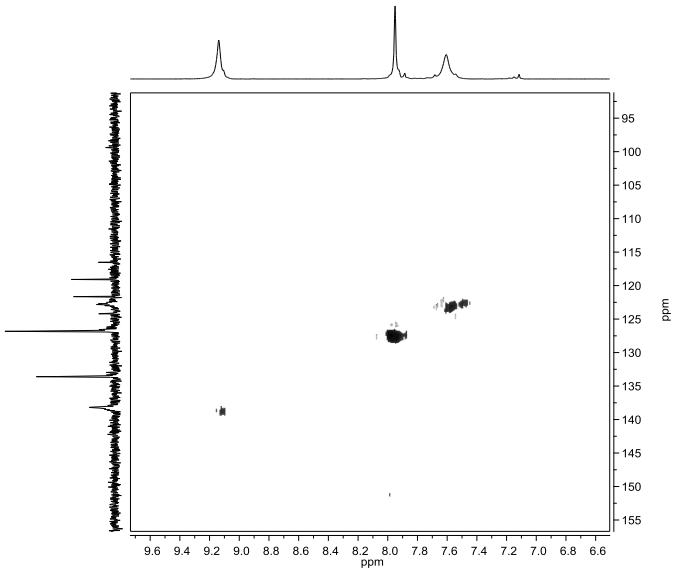


**Figure 5.3** $^{1}$H-$^{13}$C gHSQC spectrum of **[LH]$_6$(OTf)$_6$** in DMSO-$d_6$

**Synthesis of hexa(3-ethylimidazol-1-yl)benzene hexa tetrafluoroborate, [MH]$_6$(BF$_4$)$_6$**

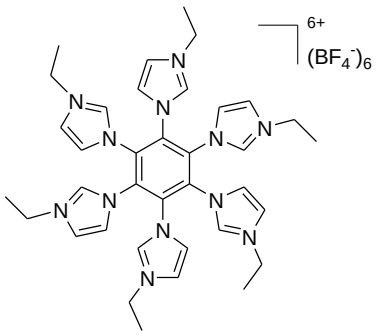


A suspension of hexa(imidazol-1-yl)benzene[13] (350 mg, 0.74 mmol) and triethyloxonium tetrafluoroborate (928 mg, 4.9 mmol) in $CH_3CN$ (20 mL), was stirred at room temperature for 1h under aerobic conditions. After this time, the generated solid was filtered and washed with $CH_2Cl_2$. Compound **[MH]$_6$(BF$_4$)$_6$** was isolated as a white, air and moisture stable solid. Yield: 668 mg (78%). $^{1}$H NMR (300 MHz, $CD_3CN$, 303 K): δ 8.82 (s, 6H, NC*H*N), 7.66 (s, 6H, C$H_{imz}$), 7.62 (s, 6H, C$H_{imz}$), 4.26 (m, 12H, C$H_2$CH$_3$), 1.40 (t, 18H, CH$_2$C$H_3$). $^{13}$C{1H} NMR (75 MHz, $CD_3CN$, 303 K): δ 138.1, 136.0, 126.7, 125.5 (s, N*C*HN, $C_{qarom}$, *C*H$_{imz}$), 47.9 (s, *C*H$_2$CH$_3$), 15.0 (s, CH$_2$*C*H$_3$). HRMS (+)-ESI-TOF-MS of [M-4(BF$_4$)]$^{4+}$, monoisotopic peak 205.6036, calcd 205.6049, $\varepsilon_r$= 6 ppm.

## 5.2.2 Synthesis of Pd(II) complexes

### General procedure for the synthesis of compounds (1A-3C)

A solution of the appropriate sulfonate-functionalised-imidazolium precursor ligand (1 equivalent), $Pd(OAc)_2$ (0.5 or 1 equivalents) and KI (1 or 2 equivalent) in degassed DMSO (5 mL), was heated at 80ºC for 2-12h and 140-160 ºC for 3-12h, depending on the reaction, under aerobic conditions. After this time, the reaction mixture was cooled to room temperature and the solvent was removed under reduced pressure at 60ºC to give a crude product that was purified by washing or column chromatography.

### Synthesis of 1A

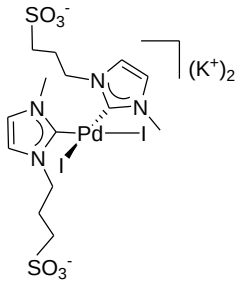


The reaction was carried out with **AH**, (182 mg, 0.892 mmol), $Pd(OAc)_2$ (100 mg, 0.446 mmol) and KI (148 mg, 0.892 mmol). The mixture was heated at 80ºC for 12h and then at 160ºC for further 3h. During this time the reaction solution turned from red to bright orange. After removing DMSO, the generated crude solid was washed three times with hot $CH_3OH$. Compound **1A** was isolated as an orange, air and moisture stable solid. Yield: 277 mg (75 %). $^1$H NMR (300 MHz, $D_2O$, 303 K): δ = 7.18 (s, 2H, C*H*$_{imz}$), 7.13 (s, 2H, C*H*$_{imz}$), 4.40 (m, 4H, NC*H*$_2$), 3.85 (s, 6H, NC*H*$_3$), 2.95 (m, 4H, $CH_2CH_2SO_3$), 2.45 (m, 4H, $CH_2CH_2SO_3$). $^{13}$C{$^1$H} NMR (125 MHz, $D_2O$, 303K): δ = 163.9 (s, Pd*C*$_{imz}$), 124.0 (s, *C*$_{imz}$), 122.4 (s, *C*$_{imz}$), 49.4 (s, N*C*H$_2$), 48.9 (s, N*C*H$_3$), 38.2 (s, $CH_2CH_2SO_3$), 25.5 (s, $CH_2CH_2SO_3$). HRMS (+)-ESI-TOF-MS of [M-I]$^-$, 638.9060, calcd. 638.9065, $\varepsilon_r$ = 0.8 ppm; [M+H]$^-$, 766.8204, calcd. 766.8188, $\varepsilon_r$ = 2.1 ppm. Anal. calcd. for $C_{14}S_2O_6N_4H_{22}PdI_2K_2$ (mol wt. 844.90): C, 19.90; H, 2.62; N, 6.63. Found: C, 20.12; H, 2.95; N, 7.3.

### Synthesis of 2B

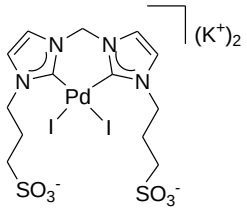


The reaction was carried out with **BH$_2$** (129.4 mg, 0.330 mmol), $Pd(OAc)_2$ (75 mg, 0.330 mmol) and KI (109.6 mg, 0.660 mmol). The mixture was heated at 80ºC for 2h and then at 140ºC for further 12h. After removing the DMSO, the generated crude solid was dissolved in hot $CH_3OH$ and

transferred to a column chromatography packed with $CH_2Cl_2/CH_3OH$ (1:1). Elution with $CH_2Cl_2/CH_3OH$ (1:9) afforded the separation of a yellow band that contained **2B**. Compound **2B** was isolated as a yellow, air and moisture sensitive solid. Yield: 78.6 mg (29 %). $^1$H NMR (300 MHz, $D_2O$, 303 K): δ = 7.54 (d, $^3J_{HH}$ = 2.0 Hz, 2H, C$H_{imz}$), 7.24 (d, $^3J_{HH}$ = 2.0 Hz, 2H, C$H_{imz}$), 6.61 (d, $^2J_{HH}$ = 13.5 Hz, 1H, aC$H_{bridge}$), 6.27 (d, $^2J_{HH}$ = 13.5 Hz, 1H, bC$H$b$_{bridge}$), 3.92 (m, 2H, NC$H_2$), 3.56 (m, 2H, NC$H_2$), 2.61 (m, 4H, $CH_2CH_2SO_3$), 2.01 (m, 4H, $CH_2CH_2SO_3$). $^{13}$C{$^1$H} NMR (75 MHz, $D_2O$, 303 K): δ = 169.3 (s, PdC$_{imz}$), 123.2 (s, $C_{imz}$), 122.3 (s, $C_{imz}$), 64.1 (s, N$CH_2$N), 49.3 (s, N$CH_2$), 47.9 (s, $CH_2CH_2SO_3$), 26.6 (s, $CH_2CH_2SO_3$). HRMS (+)-ESI-TOF-MS of [M-I]$^-$, 622.8765, calcd. 622.8752, $\varepsilon_r$ = 2.1 ppm. Several attempts to obtain satisfactory elemental analysis of **2B** failed, probably because this species is highly hygroscopic.

**Synthesis of 3C**

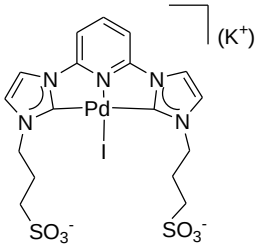


The reaction was carried out with **$CH_2$** (304 mg, 0.67 mmol), $Pd(OAc)_2$ (150 mg, 0.67 mmol) and KI (111.2 mg, 0.67 mmol). The mixture was heated at 80ºC for 2h and at 140ºC for further 12h. After removing the DMSO, the generated crude solid was dissolved in the minimum amount of water and transferred to a column chromatography packed with $CH_2Cl_2/CH_3OH$ (1:1). Elution with $CH_3OH$ afforded the separation of an orange band that contained compound **3C**. Compound **3C** was isolated as an orange, air and moisture sensitive solid. Yield: 87.2 mg (18 %). $^1$H NMR (300 MHz, $D_2O$, 303 K): δ = 8.27 (t, $^3J_{HH}$ = 8.1 Hz, 1H, C$H_{pyr}$), 7.86 (d, $^3J_{HH}$ = 2.1 Hz, 2H, C$H_{imz}$), 7.54 (d, $^3J_{HH}$ = 8.4 HZ, 2H, C$H_{pyr}$), 7.37 (d, $^3J_{HH}$ = 2.1 Hz, 2H, C$H_{imz}$), 4.36 (m, 4H, NC$H_2$), 2.90 (m, 4H, $CH_2CH_2SO_3$), 2.08 (m, 4H, $CH_2CH_2SO_3$). $^{13}$C{$^1$H} NMR (75 MHz, $D_2O$, 303 K): δ = 166.5 (s, PdC$_{imz}$), 149.7 (s, $C_{qpyr\text{-}ortho}$), 147.1 (s, $C$H$_{pyr\text{-}para}$), 124.7 (s, $C$H$_{imz}$), 118.3 (s, $C$H$_{imz}$), 109.1 (s, $C$H$_{pyr\text{-}meta}$), 51.1 (s, N$CH_2$), 47.7 (s, $CH_2CH_2SO_3$), 27.1 (s, $CH_2CH_2SO_3$). HRMS (+)-ESI-TOF-MS of [M]$^-$, 685.8868, calcd. 685.8862, $\varepsilon_r$ = 0.9 ppm. Several attempts to obtain satisfactory elemental analysis of **3C** failed, probably because this species is highly hygroscopic.

**Synthesis of 4C**

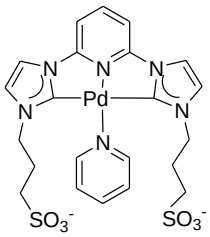

Silver triflate (7.0 mg, 0.027 mmol) was added slowly to a solution of **3C** (17.7 mg, 0.025 mmol) in $CH_3OH$ (5 mL). Pyridine (1 mL) was then added and the resulting solution was refluxed overnight. The reaction mixture was filtered through Celite and concentrated under reduced pressure. Compound **4C** was isolated as a pale yellow, air and moisture stable solid.Yield: 15.6 mg (98 %). $^1$H NMR (300 MHz, $D_2O$, 303 K): δ = 9.14 (d, $^3J_{HH}$ = 5.1 Hz, 2H, C$H_{pyr}$), 8.37 (t, $^3J_{HH}$ = 8.4 Hz, 1H, C$H_{pyr}$), 8.25 (t, $^3J_{HH}$ = 8.1 Hz, 1H, C$H_{pyr}$), 7.94 (d, $^3J_{HH}$ = 2.1 Hz, 2H, C$H_{imz}$), 7.85 (t, $^3J_{HH}$ = 7.5 Hz, C$H_{pyr}$), 7.67 (d, $^3J_{HH}$ = 8.1 Hz, 2H, C$H_{pyr}$), 7.36 (d, $^3J_{HH}$ = 2.1 Hz, 2H, C$H_{imz}$), 3.41 (t, $^3J_{HH}$ = 7.5 Hz, 4H, NC$H_2$), 2.42 (t, $^3J_{HH}$ = 7.5 Hz, 4H, $CH_2CH_2SO_3$), 1.86 (m, 4H, $CH_2CH_2SO_3$). $^{13}$C{$^1$H} NMR (75 MHz, $D_2O$, 303 K): δ = 172.8 (s, *C*$H_{pyr}$), 167.9 (s, Pd$C_{imz}$), 152.7 (s, $C_{qpyr}$), 151.5 (s, *C*$H_{pyr}$), 128.5 (s, *C*$H_{pyr}$), 123.7 (s, *C*$H_{imz}$), 118.4 (s, *C*$H_{imz}$), 109.2 (s, *C*$H_{pyr}$), 82.1 (s, *C*$H_{pyr}$), 49.1 (s, N*C*$H_2$), 47.7 (s, $CH_2CH_2SO_3$), 26.5 (s, $CH_2CH_2SO_3$). HRMS (+)-ESI-TOF-MS of $[M\text{-pyr+Na}]^+$, 581.9719, calcd. 581.9715, $\varepsilon_r$ = 0.7 ppm. Anal. calcd. for $C_{22}S_2O_6N_6H_{24}Pd$ (mol. wt. 639.01): C, 41.55; H, 3.79; N, 13.15. Found: C, 41.23; H, 3.61; N, 14.6.

## 5.2.3 Synthesis of Ir(III) and Rh(III) complexes

**Synthesis of 5D**

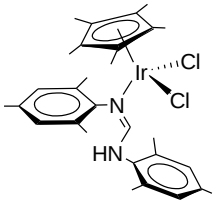

A solution of $[IrCp^*Cl_2]_2$ (100 mg, 0.126 mmol) and compound **D**, (70 mg, 0.250 mmol) in dry $CH_2Cl_2$ (10 mL), was stirred at room temperature for 2h under nitrogen atmosphere. After this time, the solvent was evaporated under reduced pressure and the remaining solid obtained was washed with hexane. Compound **5D** was isolated as a crystalline orange, air and moisture stable solid. Yield 153 mg (90%). $^1$H NMR (300 MHz, $CDCl_3$, 303 K): δ = 8.09 (d, $^3J_{HH}$ = 13 Hz, 1H, C*H*), 7.01 (s, 2H, C$H_{Mes}$), 6.78 (s, 2H, C$H_{Mes}$), 5.76 (d, $^3J_{HH}$ = 12 Hz, 1H, N*H*), 2.35 (s, 3H, C$H_3$), 2.32 (s, 6H, C$H_3$), 2.20 (s, 3H, C$H_3$), 2.17 (s, 6H, C$H_3$), 1.30 (s, 15H, (C$H_3$)$_5$Cp*). $^{13}$C{$^1$H} NMR (125 MHz, $CDCl_3$, 303 K): δ = 160.8 (s, *C*H), 140.4 (s, $C_{Mes}$), 136.8 (s, $C_{Mes}$), 136.4 (s, $C_{Mes}$), 133.9 (s, $C_{Mes}$), 133.2 (s, $C_{Mes}$), 132.7 (s, $C_{Mes}$), 129.6 (s, *C*$H_{Mes}$), 129.4 (s, *C*$H_{Mes}$), 85.6 (s, $C_5$Cp*), 21.0 (s, *C*$H_3$), 20.9 (s, *C*$H_3$), 19.1

(s, *C*$H_3$), 17.8 (s, *C*$H_3$), 8.6 (s, (*C*$H_3$)$_5$Cp*). ESI-MS (25V, $CH_3OH$): *m/z* 634.4 [M-Cl]$^+$. Anal. calcd. for $C_{29}H_{39}N_2IrCl_2$ (mol. wt. 678.76) C, 51.32; H, 5.79; N, 4.13. Found: C, 51.47; H, 5.70; N, 4.22.

**Synthesis of 6D**

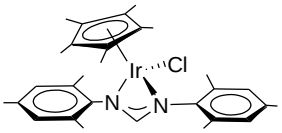


The synthesis of compound **6D** was achieved following the procedure described in the literature.[16] A suspension compound **D**, (70 mg, 0.250 mmol) in dry THF, was cooled at 0ºC under nitrogen atmosphere. *n*BuLi (120 µL, 2.5M in hexane) was added, and the solution was stirred for 10 minutes. The resulting yellow solution was transferred via oven dried cannula into a solution of [IrCp$^*$Cl$_2$]$_2$ (100 mg, 0.126 mmol) in dry THF (10 mL). The resulting solution was stirred at 0ºC for 10 minutes and then at room temperature for further 2h. After this time, the solvent was evaporated under reduced pressure and the remaining solid obtained was extracted with dry $C_6H_6$. After evaporation of the benzene, the solid obtained was washed with hexane. Compound 6D was isolated as a yellow, air and moisture stable solid. Yield 113 mg (70%). $^1$H NMR (300 MHz, $C_6D_6$, 303 K): δ = 9.15 (s, 1H, C*H*), 6.83 (s, 4H, C*H*$_{Mes}$), 2.57 (s, 12H, C*H*$_3$), 2.17 (s, 6H, C*H*$_3$), 1.21 (s, 15H, (C*H*$_3$)$_5$Cp*). $^{13}$C{$^1$H} NMR (75 MHz, $C_6D_6$, 303 K): δ = 167.6 (s, *C*H), 140.4 (s, *C*$_{Mes}$), 134.2 (s, *C*$_{Mes}$), 133.1 (s, *C*$_{Mes}$), 129.6 (s, *C*H$_{Mes}$), 83.2 (s, *C*$_5$Cp*), 21.8 (s, *C*$H_3$), 20.7 (s, *C*$H_3$), 9.0 (s, (*C*$H_3$)$_5$Cp*). Anal. calcd. for $C_{29}H_{38}N_2IrCl$ (mol. wt. 642.30): C, 54.23; H, 5.96; N, 4.36. Found: C, 54.11; H, 6.00; N, 4.28.

**General procedure for the synthesis of compounds, 7E-16I**

A solution of the appropriate imidazolium-pyridinium salt (1 equivalent), metal precursor [MCl(diene)]$_2$ (M = Rh, Ir; diene = COD, NBD) (0.5 equivalents) and KI (1 equivalent) in $CH_3CN$ (50 mL), was heated at 65ºC for 12h. After this time, the reaction mixture was cooled to room temperature and filtered through Celite. The solvent was removed under reduced pressure to give a crude product that was purified by column chromatography.

**Synthesis of 7E**

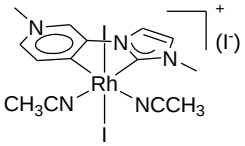

The reaction was carried out with **[EH$_2$]I$_2$**, (87 mg, 0.2 mmol), [RhCl(COD)]$_2$ (50 mg, 0.1 mmol), and KI (34 mg, 0.2 mmol). The crude solid was purified by column chromatography. Elution with $CH_2Cl_2$ separated a minor yellow band containing [RhCl(COD)]$_2$. Further elution with $CH_2Cl_2$/$CH_3CN$ (1:1) afforded the separation of a red band that contained compound **7E**. Compound **7E** was isolated as a red, air and moisture stable solid. Yield: 72.5 mg (50 %). $^1$H NMR (300 MHz, $CD_3CN$, 303 K): δ = 8.86 (s, 1H, C$H_{pyr}$), 8.45 (d, $^3J_{HH}$ = 6 Hz, 1H, C$H_{pyr}$), 8.08 (d, $^3J_{HH}$ = 2 Hz, 1H, C$H_{imz}$), 7.95 (d, $^3J_{HH}$ = 6 Hz, 1H, C$H_{pyr}$), 7.37 (d, $^3J_{HH}$ = 2 Hz, 1H, C$H_{imz}$), 4.28 (s, 3H, C$H_{3pyr}$), 3.99 (s, 3H, C$H_{3imz}$). $^{13}$C{$^1$H} NMR (75 MHz, $CD_3CN$, 303 K): δ = the signal corresponding to Rh-$C_{imz}$ could not be observed, 183.6 (d, $^1J_{RhC}$ = 28 Hz, Rh-$C_{pyr}$), 147.5 (s, $C_{pyr}$), 137.0 (s, $C$H$_{pyr}$), 136.4 (s, $C$H$_{pyr}$), 126.9 (s, $C$H$_{imz}$), 125.2 (s, $C$H$_{pyr}$), 117.8 (s, $C$H$_{imz}$), 47.7 (s, $C$H$_{3pyr}$), 38.3 (s, $C$H$_{3imz}$). ESI-MS (20V, $CH_3CN$): *m/z* 611.7 [M-I]$^+$, *m/z* 570.7 [M-I-$CH_3CN$]$^+$. Anal. calcd. for $C_{14}H_{17}N_5I_3Rh$ (mol. wt. 738.94): C, 28.76; H, 2.32; N, 9.48. Found: C, 28.43; H, 2.75; N, 9.50.

**Synthesis of 8E**

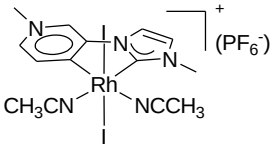

Compound **8E** was obtained using the same quantities as for **7E**, in this case, **[EH$_2$](PF$_6$)$_2$** (94 mg, 0.2 mmol) was employed as ligand precursor. Compound purified by column chromatography. Elution with $CH_2Cl_2$ separated a yellow band containing [RhCl(COD)]$_2$. Further elution with $CH_2Cl_2$/$CH_3CN$ (9:1) afforded the separation of an orange band that contained compound **8E**. Compound **8E** was isolated as an orange, air and moisture stable solid. Yield: 85 mg (56 %). $^1$H NMR (300 MHz, $CD_3CN$, 303 K): δ = 8.42 (d, $^3J_{HH}$ = 6 Hz, 1H, C$H_{pyr}$), 8.34 (s, 1H, C$H_{pyr}$), 7.87 (d, $^3J_{HH}$ = 6 Hz, 1H, C$H_{pyr}$), 7.80 (d, $^3J_{HH}$ = 2 Hz, 1H, C$H_{imz}$), 7.34 (d, $^3J_{HH}$ = 2 Hz, 1H, C$H_{imz}$), 4.22 (s, 3H, C$H_{3pyr}$), 3.99 (s, 3H, C$H_{3imz}$). $^{13}$C{$^1$H} NMR (75 MHz, $CD_3CN$, 303 K): δ = 183.9 (d, $^1J_{RhC}$ = 28 Hz, Rh-$C_{pyr}$), 167.4 (d, $^1J_{RhC}$ = 43 Hz, Rh-$C_{imz}$), 147.6 (s, $C_{pyr}$), 136.9 (s, $C$H$_{pyr}$), 136.4 (s, $C$H$_{pyr}$), 127.0 (s, $C$H$_{imz}$), 124.9 (s, $C$H$_{pyr}$), 117.3 (s, $C$H$_{imz}$), 47.8 (s, $C$H$_{3pyr}$), 38.3 (s, $C$H$_{3imz}$). ESI-MS (20V, $CH_3CN$): *m/z* 570.9 [M-$PF_6$-$CH_3CN$]$^+$, *m/z* 529.9 [M-$PF_6$-($CH_3CN$)$_2$]$^+$ Anal. calcd. for $C_{14}H_{17}N_5I_2RhPF_6$ (mol. wt. 757.00): C, 22.21; H, 2.26; N, 9.25. Found: C, 22.43; H, 2.25; N, 9.43.

**Synthesis of 9E**

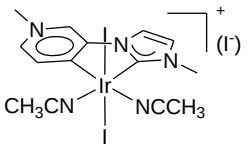


The reaction was carried out with **$[EH_2]I_2$** (64 mg, 0.15 mmol), $[IrCl(COD)]_2$ (50 mg, 0.075 mmol), and KI (25 mg, 0.15 mmol). The crude solid was purified by column chromatography. Elution with $CH_2Cl_2$ separated a minor red band containing $[IrCl(COD)]_2$. Further elution with $CH_2Cl_2/CH_3CN$ (1:1) afforded the separation of an orange band that contained compound **9E**. Compound **9E** was isolated as an orange, air and moisture stable solid. Yield: 74 mg (60 %). $^1$H NMR (300 MHz, $CD_3CN$, 303 K): δ = 8.75 (s, 1H, C$H_{pyr}$), 8.23 (d, $^3J_{HH}$ = 7 Hz, 1H, C$H_{pyr}$), 7.92 (s, 1H, C$H_{imz}$), 7.78 (d, $^3J_{HH}$ = 7 Hz, 1H, C$H_{pyr}$), 7.32 (s, 1H, C$H_{imz}$), 4.22 (s, 3H, C$H_{3pyr}$), 4.00 (s, 3H, C$H_{3imz}$). $^{13}$C{$^1$H} NMR (75 MHz, DMSO-$d_6$, 303 K): δ = 164.7 (s, Ir-$C_{pyr}$), 148.1 (s, Ir-$C_{imz}$), 146.8 (s, $C_{pyr}$), 136.2 (s, $C$H$_{pyr}$), 133.8 (s, $C$H$_{pyr}$), 126.3 (s, $C$H$_{imz}$), 123.6 (s, $C$H$_{pyr}$), 117.9 (s, $CH_3C$N), 115.3 (s, $C$H$_{imz}$), 46.0 (s, $C$H$_{3pyr}$), 42.6 (s, $C$H$_{3imz}$), 1.2 (s, $C$H$_3$CN). ESI-MS (15 V, $CH_3CN$): *m/z* 701.9 $[M\text{-}I]^+$, *m/z* 660.9 $[M\text{-}I\text{-}CH_3CN]^+$. Anal. calcd. for $C_{14}H_{17}N_5I_3Ir$ (mol. wt. 828.25): C, 20.30; H, 2.07; N, 8.46. Found: C, 20.46; H, 1.99; N, 8.50.

**Synthesis of 10E**

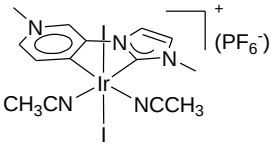


Compound **10E** was obtained using the same quantities as for **9E**, in this case, **$[EH_2](PF_6)_2$** (70 mg, 0.15 mmol) was employed as ligand precursor. Compound purified by column chromatography. Elution with $CH_2Cl_2$ separated a red band containing $[IrCl(COD)]_2$. Further elution with $CH_2Cl_2/CH_3CN$ (9:1) afforded the separation of a yellow band that contained compound **10E**. Compound **10E** was isolated as yellow, air and moisture stable solid. Yield: 70 mg (55 %). $^1$H NMR (300 MHz, $CD_3CN$, 303 K): δ = 8.32 (s, 1H, C$H_{pyr}$), 8.20 (d, $^3J_{HH}$ = 6 Hz, 1H, C$H_{pyr}$), 7.72 (d, $^3J_{HH}$ = 6 Hz, 1H, C$H_{pyr}$), 7.68 (s, 1H, C$H_{imz}$), 7.30 (s, 1H, C$H_{imz}$), 4.17 (s, 3H, $CH_{3pyr}$), 4.01 (s, 3H, $CH_{3imz}$). $^{13}$C{$^1$H} NMR (75 MHz, $CD_3CN$, 303 K): δ = 164.6 (s, Ir-$C_{pyr}$), 149.4 (s, Ir-$C_{imz}$), 145.6 (s, $C_{pyr}$), 138.1 (s, $C$H$_{pyr}$), 134.9 (s, $C$H$_{pyr}$), 125.8 (s, $C$H$_{imz}$), 124.3 (s, $C$H$_{pyr}$), 116.8 (s, $C$H$_{imz}$), 47.5 (s, $C$H$_{3pyr}$), 37.7 (s, $C$H$_{3imz}$). ESI-MS (20V, $CH_3CN$): *m/z* 701.9 $[M\text{-}PF_6]^+$, *m/z* 660.8 $[M\text{-}PF_6\text{-}CH_3CN]^+$. Anal. calcd. for $C_{14}H_{17}N_5I_2IrPF_6$ (mol. wt. 846.31): C,19.87; H, 2.02; N, 8.28. Found: C, 19.93; H, 2.07; N, 8.41.

**Synthesis of 11F**

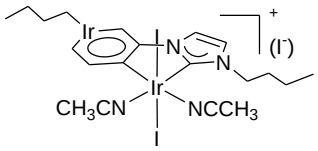


Compound **11F** was obtained using the same quantities as for **9E**, in this case, **[FH$_2$]I$_2$** (77 mg, 0.15 mmol) was employed as ligand precursor. Compound purified by column chromatography. Elution with $CH_2Cl_2$ separated a red band containing $[IrCl(COD)]_2$. Further elution with $CH_2Cl_2$/$CH_3CN$ (7:3) afforded the separation of an orange band that contained compound **11F**. Compound **11F** was isolated as an orange, air and moisture stable solid. Slow evaporation of a concentrated solution of compound **11F** in $CH_3CN$ gave crystals suitable for X-Ray crystallography. Yield: 68 mg (50 %). $^1$H NMR (500 MHz, $CD_3CN$, 303 K): δ = 8.54 (d, $^3J_{HH}$ = 2 Hz, 1H, C$H_{pyr}$), 8.23 (d, $^3J_{HH}$ = 10 Hz, 1H, C$H_{pyr}$), 7.83 (d, $^3J_{HH}$ = 3 Hz, 1H, C$H_{imz}$), 7.81 (dd, $^3J_{HH}$ = 2 Hz, $^3J_{HH}$ = 10 Hz, 1H, C$H_{pyr}$), 7.34 (d, $^3J_{HH}$ = 3 Hz, 1H, C$H_{imz}$), 4.40 (t, $^3J_{HH}$ = 12 Hz, 2H, NC$H_{2pyr}$), 4.35 (t, $^3J_{HH}$ = 12 Hz, 2H, NC$H_{2imz}$), 2.00 (m, 4H, $CH_2CH_2CH_2$), 1.40 (m, 4H, $CH_2CH_3$), 0.98 (m, 6H, C$H_3$). $^{13}$C{$^1$H} NMR (125 MHz, $CD_3CN$, 303 K): δ = 164.8 (s, Ir-$C_{pyr}$), 149.4 (s, Ir-$C_{imz}$), 146.8 (s, $C_{pyr}$), 137.1 (s, $CH_{pyr}$), 133.7 (s, $CH_{pyr}$), 124.8 (s, $CH_{imz}$), 123.4 (s, $CH_{pyr}$), 117.3 (s, $CH_{imz}$), 60.9 (s, $CH_{2pyr}$), 50.4 (s, $CH_{2imz}$), 33.6 (s, $CH_2CH_{2pyr}CH_2$), 33.3 (s, $CH_2CH_{2imz}CH_2$), 20.6 (s, $CH_{2pyr}CH_3$), 20.1 (s, $CH_{2imz}CH_3$), 14.1 (s, $CH_{3pyr}$), 13.7 (s, $CH_{3imz}$). ESI-MS (15 V, $CH_3CN$): *m/z* 786 $[M\text{-}I]^+$, *m/z* 745 $[M\text{-}I\text{-}CH_3CN]^+$. Anal. calcd. for $C_{20}H_{29}N_5I_3Ir$ (mol. wt. 912.41): C, 26.33; H, 3.20; N, 7.68. Found: C, 26.45; H 3.00; N 7.80.

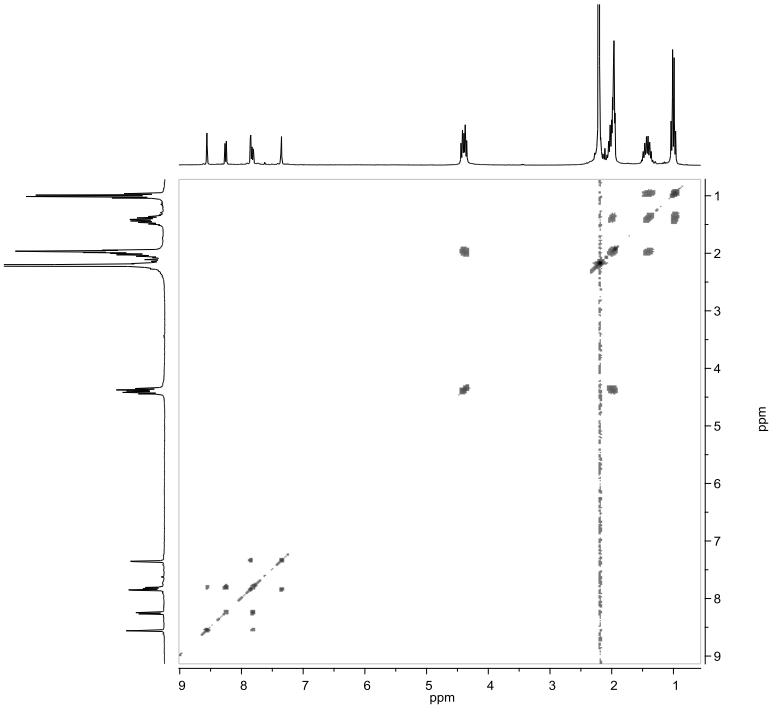


**Figure 5.4** $^{1}$H-$^{1}$H gCOSY spectrum of **11F** in $CD_3CN$

**Synthesis of 12E**

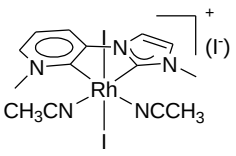


The reaction was carried out with **[EH$_2$]I$_2$** (93 mg, 0.22 mmol), [RhCl(NBD)]$_2$ (50 mg, 0.11 mmol), and KI (36 mg, 0.22 mmol). The crude solid was purified by column chromatography. Eluton with $CH_2Cl_2$ separated a yellow band containing [RhCl(NBD)]$_2$. Further elution with $CH_2Cl_2$/$CH_3CN$ (1:1) afforded the separation of a red band that contained compound **12E**. Compound **12E** was isolated as a red, air and moisture stable solid. Slow diffusion of $Et_2O$ into a concentrated solution of compound **12E** in $CH_3CN$ gave crystals suitable for X-Ray crystallography. Yield: 107 mg (66 %). $^{1}$H NMR (500 MHz, DMSO-$d_6$, 303 K): δ = 8.60 (d, $^{3}J_{HH}$ = 6 Hz, 1H, C$H_{pyr}$), 8.30 (d, $^{3}J_{HH}$ = 2 Hz, 1H, C$H_{imz}$), 8.17 (d, $^{3}J_{HH}$ = 8 Hz, 1H, C$H_{pyr}$), 7.63 (d, $^{3}J_{HH}$ = 2 Hz, 1H, C$H_{imz}$), 7.54 (dd, $^{3}J_{HH}$ = 6 Hz, $^{3}J_{HH}$ = 8 Hz, 1H, C$H_{pyr}$), 4.52 (s, 3H, C$H_{3pyr}$), 4.04 (s, 3H, C$H_{3imz}$), 2.07 (s, 6H, C$H_3$CN). $^{13}$C{$^{1}$H} NMR (125 MHz, DMSO-$d_6$, 303 K): δ = the signals corresponding to Rh$C_{imz}$ and Rh$C_{pyr}$ could not be observed, 147.7 (s, $C_{pyr}$), 143.0 (s, $C$H$_{pyr}$), 127.2 (s, $C$H$_{imz}$), 121.1

(s, *C*$H_{pyr}$), 119.1 (s, *C*$H_{pyr}$), 118.0 (s, $CH_3$*C*N), 117.0 (s, *C*$H_{imz}$), 51.6 (s, *C*$H_{3pyr}$), 37.1 (s, *C*$H_{3imz}$), 1.1 (s, *C*$H_3$CN). ESI-MS (20 V, $CH_3CN$): *m/z* 571.0 $[M\text{-}I\text{-}CH_3CN]^+$, *m/z* 529.9 $[M\text{-}I\text{-}(CH_3CN)_2]^+$. Anal. calcd. for $C_{14}H_{17}N_5I_3Rh$ (mol. wt. 738.94): C, 28.76; H, 2.32; N, 9.48. Found: C, 28.43; H, 2.75; N, 9.50.

**Synthesis of 13E**

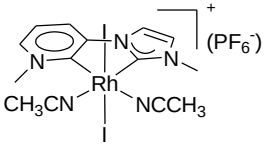


Compound **13E** was obtained using the same quantities as for **12E**, in this case, **[EH$_2$](PF$_6$)$_2$** (101 mg, 0.22 mmol) was employed as ligand precursor. The compound was purified by column chromatography. Elution with $CH_2Cl_2$ separated a yellow band containing $[RhCl(NBD)]_2$. Further elution with $CH_2Cl_2$/$CH_3CN$ (9:1) afforded the separation of an orange band that contained compound **13E**. Compound **13E** was isolated as an orange, air and moisture stable solid. Yield: 88 mg (54 %). $^1$H NMR (300 MHz, $CD_3CN$, 303 K): δ = 8.36 (d, $^3J_{HH}$ = 6 Hz, 1H, C*H*$_{pyr}$), 7.93 (d, $^3J_{HH}$ = 8 Hz, 1H, C*H*$_{pyr}$), 7.85 (s, 1H, C*H*$_{imz}$), 7.47 (m, 1H, C*H*$_{pyr}$), 7.34 (s, 1H, C*H*$_{imz}$), 4.52 (s, 3H, C*H*$_{3pyr}$), 4.03 (s, 3H, C*H*$_{3imz}$). $^{13}$C{$^1$H} NMR (75 MHz, $CD_3CN$, 303 K): δ = 175.7 (d, $^1J_{RhC}$ = 36 Hz, Rh-*C*$_{pyr}$), 162.7 (d, $^1J_{RhC}$ = 42 Hz, Rh-*C*$_{imz}$), 148.1 (s, *C*$_{pyr}$), 143.7 (s, *C*$H_{pyr}$), 127.8 (s, *C*$H_{imz}$), 122.7 (s, *C*$H_{pyr}$), 121.5 (s, *C*$H_{pyr}$), 117.5 (s, *C*$H_{imz}$), 54.7 (s, *C*$H_{3pyr}$), 39.0 (s, *C*$H_{3imz}$). ESI-MS (20 V, $CH_3OH$): *m/z* 529.8 $[M\text{-}PF_6\text{-}(CH_3CN)_2]^+$. Anal. calcd. for $C_{14}H_{17}N_5I_2RhPF_6$ (mol. wt. 757.00): C, 22.21; H, 2.26; N, 9.25. Found: C, 22.38; H, 2.33; N, 9.20.

**Synthesis of 14G**

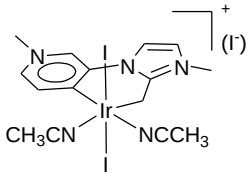


The reaction was carried out with **[GH$_2$]I$_2$** (67 mg, 0.15 mmol), $[IrCl(COD)]_2$ (50 mg, 0.075 mmol), and KI (25 mg, 0.15 mmol) in refluxing $CH_3CN$ (20 mL) for 18h. The crude solid was purified by column chromatography. Elution with $CH_2Cl_2$ separated a red band containing $[IrCl(COD)]_2$. Further elution with $CH_2Cl_2$/$CH_3CN$ (1:1) afforded the separation of an orange band that contained compound **14G**. Compound **14G** was isolated as an orange, air and moisture stable solid. Slow diffusion of $Et_2O$ into a concentrated solution of compound **14G** in $CH_3CN$ gave crystals suitable for X-Ray crystallography. Yield: 78 mg (62 %). $^1$H NMR (300 MHz, $CD_3CN$, 303 K): δ = 8.51 (d, $^3J_{HH}$ = 6 Hz, 1H, C*H*$_{pyr}$), 8.21 (s, 1H, C*H*$_{pyr}$), 7.64 (d, $^3J_{HH}$ = 6 Hz, 1H, C*H*$_{pyr}$), 7.52 (d, $^3J_{HH}$ = 2 Hz, 1H,

C$H_{imz}$), 7.15 (d, $^{3}J_{HH}$ = 2 Hz, 1H, C$H_{imz}$), 4.09 (s, 3H, C$H_{3pyr}$), 3.98 (s, 2H, Ir-C$H_{2imz}$), 3.71 (s, 3H, C$H_{3imz}$). $^{13}$C{$^{1}$H} NMR (75 MHz, $CD_3CN$, 303 K): δ = 168.9 (s, Ir-$C_{pyr}$), 163.5 (s, $C_{imz}$), 145.8 (s, $C$H$_{pyr}$), 144.9 (s, $C_{pyr}$), 135.2 (s, $C$H$_{pyr}$), 130.0 (s, $C$H$_{pyr}$), 121.9 (s, $C$H$_{imz}$), 118.7 (s, $C$H$_{imz}$), 46.9 (s, $C$H$_{3pyr}$), 35.9 (s, $C$H$_{3imz}$), -25.5 (s, Ir-$C$H$_{2imz}$). ESI-MS (20 V, $CH_3CN$): *m/z* 674.0 [M-I-$CH_3CN$]$^{+}$, *m/z* 633.9 [M-I-$(CH_3CN)_2$]$^{+}$. Anal. calcd. for $C_{15}H_{19}N_5I_3Ir$ (mol. wt. 842.28): C, 21.39; H, 2.27; N, 8.31. Found: C, 21.43; H, 2.35; N, 8.23.

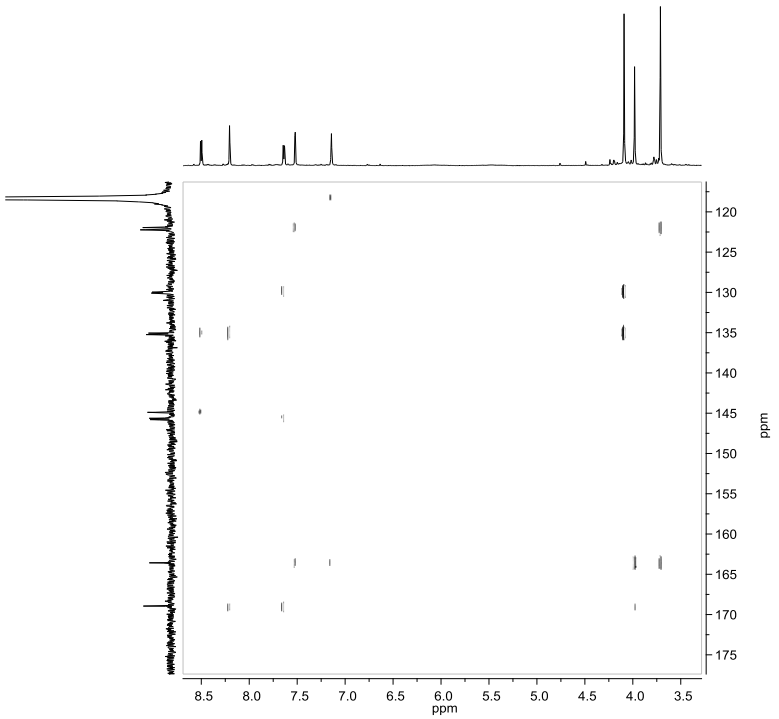


**Figure 5.5** $^{1}$H-$^{13}$C gHMBC spectrum of **14G** in $CD_3CN$

**Synthesis of 15I**

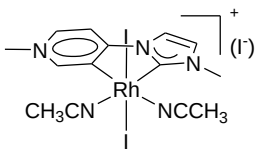


**Method a)** The reaction was carried out with **[IH$_2$]I$_2$** (87 mg, 0.2 mmol), [RhCl(COD)]$_2$ (50 mg, 0.1 mmol), and KI (34 mg, 0.2 mmol). The crude solid was purified by column chromatography. Elution with $CH_2Cl_2$ separated a yellow band containing [RhCl(COD)]$_2$. Further elution with $CH_2Cl_2$/$CH_3CN$ (7:3) afforded the separation of an orange band that contained compound **15I**. Compound **15I** was

isolated as an orange, air and moisture stable solid. Slow diffusion of $Et_2O$ into a concentrated solution of compound **15I** in $CH_3CN$ gave crystals suitable for X-Ray crystallography. Yield: 79 mg (54 %). **Method b)** Compound **15I** was obtained using the same quantities and purification process as in method a, in this case, **$[JH_2]I_2$** (90 mg, 0.2 mmol) was employed as ligand precursor. Yield: 29 mg (20 %). $^1$H NMR (300 MHz, $CD_3CN$, 303 K): δ = 8.60 (s, 1H, C$H_{pyr}$), 8.24 (d, $^3J_{HH}$ = 11 Hz, 1H, C$H_{pyr}$), 7.99 (d, 1H, $^3J_{HH}$ = 4 Hz, C$H_{imz}$), 7.77 (d, $^3J_{HH}$ = 11 Hz, 1H, C$H_{pyr}$), 7.39 (d, $^3J_{HH}$ = 4 Hz, 1H, C$H_{imz}$), 4.26 (s, 3H, C$H_{3pyr}$), 4.01 (s, 3H, C$H_{3imz}$). $^{13}$C{$^1$H} NMR (75 MHz, DMSO-$d_6$, 303 K): δ = 169.6 (d, $^1J_{RhC}$ = 47 Hz, Rh-$C_{pyr}$), 157.9 (s, $C_{pyr}$), 153.5 (s, $C$H$_{pyr}$), 143.1(s, $C$H$_{pyr}$), 139.6 (d, $^1J_{RhC}$ = 34 Hz, Rh-$C_{imz}$), 127.0 (s, $C$H$_{pyr}$), 118.0 (s, $CH_3C$N), 117.5 ($C$H$_{imz}$), 109.0 (s, $C$H$_{imz}$), 47.3 (s, $C$H$_{3pyr}$), 36.0 (s, $C$H$_{3imz}$), 1.2 (s, $CH_3C$N). ESI-MS (20 V, $CH_3CN$): *m/z* 570.7 [M-I-$CH_3CN$]$^+$, *m/z* 529.7 [M-I-$(CH_3CN)_2$]$^+$. Anal. calcd. for $C_{14}H_{17}N_5I_3Rh$ (mol. wt. 738.94): C, 22.76; H, 2.32; N, 9.48. Found: C, 22.89; H, 2.26; N, 9.36.

**Synthesis of 16I**

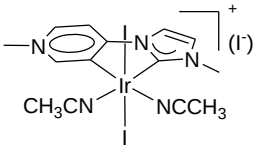


**Method a)** The reaction was carried out with **$[IH_2]I_2$** (64 mg, 0.15 mmol), $[IrCl(COD)]_2$ (50 mg, 0.075 mmol), and KI (25 mg, 0.15 mmol) were used. The crude solid was purified by column chromatography. Elution with $CH_2Cl_2$ separated a red band containing $[IrCl(COD)]_2$. Further elution with $CH_2Cl_2/CH_3CN$ (9:1) afforded the separation of a yellow band that contained compound **16I**. Compound **16I** was isolated as a yellow, air and moisture stable solid. Yield: 70 mg (56 %). **Method b)** Compound **16I** was obtained using the same quantities and purification process as in method a, in this case, **$[JH_2]I_2$** (66 mg, 0.15 mmol) was employed as ligand precursor. Yield: 30 mg (24 %). $^1$H NMR (500 MHz, $CD_3CN$, 303 K): δ = 8.42 (s, 1H, C$H_{pyr}$), 8.04 (d, $^3J_{HH}$ = 6 Hz, 1H, C$H_{pyr}$), 7.80 (d, 1H, $^3J_{HH}$ = 2 Hz, C$H_{imz}$), 7.69 (d, $^3J_{HH}$ = 6 Hz, 1H, C$H_{pyr}$), 7.33 (d, $^3J_{HH}$ = 2 Hz, 1H, C$H_{imz}$), 4.21 (s, 3H, C$H_{3pyr}$), 4.04 (s, 3H, C$H_{3imz}$). $^{13}$C{$^1$H} NMR (125 MHz, $CD_3CN$, 303 K): δ = 160.8 (s, Ir-$C_{pyr}$), 152.0 (s, Ir-$C_{imz}$), 148.4 (s, $C$H$_{pyr}$), 142.4 (s, $C$H$_{pyr}$), 128.5 (s, $C_{pyr}$), 125.4 (s, $C$H$_{pyr}$), 116.6 (s, $C$H$_{imz}$), 107.6 (s, $C$H$_{imz}$), 47.1 (s, $C$H$_{3pyr}$), 36.9 (s, $C$H$_{3imz}$). ESI-MS (20 V, $CH_3CN$): *m/z* 701.9 [M-I]$^+$, *m/z* 660.8 [M-I-$CH_3CN$]$^+$. Anal. calcd. for $C_{14}H_{17}N_5I_3Ir$ (mol. wt. 828.25): C, 20.30; H, 2.07; N, 8.86. Found: C, 20.18; H, 2.32; N, 8.72.

**General procedure for the synthesis of compounds, 17E-24I**

A solution of the appropriate imidazolium-pyridinium salt (1 equivalent), metal precursor $[MCp^*Cl_2]_2$ (M = Rh, Ir) (0.5 equivalents), base (2.5 equivalents) and KI (2.5 equivalents) in $CH_3CN$ (20 mL), was heated at 90 ºC for 12h. After this time, the reaction mixture was cooled to room temperature and filtered through Celite. The solvent was removed under reduced pressure to give a crude product that was purified by column chromatography or precipitation.

**Synthesis of 17E**

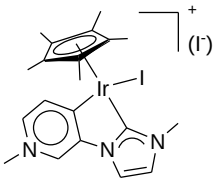


The reaction was carried out with **$[EH_2]I_2$** (53.9 mg, 0.125 mmol), $[IrCp^*Cl_2]_2$ (50 mg, 0.063 mmol), $Cs_2CO_3$ (102.3 mg, 0.314 mmol) and KI (52 mg, 0.314 mmol). Compound **17E** was isolated as a yellow, air and moisture stable solid. Yield: 71 mg (75 %). $^1$H (300 MHz, $CDCl_3$, 303 K): δ = 10.01 (s, 1H, C$H_{pyr}$), 8.50 (d, $^3J_{HH}$ = 2.4 Hz, 1H, C$H_{imz}$), 8.11 (d, $^3J_{HH}$ = 6 Hz, 1H, C$H_{pyr}$), 7.79 (d, $^3J_{HH}$ = 6 Hz, 1H, C$H_{pyr}$), 7.23 (d, $^3J_{HH}$ = 2.4 Hz, C$H_{imz}$), 4.37 (s, 3H, C$H_{3pyr}$), 3.89 (s, 3H, C$H_{3imz}$), 1.94 (s, 15H, (C$H_3$)$_5$Cp*). $^{13}$C{$^1$H} (75 MHz, $CDCl_3$, 303 K): δ = 175.1 (s, Ir-$C_{pyr}$), 163.7 (s, Ir-$C_{imz}$), 148.5 (s, $C_{pyr}$), 136.4 (s, $C$H$_{pyr}$), 135.0 (s, $C$H$_{pyr}$), 124.1 (s, $C$H$_{pyr}$), 124.0 (s, $C$H$_{imz}$), 118.0 (s, $C$H$_{imz}$), 94.6 (s, $C_5$Cp*), 46.7 (s, $C$H$_{3pyr}$), 37.9 (s, $C$H$_{3imz}$), 10.5 (s, ($C$H$_3$)$_5$Cp*). ESI-MS (15 V, $CH_2Cl_2$/MeOH): *m/z* 628.1 $[M\text{-}I]^+$. HRMS (+)-ESI-TOF-MS of $[M]^+$, 628.0801, calcd. 628.0801, $\varepsilon_r$ = 0.8 ppm. Anal. calcd. for $C_{20}H_{26}N_3IrI_2$ (mol. wt. 754.47): C, 31.84; H 3.47; N 5.57. Found: C, 31.78; H 3.50; N 5.63.

**Synthesis of 18E, 19E and 20E**

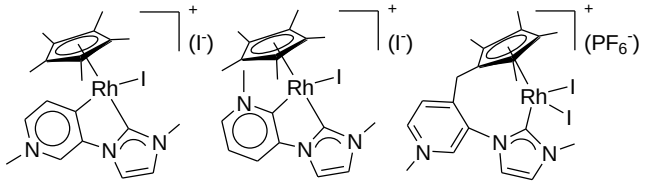


**18E** **19E** **20E**

The reaction was carried out with **$[EH_2]I_2$** (139 mg, 0.32 mmol), $[RhCp^*Cl_2]_2$ (100 mg, 0.16 mmol), NaOAc (265 mg, 3.24 mmol) and KI (269 mg, 1.6 mmol). The crude solid was purified by column chromatography. Elution with $CH_2Cl_2$ separated a minor red band containing $[RhCp^*Cl_2]_2$. Elution with $CH_2Cl_2$/acetone (9:1) afforded the separation of a pink band containing diiodine. Additional elution with

$CH_2Cl_2$/acetone (1:1) afforded the separation of a major orange band that contained compounds **18E** and **19E**. Further elution with acetone and $KPF_6$ separated a red band that contained compound **20E**. Attempts to separate isomers **18E** and **19E** gave no satisfactory results.

Data for **18E** and **19E**: The mixture of compounds **18E** and **19E** was isolated as an orange, air and moisture stable solid in a molar ratio 7:3, respectively. Slow diffusion of $Et_2O$ into a concentrated solution of the mixture of compounds **18E** and **19E** in $CH_3CN$ gave crystals, only for compound **18E**, suitable for X-Ray crystallography. Yield: 116 mg (54%). **18E**; Yield: 81 mg (38%). $^1$H (300 MHz, $CDCl_3$, 303 K): δ = 9.93 (s, 1H, C$H_{pyr}$), 8.55 (d, $^3J_{HH}$ = 2 Hz, 1H, C$H_{imz}$), 8.07 (d, $^3J_{HH}$ = 6 Hz, 1H, C$H_{pyr}$), 7.05 (d, $^3J_{HH}$ = 6 Hz, 1H, C$H_{pyr}$), 7.26 (d, $^3J_{HH}$ = 2 Hz, 1H, C$H_{imz}$), 4.43 (s, 3H, C$H_{3pyr}$), 3.87 (s, 3H, C$H_{3imz}$), 1.86 (s, 15H, (C$H_3$)$_5$Cp*). $^{13}$C{$^1$H} (125 MHz, $CDCl_3$, 303 K): δ = 194.8 (d, $^1J_{RhC}$ = 37 Hz, Rh-$C_{pyr}$), 181.7 (d, $^1J_{RhC}$ = 55 Hz, Rh-$C_{imz}$), 147.3 (s, $C_{pyr}$), 136.5 (s, $C$H$_{pyr}$), 135.0 (s, $C$H$_{pyr}$), 125.0 (s, $C$H$_{pyr}$), 124.2 (s, $C$H$_{imz}$), 118.4 (s, $C$H$_{imz}$), 100.1 (d, $^1J_{RhC}$ = 5, Rh-$C_5$Cp*), 46.8 (s, $C$H$_{3pyr}$), 38.3 (s, $C$H$_{3imz}$), 10.8 (s, ($C$H$_3$)$_5$Cp*). ESI-MS (20V, MeOH): *m/z* 538.1 [M]$^+$. **19E**; Yield: 35 mg (16%). $^1$H (300 MHz, $CDCl_3$, 303 K): δ = 8.74 (d, $^3J_{HH}$ = 7 Hz, 1H, C$H_{pyr}$), 8.32 (d, $^3J_{HH}$ = 8 Hz, 1H, C$H_{pyr}$), 8.22 (d, $^3J_{HH}$ = 2 Hz, 1H, C$H_{imz}$), 7.51 (dd, $^3J_{HH}$ = 7 Hz, $^3J_{HH}$ = 8 Hz, 1H, C$H_{pyr}$), 7.39 (d, $^3J_{HH}$ = 2 Hz, 1H, C$H_{imz}$), 4.52 (s, 3H, C$H_{3pyr}$), 3.87 (s, 3H, C$H_{3imz}$), 1.84 (s, 15H, (C$H_3$)$_5$Cp*). $^{13}$C{$^1$H} (125 MHz, $CDCl_3$, 303 K): δ = 192.6 (d, $^1J_{RhC}$ = 45 Hz, Rh-$C_{pyr}$), 179.9 (d, $^1J_{RhC}$ = 54 Hz, Rh-$C_{imz}$), 146.9 (s, $C_{pyr}$), 141.0 (s, $C$H$_{pyr}$), 125.6 (s, $C$H$_{pyr}$), 122.0 (s, $C$H$_{pyr}$), 120.6 (s, $C$H$_{imz}$), 119.1 (s, $C$H$_{imz}$), 101.0 (d, $^1J_{RhC}$ = 5, Rh-$C_5$Cp*), 54.3 (s, $C$H$_{3pyr}$), 38.9 (s, $C$H$_{3imz}$), 10.8 (s, ($C$H$_3$)$_5$Cp*). ESI-MS (20 V, MeOH): *m/z* 538.1 [M]$^+$. Anal. calcd. for **18E** and **19E** $C_{20}H_{26}N_3RhI_2$ (mol. wt. 665.15): C, 36.11; H, 3.94; N, 6.32. Found: C, 36.12; H, 4.48; N, 5.89.

Data for **20E**: Compound **20E** was obtained as a red, air and moisture sensitive solid. Slow diffusion of $Et_2O$ into a concentrated solution of compound **20E** in $CH_3CN$ gave crystals suitable for X-Ray crystallography. Yield: 62 mg (25%). $^1$H (300 MHz, $CD_3CN$, 303 K): δ = 8.77 (s, 1H, C$H_{pyr}$), 8.59 (d, $^3J_{HH}$ = 6 Hz, 1H, C$H_{pyr}$), 8.12 (d, $^3J_{HH}$ = 6 Hz, 1H, C$H_{pyr}$), 7.56 (s, 1H, C$H_{imz}$), 7.52 (s, 1H, C$H_{imz}$), 4.25 (s, 3H, C$H_{3pyr}$), 4.18 (s, 3H, C$H_{3imz}$), 3.62 (d, $^2J_{HH}$ = 15 Hz, 1H, aC$H_2$-Cp*), 3.44 (d, $^2J_{HH}$ = 15 Hz, 1H, bC$H_2$-Cp*), 2.25, 2.21, 1.84, 1.35 (s, 3H, (C$H_3$)$_4$Cp*). $^{13}$C{$^1$H} (75 MHz, $CD_3CN$, 303 K): δ = 170.1 (d, $^1J_{RhC}$ = 57 Hz, Rh-$C_{imz}$), 152.1 (s, $C_{pyr}$), 147.3 (s,

*C*H$_{pyr}$), 144.2 (s, *C*H$_{pyr}$), 142.7 (s, *C*$_{pyr}$CH$_2$), 131.6 (s, *C*H$_{pyr}$), 127.8 (s, *C*H$_{imz}$), 126.0 (s, *C*H$_{imz}$), 113.3, 108.1, 97.4, 94.6, 80.6 (d, $^1J_{RhC}$ = 7, Rh-*C*$_5$Cp*), 48.8 (s, *C*H$_{3pyr}$), 44.1 (s, *C*H$_{3imz}$), 28.7 (s, *C*H$_2$Cp*), 13.2, 13.1, 9.5, 9.0 (s, (*C*H$_3$)$_4$Cp*). ESI-MS (20V, CH$_3$CN): *m/z* 289.2 [M-I+CH$_3$CN]$^{2+}$. Several attempts to obtain satisfactory elemental analysis of **20E** failed, probably because this species is highly hygroscopic.

**Synthesis of 21G**

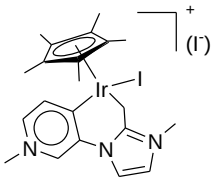


Compound **21G** was obtained using the same quantities as for **17E**, in this case, **[GH$_2$]I$_2$** (55.6 mg, 0.125 mmol) was employed as ligand precursor. Compound purified by column chromatography. Elution with CH$_2$Cl$_2$/Acetone (9:1) separated an orange band that contained [IrCp*Cl$_2$]$_2$. Further elution with CH$_2$Cl$_2$/Acetone (1:1) afforded the separation of a major orange band that contained compound **21G**. Compound **21G** was isolated as an orange, air and moisture stable solid. Yield: 62 mg (65%). $^1$H (500 MHz, CD$_3$CN, 303 K): δ = 8.39 (d, $^3J_{HH}$ = 6 Hz, 1H, C*H*$_{pyr}$), 8.06 (s, 1H, C*H*$_{pyr}$), 7.57 (d, $^3J_{HH}$ = 6 Hz, 1H, C*H*$_{pyr}$), 7.36 (d, $^3J_{HH}$ = 2 Hz, 1H, C*H*$_{imz}$), 7.17 (d, $^3J_{HH}$ = 2 Hz, C*H*$_{imz}$), 4.33 (s, 3H, C*H*$_{3pyr}$), 3.96 (d, $^2J_{HH}$ = 13 Hz, 1H, Ir-aC*H*$_2$), 3.87 (s, 3H, C*H*$_{3imz}$), 2.63 (d, $^2J_{HH}$ = 13 Hz, 1H, Ir-bC*H*$_2$), 1.65 (s, 15H, (C*H*$_3$)$_5$Cp*). $^{13}$C{$^1$H} (125 MHz, CD$_3$CN, 303 K): δ = 187.4 (s, Ir-*C*$_{pyr}$), 159.6 (s, *C*$_{imz}$), 147.4 (s, *C*H$_{pyr}$), 140.8 (s, *C*$_{pyr}$), 134.3 (s, *C*H$_{pyr}$), 128.3 (s, *C*H$_{pyr}$), 120.5 (s, *C*H$_{imz}$), 119.6 (s, *C*H$_{imz}$), 90.8 (s, *C*$_5$Cp*), 46.9 (s, *C*H$_{3pyr}$), 35.3 (s, *C*H$_{3imz}$), 9.8 (s, (*C*H$_3$)$_5$Cp*), -13.7 (s, Ir-*C*H$_2$). ESI-MS (20 V, CH$_2$Cl$_2$/MeCN (8:2)): *m/z* 642.6 [M]$^+$. Anal. calcd. for C$_{21}$H$_{28}$N$_3$IrI$_2$ (mol. wt. 768.49): C, 32.82; H, 3.67; N, 5.47. Found: C, 32.99; H 3.55; N 5.58.

**Synthesis of 22G**

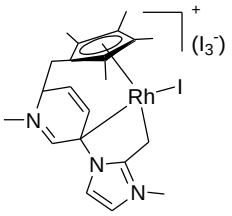


The reaction was carried out with **[GH$_2$]I$_2$** (71.7 mg, 0.162 mmol), [RhCp*Cl$_2$]$_2$ (50 mg, 0.081 mmol), Cs$_2$CO$_3$ (132 mg, 0.405 mmol) and KI (269 mg, 1.6 mmol). The crude solid was purified by column chromatography. Elution with CH$_2$Cl$_2$/Acetone (9:1) separated a red band containing [RhCp*Cl$_2$]$_2$. Further elution with CH$_2$Cl$_2$/Acetone (1:1) afforded the separation of a major orange band that contained compound **22G**. Compound **22G** was isolated as an orange, air and moisture stable solid. Slow diffusion of hexane into a concentrated

solution of compound **22G** in $CH_2Cl_2$ gave crystals suitable for X-Ray crystallography. Yield: 91 mg (60 %). $^1$H (500 MHz, $CDCl_3$, 303 K): δ = 7.60 (s, 1H, C*H*$_{pyr}$), 7.30 (d, $^3J_{HH}$ = 2 Hz, 1H, C*H*$_{imz}$), 7.02 (d, $^3J_{HH}$ = 2 Hz, 1H, C*H*$_{imz}$), 6.62 (dd, $^4J_{HH}$ = 1.5 Hz, $^3J_{HH}$ = 9.5 Hz, 1H, C*H*$_{pyr}$), 5.44 (dd, $^3J_{HH}$ = 5.5 Hz, $^3J_{HH}$ = 9.5 Hz, 1H, C*H*$_{pyr}$), 5.17 (td, $^3J_{HH}$ = 2 Hz, $^3J_{HH}$ = 5.5 Hz, 1H, C*H*$_{pyr}$), 3.68 (s, 3H, C*H*$_{3pyr}$), 3.46 (dd, $^2J_{RhH}$ = 3 Hz, $^2J_{HH}$ = 14 Hz, 1H, Rh-aC*H*$_2$), 3.08 (s, 3H, C*H*$_{3imz}$), 2.71 (dd, $^2J_{RhH}$ = 3 Hz, $^2J_{HH}$ = 14 Hz, 1H, Rh-bC*H*$_2$), 2.15 (s, 3H, C*H*$_3$Cp*), 1.97 (dd, $^3J_{HH}$ = 1.5 Hz, $^2J_{HH}$ = 14 Hz, 1H, aC*H*$_2$-Cp*), 1.82 (s, 3H, C*H*$_3$Cp*), 1.74 (s, 3H, C*H*$_3$Cp*), 1.68 (dd, $^3J_{HH}$ = 2 Hz, $^2J_{HH}$ = 14 Hz, 1H, bC*H*$_2$-Cp*), 1.12 (s, 3H, C*H*$_3$Cp*). $^{13}$C{$^1$H} (125 MHz, $CDCl_3$, 303 K): δ = 165.1 (s, *C*$_{imz}$), 139.9 (s, *C*H$_{pyr}$), 131.4 (s, *C*H$_{pyr}$), 123.5 (s, *C*H$_{imz}$), 118.7 (s, *C*H$_{imz}$), 115.5 (s, *C*H$_{pyr}$), 106.0 (d, $^1J_{RhC}$ = 5.0, Rh-*C*Cp*), 101.0 (d, $^1J_{RhC}$ = 6.2, Rh-*C*Cp*), 99.1 (d, $^1J_{RhC}$ = 4.4, Rh-*C*Cp*), 89.8 (d, $^1J_{RhC}$ = 4.6, Rh-*C*Cp*), 87.4 (d, $^1J_{RhC}$ = 8.8, Rh-*C*Cp*), 64.6 (d, $^1J_{RhC}$ = 15.1, Rh-*C*$_{pyr}$), 55.6 (s, *C*H$_{pyr}$), 41.2 (s, *C*H$_{3pyr}$), 33.6 (s, *C*H$_{3imz}$), 11.6, 10.5, 9.0, 6.9, (s, (*C*H$_3$)$_4$Cp*), 8.3 (s, C*H*$_2$Cp*), 2.0 (d, $^1J_{RhC}$ = 26.9, Rh-*C*H$_2$). ESI-MS (15 V, $CH_2Cl_2$/MeCN (8:2)): *m/z* 552 $[M]^+$. Anal. calcd. for $C_{21}H_{28}N_3RhI_4$ (mol. wt. 932.99): C, 27.03; H, 3.02; N, 4.50. Found: C, 27.15; H, 3.28; N, 4.8.

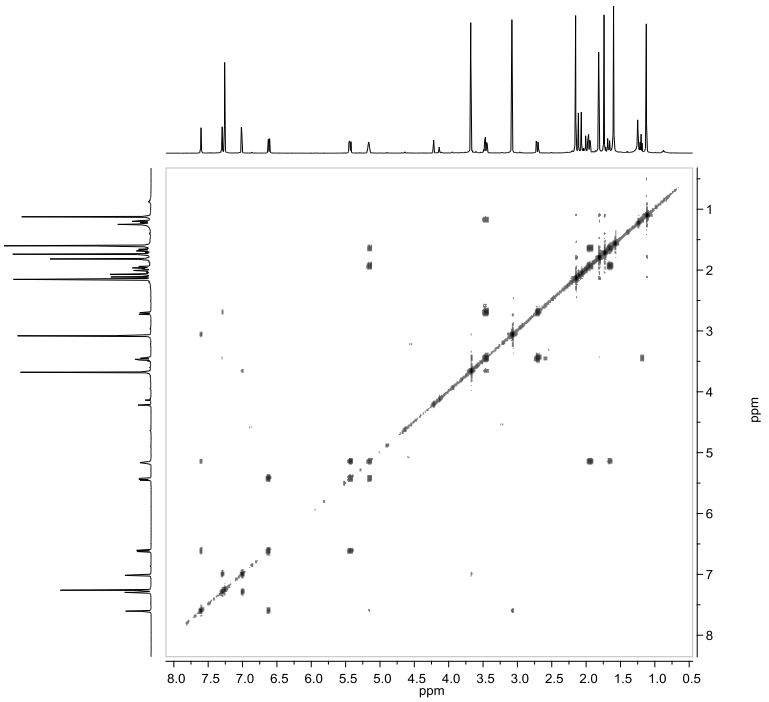


**Figure 5.6** $^{1}$H-$^{1}$H gCOSY spectrum of **22G** in $CDCl_3$

**Synthesis of 23I and 24I**

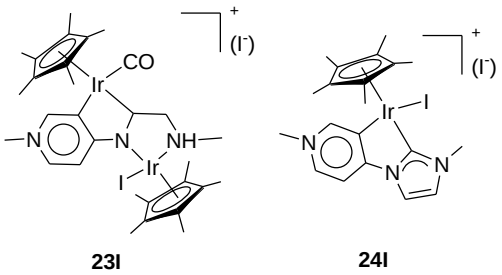


**23I** **24I**

The reaction was carried out with **$[IH_2]I_2$** (54 mg, 0.125 mmol), $[IrCp^*Cl_2]_2$ (50 mg, 0.063 mmol), $Cs_2CO_3$ (102 mg, 0.32 mmol) and KI (52 mg, 0.32 mmol). The crude solid was purified by column chromatography. Elution with $CH_2Cl_2$ separated a yellow band containing $[IrCp^*Cl_2]_2$. Further elution with $CH_2Cl_2$/acetone (8:2) afforded the separation of a yellow band that contained compound **23I**. Further elution with acetone separated an orange band that contained compound **24I**.

Data for **23I**: Compound **23I** was isolated as an orange, air and moisture stable solid. Slow diffusion of $Et_2O$ into a concentrated solution of compound **23I** in $CHCl_3$ gave crystals suitable for X-Ray crystallography. Yield: 10 mg (15%). $^{1}$H (500 MHz,

$CDCl_3$, 303 K): δ = 7.16 (m, 1H, N*H*), 6.83 (dd, $^3J_{HH}$ = 3 Hz, $^3J_{HH}$ = 9 Hz, 1H, C$H_{pyr}$), 6.27 (d, $^3J_{HH}$ = 3 Hz, 1H, C$H_{pyr}$), 5.83 (d, $^3J_{HH}$ = 6 Hz, 1H, C$H_{pyr}$), 4.38 (dd, $^3J_{HH}$ = 3 Hz, $^3J_{HH}$ = 12 Hz, 1H, C$H_{imz}$), 3.50 (s, 3H, C$H_{3pyr}$), 2.97 (d, $^3J_{HH}$ = 6 Hz, 3H, C$H_{3imz}$), 2.87 (m, 2H, C$H_{imz}$), 2.01 (s, 15H, (C$H_3$)$_5$Cp*), 1.91 (s, 15H, (C$H_3$)$_5$Cp*). $^{13}$C{$^1$H} (125 MHz, $CD_3CN$, 303 K): δ = 171.8 (s, Ir-$C_{pyr}$), 170.4 (s, *C*O), 136.8 (s, *C*H$_{pyr}$), 136.8 (s, *C*H$_{pyr}$), 119.9 (s, $C_{pyr}$), 105.0 (s, *C*H$_{pyr}$), 99.5 (s, $C_5$Cp*), 86.6 (s, $C_5$Cp*), 66.6 (s, *C*H$_2$), 60.8 (s, *C*H$_{3pyr}$), 44.7 (s, *C*H$_{3imz}$), 42.3 (s, *C*H), 10.6 (s, (*C*H$_3$)$_5$Cp*), 9.7 (s, (*C*H$_3$)$_5$Cp*). ESI-MS (20 V, $CH_3OH$): *m/z* 972.3 [M-I]$^+$. IR (KBr): 1986 (ν $_{C=O}$) cm$^{-1}$.

Data for **24I**: Compound **24I** was isolated as an orange, air and moisture stable solid. Slow diffusion of $Et_2O$ into a concentrated solution of compound **24I** in $CH_3CN$ gave crystals suitable for X-Ray crystallography. Yield: 55 mg (58%). $^1$H (300 MHz, $CD_3CN$, 303 K): δ = 8.31 (s, 1H, C$H_{pyr}$), 8.11 (d, $^3J_{HH}$ = 6 Hz, 1H, C$H_{pyr}$), 7.78 (d, $^3J_{HH}$ = 2 Hz, 1H, C$H_{imz}$), 7.73 (d, $^3J_{HH}$ = 6 Hz, 1H, C$H_{pyr}$), 7.38 (d, $^3J_{HH}$ = 2 Hz, 1H, C$H_{imz}$), 4.20 (s, 3H, C$H_{3pyr}$), 3.90 (s, 3H, C$H_{3imz}$), 1.96 (s, 15H, (C$H_3$)$_5$Cp*). $^{13}$C{$^1$H} (75 MHz, $CD_3CN$, 303 K): δ = 169.3 (s, Ir-$C_{pyr}$), 159.9 (s, Ir-$C_{imz}$), 149.1 (s, *C*H$_{pyr}$), 141.5 (s, C$_{pyr}$), 140.9 (s, *C*H$_{pyr}$), 125.9 (s, *C*H$_{pyr}$), 116.9 (s, *C*H$_{imz}$), 107.9 (s, *C*H$_{imz}$), 94.1 (s, $C_5$Cp*), 46.7 (s, *C*H$_{3pyr}$), 37.9 (s, *C*H$_{3imz}$), 10.5 (s, (*C*H$_3$)$_5$Cp*). ESI-MS (20 V, $CH_3OH$): *m/z* 628.2 [M]$^+$. Anal. calcd. for $C_{20}H_{26}N_3IrI_2$ (mol. wt. 754.47): C, 31.84; H, 3.47; N, 5.57. Found: C, 31.88; H, 3.23; N, 5.62.

### 5.2.4 Synthesis of poly-NHC complexes of Rh(I), Ag(I) and Au(I)

**Synthesis of 25K**

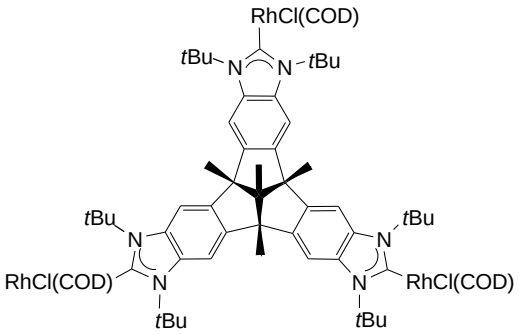


A suspension of compound **[KH$_3$](BF$_4$)$_3$** (200 mg, 0.19 mmol) in THF (10 mL), was stirred at 0 °C for 20 minutes. KHMDS was added dropwise (0.5 M in toluene, 1.48 mL, 0.74 mmol) and the slurry was stirred at 0 ºC for further 30 minutes. After this time, the resulting cloudy dark brown solution was filtered through oven dried cannula into a solution of $[Rh(COD)Cl]_2$ (154 mg, 0.313 mmol) in THF (10 mL). The reaction mixture was stirred at room temperature

for 12h. Solvent was removed under reduced pressure and the crude solid was purified by column chromatrography. Elution with $CH_2Cl_2$ separated a yellow band containing $[Rh(COD)Cl]_2$. Further elution with $CH_2Cl_2$/acetone (9:1) separated a light yellow band that contained compound **25K**. Compound **25K** was isolated as a pale yellow, air and moisture sensitive solid. Yield: 94 mg (32 %). $^1$H NMR (300 MHz, $CDCl_3$, 303 K): δ = 7.61 (s, 3H, C$H_{arom}$), 7.58 (s, 3H, C$H_{arom}$), 4.99 (br, 6H, COD), 3.01 (br, 3H, COD), 2.72 (br, 3H, COD), 2.41 (br, 12H, COD), 2.37 (s, 27 H, C(C$H_3$)$_3$), 2.36 (s, 27 H, C(C$H_3$)$_3$), 1.97 (s, 9H, C$H_3$), 1.83 (s, 3H, C$H_{3central}$), 1.77 (br, 12H, COD). $^{13}$C{$^1$H} NMR (125 MHz, $CD_2Cl_2$, 303 K): δ = 195.9 (d, $^1J_{RhC}$ = 49.0 Hz, Rh-$C_{carbene}$), 195.7 (d, $^1J_{RhC}$ = 49.0 Hz, Rh-$C_{carbene}$), 142.5 (s, $C_{qarom}$), 136.1 (s, $C_{qarom}$), 108.3 (s, $C$H$_{arom}$), 93.3 (d, $^1J_{RhC}$ = 15.8 Hz, Rh-$C$HCOD), 72.2 (s, $C$CH$_{3\ central}$), 67.5 (d, $^1J_{RhC}$ = 15.8 Hz, Rh-$C$HCOD), 61.7 (s, $C$CH$_3$), 60.2 (s, $C$(CH$_3$)$_3$), 32.5 (s, C($C$H$_3$)$_3$), 32.4 (s, C($C$H$_3$)$_3$), 31.0 (s, $C$H$_2$-COD), 28.6 (s, $C$H$_2$-COD). 27.2 (s, $C$H$_3$), 16.7 (s, $C$H$_{3central}$). ESI-MS (20 V, $CH_3CN$): *m/z* 516.6 $[M\text{-}3Cl\text{+}3CH_3CN]^{3+}$. Several attempts to obtain satisfactory elemental analysis of **25K** failed, probably because this species is highly hygroscopic.

**Synthesis of 26L**

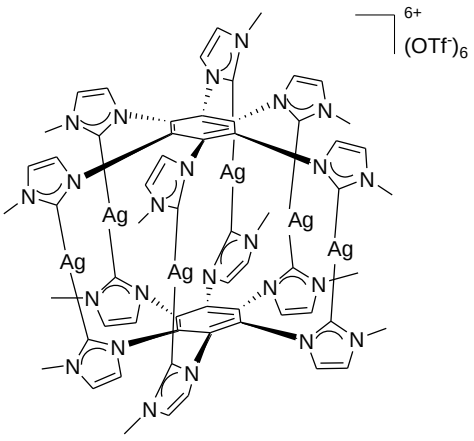


A solution of compound **[LH$_6$](OTf)$_6$** (200 mg, 0.137 mmol) and $Ag_2O$ (105 mg, 0.453 mmol) in $CH_3OH$ (20 mL), was heated at 50 ºC for 24h under exclusion of light. After this time, the reaction mixture was cooled to room temperature and filtered through Celite. The filtrate was concentrated to 5 mL and added over $Et_2O$ (20 mL), leading to the formation of a white microcrystalline solid, which was collected by filtration and washed with $Et_2O$. Compound **26L** was isolated as a white, air and moisture sensitive solid. Yield: 162 mg (89 %). $^1$H NMR (500 MHz, $CD_3OD$, 303 K): δ = 7.47 (s, 12H, C$H_{imz}$) 7.37 (s, 12H, C$H_{imz}$), 3.88 (s, 36H, C$H_3$). $^{13}$C{$^1$H} NMR (125 MHz, $CD_3OD$, 303 K): δ = 181.4 (dd, $^1J_{Ag107C}$ = 182.0 Hz, $^1J_{Ag109C}$ = 210.1 Hz, Ag-$C_{imz}$), 138.1 (s, $C_{qarom}$), 126.7 (s, $C$H$_{imz}$), 124.7 (s, $C$H$_{imz}$), 40.1 (s, $C$H$_3$).

HRMS (+)-ESI-TOF-MS of $[M\text{-}3(CF_3SO_3)]^{3+}$, monoisotopic peak 736.9399, calcd 736.9432, $\varepsilon_r$ = 4.5 ppm.

**Synthesis of 27M**

A solution of compound **$[MH_6](BF_4)_6$** (200 mg, 0.171 mmol) and $Ag_2O$ (119 mg, 0.513 mmol) in $CH_3CN$ (15 mL), was heated at 60 ºC for 24h under exclusion of light. After this time, the reaction mixture was cooled to room temperature and filtered through Celite. The filtrate was concentrated to 5 mL and added over $Et_2O$ (20 mL), leading to the formation of a white microcrystalline solid, which was collected by filtration and washed with $Et_2O$. Compound **27M** was isolated as a white, air and moisture sensitive solid. Slow diffusion of $Et_2O$ into a concentrated solution of compound **27M** in $CH_3CN$ gave crystals suitable for X-Ray crystallography. Yield: 195 mg (93 %). $^1$H NMR (500 MHz, $CD_3CN$, 303 K): δ 7.37 (s, 12H, C*H*$_{imz}$) 7.16 (s, 12H, C*H*$_{imz}$), 3.99 (m, 24H, C*H*$_2$CH$_3$), 1.26 (m, 36H, CH$_2$C*H*$_3$). $^{13}$C{$^1$H} NMR (125 MHz, $CD_3CN$, 303 K): δ 180.6 (br, AgC$_{imz}$), 136.2 (s, *C*$_{qarom}$), 123.5 (s, *C*H$_{imz}$), 122.1 (s, *C*H$_{imz}$), 47.7 (s, *C*H$_2$CH$_3$), 16.7 (s, CH$_2$*C*H$_3$). HRMS (+)-ESI-TOF-MS of $[M - 4(BF_4)]^{4+}$, monoisotopic peak 526.5422, calcd 526.5424, $\varepsilon_r$ = 0.4 ppm.

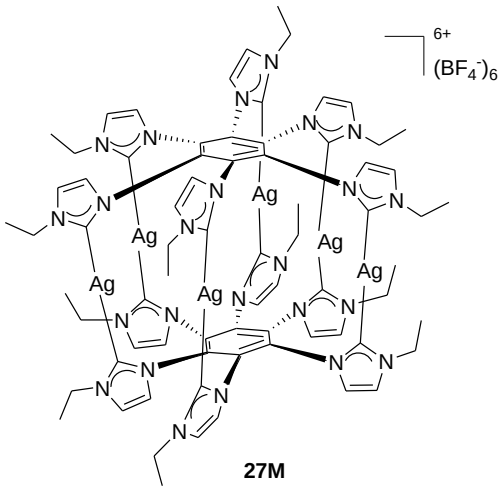


**Synthesis of 28L**

A solution of compound **26L** (133 mg, 0.05 mmol) and [AuCl(SMe$_2$)] (88.4 mg, 0.3 mmol) in $CH_3OH$ (10 mL), was heated at 50 ºC for 12h under exclusion of light. After this time, the reaction mixture was cooled to room temperature and filtered through Celite. The filtrate was concentrated to 5 mL and added over $Et_2O$

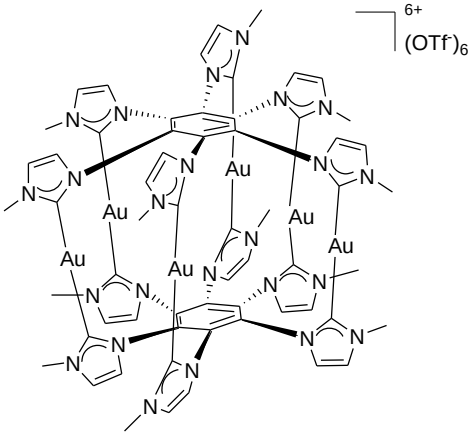

(20 mL), leading to the formation of a white microcrystalline solid, which was collected by filtration and washed with $Et_2O$. Compound **28L** was isolated as a white, air and moisture sensitive solid. Yield: 128 mg (80 %). $^1$H NMR (300 MHz, $CD_3OD$, 303K): δ = 7.44 (s, 12H, C$H_{imz}$), 7.35 (s, 12H, C$H_{imz}$), 3.84 (s, 36H, C$H_3$). $^{13}$C{$^1$H} NMR (125 MHz, $CD_3CN$, 303 K): δ = 183.9 (s, Au-$C_{imz}$), 137.9 (s, $C_{qarom}$), 126.9 (s, $C$H$_{imz}$), 123.8 (s, $C$H$_{imz}$), 40.3 (s, $C$H$_3$). ESI-MS (20 V, $CH_3OH$): m/z 649.4 [M - 4($CF_3SO_3$)]$^{4+}$.

**Synthesis of 29M**

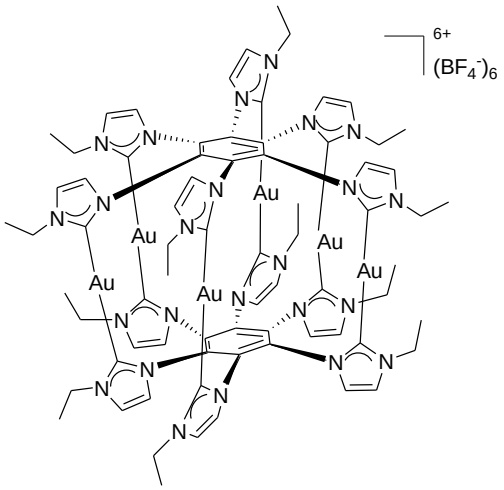


A solution of compound **27M** (123 mg, 0.05 mmol) and [AuCl($SMe_2$)] (88.4 mg, 0.3 mmol) in $CH_3OH$ (15 mL), was heated at 50 ºC for 12h under exclusion of light. After this time, the reaction mixture was cooled to room temperature and filtered through Celite. The filtrate was concentrated to 5 mL and added over $Et_2O$ (20 mL), leading to the formation of a white microcrystalline solid, which was collected by filtration and washed with $Et_2O$. Compound **29M** was isolated as a white, air and moisture sensitive solid. Yield: 125 mg (84 %). $^1$H NMR (500 MHz, $CD_3OD$, 333K): δ = 7.38 (s, 12H, C$H_{imz}$), 7.28 (s, 12H, C$H_{imz}$), 4.16 (s, 24H, C$H_2$CH$_3$), 1.35 (s, 36H, CH$_2$C$H_3$). $^{13}$C{$^1$H} NMR (125 MHz, $CD_3CN$, 333 K): δ = 182.2 (s, Au-$C_{imz}$), 136.5 (s, $C_{qarom}$), 125.0 (s, $C$H$_{imz}$), 122.7 (s, $C$H$_{imz}$), 47.6 (s, CH$_2$$C$H$_3$), 16.6 (s, CH$_2$$C$H$_3$). HRMS (+)-ESI-TOF-MS of [M - 2($BF_4$)]$^{4+}$, monoisotopic peak 660.1340, calcd 660.1346, $\varepsilon_r$ = 0.9 ppm.

# 5.3 CATALYTIC ASSAYS

## 5.3.1 Suzuki-Miyaura C-C Coupling in water

A mixture of arylhalide (1 mmol), phenylboronic acid (1.2 mmol), $K_2CO_3$ (1.5 mmol) and catalyst (1, $10^{-1}$, $10^{-2}$, $10^{-3}$ mol%), in 5 mL of degassed Milli-Q water or in a degassed mixture 1:1 Milli-Q water/*i*PrOH, was vigorously stirred at 110ºC under aerobic conditions, in a Pyrex tube. The activation of aryl chlorides required the addition of 1.5 mmol of TBABr as phase transfer catalyst. After the desired reaction time, the solution was allowed to cool to room temperature. The reaction mixture was extracted with $CH_2Cl_2$ (3 x 5mL) and the organic phase dried over $Na_2SO_4$. The solvent was removed by evaporation to give a crude product. Yields were determined by GC using anisole as internal standard. The confirmation of the nature of the products was performed by comparison with the commercial available products.

## 5.3.2 *Borrowing-Hydrogen* processes

### 5.3.2.1 *β*-Alkylation of secondary alcohols with primary alcohols

A mixture of primary alcohol (1 or 2 mmol), 1-phenylethanol (1 mmol), KOH (1 mmol) and catalyst (1 or 0.1 mol %), in 0.3 mL of toluene, was stirred at 100ºC under aerobic conditions, in a sealed tube. After the desired reaction time, the solution was allowed to cool to room temperature. Yields were determined by $^1$H NMR taking aliquots (5 μL), using anisole as internal standard and $CDCl_3$ as deuterated solvent. The confirmation of the nature of the products was performed by comparison with the literature data, 1,3-diphenyl-1-propanol, 1,3-diphenyl-1-propanone, 1-phenyl-1-hexanol and 1-phenyl-1-hexanone,[17] 3-(3-chlorophenyl-1-penyl-1-propanol), 3-(3-chlorophenyl-1-penyl-1-propanone), 3-(4-chlorophenyl-1-penyl-1-propanol) and 3-(4-chlorophenyl-1-penyl-1-propanone).[18]

### 5.3.2.2 Alkylation of ammonia with primary alcohols

A mixture of the ammonium source (1 mmol of ammonium salt), alcohol (3 or 3.6 mmol) and catalyst (1 mol %) was stirred at 130ºC under inert atmosphere, in a sealed tube. After the desired reaction time, the solution was allowed to cool. Then, a solution of NaOH in water (2.0M, 10 mL) was added to the reaction mixture, and the product was extracted with $CH_2Cl_2$ (30 mL). Yields were determined by GC using

anisole as internal standard. All products were isolated by column chromatography and characterised by $^{1}H$ and $^{13}C$ NMR spectroscopy. The confirmation of the nature of the products was performed by comparison with the commercial available products or literature data.[19]

#### 5.3.2.3 Dehydrogenation of benzyl alcohol

A mixture of benzyl alcohol (0.4 mmol), catalyst (5 mol %) and $Cs_2CO_3$ (20 mol %) was refluxed in toluene (1 mL) under aerobic conditions, in a small round bottom flask for 15h. After the desired reaction time, the solution was allowed to cool. Yield was determined by $^{1}H$ NMR spectroscopy taking aliquots (5 µL), using anisole as internal standard and $CDCl_3$ as deuterated solvent. The confirmation of the nature of benzaldehyde was performed by comparison with literature data.[18]

## 5.4 X-RAY DIFFRACTION

Single crystals suitable for X-Ray Diffraction were mainly obtained by slow diffusion of hexane or $Et_2O$ into a concentrated solution of the compound in different solvents or slow evaporation of a concentrated solution of the compound in appropriated solvent. Diffraction data was collected on a Agilent SuperNova diffractometer equipped with an Atlas CCD detector using Mo-Kα radiation (λ = 0.71073 Å). Single crystals were mounted on a MicroMount® polymer tip (MiteGen) in a random orientation. Absorption corrections based on the multiscan method were applied.[20] Structures were solved by direct methods in SHELXS-97 and refined by the full-matrix method based on $F^2$ with the program SHELXL-97 using the OLEX software package.[21-22]

In the following tables the structural parameters, registering conditions and refinement for these structures are described.

**Table 5.1** Crystallographic data and structure refinement for complexes **5D** and **6D**

| | **5D** | **6D** |
|---|---|---|
| Empirical Formula | $C_{29}H_{39}Cl_2IrN_2$ | $C_{29}H_{38}ClIrN_2$ |
| $M_w$ | 678.72 | 642.26 |
| Temperature (K) | 293 | 293 |
| Crystalline System | Monoclinic | Orthorhombic |
| Space Group | I2/a | P2(1)2(1)2(1) |
| *a* (Å) | 16.4387(7) | 7.726(4) |
| *b* (Å) | 11.5763(5) | 15.760(8) |
| *c* (Å) | 30.8766(12) | 24.788(12) |
| $\alpha$/º | 90 | 90 |
| $\beta$/º | 100.1160 | 90 |
| $\gamma$/º | 90 | 90 |
| *V* (Å)$^3$ | 5784.5(4) | 3018(2) |
| Z | 8 | 4 |
| $D_{calcd}$ (mg/mm$^3$) | 1.559 | 1.413 |
| $\mu$(Mo Kα) (mm$^{-1}$) | 4.820 | 4.529 |
| Nº total reflections | 6641 | 6921 |
| $R_{int}$ | 0.0378 | 0.0485 |
| $R^a$, $R_w{}^b$ (I>2σ) | 0.0273, 0.0378 | 0.0430, 0.0590 |
| Goodnes-of-fit F$^2$ | 1.151 | 1.104 |

**Table 5.2** Crystallographic data and structure refinement for complexes **11F** and **12E**

| | **11F** | **12E** |
|---|---|---|
| Empirical Formula | $C_{20}H_{29}N_5I_3Ir$ | $C_{14}H_{20}I_3N_5O_2Rh$ |
| $M_w$ | 912.38 | 773.96 |
| Temperature (K) | 293(2) | 293(2) |
| Crystalline System | triclinic | orthorhombic |
| Space Group | P-1 | Pnma |
| *a* (Å) | 8.1564(4) | 7.3202(6) |
| *b* (Å) | 13.2101(6) | 11.6155(13) |
| *c* (Å) | 14.2977(7) | 27.281(2) |
| $\alpha$/º | 108.985 | 90.00 |
| $\beta$/º | 102.089 | 90.00 |
| $\gamma$/º | 98.667 | 90.00 |
| *V* (Å)$^3$ | 1383.96(11) | 2319.6(4) |
| Z | 2 | 4 |
| $D_{calcd}$ (mg/mm$^3$) | 2.189 | 2.216 |
| $\mu$(Mo K$\alpha$) (mm$^{-1}$) | 8.185 | 4.745 |
| Reflections collected | 17980 | 12087 |
| $R_{int}$ | 0.0321 | 0.0704 |
| $R^a$, $R_w^b$ (I>2$\sigma$) | 0.0322, 0.0689 | 0.0432, 0.0839 |
| Goodnes-of-fit F$^2$ | 1.041 | 1.212 |

**Table 5.3** Crystallographic data and structure refinement for complexes **14G** and **15I**

| | **14G** | **15I** |
|---|---|---|
| Empirical Formula | $C_{17}H_{22}I_3IrN_6$ | $C_{14}H_{17}I_3N_5Rh$ |
| $M_w$ | 883.31 | 738.94 |
| Temperature (K) | 220(2) | 199.95(10) |
| Crystalline System | triclinic | monoclinic |
| Space Group | P-1 | $P2_1/c$ |
| *a* (Å) | 10.1810(6) | 11.3673(4) |
| *b* (Å) | 11.0855(5) | 24.5851(7) |
| *c* (Å) | 12.6852(7) | 7.6286(3) |
| $\alpha$/º | 107.112(4) | 90.00 |
| $\beta$/º | 94.167(4) | 100.612(3) |
| $\gamma$/º | 112.461(5) | 90.00 |
| *V* (Å)$^3$ | 1236.42(11) | 2095.48(12) |
| Z | 2 | 4 |
| $D_{calcd}$ (mg/mm$^3$) | 2.373 | 2.342 |
| $\mu$(Mo Kα) (mm$^{-1}$) | 9.158 | 5.240 |
| Reflections collected | 27397 | 24019 |
| $R_{int}$ | 0.0658 | 0.0414 |
| $R^a$, $R_w{}^b$ (I>2σ) | 0.0462, 0.1021 | 0.0417, 0.0945 |
| Goodnes-of-fit $F^2$ | 1.030 | 1.057 |

**Table 5.4** Crystallographic data and structure refinement for complexes **18E** and **20E**

| | **18E** | **20E** |
|---|---|---|
| Empirical Formula | $C_{22}H_{30}Cl_4I_2N_3Rh$ | $C_{22}H_{28}F_6I_2N_4PRh$ |
| $M_w$ | 835.00 | 850.16 |
| Temperature (K) | 293(2) | 150.00(10) |
| Crystalline System | triclinic | monoclinic |
| Space Group | P-1 | $P2_1$ |
| *a* (Å) | 13.7969(5) | 14.1135(4) |
| *b* (Å) | 15.4932(5) | 8.5326(2) |
| *c* (Å) | 15.9750(5) | 23.1568(7) |
| $\alpha$/º | 104.678 | 90.00 |
| $\beta$/º | 94.849 | 90.479 |
| $\gamma$/º | 113.955 | 90.00 |
| *V* (Å)$^3$ | 2950.19(16) | 2788.55(13) |
| Z | 4 | 4 |
| $D_{calcd}$ (mg/mm$^3$) | 1.880 | 2.025 |
| $\mu$(Mo Kα) (mm$^{-1}$) | 3.050 | 2.943 |
| Reflections collected | 66040 | 33737 |
| $R_{int}$ | 0.0599 | 0.0322 |
| $R^a$, $R_w{}^b$ (I>2σ) | 0.0457, 0.0938 | 0.0262, 0.0484 |
| Goodnes-of-fit $F^2$ | 1.042 | 1.041 |

**Table 5.5** Crystallographic data and structure refinement for complexes **22G**

| | **22G** |
|---|---|
| Empirical Formula | $C_{21}H_{28}I_4N_3Rh$ |
| $M_w$ | 932.97 |
| Temperature (K) | 220.1(3) |
| Crystalline System | triclinic |
| Space Group | P-1 |
| *a* (Å) | 9.0134(4) |
| *b* (Å) | 9.2489(3) |
| *c* (Å) | 17.7845(6) |
| *α*/º | 76.233(3) |
| *β*/º | 75.331(3) |
| *γ*/º | 71.979(3) |
| *V* (Å)$^3$ | 1343.22(8) |
| Z | 2 |
| $D_{calcd}$ (mg/mm$^3$) | 2.307 |
| $\mu$(Mo Kα) (mm$^{-1}$) | 5.245 |
| Reflections collected | 30192 |
| $R_{int}$ | 0.0602 |
| $R^a$, $R_w{}^b$ (I>2σ) | 0.0390, 0.0887 |
| Goodnes-of-fit $F^2$ | 1.069 |

**Table 5.6** Crystallographic data and structure refinement for complexes **23I** and **24I**

| | **23I** | **24I** |
|---|---|---|
| Empirical Formula | $C_{125}H_{183}Cl_3I_8Ir_8N_{12}O_5$ | $C_{20}H_{26}I_2IrN_3$ |
| $M_w$ | 4592.98 | 754.44 |
| Temperature (K) | 200.00(10) | 200.00(10) |
| Crystalline System | triclinic | monoclinic |
| Space Group | P-1 | $P2_1/c$ |
| *a* (Å) | 8.6951(3) | 8.37605(14) |
| *b* (Å) | 19.7945(4) | 15.7756(3) |
| *c* (Å) | 22.8934(6) | 17.2828(3) |
| $\alpha$/º | 86.5179 | 90.00 |
| $\beta$/º | 81.711 | 97.0408(16) |
| $\gamma$/º | 80.528 | 90.00 |
| *V* (Å)$^3$ | 3843.24(18) | 2266.49(6) |
| Z | 1 | 4 |
| $D_{calcd}$ (mg/mm$^3$) | 1.984 | 2.211 |
| $\mu$(Mo Kα) (mm$^{-1}$) | 8.603 | 8.624 |
| Reflections collected | 72351 | 23406 |
| $R_{int}$ | 0.0427 | 0.0356 |
| $R^a$, $R_w{}^b$ (I>2σ) | 0.0298, 0.0752 | 0.0240, 0.0420 |
| Goodnes-of-fit $F^2$ | 1.050 | 1.060 |

**Table 5.7** Crystallographic data and structure refinement for complexes **$[KH_3](BF_4)_3$** and **27M**

| | **$[KH_3](BF_4)_3$** | **27M** |
|---|---|---|
| Empirical Formula | $C_{53}H_{72}B_3F_{12}N_6$ | $C_{72}H_{84}Ag_6N_{24}$ |
| $M_w$ | 1053.60 | 1932.85 |
| Temperature (K) | 200.00(14) | 200.15 |
| Crystalline System | hexagonal | orthorhombic |
| Space Group | $P6_3cm$ | Ccce |
| *a* (Å) | 15.7431(5) | 22.9670(10) |
| *b* (Å) | 15.7431(5) | 28.073(2) |
| *c* (Å) | 12.5624(5) | 16.2980(10) |
| *α*/º | 90.00 | 90 |
| *β*/º | 90.00 | 90 |
| *γ*/º | 120.00 | 90 |
| *V* (Å)$^3$ | 2696.41(16) | 10508.2(11) |
| Z | 2 | 4 |
| $D_{calcd}$ (mg/mm$^3$) | 1.298 | 1.222 |
| $\mu$(Mo Kα) (mm$^{-1}$) | 0.886 | 1.139 |
| Reflections collected | 16021 | 19719 |
| $R_{int}$ | 0.0284 | 0.0253 |
| $R^a$, $R_w{}^b$ (I>2σ) | 0.0696, 0.1947 | 0.0870, 0.2747 |
| Goodnes-of-fit $F^2$ | 1.026 | 1.049 |

## 5.5 REFERENCES


1. Herde, J. L.; Lambert, J. C.; Senoff, C. V., *Inorg. Synth.* **1974**, *14*, 18-20.
2. Ball, R. G.; Graham, W. A. G.; Heinekey, D. M.; Hoyano, J. K.; McMaster, A. D.; Mattson, B. M.; Michel, S. T., *Inorg. Chem.* **1990**, *29*, 2023-2025.
3. Giordano, G.; Crabtree, R. H., *Inorg. Synth.* **1990**, *28*, 88-90.
4. White, C. Y., A.; Maitlis, P.M., *Inorg. Synth.* **1992**, *29*, 228.
5. Abel, E. W.; Bennett, M. A.; Wilkinson, G., *Journal of the Chemical Society* **1959**, 3178-3182.
6. Uson, R.; Laguna, A.; Laguna, M.; Briggs, D. A.; Murray, H. H.; Fackler, J. P., *Inorg. Synth.* **1989**, *26*, 85-91.
7. Azua, A.; Sanz, S.; Peris, E., *Organometallics* **2010**, *29*, 3661-3664.
8. Diezbarra, E.; Delahoz, A.; Sanchezmigallon, A.; Tejeda, J., *Heterocycles* **1992**, *34*, 1365-1373.
9. Caballero, A.; Diez-Barra, E.; Jalon, F. A.; Merino, S.; Rodriguez, A. M.; Tejeda, J., *J. Organomet. Chem.* **2001**, *627*, 263-264.
10. Kuhn, K. M.; Grubbs, R. H., *Org. Lett.* **2008**, *10*, 2075-2077.
11. Kuck, D.; Schuster, A.; Krause, R. A.; Tellenbroker, J.; Exner, C. P.; Penk, M.; Bogge, H.; Muller, A., *Tetrahedron* **2001**, *57*, 3587-3613.
12. Arduengo, A. J.; Krafczyk, R.; Schmutzler, R.; Craig, H. A.; Goerlich, J. R.; Marshall, W. J.; Unverzagt, M., *Tetrahedron* **1999**, *55*, 14523-14534.
13. Henrie, R. N.; Yeager, W. H., *Heterocycles* **1993**, *35*, 415-426.
14. Er, J. A. V.; Tennyson, A. G.; Kamplain, J. W.; Lynch, V. M.; Bielawski, C. W., *Eur. J. Inorg. Chem.* **2009**, 1729-1738.
15. Papini, G.; Pellei, M.; Lobbia, G. G.; Burini, A.; Santini, C., *Dalton Trans.* **2009**, 6985-6990.
16. Gerhardt, C., *Annalen* **1858**, *108*, 219.
17. Fujita, K.; Asai, C.; Yamaguchi, T.; Hanasaka, F.; Yamaguchi, R., *Org. Lett.* **2005**, *7*, 4017-4019.
18. Martinez, R.; Ramon, D. J.; Yus, M., *Tetrahedron* **2006**, *62*, 8982-8987.

19. Yamaguchi, R.; Kawagoe, S.; Asai, C.; Fujita, K. I., *Org. Lett.* **2008**, *10*, 181-184.
20. Clark, R. C.; Reid, J. S., *Acta Crystallographica Section A* **1995**, *51*, 887-897.
21. Dolomanov, O. V.; Bourhis, L. J.; Gildea, R. J.; Howard, J. A. K.; Puschmann, H., *J. Appl. Crystallogr.* **2009**, *42*, 339-341.
22. Sheldrick, G. M., *Acta Crystallographica Section A* **2008**, *64*, 112-122.

# CHAPTER 6

# CATALITZADORS HOMOGENIS PER A PROCESSOS VERDS I COMPLEXOS BASATS EN LLIGANDS NHC NO CONVENCIONALS

En aplicació de la normativa d'estudis de doctorat sobre l'elaboració de Tesis doctorals segons el programa RD 99/2011, per a qual s'estableix que: la tesi doctoral escrita en una llengua diferent del valencià o el castellà, en el moment de ser dipositada, ha de contenir un apartat suficientment ampli en una d'aquestes dues llengües, i ha de formar part de l'enquadernació de la tesi; el següent capítol conté un resum en valencià del treball recollit en la present tesi doctoral.

## 6.1 INTRODUCCIÓ

Des del 2001, el grup de Química Organometàl·lica i Catàlisis Homogènia de la Universitat Jaume I, QOMCAT, dirigit pel professor Eduardo Peris, ha centrat els seus esforços en la investigació i desenvolupament de nous lligands de tipus carbè N-heterocíclics (NHCs) per a la preparació de catalitzadors metàl·lics millorats. La versatilitat dels lligands de tipus NHC, a més de la fàcil preparació dels seus precursors (normalment sals d'azoli), han permès dissenyar una gran varietat de topologies i formes de coordinació. Dins d'aquest context, aquest grup va iniciar algunes línies d'investigació relacionades amb la 'Química Verda'. Així, nous complexos que contenien lligands NHC van ser sintetitzats per a la reducció de $CO_2$ utilitzant *i*PrOH en lloc de $H_2$, fent el procés més segur i respectuós amb el medi ambient. A més, la funcionalització de lligands NHC amb grups polars va permetre la síntesi de catalitzadors solubles en dissolvents sostenibles (aigua i glicerol),[1-6] i també l'ús d'altres eines d'activació de calefacció d'energia alternativa (MW or US).[4-5] Més recentment, el grup va reorientar els seus esforços en el disseny d'estructures rígides basades en lligands poli-NHC per a la preparació de catalitzadors homo- i heterometàl·lics.[7-10] Aquest tipus de policarbens poden estar units mitjançant sistemes rígids π-conjugats i poden ser capaços de comunicar electrònicament les unitats carbèniques. Aquesta característica dels complexos poli-NHC pot tindre molt d'interès per a la fabricació de dispositius electrònics moleculars a més de les importants millores catalítiques que pot implementar. A continuació s'inclou una breu ressenya sobre els avanços fets durant aquesta tesi doctoral: Disseny de catalitzadors per al desenvolupament de processos verds i síntesi de nous complexos basats en lligands imidazolilidè-piridilidè i poli-NHC.

Els processos verds que decidírem estudiar són la reacció Suzuki-Miyaura d'acoblament C-C en aigua i l'alquilació d'amoníac amb alcohols primaris que transcorre a través d'un mecanisme de "préstec d'hidrogen", conegut més habitualment pel terme anglès *Borrowing-Hydrogen*.

Les reaccions d'acoblament C-C catalitzades per metalls de transició són un dels mètodes més utilitzats per a la formació d'enllaços C-C, sent el pal·ladi el metall més utilitzat per a desenvolupar aquest tipus de reaccions. Entre aquests processos, la reacció d'acoblament Suzuki-Miyaura, és a dir, l'acoblament entre un àcid arilborònic i un halur d'aril,[11] és el protocol més utilitzat per a sintetitzar bifenils atesa la bona tolerància davant diferents grups funcionals. Per aquesta raò, trobar una alternativa més respectuosa amb el medi ambient per a dur a terme aquesta reacció és un repte per als investigadors en el camp de la catàlisi homogènia.

Els processos catalítics que s'engloben sota el terme "B*orrowing-Hydrogen*" constitueixen un ampli ventall de reaccions en les que el nexe comú és determinat per la intermediació d'un catalitzador que serveix com a transportador d'hidrogen entre un parell de substrats.[12-15] En una reacció típica de *Borrowing-Hydrogen* es produeix l'oxidació d'un substrat, normalment un alcohol (o una amina), per un catalitzador metàl·lic que 'agafa com a préstec' dos àtoms d'hidrogen. Depenent si l'alcohol és primari o secundari, es generarà un aldehid o una cetona, respectivament. Aquests compostos de carbonil poden sofrir una àmplia gama de transformacions ja que poden reaccionar *in situ* per a donar imines, alquens i compostos de carbonil funcionalitzats. El catalitzador metàl·lic, que havia agafat com a préstec l'hidrogen, el "torna" al nou compost, produint la seua reducció. Aquests processos catalítics compleixen el principi d'economia atòmica ja que, normalment, tots els àtoms dels substrats apareixen en els productes o, com a màxim, l'únic subproducte obtingut és $H_2O$ o $NH_3$, per la qual cosa es consideren processos que contribueixen a la química verda.

Els lligands de tipus imidazolilidè-piridilidè (*C,C'*-imz-pyr) se formen com a conseqüència de la unió d'una unitat d'imidazolilidè i una unitat piridilidè. El primers complexos que presentaven aquest tipus de lligands (*C,C'*-imz-pyr) foren descrits per Colbran,[16] **6.1** en Esquema 6.1.

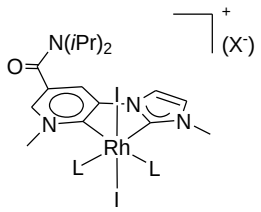


**6.1**

**Esquema 6.1**

En els últims anys els lligands de tipus poli-NHC han donant lloc a una gran varietat de complexos polimetàl·lics, amb diferents topologies que condueixen a l'obtenció de propietats catalítiques inusuals[17-20] En aquest sentit, el nostre grup d'investigació ha descrit recentment lligands di- i tri-NHC amb sistemes π-electrònics conjuminats per a la preparació de compostos polimetàl·lics millorats.[8, 21] En particular, el lligand tri-NHC **6.2** (Esquema 6.2) va donar lloc a compostos que augmentaven la seua capacitat catalítica en comparació amb altres compostos mono metàl·lics o tri metàl·lics amb les mateixes característiques esteroelectròniques

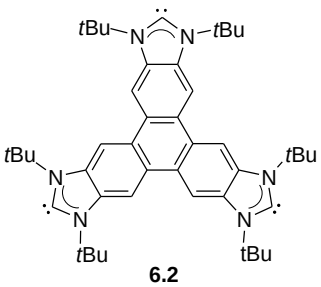


**6.2**

**Esquema 6.2**

Hahn i col·laboradors van ser els primers a descriure una estructura supramolecular metàl·lica tridimensional que contenia exclusivament enllaços metall-NHC (**6.3**, Esquema 6.3).[22] Aquesta estructura es va sintetitzar per reacció directa de dos lligands hexa-NHC amb $Ag_2O$. En principi, aquest tipus d'estructures poden ser utilitzades com a caixes macromoleculars encercladores de molècules menudes neutres o iòniques i, per tant, funcionar com a detectors químics.[23-28] En concret en el compost **6.3** es mostra la presència d'un ió bromur a l'interior de la caixa.

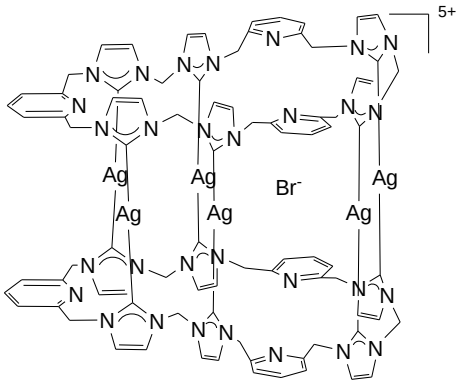


**6.3**

**Esquema 6.3**

## 6.2 OBJECTIUS

L'objectiu general d'aquesta tesi doctoral és la síntesi de catalitzadors homogenis amb propietats esteroelectròniques millorades. En aquest sentit, el treball es centra en la preparació i caracterització de nous complexos metàl·lics amb diferents lligands de tipus carbè N-heterocíclic (NHC) o lligands anàlegs, l'estudi dels seus patrons de reactivitat i l'exploració de les seues propietats catalítiques. Els objectius concrets que se'n deriven son els següents:

- Síntesi de complexos de pal·ladi i iridi per al desenvolupament de processos verds. Principalment, s'intentaran realitzar reaccions catalítiques amb les condicions més respectuoses amb el medi ambient, utilitzant dissolvents no tòxics, amb la màxima economia atòmica i sense malbaratament d'energia.
- Estudi sistemàtic de la reactivat de lligands imidazolilidè-piridilidè mitjançant la seua coordinació a precursors de rodi i iridi.
- Disseny, síntesi i coordinació de lligands poli-NHC per a la preparació de complexos polimetàl·lics amb estructures inusuals i altament simètriques. Estudi de les seues propietats electròniques.

# 6.3 DISCUSSIÓ DE RESULTATS

## 6.3.1 Síntesi de compostos de Pd(II) hidrofílics amb lligands NHC. Aplicacions catalítiques

### 6.3.1.1 Síntesi de compostos de Pd(II) hidrofílics amb lligands NHC

L'Esquema 6.4, mostra els tres precursors dels lligands NHC, funcionalitzats amb cadenes sulfonatades, que han sigut utilitzats. El compost **AH**,[3] ha sigut prèviament descrit en la bibliografia, mentre que, els compostos **$BH_2$** i **$CH_2$** s'han sintetitzat i caracteritzat per primera vegada al llarg del treball d'investigació que es presenta.

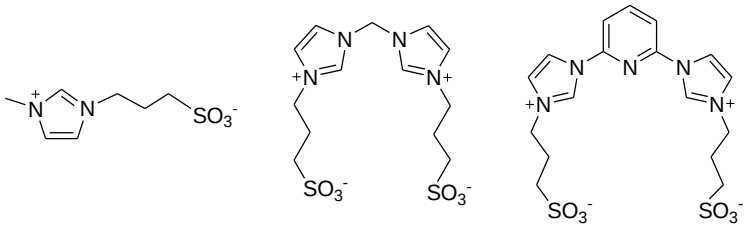


**AH** **$BH_2$** **$CH_2$**

**Esquema 6.4**

A partir d'aquests lligands s'han obtingut complexos de Pd(II) en els quals els lligands s'uneixen al metall de forma mono coordinada, quelat i pinça. Hem tractat que l'elecció d'aquest tipus de modes de coordinació donen lloc a un ampli conjunt de topologies de complexos de pal·ladi NHC que ja han demostrat propietats catalítiques eficients en dissolvents orgànics.[29-30] L'estratègia de metal·lació utilitzada ha sigut l'ús d'una base dèbil incorporada en el precursor de pal·ladi per a desprotonar els compostos d'imidazolilidè segons es mostra en l'Esquema 6.5.

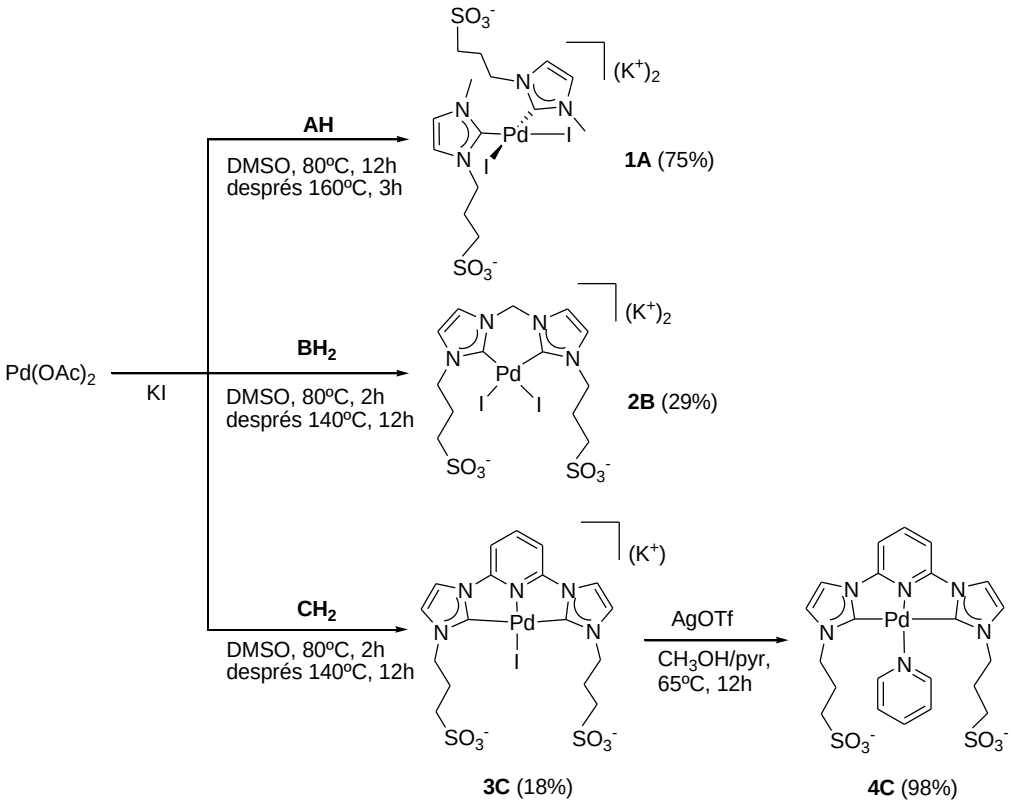


**Esquema 6.5**

Els compostos d'imidazoli **$BH_2$** i **$CH_2$** junt amb els catalitzadors **1A-4C** descrits en aquesta secció, han sigut sintetitzats per primera vegada al llarg del treball d'investigació que es presenta i han sigut caracteritzats per espectroscòpia d'RMN, espectrometria de masses i per anàlisi elemental. El complex **4C** va ser sintetitzat, ja que la introducció d'un lligand piridina ha demostrat millorar l'activitat catalítica dels compostos amb els quals es coordina per efecte "PEPPSI".[31-33]

### 6.3.1.2 Aplicacions catalítiques

Amb la finalitat d'avaluar les propietats catalítiques dels complexos hidrofílics preparats en l'apartat anterior, decidírem utilitzar-los en la reacció d'acoblament C-C de Suzuki-Miyaura en aigua, on un àcid arilborònic reacciona amb un halur d'aril per a donar un compost biarilat. Així, es va fer reaccionar l'àcid fenilborònic amb vuit halurs d'aril diferents (4-brom, i 4-cloracetofenona; 4-brom, i 4-clorbenzè; 4-brom, i

4-clortoluè; 4-brom, i 4-cloranisol), tal com es mostra en l'Esquema 6.6. Les reaccions es van fer en una mescla d'aigua/*i*PrOH (1:1) a 110ºC, amb 1 mol% de catalitzador i en presència de $K_2CO_3$.

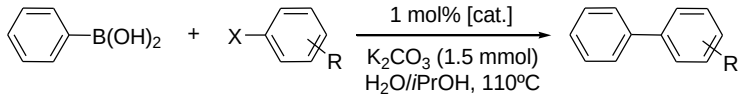


X=Br or Cl R=$COCH_3$
X=Br or Cl R=$OCH_3$
X=Br or Cl R=$CH_3$
X=Br or Cl R=H

**Esquema 6.6**

Els resultats obtinguts ens van permetre concloure que els compostos **1A** i **3C** són els més actius, ja que faciliten rendiments molt elevats en temps de reacció curts (4h, per als bromur d'aril i 12h, per als clorur d'aril). Però és el catalitzador **1A** amb què obtenim els resultats més espectaculars quan utilitzem 4-bromacetofenona i 4-cloracetofenona, ja que obtenim rendiments superiors al 99% en 4h i 12h, respectivament.

Els resultats catalítics obtinguts suggereixen que la presència del lligand piridina en el compost **4C** no augmenta l'activitat catalítica d'aquest per efecte "PEPPSI" en comparació al catalitzador **3C**.

## 6.3.2 Síntesi de compostos de Ir(III) amb lligands formamidina. Aplicacions catalítiques

### 6.3.2.1 Síntesi de compostos de Ir(III) amb lligands formamidina

El lligand 1,3-bis(2,4,6-trimetilfenil)formamidina, **D**, va ser sintetitzat seguint el procediment descrit en la literatura[34] i a partir d'aquest vam obtenir dos compostos diferents de 'IrCp*' depenent de la forma de coordinar-se d'aquest. Si el lligand **D** adopta coordinació monodentada s'obté el compost **5D**, però si la coordinació es en forma quelat obtenim el compost **6D** (Esquema 6.7).

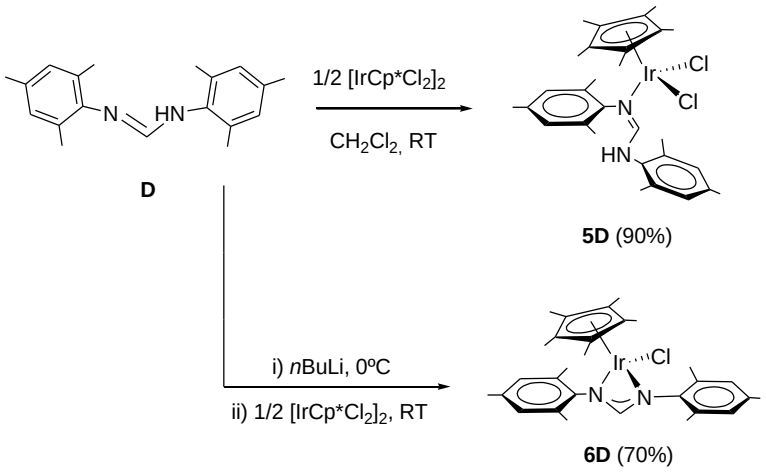


**Esquema 6.7**

Aquests dos nous compostos, **5D** i **6D**, han sigut caracteritzats per espectroscòpia d'RMN, espectrometria de masses i per anàlisi elemental. Les estructures moleculars dels dos compostos han sigut confirmades mitjançant Difracció de Raigs X (DRX) sobre monocristall.

### 6.3.2.2 Aplicacions catalítiques

En aquest cas, decidírem comprovar l'activitat catalítica dels compostos **5D** i **6D** en dues reaccions governades per processos de *Borrowing-Hydrogen*. En primer lloc començàrem amb la reacció de *β*-alquilació d'alcohols secundaris amb alcohols primaris per a després estendre l'estudi de l'activitat catalítica dels dos complexos en una reacció més interessant, com és l'alquilació d'amoníac amb alcohols primaris.

*a) β-Alquilació d'alcohols secundaris amb alcohols primaris*

Aquesta reacció es va dur a terme en condicions de màxima economia atòmica, és a dir, intentant que tots els materials utilitzats com a reactius s'incorporen als productes. Així, tal com es mostra en l'Esquema 6.8, es va fer reaccionar una mescla equimolecular de l'alcohol primari, alcohol secundari i una base (KOH), en presència de 0.1-1 mol% de catalitzador en toluè a 100ºC.

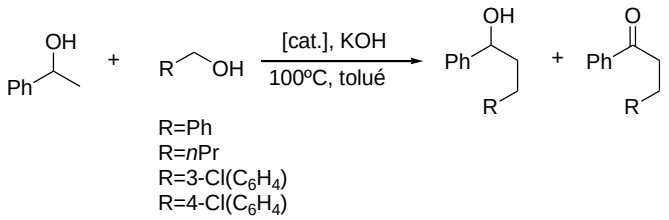


**Esquema 6.8**

La reacció pot donar lloc a dos productes, l'alcohol alquilat i/o la cetona alquilada. La reacció es va dur a terme utilitzant 2-feniletanol com a alcohol secundari i quatre alcohols primaris diferents (bencilalcohol, butanol, 3-clorbencilalcohol i 4-clorbencilalcohol), utilitzant els catalitzadors **5D** i **6D**. Els resultats obtinguts van permetre concloure que **5D** és molt més eficient que **6D**, tant en termes de conversió cap als productes finals com en selectivitat cap a l'alcohol *β*-alquilat. El catalitzador **5D** també és molt actiu fins i tot a concentracions de 0.1 mol%, sobretot quan utilitzem bencilalcohol i 4-clorbencilalcohol.

Els resultats catalítics obtinguts suggereixen que el grup NH en el lligand formamidina del complex **5D** aporta un 'efecte NH'[35-36] cooperatiu fent que aquest compost siga més actiu que **6D**.

*b) Alquilació d'amoníac amb alcohols primaris*

En primer lloc vam comparar l'activitat catalítica de $[IrCp^*Cl_2]_2$, el catalitzador d'Shvo i els nous compostos **5D** i **6D**. Com es mostra en l'Esquema 6.9, per a dur a terme la reacció es va fer reaccionar diferents sals d'amoni amb bencilalcohol a 110 o 130ºC, utilitzat diverses carregues de catalitzador, en presència d'un 3 mol% de $NaHCO_3$ i amb proporcions de bencilalcohol/sal d'amoni de 3:1 o 3.6:1.

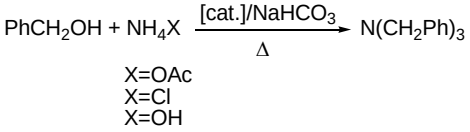


**Esquema 6.9**

El complex **5D** i el catalitzador d'Shvo mostraren excel·lents resultats catalítics en l'alquilació de la sal d'amoni $NH_4OAc$ per a obtindre trifenilamina, en comparació amb els resultats obtinguts amb $[IrCp^*Cl_2]_2$ i el complex **6D** sota les mateixes

condicions de reacció. A més, **5D** va ser moderadament actiu en l'alquilació del $NH_4OH$.

Tenint en compte les dades anteriors, decidírem ampliar l'abast del catalitzador d'Shvo i el complex **5D,** estudiant la seva activitat catalítica davant una varietat d'alcohols primaris. Tal i com es mostra en l'Esquema 6.10, l'alquilació de sals d'amoni amb diferents alcohols primaris es va dur a terme a 130 o140ºC, utilitzant carregues de catalitzador d'1, 3 i 5 mol%, en presència de KOH o sense base i amb proporcions d'alcohol primari/sal d'amoni de 3.6:1 o 6:1.

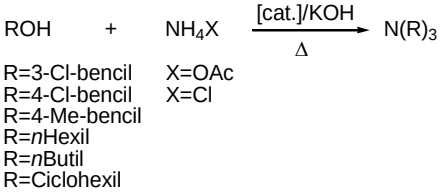


**Esquema 6.10**

En aquest cas la reacció pot donar lloc a diferents amines, segons l'alcohol primari utilitzat (4-clorbencilalcohol, 3-clorbencilalcohol, 4-metilbencilalcohol, 1-hexanol, 1-butanol i 1-ciclohexanol).

Els resultats obtinguts ens van permetre concloure que amb el catalitzador **5D** s'obtenen resultats catalítics extraordinaris, sobretot quan utilitzem bencilalcohol, però, la seua eficiència baixa quan utilitzem alcohols alquílics. La activitat del catalitzador d'Shvo és en la majoria del casos més elevada, mostrant així la gran aplicabilitat d'aquest catalitzador exepcional.

A la vista dels resultats obtinguts en les dues reaccions governades per processos de *Borrowing-Hydrogen*, i tal com havíem comentat anteriorment, creiem que la presència del grup NH en el lligand formamidina del complex **5D** està incrementant l'activitat catalítica d'aquest davant el complex **6D** i $[IrCp^*Cl_2]_2$. Aquet 'efecte NH' pot estar facilitant la deshidrogenació de l'alcohol primari per a passar a aldehid en el primer pas del cicle catalític,[37] d'una manera similar a les observacions descrites per Noyori en les reaccions d'hidrogenació de cetones.[35-36]

### 6.3.3 Síntesi de compostos de Rh(III) i Ir(III) basats en lligands imidazolilidè-piridilidè i estudi de la seua reactivitat no convencional

Durant aquesta tesi doctoral també ens vam interessar en la síntesi de compostos de rodi i iridi amb lligands imidazolilidè-piridilidè (*C,C'*-imz-pyr) coordinats en forma quelat. A més d'obtenir els compostos di-NHC esperats, també es varen sintetitzar una sèrie de compostos amb els lligands reordenats en formes poc convencionals. L'estudi d'aquests nous compostos amb lligands *C,C'*-imz-pyr ofereix una bona oportunitat per a comparar les diferències estructurals i de reactivitat d'aquests complexos depenent del tipus de la coordinació del carbè (*normal*, *abnormal* o *remota*), tant del imidazolilidè com del piridilidè.

L'Esquema 6.11 mostra les diferents sals precursores dels lligands *C,C'*-imz-pyr que han sigut utilitzades. Totes aquestes sals s'han sintetitzat i caracteritzat, per primera vegada, al llarg del treball d'investigació que es presenta.

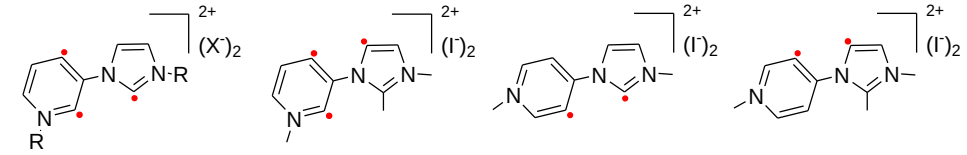

R=Me, X=I; **[EH$_2$]I$_2$** **[GH$_2$]I$_2$** **[IH$_2$]I$_2$** **[JH$_2$]I$_2$**

R=Me, X=PF$_6$; **[EH$_2$](PF$_6$)$_2$**

R=*n*Bu, X=I; **[FH$_2$]I$_2$**

**Esquema 6.11** Sals d'imidazoli-piridini utilitzades en aquest treball. Els punts rojos indiquen els llocs de coordinació esperats.

#### 6.3.3.1 Síntesi i caracterització dels complexos [MI$_2$(*C,C'*-imz-pyr)(CH$_3$CN)$_2$]$^+$ (M = Rh, Ir)

En primer lloc, vam obtenir una sèrie de complexos de tipus [MI$_2$(*C,C'*-imz-pyr)(CH$_3$CN)$_2$]$^+$ (M = Rh, Ir) (Esquema 6.13). L'estratègia sintètica per a sintetitzar estos compostos va consistir a fer reaccionar la sal d'imidazoli-piridini corresponent, **[EH$_2$]I$_2$-[JH$_2$]I$_2$**, amb el precursor metàl·lic [MCl(diolefina)]$_2$ (M = Rh, Ir; diolefina = COD, NBD) i KI en CH$_3$CN a 65ºC durant 12h. Com a exemple la síntesi del compost **7E** es mostra en l'Esquema 6.12.

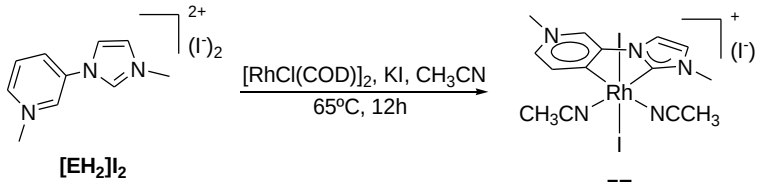


**[EH$_2$]I$_2$** **7E**

**Esquema 6.12**

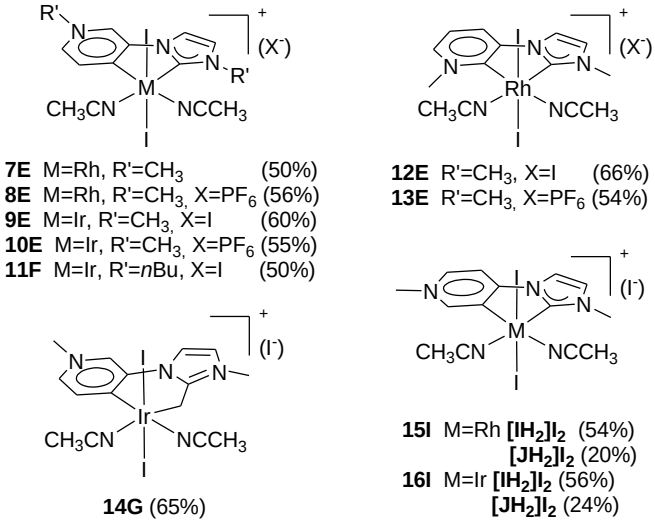


**7E** M=Rh, R'=$CH_3$ (50%)
**8E** M=Rh, R'=$CH_3$, X=$PF_6$ (56%)
**9E** M=Ir, R'=$CH_3$, X=I (60%)
**10E** M=Ir, R'=$CH_3$, X=$PF_6$ (55%)
**11F** M=Ir, R'=*n*Bu, X=I (50%)

**12E** R'=$CH_3$, X=I (66%)
**13E** R'=$CH_3$, X=$PF_6$ (54%)

**14G** (65%)

**15I** M=Rh **[IH$_2$]I$_2$** (54%)
**[JH$_2$]I$_2$** (20%)
**16I** M=Ir **[IH$_2$]I$_2$** (56%)
**[JH$_2$]I$_2$** (24%)

**Esquema 6.13**

Les noves sals d'imidazoli-piridini, **[EH$_2$]I$_2$-[JH$_2$]I$_2$**, i els nous complexos metàl·lics de Rh(III) i Ir(III), **7E-16I**, descrits en aquesta secció han sigut caracteritzats per espectroscòpia d'RMN, espectrometria de masses i per anàlisi elemental. Les estructures moleculars dels complexos **11F**, **14G** i **15I** han sigut confirmades mitjançant Difracció de Raigs-X sobre monocristall.

L'avaluació de l'espectroscòpia de RMN d'aquests complexos revela algunes característiques que interessa mencionar. Pel que fa a l'espectroscòpia $^{13}C$ RMN d'aquests compostos, es va observar que les freqüències degudes als carbens dels piridilidens decreixen en l'ordre: *remot*, *normal*, *abnormal*, per al rodi, i *remot*, *abnormal* per a l'iridi.

Rodi: *remot* ($\delta_c$ = 183.9) > *normal* ($\delta_c$ = 175.7) > *abnormal* ($\delta_c$ = 169.3)

Iridi: *remot* ($\delta_c$ = 164.7) > *abnormal* ($\delta_c$ = 160.8)

L'anàlisi de les longituds d'enllaç en les estructures moleculars del compostos **11F** i **15I** (Esquema 6.14) en han permès constatar que els piridilidens aporten una influència *trans* major que els imidazolilidens, com ja han suggerit altres grups d'investigació.[38-39]

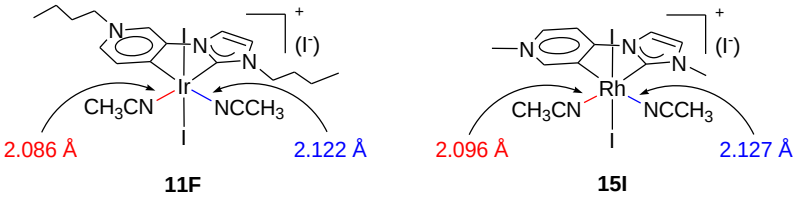


**Esquema 6.14**

### 6.3.3.2 Síntesi i caracterització dels complexos [MCp*I(*C,C'*-imz-pyr)]$^+$ (M = Rh, Ir)

Decidírem estendre la coordinació dels lligands derivats de les sals, **[EH$_2$]I$_2$**, **[GH$_2$]I$_2$** i **[IH$_2$]I$_2$**, a altres precursors metàl·lics com són [MCp*Cl$_2$]$_2$ (M = Rh, Ir) i una sèrie de compostos [MCp*I(C,C'-imz-pyr)]$^+$ (M = Rh, Ir) foren sintetitzats (Esquema 6.16). L'estratègia sintètica per a sintetitzar estos compostos és similar a la utilitzada anteriorment, però en aquest es va afegir base i es va calfar a 90ºC durant 12h. Com a exemple la síntesi del compost **17E** es mostra en l'Esquema 6.15.

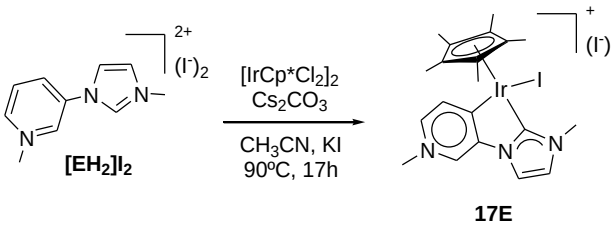


**Esquema 6.15**

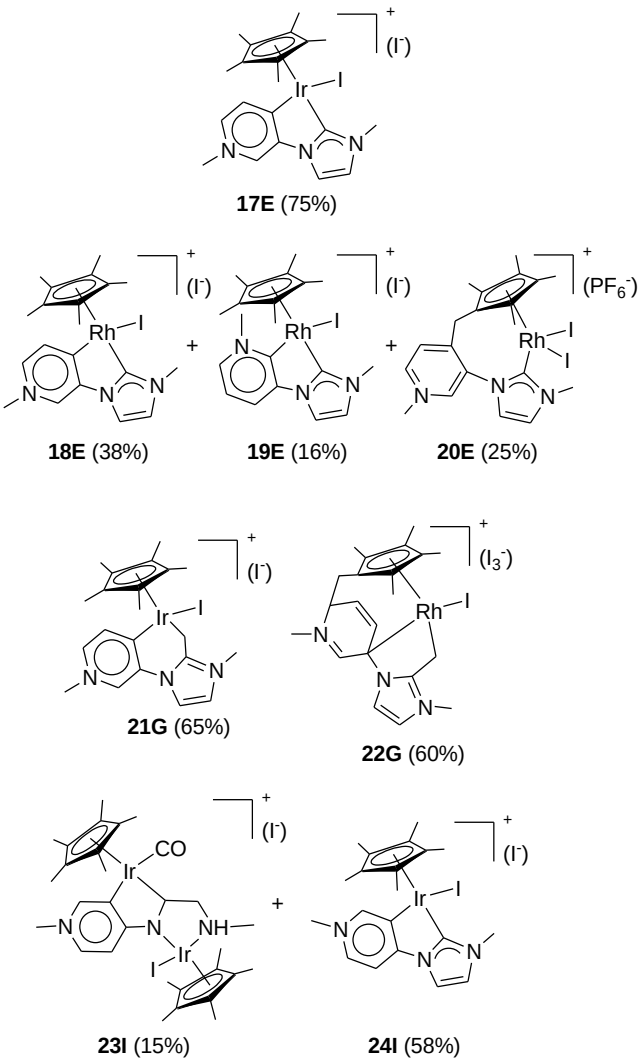
(I-)
Ir
I
N
N
N
17E (75%)
(I-)
Rh
I
18E (38%)
(I-)
19E (16%)
(PF6-)
20E (25%)
(I-)
21G (65%)
(I3-)
22G (60%)
(I-)
CO
NH
23I (15%)
24I (58%)

**Esquema 6.16**

Els nous complexos metàl·lics de Rh(III) i Ir(III), **17E-24I**, descrits en aquesta secció han sigut caracteritzats per espectroscòpia d'RMN, espectrometria de masses i per anàlisi elemental. Les estructures moleculars dels complexos **18E**, **19E**, **20E**, **22G** i **23I** han sigut confirmades mitjançant Difracció de Raigs-X sobre monocristall.

Els compostos **20E**, **22G** i **23I** presenten reactivitats molt inusuals. En el cas de **20E**, l'imidazolilidè esta coordinat al centre metàl·lic mentre que el piridilidè esta acoblat a l'anell de Cp*, així s'obté un anell Cp* funcionalitzat amb un imidazolilidè penjant. Pel que fa al compost **22G**, a més de l'activació C-H esperada del $CH_3$ del C2 de l'imidazoli un acoblament reductiu entre el Cp* i l'anell de piridini te lloc. Tant en el cas del complex **20E** com per a **22G**, creiem que aquests dos compostos se generen *via* la formació d'un intermedi de tetrametilfulvè de rodi. Tal com s'ha descrit per a compostos amb reactivitats similars.[40-45]

El compost **23I** és un dímer d'iridi en el qual l'obertura de l'anell d'imidazoli ha tingut lloc com a conseqüència de la hidròlisi de l'imidazolilidè. La hidròlisi de carbens no és un fet tant estrany i ha sigut descrit en més ocasions.[46] En el nostre cas, a banda de l'obertura de l'anell d'imidazolilidè, es produeixen altres reorganitzacions que tenen a veure amb la descarboxilació de l'aldehid per a generar el lligand carbonil i el lligand imino.

### 6.3.4 Síntesi de compostos de Rh(I) Ag(I) i Au(I) basats en lligands poli-NHC

Durant aquesta tesi doctoral, també hem centrat els nostres esforços en sintetitzar compostos que contenen lligands poli-NHC. En primer lloc, varem sintetitzar i coordinar un lligand tri-NHC amb una estructura central basada en un tribenzotriquinacè (TBTQ) i amb simetria $C_{3v}$ a Rh(I). La segona família de compostos es va obtenir a partir de dues sals d'hexa-imidazoli, els lligands derivats d'elles es varen coordinar a Ag(I) obtenint complexos amb sis àtoms de plata en forma cilíndrica. Els compostos d'or anàlegs també es varen obtenir mitjançant transmetal·lació.

### 6.3.4.1 Síntesi i caracterització del complex de Rh(I) amb el lligand tri-NHC-TBTQ

L'estratègia sintètica per a preparar compostos amb lligands poli-NHC comença amb l'aminació múltiple de Buchwald-Hartwig de molècules poliaromàtiques amb bromurs adjacents. Aquesta metodologia ha sigut utilitzada per Bielawski i col·laboradors i nosaltres aplicàrem aquesta metodologia a hexabromtribenzotriquinacè **6.5**[47] (Esquema 6.17). D'aquesta manera, tal com es mostra en l'Esquema 6.17, el compost **6.5** reacciona amb *tert*-butilamina ($t$BuNH$_2$) en presència de [Pd(OAc)$_2$], IPr·HCl i NaO$t$Bu en toluè a 115ºC, per a donar hexaaminotribenzotriquinacè, **hexaNH$_2$-TBTQ**, que posteriorment es ciclat amb trietilortoformat (HC(OEt)$_3$) en presència de HBF$_4$ a 80ºC, obtenint-se la sal **[KH$_3$](BF$_4$)$_3$**. Aquesta sal es desprotonada amb KHMD en THF a 0ºC, i amb la posterior addició de [RhCl(COD)]$_2$ a temperatura ambient s'obté el complex **25K** que es purificat mitjançant cromatografia de columna.

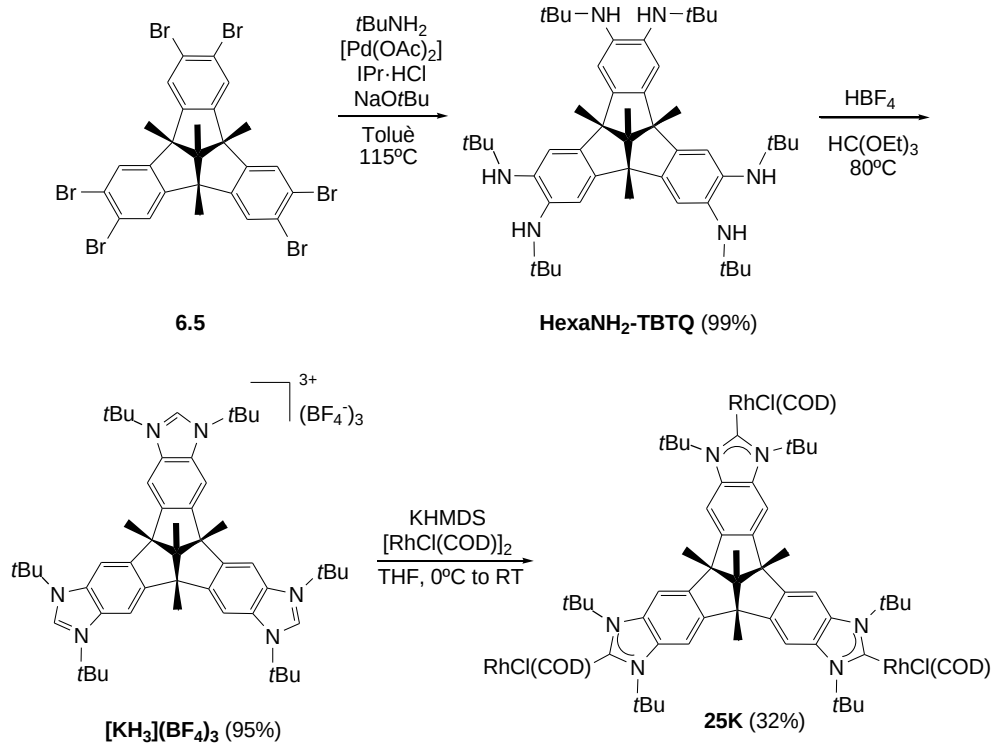


**Esquema 6.17**

Els nous compostos, **hexa$NH_2$-TBTQ**, **$[KH_3](BF_4)_3$** i **25K**, descrits en aquesta secció han sigut caracteritzats per espectroscòpia d'RMN i espectrometria de masses. L'estructura molecular de **$[KH_3](BF_4)_3$** ha sigut confirmada mitjançant Difracció de Raigs-X sobre monocristall.

### 6.3.4.2 Síntesi i caracterització de complexos de Ag(I) i Au(I) amb lligands hexa-NHC

Amb la finalitat d'augmentar el nombre d'estructures supramoleculars generades a partir de lligands poli-NHC, pensàrem que les sals 1,2,3,4,5,6-hexa(N-alquil imidazoli)benzè **$[LH_6](OTf)_6$** i **$[MH_6](BF_4)_6$** (alquil = Me i Et, respectivament) (Esquema 6.18), podrien ser bones precursores.

Aquestes sals s'obtenen a partir de l'alquilació de hexa(imidazol-1-il)benzè amb metil trifluorometasulfonat per a donar **$[LH_6](OTf)_6$**, o amb trietiloxoni tetrafluoroborat per a donar **$[MH_6](BF_4)_6$** (Esquema 6.18). La reacció d'aquestes dues sals amb $Ag_2O$ en $CH_3OH$ a 50ºC dona lloc als corresponents complexos cilíndrics, **26L** i **27M**, que contenen sis centres de Ag(I). Els compostos anàlegs d'or, **28L** i **29M**, s'obtenen mitjançant la reacció de **26L** i **27M** en $CH_3OH$ a 50ºC i en presència de $AuCl(SMe_2)$ (Esquema 6.18).

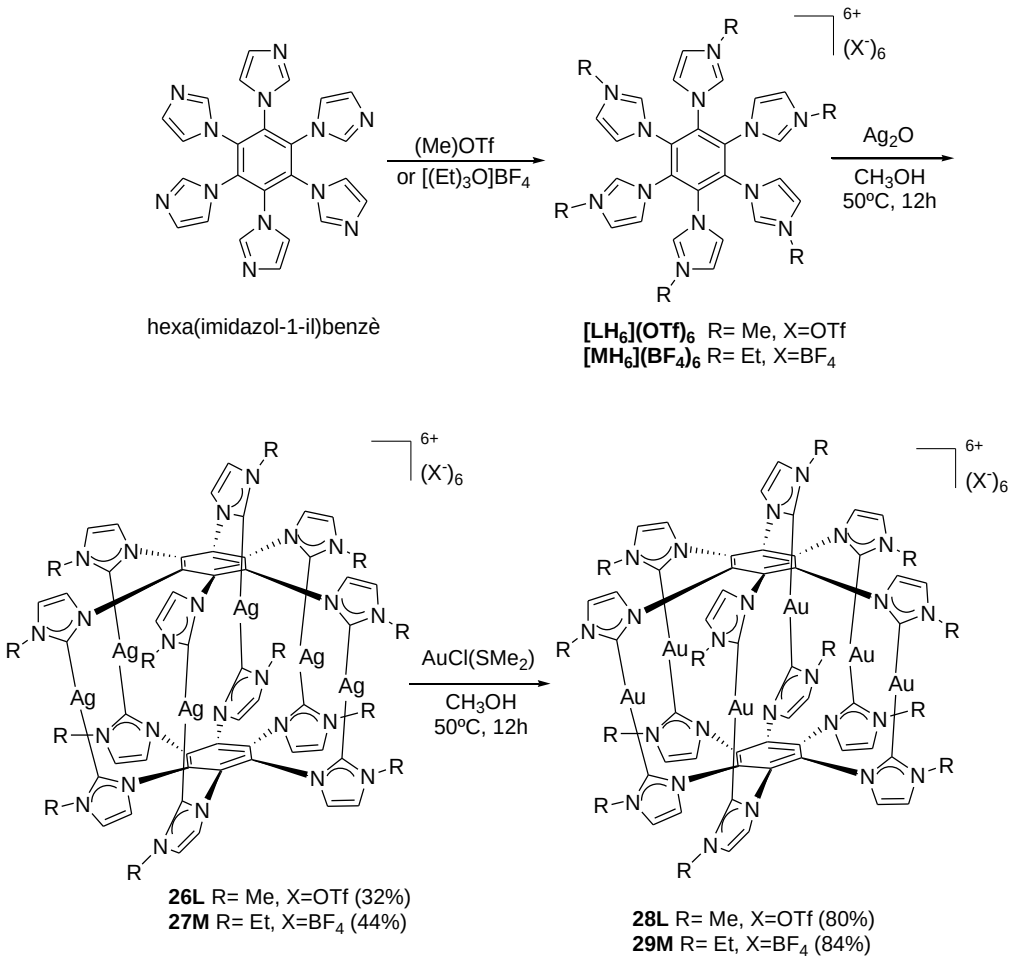


hexa(imidazol-1-il)benzè

**[LH$_6$](OTf)$_6$** R= Me, X=OTf
**[MH$_6$](BF$_4$)$_6$** R= Et, X=BF$_4$

**26L** R= Me, X=OTf (32%)
**27M** R= Et, X=BF$_4$ (44%)

**28L** R= Me, X=OTf (80%)
**29M** R= Et, X=BF$_4$ (84%)

**Esquema 6.18**

Les noves sals, **[LH$_6$](OTf)$_6$** i **[MH$_6$](BF$_4$)$_6$** i els nous complexos **26L**, **27M**, **28L** i **29M**, descrits en aquesta secció han sigut caracteritzats per espectroscòpia d'RMN i espectrometria de masses. L'estructura molecular de **28M** ha sigut confirmada mitjançant Difracció de Raigs-X sobre monocristall.

## 6.4 CONCLUSIONS

En aquesta tesi doctoral s'han obtingut una sèrie de complexos de pal·ladi amb lligands NHC hidrofílics i complexos d'iridi amb el lligand formamidina. Aquests complexos han sigut avaluats en processos verds com són la reacció Suzuki-Miyaura d'acoblament C-C en aigua i les reaccions governades per processos de *Borrowing-Hydrogen*: *β*-alquilació d'alcohols secundaris amb alcohols primaris i alquilació d'amoníac amb alcohols primaris.

El compost **3C** ha sigut el més actiu en la reacció Suzuki-Miyaura d'acoblament C-C en aigua i el compost **5D**, junt amb el catalitzador d'Shvo, han presentat les millors activitats en les reaccions governades per processos de *Borrowing-Hydrogen*.

Durant aquesta tesi doctoral, també s'han sintetitzat compostos de Rh(III) i Ir(III) amb lligands imidazolilidè-piridilidè que han presentat reactivitats molt inusuals. La comparació entre els diferents compostos obtinguts ens ha permès determinar que els piridilidens ocasionen un major efecte *trans* que els imidazolilidens.

Finalment, s'han sintetitzat dos lligands nous poli-NHC per a la preparació de complexos polimetàl·lics amb estructures altament simètriques.

La possibilitat de preparar complexos homo-polimetàl·lics suggereix que prompte podrem trobar la via per a sintetitzar espècies hetero-polimetàl·liques. Per la nostra experiència, aquests complexos solen ser potencialment útils per al disseny de nous processos catalítics tàndem.

A més, una de les propostes que ens hem plantejat és la combinació dels lligands piridilidens amb estructures politòpiques que obri una nova línea d'investigació dins del camp dels carbens N-heterocíclics.

## 6.5 REFERÈNCIES

1. Azua, A.; Mata, J. A.; Heymes, P.; Peris, E.; Lamaty, F.; Martinez, J.; Colacino, E., *Adv. Synth. Catal.* **2013**, *355*, 1107-1116.
2. Azua, A.; Sanz, S.; Peris, E., *Chem.-Eur. J.* **2011**, *17*, 3963-3967.
3. Azua, A.; Sanz, S.; Peris, E., *Organometallics* **2010**, *29*, 3661-3664.
4. Azua, A.; Mata, J. A.; Peris, E., *Organometallics* **2011**, *30*, 5532-5536.
5. Azua, A.; Mata, J. A.; Peris, E.; Lamaty, F.; Martinez, J.; Colacino, E., *Organometallics* **2012**, *31*, 3911-3919.
6. Sanz, S.; Azua, A.; Peris, E., *Dalton Trans.* **2010**, *39*, 6339-6343.
7. Zanardi, A.; Mata, J. A.; Peris, E., *J. Am. Chem. Soc.* **2009**, *131*, 14531-14537.
8. Gonell, S.; Poyatos, M.; Peris, E., *Angew. Chem. Int. Ed.* **2013**, *52*, 7009-7013.
9. Mas-Marza, E.; Mata, J. A.; Peris, E., *Angew. Chem. Int. Ed.* **2007**, *46*, 3729-3731.
10. Sabater, S.; Mata, J. A.; Peris, E., *Nat. Commun.* **2013**, *4*.
11. Miyaura, N.; Yamada, K.; Suginome, H.; Suzuki, A., *J. Am. Chem. Soc.* **1985**, *107*, 972-980.
12. Hamid, M.; Slatford, P. A.; Williams, J. M. J., *Adv. Synth. Catal.* **2007**, *349*, 1555-1575.
13. Guillena, G.; Ramon, D. J.; Yus, M., *Angew. Chem. Int. Ed.* **2007**, *46*, 2358-2364.
14. Guillena, G.; Ramon, D. J.; Yus, M., *Chem. Rev.* **2010**, *110*, 1611-1641.
15. Dobereiner, G. E.; Crabtree, R. H., *Chem. Rev.* **2010**, *110*, 681-703.
16. McSkimming, A.; Bhadbhade, M.; Colbran, S. B., *Dalton Trans.* **2010**, *39*, 10581-10584.
17. Hahn, F. E., *Angew. Chem. Int. Ed.* **2006**, *45*, 1348-1352.
18. Herrmann, W. A.; Kocher, C., *Angew. Chem. Int. Ed.* **1997**, *36*, 2163-2187.
19. Poyatos, M.; Mata, J. A.; Peris, E., *Chem. Rev.* **2009**, *109*, 3677-3707.
20. de Fremont, P.; Marion, N.; Nolan, S. P., *Coord. Chem. Rev.* **2009**, *253*, 862-892.

21. Gonell, S.; Alabau, R. G.; Poyatos, M.; Peris, E., *Chem. Commun.* **2013**, *49*, 7126-7128.

22. Hahn, F. E.; Radloff, C.; Pape, T.; Hepp, A., *Chemistry-a European Journal* **2008**, *14*, 10900-10904.

23. Han, Y.-F.; Jia, W.-G.; Lin, Y.-J.; Jin, G.-X., *Angew. Chem. Int. Ed.* **2009**, *48*, 6234-6238.

24. Yoon, J.; Kim, S. K.; Singh, N. J.; Kim, K. S., *Chem. Soc. Rev.* **2006**, *35*, 355-360.

25. Birkmann, B.; Froehlich, R.; Hahn, F. E., *Chem.-Eur. J.* **2009**, *15*, 9325-9329.

26. Wong, W. W. H.; Vickers, M. S.; Cowley, A. R.; Paul, R. L.; Beer, P. D., *Org. Biomol. Chem.* **2005**, *3*, 4201-4208.

27. Pluth, M. D.; Bergman, R. G.; Raymond, K. N., *Science* **2007**, *316*, 85-88.

28. Yoshizawa, M.; Tamura, M.; Fujita, M., *Science* **2006**, *312*, 251-254.

29. Loch, J. A.; Albrecht, M.; Peris, E.; Mata, J.; Faller, J. W.; Crabtree, R. H., *Organometallics* **2002**, *21*, 700-706.

30. Peris, E.; Loch, J. A.; Mata, J.; Crabtree, R. H., *Chem. Commun.* **2001**, 201-202.

31. Organ, M. G.; Abdel-Hadi, M.; Avola, S.; Hadei, N.; Nasielski, J.; O'Brien, C. J.; Valente, C., *Chem.-Eur. J.* **2007**, *13*, 150-157.

32. Organ, M. G.; Avola, S.; Dubovyk, I.; Hadei, N.; Kantchev, E. A. B.; O'Brien, C. J.; Valente, C., *Chem.-Eur. J.* **2006**, *12*, 4749-4755.

33. O'Brien, C. J.; Kantchev, E. A. B.; Chass, G. A.; Hadei, N.; Hopkinson, A. C.; Organ, M. G.; Setiadi, D. H.; Tang, T. H.; Fang, D. C., *Tetrahedron* **2005**, *61*, 9723-9735.

34. Kuhn, K. M.; Grubbs, R. H., *Org. Lett.* **2008**, *10*, 2075-2077.

35. Ohkuma, T.; Ooka, H.; Hashiguchi, S.; Ikariya, T.; Noyori, R., *J. Am. Chem. Soc.* **1995**, *117*, 2675-2676.

36. Noyori, R.; Ohkuma, T., *Angew. Chem. Int. Ed.* **2001**, *40*, 40-73.

37. Yamaguchi, R.; Kawagoe, S.; Asai, C.; Fujita, K. I., *Org. Lett.* **2008**, *10*, 181-184.

38. Schneider, S. K.; Julius, G. R.; Loschen, C.; Raubenheimer, H. G.; Frenking, G.; Herrmann, W. A., *Dalton Trans.* **2006**, 1226-1233.
39. Herde, J. L.; Lambert, J. C.; Senoff, C. V., *Inorg. Synth.* **1974**, *14*, 18-20.
40. Fujita, K.; Nakamura, M.; Yamaguchi, R., *Organometallics* **2001**, *20*, 100-105.
41. Klahn, A. H.; Oelckers, B.; Godoy, F.; Garland, M. T.; Vega, A.; Perutz, R. N.; Higgitt, C. L., *J. Chem. Soc. Dalton* **1998**, 3079-3086.
42. Fan, L.; Turner, M. L.; Adams, H.; Bailey, N. A.; Maitlis, P. M., *Organometallics* **1995**, *14*, 676-684.
43. Kolle, U.; Grub, J., *J. Organomet. Chem.* **1985**, *289*, 133-139.
44. Fairchild, R. M.; Holman, K. T., *Organometallics* **2008**, *27*, 1823-1833.
45. Gusev, O. V.; Sergeev, S.; Saez, I. M.; Maitlis, P. M., *Organometallics* **1994**, *13*, 2059-2065.
46. Zuo, W. W.; Braunstein, P., *Dalton Trans.* **2012**, *41*, 636-643.
47. Kuck, D.; Schuster, A.; Krause, R. A.; Tellenbroker, J.; Exner, C. P.; Penk, M.; Bogge, H.; Muller, A., *Tetrahedron* **2001**, *57*, 3587-3613.